Title	Wave-Induced Morphological Change of Composite Sand-Gravel Beach
Author(s)	Muhajjir
Citation	大阪大学, 2019, 博士論文
Version Type	VoR
URL	https://doi.org/10.18910/73583
rights	
Note	

Doctoral Dissertation

Wave-Induced Morphological Change of Composite
Sand-Gravel Beach

Muhajjir

July 2019

Graduate School of Engineering

Department of Civil Engineering

Osaka University

Abstracts

One of the significant impacts of storm wave is coastal erosion. Coastal erosion occurs due to the inability of beach to defend itself from severe wave attack. Under extreme wave condition, the beach could lose their shoreline massively; even it could cause disaster such as flooding and landslide/cliff collapse. Even under moderate wave condition, wave induces the morphological change of the beach. The topographic change also depends on the type of the beach itself (e.g., sandy beach, gravel beach, etc.). The kind of beach determines the capability of the beach in protecting the coastline and adjacent area. One of the beach types that is well known to have better performance in protecting the beach from erosion is gravel beach.

The gravel beach is classified into three types based on the morphodynamic characteristics; pure gravel (G) mixed sand-gravel (MSG) and composite sand-gravel (CSG). The composite sand-gravel beach was selected as the main target in this research, because there is an actual composite sand-gravel beach that suffers from erosion and because there is limited research related to this topic, especially in terms of laboratory study.

Chapter one describes the background issues of beach erosion of sandy beach and composite sand-gravel beach. Along with that, the goals and objectives of this study are shown. Overview of the field measurement and the laboratory experiment is shown, by which morphological change of the composite sand-gravel beach was studied.

In chapter two, the field measurement was conducted for three years at one of the composite sand-gravel beaches of Ojigahama Coast, Wakayama, Japan. The purpose of the field study was to investigate the characteristics of the morphological change of the beach and wave condition off the beach. The topographic change of the beach was discussed in relation to the wave condition and the behaviour of the typhoons.

In chapter three, a two-dimensional physical experiment was performed in a wave flume. By adopting some of the parameters of the real condition into the experiment, the morphological change of composite sand-gravel beach was observed under various experimental conditions. The beach profile started eroding with a normal wave and became massive with storm wave. Under storm condition, the formation of berm occurred and a strong backwash current was observed, which caused a steep foreshore slope and flat part off the berm.

In chapter four, a three-dimensional physical experiment was conducted in a wave basin. In this experiment, the longshore transport of the gravel was observed through the distribution

of colored gravel (tracer material) on the beach. It was found that the gravel was transported in two steps; first, the gravel moved seaward as the effect of steep profile formation associated with strong backwash current, second, when the gravel reached nearshore, the gravel turned to move by the longshore current developed.

In chapter five, additional experiments were carried out to investigate a protection work by gravel nourishment. The gravel nourishment was selected as the gravel has recently used as one of the elements of shoreline protection. Based on the results of the experiment, it revealed that the volume factor of nourishment was more critical than the location factor in protecting the beach from severe erosion. Moreover, the armouring effect and mixture effect have significant role in reducing sediment transport rate.

In chapter six, the conclusions of overall studies were summarized.

Acknowledgments

Osaka, June 2019

Muhajjir

Table of Contents

List of Figures

Chapter 3

Chapter 4

Chapter 5

List of Tables

Chapter 1
Introduction

1.1. Background

Coastal morphodynamics is a term that has been used to study the dynamics of coast-seafloor topography change involving hydrodynamic processes such as waves, tides, wind-induced current, and sediment transport. Besides, the morphological change is also influenced by environmental boundary conditions such as the presence of coastal structure, the geology of the coast, sediment size of the coast, and many other factors. The morphodynamic approach to beach and coastal system recognize a wide range of interactions among the above process to full beach system. It measures both process and response of the morphological change itself along with positive and negative feedbacks between process and response, which determine the dynamic equilibrium of the coastal system. [1]

In the process of morphological change and response to hydrodynamic force, sediment transport plays an important role in maintaining the equilibrium condition of the beach. Sediment transport on the beach is classified into cross-shore and longshore transport. The cross-shore sediment transport process is controlled by a balance between onshore transport due to incident wave skewness/asymmetry and offshore transport by the bed return flow [2]. While longshore transport is the transport of sediment within the surf zone, which directed parallel to the beach. The effect of sediment transport could lead to the changing of morphological features of the beach, such as beach erosion. The morphological change of the beach is triggered by many factors such as sediment characteristics, wave condition, tide, and human activities. However, not a little case the change depends also on the type of the beach itself (e.g., sandy beach types, gravel beach types). The type of beach determines the capability of the beach itself in protecting the coastline and adjacent area.

Sandy beach is the simplest beach to find worldwide. The beach provides recreational areas for people and also living area for a marine animal. Sandy beach is formed deposition of particles carried by currents and waves. The beach is mainly composed of sand from fine to coarse-grained, which acts as a buffer zone to protect the coastline, sea cliff, or dune from direct wave attack [3]. However, most of the natural sandy beach is not sufficient to protect the beach itself against extreme wave and storm surge (e.g., beach erosion). Therefore, for some area, additional counter measures for coastal protection are necessary. There are two types of

coastal protection method which are soft and hard shore protection. Hard shore protection method is mainly using structures to protect the coast (e.g., breakwater, detached breakwater, groin, seawall, etc.), however, sometimes in several cases, the structures even trigger the erosion. While soft shore protection working on a modification of beach profile (sand bypass, nourishment, scrapping). This method has become a preference among coastal engineers, considering less expensive, ease of work and especially environment conscious. Moreover, this method also could be combined hard shore protection such seawall which may continue to be the last line of coastal defense.

Another type of the beach is gravel beach or known as shingle beach. According to Jennings and Shulmeister [4] which have classified the scheme for gravel beaches based on morphodynamic characteristics into three types; pure gravel (G), mixed sand-gravel (MSG), composite gravel/composite sand-gravel (CSG) as seen in Fig.1.1.
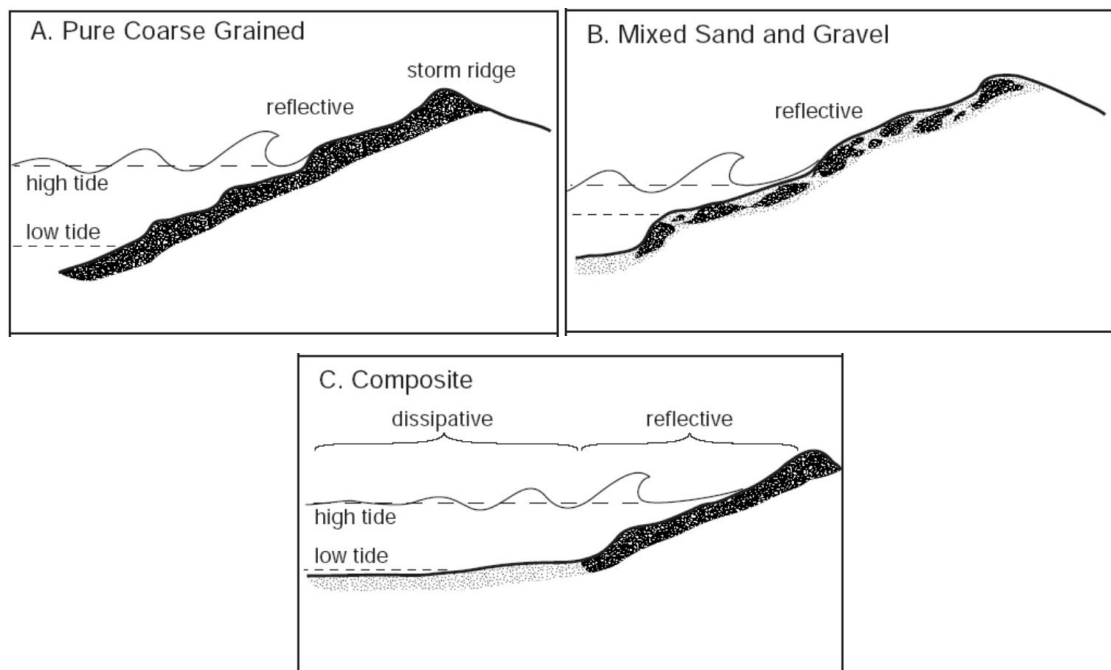
Figure 1.1 The classification of gravel beaches based distribution of sediments (sand, gravel and cobbles) and the resulting wave response

The response of each type of gravel beach to wave is distinctly different from each other in terms of profile response to hydrodynamic force, characteristics of sediment, and distribution of sediment [5]. Therefore, it is vital to understand the differentiation of gravel beach types, so that the object of the study could be addressed appropriately to the specific type of gravel beach, not to be misdirected. One of the beach type concerned in this study is composite gravel-sand beach (CSG). The beach is composed of gravel in inter-to supra-tidal swash zone and sand

lower to sub-tidal surf zone [6]. The beach can be found both in natural condition and in the design beach construction such as nourishment scheme [7]. In the nourishment scheme, the beach face which originally composed of sand is replaced by gravels, so beach type change from the sandy beach to composite sand-gravel. The changing in the beach face is done to reduce the serious impacts of coastal erosion.

On the other hand, recently, the gravel beach has turned up as elemental part of shoreline protection, regardless of any types of gravel beach itself [8]. The number of researches pertaining gravel used on coastal protection has been broadly developed in the past two decades, especially pure gravel beach (G) and mixed sand-gravel beach (MSG). Bascombe, D and Masselink, G [9] introduce one of the comprehensive studies of gravel beach in 2006, in which his study discussed the concept in the gravels beach dynamic. The gravel beach dynamic depends on the variation of the grain size, active beach step which controlling the influence of morphodynamics change. Masselink, G et al.[10] continued his previous study by conducting field monitoring in Slapton Sands (UK) in 2010. The average diameter of the beach (d50) is about 2-10 mm, which is classified as fine-gravel. He finds that on the upper part of the beach, berm formed (deposited) during swell with low steepness (H/L < 0.01) and the erosion take place under high steepness of wind-wave (H/L > 0.01). However, the opposite trends occur in the intertidal zone, which is the sediment losses occur during the swell condition and an increase deposited sediment volume due to wind wave.

Ikeda and Iseya [11] initiate the study on the effect of sand feeding to gravel bed under the experimental condition in 1988. They reveal that as sand is added to the gravel bed, the bed shear stress decreases, although the transport rate is getting larger. Wilcock, PR et al.[12] develop an experimental study of mixed sand-gravel with relying on the study of Ikeda and Iseya [11]. They measure the transport rate of five cases of mixed sand-gravel. The mixture containing 6, 15, 21, 27 and 34 % of sand was added with the same gravel diameter. Based on the result, they conclude that as the percentage of the sand content increases, the gravels transport rate also increases. The most rapid rate occurs in the case of sand content between 15 and 27 %. Furthermore, they also found that the surface grain size varies with the sand content, but no coarsening bed surface is found under strong flows and transport rate. This indicates that the formation of an armour layer occurs at small flows, demolish with increasing flow, and transport rate.

There are still many studies that discuss the gravel beach or mixed sand-gravel with different goals and objectives which rely on one and another previous study[13][14][15][16]. However,

the reviews on composite sand-gravel (CSG) are still limited, which mostly in-field monitoring study. Karunarathna et al. [6] study the cross-shore profile evolution and sediment characteristics by comparing two locations of the composite sand-gravel beach in the UK, which are Milford-on-Sea Beach and Narrabeen Beach. They discover that composite sand-gravel beach becomes critical in a sub-aerial zone against the erosion during storm wave which following by the formation of the steep slope (i.e. sandy zone below the water destabilise due to strong backwash). The recovery process of the beach come more difficult under a post-storm wave as steep profile formed in nearshore. Therefore, along with increasing use of gravel as part of shore protection and lack of studies of composite sand-gravel, a comprehensive study related to the specific type of gravel beach (CSG) need to be assessed appropriately. Furthermore, an additional work of gravel nourishment is performed to observe the morphodynamic response of the beach before and after the nourishment, including transformation effect from the sandy beach to composite sand-gravel beach as nourishment scheme. Hence, relying on some theories, this research is attempting to provide a fundamental idea of a composite sand-gravel beach based on field measurements and laboratory studies. Detailed information of this study will be explained in the next section.

1.2. Goals and Objectives of the Study

The goals of this study are to assess deeply the morphodyanmics of composite sand-gravel beach along with the additional development of countermeasure work of beach erosion on the sandy beach. To accomplish the goals, several objectives are considered in to specific chapters as follows:

Chapter 2: Understands the behaviour of a composite sand-gravel beach based on the observation and field study of one representative beach case (Ojigahama Beach, Wakayama Prefecture).

Chapter 3: Investigates the response of composite sand-gravel beach profile to the waves. Identify the mixture sand-gravel effect on sediment transport.

Chapter 4: Observes the longshore sediment transport process of composite sand-gravel. Identify alongshore and cross-shore gravel transport on the beach.

Chapter 5: Assesses the effectiveness of gravel nourishment to encounter beach erosion issues. Identify the armoring and mixture effect on sediment transport.

1.3. Methodology of the Study

In order to achieve the goals, the methodologies used in this research are field study and laboratory experiment. The location of the field study was selected as a representative composite sand-gravel beach in Japan, located in Shigu, Wakayama Prefecture. The beach was attacked by storm wave in 2015, which caused severe erosion. One of the major factors caused the erosion was no protection along the coast. Furthermore, the beach is one of the preserved areas of local communities, which is maintained by strict rules under local government, any kinds of structures are prohibited from building around the coast despite the reason of coastal protection. Based on this issue, the development of "soft-shore protection" (e.g., beach nourishment) for the coast will be more suitable.

The field study triggered overall work in this research, by looking at characteristics, condition pre and post-disaster, and the problem experienced on the coast; it encourages us to develop comprehensive research on it. Therefore, in order to enhance the study, laboratory experiments were conducted. The laboratory study was designed into two series test in 2D wave flume (chapter 3 and 5) and a series test in 3D wave basin (chapter 4). By completing all the study on this research, it may have a definite understanding regarding how a composite-sand-gravel works under various circumstances and in what condition the countermeasure of beach erosion could be done.

1.4. Structure of the Study

The flow of the research is described in this section. The thesis consists of five chapters, which discuss separately but sustainably of each chapter.

Chapter One: the author introduces the background of research along with the goals and methodologies of the research. In part 1.1 (background), it describes briefly about the definition of beach morphodynamics along with factors contributes to the morphological change such wave, tides, wind-induced current, sediment transport. Besides, the author also gives some introductions to the classification of sediment transport, which has an essential role in morphological change. A brief understanding of cross-shore and longshore sediment transport is necessary in order to know the fundamental concept of the phenomenon. Furthermore, regarding the process and response of morphological features, an introduction about the types of the beach are included in this chapter. It is important to know the types of beach (e.g., sandy beach types, gravel beach types) and classification within each type (e.g., fine sand, coarse

sand, pure gravel (G), mixed-sand gravel (MSG), composite sand-gravel (CSG)), because each type has different characteristics, so the response of the beach to the hydrodynamic forces will be different as well. Therefore, based on the understanding of the above types and the class of the beaches, so a specific study could be addressed appropriately. In this regard, the author has selected one of the classes in gravel beach type, which is composite sand-gravel beach (CSG) to be the main subject/topic in this research. There are two consideration in selecting composite sand-gravel (CSG) to be the topic in this research; first, departing from the experience when working in a small project about beach erosion in Ojigahma Beach, Wakayama, the author have realized something unique about the formation of beach, which eventually known as composite sand-gravel beach type. Secondly, there is motivation to expand the study of the small project, since the study about CSG is also still limited (some field studies), especially in term of the laboratory study, so this would be a good opportunity to expand the knowledge about that. On the other hand, part 1.2 contains the goals and objectives of the research. The objectives of the research are designed based on the target of each chapter. However, the main goals of each chapter are the same. While part 1.3 describes the methodology of the research.

Chapter Two: in part 2.1, a brief explanation of the background of a field study in one of the representatives a composite sand-gravel beach is described. The study had been done since 2016 to 2018. In part 2.2, the structure of the study is explained in details. Based on the structure of the study, two main topics would be discussed in the next parts, which are wave data analysis and topographic analysis. Those topics would be discussed year by year sustainably. In part 2.3, overviews of field measurement are discussed in details. The overview covers the wave-current measurement, topographic measurement, and sediment sampling as primary data. Also, the secondary data such as wave data from nearby wave station, typhoon data, and wind data are used as supporting data to elaborate the result of primary data. Those data are evaluated year by year. In part 2.4 to part 2.5, a series of discussion topics of wave and topographic analysis in 2016 is done. In part 2.6 to 2.7, the advanced study of the condition in 2017 about those two topics above is provided in these parts. While the discussion of the last measurement condition in 2018 is provided in part 2.8 and 2.9 for the wave and topographic analysis, respectively. Between the topics, direct and indirect relationship are discovered. Thus, it would be interesting to know the valid information based on the actual data and assessment.

Chapter Three: a 2D experimental study on cross-shore sediment transport of composite sand-gravel beach are discussed. The beach profile response to the various wave condition is the main topic that would be elaborated in this chapter. Chapter 3 consists of three main parts.

Part 3.1 and 3.2 discuss the introduction and experiment set up of the study, respectively. In part 3.2, the parameters in the experiment were adopted based on field measurement study in chapter two. The author realizes that not all the parameters on the field could be scaled similarly and perfect with the experiment. There would be a scale-effect issue which might affect the experimental results. Consideration of the scale-effect of each parameter (e.g., sand, gravel, wave height, wave period, wave duration, etc.) and scale-effect combinations of the parameters are important, but it needs a comprehensive or specific study to discuss intensely. Moreover, with respect to main goal of the study which limited to clarify the general characteristics of beach response under experimental condition. In part 3.3, the section is divided in five sub-parts, which discuss the results of the experiment.

Evaluations of beach profile response to wave conditions are discussed over three different cases (C1, C2, and C3) in subpart 3.3.1. The profile changed rapidly in the first 30 minutes, showing the significant erosion along nearshore, formed steep slope and formed the berm on the top of the beach. It has prevailed (i.e., erosion phenomena and steep slope formation) for all the cases in the experiment except case-C2 with no berm on top of the beach. The recovery of the beach in post-storm condition was discovered to be very slow. In subpart 3.3.2, shoreline change was analyzed by comparing the profile between the initial and final state at the water line. Based on the result, case C2 revealed the lowest shoreline retreat among the case with 270 mm. Discussion of net sediment transport is provided in subpart 3.3.3. Significant transport rate occurred during the first 60 minutes and decreased gradually with time. Transport rates in the post-storm conditions were discovered to be inconsistent every hour. In subpart 3.3.4, the sediment mixture was estimated, and it was found that the ratio and thickness of the mixture are predominant in storm wave condition rather than post-storm wave condition.

Chapter Four: it elaborates broadly about sediment transport behavior of composite sand-gravel beach in large scale 3D experiment. This experiment also adopted some of the parameters from the field study. By conducting this experiment, it is expected that the longshore sediment transport process could be observed. This chapter consists of three main parts, like the previous chapter. In part 4.3 (result-discussion), the result is divided into four subpart. In subpart 4.3.1, it discusses the shoreline retreat as the impact of wave attack. The shoreline change was asymmetrical and inconsistent along the coast in every 30 minutes. In subpart 4.3.2, the distribution of colored gravels along the coast takes into account. The gravels distribution was traced by sampling the colored gravel along the coast with gridding-method.

Based on this result, a trajectory of gravels transport could be discussed in details. In subpart 4.3.3, the effectiveness of wave oblique generated to sediment transport is evaluated. The wave was designed to meet the real condition (i.e., incident wave angle15°-30°). However, instead of generating the oblique wave, the beach was designed 15° to the wave. It was expected that the oblique wave could generate longshore transport; in fact, offshore transport predominantly took a place beach face area. In part 4.3.4, nearshore current and profile impact on the direction of sediment transport are investigated. The oblique wave incident generated longshore current but not close enough to the beach area. Mostly, the longshore current occurred in the nearshore. Furthermore, the beach face area (toe side) collapsed after the first wave hit, and profile became steeper by the time, as the result gravels transported initially seaward and veered in the nearshore as the impact of the longshore current.

Chapter Five: an additional 2D experimental work regarding gravel nourishment is performed in this chapter, although this work is not connected directly to the main goals of this research, explicitly, it would give valuable knowledge about response of the profiles with and without gravels nourishment to various wave condition. Chapter 5 consists of three main parts, like in other chapters. Part 5.3 is divided into four subparts, which discuss the result of the experiment. Part 5.3.1 examine profiles response of eight cases (with and without gravels nourishment), which split into two series of experiment separately. There were three and five cases for the first and second series of the experiment, respectively. Based on the result of profiles response of two series experiments, it could be deduced that the nourishment scheme is conditional. It depends on what location require protection the most. If we prefer to protect the beach area, case-T2 and case-T3 could be the option, case-T5 is fit for nearshore-offshore protection. While case-E2 is entirely compatible with protecting the beach face-nearshore area for long periods, however, it will change characteristic of the beach from the sandy beach to gravel beach, and it requires a considerable amount of gravels material (i.e., increase on the budget as well). Part 5.3.2 describes a comparison of shoreline retreat overall the case as the effect of nourishment scheme. Part 5.3.3 exhibits the net sediment transport in the different wave conditions. Furthermore, the effects of different methods in nourishment scheme are explained in this section. Part 5.3.4 illustrates the distribution of gravels nourishment along with the profile with different measurement methods (i.e., sampling and images analysis).

Chapter Six: the conclusions of overall studies would be summarized in this chapter. The goal has been reached through the achievement of several objectives of every chapter.

References

1) Short, AD., and Jackson, DWT. (2013). "Beach Morphodynamics", *Treatise on Geomorphology*, Vol. 10, pp. 106-129.

2) Masselink, G., Austin, M., Tinker, J., O'Hare, T., Russell, P. (2008). "Cross-shore Sediment Transport and Morphological Response on a Macrotidal Beach with Intertidal Bar Morphology, Truc Vert, France", *Marine Geology,* Vol. 251, pp. 141-155.

3) World Register of Introduced Marine Species (2018). "Sandy shore habitat", Retrieved from http://www.marinespecies.org/introduced/wiki/Sandy_shore_habitat

4) Jenning, R., and Shulmeister, J. (2002). "A Field Based Classification Scheme for Gravel Beaches", *Marine Geology*, 211-228.

5) Pontee, NI., Pye, K., and Blott, SJ. (2004). "Morphodynamic Behaviour and Sedimentary Variation of Mixed Sand and Gravel Beaches, Suffolk, UK," *Journal of Coastal Research*, Vol. 20(1), pp. 256-276.

6) Karunarathna, H., Horillo-Caraballo, J., Ranasinghe, R., Short, A., and Reeve, D. (2012). "An Analysis of Cross-Shore Beach Morphodynamic of a Sand and a Composite Sand-Gravel Beaches," *Marine Geology*, Vol. 299-302, pp. 33-42.

7) Hicks, BS, Kobayashi, J., Puleo, JA., and Farhadzadeh, A. (2010). "Cross-Shore Transport on Gravel Beaches," *Proceedings of 32nd International Conference on Coastal Engineering*, ICCE, sediment 43, pp. 1-9.

8) Ahrens, JP (1990). "Dynamic Revetments," *Proceedings of 22nd International Conference on Coastal Engineering*, ASCE, 1837

9) Buscombe, D., Masselink, G. (2006). "Concepts in Gravel Beach Dynamics," *Earth-Science,* Vol.79, pp. 33-55

10) Masselink, G., Austin, M., Tinker, J., O'Hare, T., Russell, P. (2010). "Cross-shore Sediment Transport and Morphological Response on a Microtidal Beach with Intertidal Bar Morphology," *Marine Geology,* Vol. 251, pp. 141-155

11) Ikeda, H., Iseya, F. (1988). "Experimental Study of Heterogeneous Sediment Transport," Pap.12, Environment Research Centre, University of Tsukuba, Tsukuba, Japan

12) Wilcock, PR., Kenworthy, ST., Crowe, JC. (2001). "Experimental Study of Transport of Mixed Sand and Gravel," Water Resources Research, Vol. 37, pp. 3349-3358

13) Masselink, G., Russell, P., Blenkinsopp, C., Turner, I. (2010). "Swash Zone Sediment Transport, Step Dynamics and Morphological Response on a Gravel Beach," Marine Geology, Vol. 274, pp. 50-68

14) Masselink, G., Russell, P., Blenkinsopp, C., Turner, I. (2010). "Swash Zone Sediment Transport, Step Dynamics and Morphological Response on a Gravel Beach," Marine Geology, Vol. 274, pp. 50-68

15) Dyksterhuis, PL. (1998). *Cross-Shore Sediment Transport on Mixed Sand and Gravel* (Master Theses). University of British Columbia, Vancouver, Canada

16) Dawe, IN. (2006). *Longshore Sediment Transport on a Mixed Sand and Gravel Lakeshore* (Doctoral Dissertation). University of Canterbury, Christchurch, New Zealand

Chapter 2
Field Measurement a Study Composite Sand-Gravel Beach

2.1. Background

Ojigahama Coast had been selected as the case study area of this research. It is located in Shingu city, Wakayama Prefecture, Japan. The coast is classified as a composite sand-gravel beach, in which the upper part of the beach is composed of gravel and the fine sand spread under the water. Furthermore, as the last-line of coastal defense, the revetment is build to protect the railway that lies along the coast.

In July 2015, the revetment was damaged due to high wave which generated by Typhoon No. 11. The damage of the revetment caused the scouring of railway track (behind the revetment). The disaster was reported to inhibit the operation of the trains [1] to [3], especially in the southern end of Ojigahama Coast as shown in Fig. 2.1. On the other hand, despite the emergency restoration measures was taken by backfilling the scored hole, another high wave (storm) of Typhoon No.16 hit the coast in the same location in August 2015.

Figure 2.1 Location of erosion as a result of high wave generated by typhoons

The impact of the storm wave was not only on the revetment and track of the railway but also on the topography of the coast that changed rapidly during the event. Furthermore, based on the observation, it was confirmed that during the storm wave, the gravel in front of the revetment was wiped out entirely by the waves. Subsequently, the waves hit the revetment directly, the base of the revetment was scoured, and the soil behind the revetment had been sucked out from the lower part of the sheet pile.

Based on the issues mentioned above, the primary purpose of this study is to investigate the cause of rapid erosion at Ojigahama Coast by estimating the characteristics of the waves that hit the target coast during the disaster. On the other hand, in order to predict the damage risk of the revetment and prevent the damage in advance in the relevant coast, a classification in how and under what condition the rapid erosion on the beach could occur is necessary. Hence, the information provided in this research is expected to be useful for the railway's company and local government to maintain the beach and activities around the coast to keep run safely.

2.2. Structure of the Study

The study in this chapter is described into three main topics, which are field measurement, wave data analysis, and topographic analysis. The study had been conducted from 2016 until 2018. In a year, the topographic measurement was performed four to six times, following the cycle of a season. The comparison of those yearly data provides compressive information regarding the wave characteristic, beach topographic characteristic, and correlation between both wave and beach topographic. Furthermore, the comparison of wave measured data with nearby wave data station (Owase Station) were done. The wave data from the station is obtained by Nationwide Ocean Wave Information Network for Ports and Harbours (NOWPHAS) of the Ministry of Land, Infrastructure, Transport, and Tourism. Besides, based on oceanographic data from Owase Station in 2015, the mechanism of coastal erosion in front of revetment is discussed.

2.3. Overview of Field Measurement in 2016

2.3.1. Wave measurement

The installation of a wave gauge on target coast was conducted in August 2016. The wave height device used is WaveHunter-403 (made by IO-technic Co., L.td.) as shown in Fig. 2.1. This device is a seafloor installation type self-recording wave gauge with an ultrasonic sensor, a pressure sensor, a flow velocity sensor, and a water temperature sensor. The sampling

interval of the data was 0.5 s, and the measurement time was ± 20 minutes (total 40 minutes) every hour, and the measurement was continuously performed from August 19 7: 40-8: 20 to November 28 22: 40-20. However, although the number of data sets to be obtained was 2,441, the water level data has some defects for Sept. 20, 11: 40-12: 20, and it was excluded from the analysis.
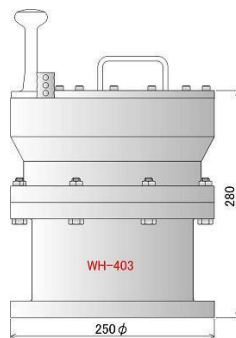
Dimensions: 280H x 259φ, Weight: 14kg

Water pressure gauge: Semiconductor pressure sensor

Flow rate: electromagnetic flow rate sensor

Wave height: ultrasonic sensor (frequency: 200 KHz)

Water temperature: platinum temperature sensor

Figure 2.2Wave gauge descriptions

The device installation was located in N33 ° 42'19.13 '', E136 ° 0'17.33'' as shown in Fig. 2.3 as "Wave Gauge." The depth of the installation position was about 13 m. The wave gauge was installed in contact with the offshore side of the reef in consideration of the impact on the fishery, based on the exploration by the diver, the bottom of the installation site had rock reefs which covered by thin sand layer. So, it was not possible to penetrate piles or pins on the site; therefore, the mount was fixed with a weight (about 200-300 kg). Besides, an anchor and a buoy (bamboo baskets, flags, flashing lights) were installed.
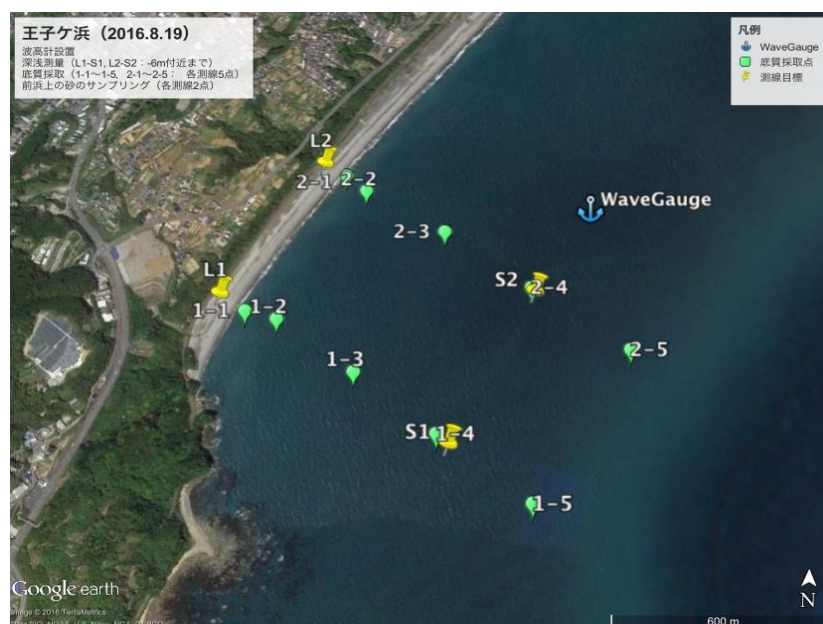
Figure 2.3 Wave height installation point (Wave Gauge), bathymetric survey lines (L1-S1, L2-S2), sediment sampling points

On the other hand, the bathymetric survey and sediment sampling were conducted after the installation of wave gauge. The bathymetric survey was conducted by using GPS and ultrasonic sounder in two lines L1-S1 and L2-S2 as shown in Fig. 2.2. The water depth could be measured only from 14m to 6m, in which 6 m water depth was about 50-60 m from the shoreline. Sediment was collected by divers using a hand collector at five points of 6m, 8m, 10m, 12m, and 14m, on two lines L1-S1 and L2-S2 respectively. The locations of sediment sampling are as shown in Table 2.1. Furthermore, foreshore sampling was collected near the two lines on the coast. The sampling points were near the beach and the top of the foreshore. A photo of measurement activities is shown in Figure 2.4.

Table 2.1 Location and time of sediment sampling

No.	Latitude / longitude	Water depth (m)	Time
1-1	N 33 ° 42'06.65 ", E 135 ° 59 '36. 64"	6	9: 10
1-2	N 33 ° 42' 05. 85 ", E 135 ° 59 '40. 38"	8	9: 14
1-3	N 33 ° 42 '00. 46 ", E 135 ° 59' 49. 62"	10	9: 20
1-4	N 33 ° 41 '54. 41 ", E 135 ° 59' 59. 15"	12	9: 26
1-5	N 33 ° 41 '47. 98 ", E 136 ° 00 '09. 69"	14	9: 33
2-1	N 33 ° 42 '22. 21 ", E 135 ° 59 '47. 57"	6	10:00
2-2	N 33 ° 42 '20. 61 ", E 135 ° 59 '50.06 "	8	9: 58
2-3	N 33 ° 42' 15. 95", E 135 ° 59 '59. 77 "	10	9: 52
2-4	N 33 ° 42' 09. 81", E 136 ° 00 '10 0.03 "	12	9: 47
2-5	N 33 ° 42 '03. 35", E 136 ° 00' 21. 28 "	14	9: 40

Wave height meter installation

L2-S2 line fron side of shoreline-side point

L1-S1 line (the slope fairly steep)

L2- S2 (the slope is lower compared to L1-S1)

The device before deployment

Situation of bathymetric survey
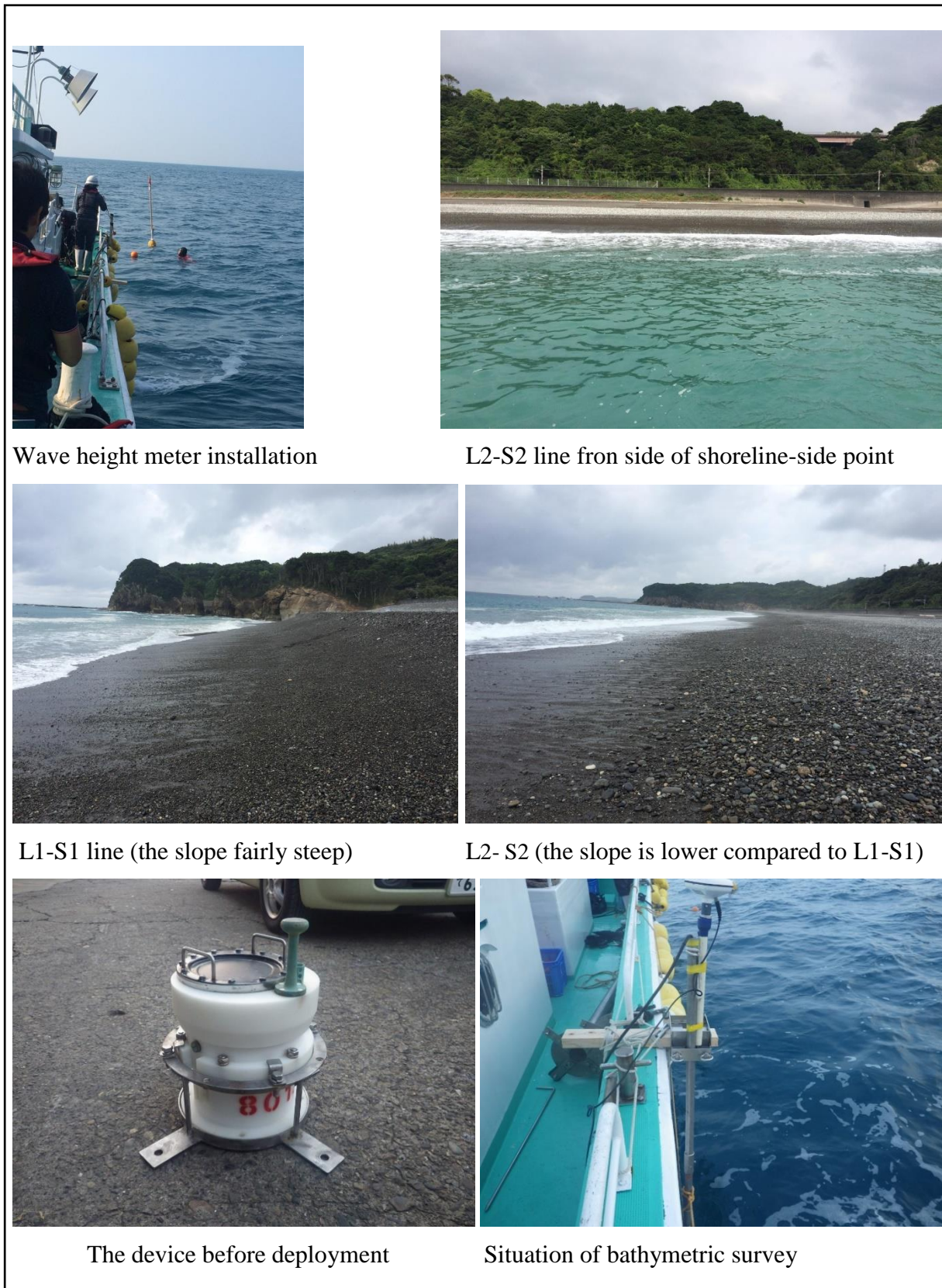
Figure 2.4 The photos on the installation day

2.3.2. Bathymetric survey and sediment sampling

Figure 2.5 illustrates the bathymetry condition which was obtained from the measurement. South line and North line in the figure correspond to the survey lines L1-S1 and L2-S2 in Fig. 2.3 respectively. Besides, the dashed line in the figure is a straight line connected by extrapolation concerning the distance of the eye measurement for the range where the sounding had not been done. Figure 2.6 is a photograph of the beachside from a point near 6 m of water depth, while the shoreline resides at ten meters from the point in this photo. By looking at Fig. 2.5, the cross-section of the Ojigahama coast had a steep slope of about 1/10 at a depth of about 7 - 8 m, and the gentle slope of about 1/150 - 1/140 up to deeper area.
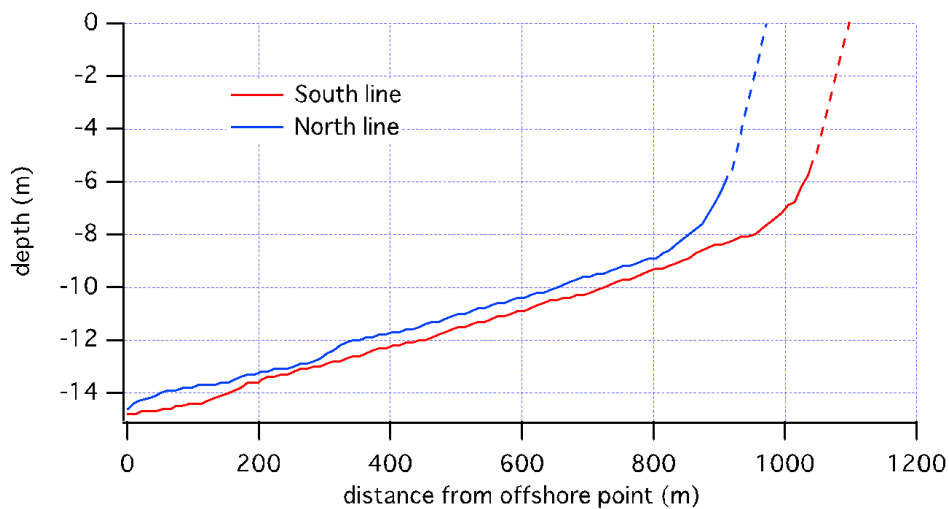
Figure 2.5 Seabed topography from bathymetric survey

Figure 2.6 The shoreline view from the water depth of 6 m

Figure 2.7 to 2.9 are grain size distribution of the sediment from the samples. Table 221 shows the summary of median grain size (d50) along with the location. It can be seen that the sediment on a gentle slope seabed was very fine sand of 0.2 mm or less. While in the foreshore, the grain size was mixed between coarse sand and gravel. The condition of foreshore is shown in Fig. 2.10.
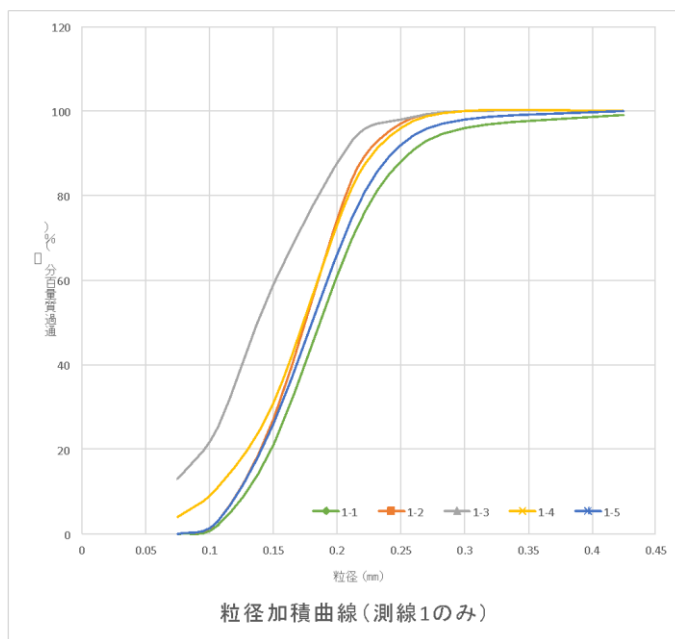
Figure 2.7 Grain size distribution of the sediment (South line)
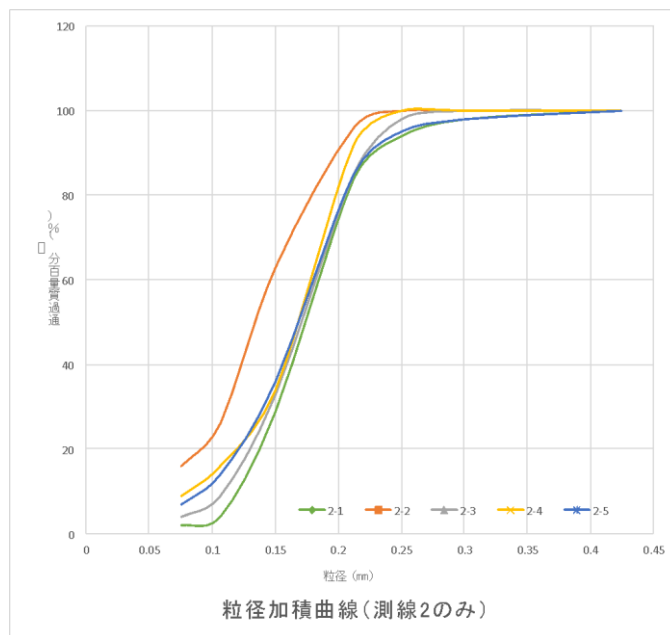
Figure 2.8 Grain size distribution of the sediment (North line)

粒径加積曲線（L1-1,2およびL2-1,2）
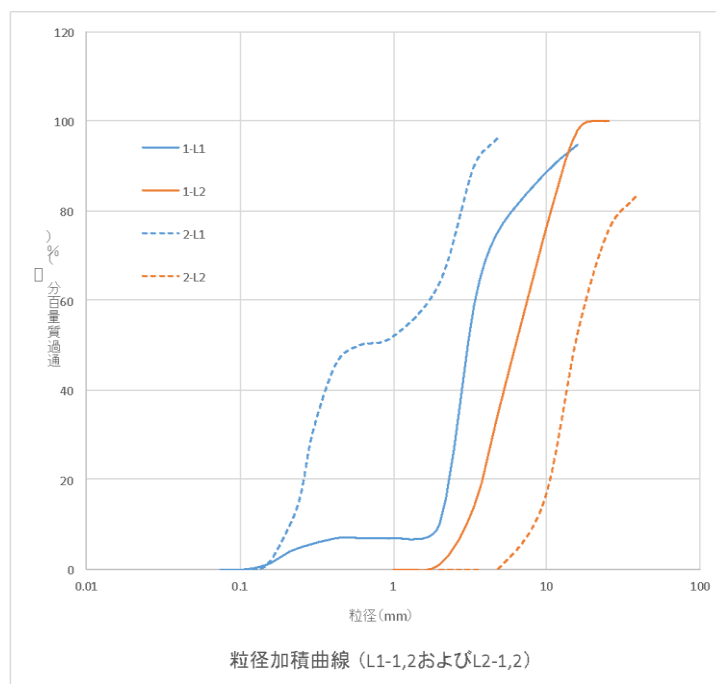
Figure 2.9 Grain size distribution on the beach area near shoreline: 1-L1, 1-L2 and top of foreshore 2-L1, 2-L2)

Table 2.2 Summary of grain size distribution of the samples

	Sampling point	Median grain size d_{50}	Remark
L1 S1 (Under the sea)	1-1	0.185 mm	water depth: 6 m
	1-2	0.175 mm	water depth: 8 m
	1-3	0.135 mm	water depth: 10 m
	1-4	0.175 mm	water depth: 12 m
	1-5	0.180 mm	water depth: 14 m
L2 to S2 (Under the sea)	2-1	0.195 mm	water depth: 6 m
	2-2	0.160 mm	water depth: 8 m
	2-3	0.190 mm	water depth: 10 m
	2- 4	0.180 mm	water depth: 12 m
	2-5	0.185 mm	water depth: 14 m
Above the foreshore (top of the beach)	11-L1	3.0 cm	near the shoreline
	1-L2	6.0 cm	top of the foreshore
	2-L1	0.6 cm	near the shoreline
	2-L2-	15.0 cm	top of the foreshore

Figure 2.10 Mixture grain between coarse sand and gravel near shoreline

2.3.3. Overview of beach topography survey

The measurement of beach topography was conducted on 22 lines set in the range of 1.2 km from the southern end of Ojigahama beach (Miwazaki side). The implementation date is shown in Table-2.3, and the position of the survey cross-section lines is as shown in Figure 2.11. The survey line is narrow at 5 m intervals on the Miwazaki side (No. 16 to No. 22), No. 11 to No. 15 are at 20 m intervals, and No. 1 to No. 11 are at 100 m intervals. The survey was leveled at intervals of about 5 m from the revetment to near the shoreline.

Table 2.3 Implementation of beach topographic survey

Date of measurement	Cross section line number	Measuring points
July 17	16-21	86
August 8	1-15	81
September 24	1-22	337
October 24	1-22	319
November 21	1-22	370
December 21	1-22	370

新宮・三輪崎間183.3k付近海岸測量

海岸測量　182k172m〜183k172m付近　@100m　10測点

182k172m

183k172m

瀬合橋りょう

狼谷橋りょう

熊野灘

王子ヶ浜

No.1　No.2　No.3　No.4　No.5　No.6　No.7　No.8　No.9　No.10

県道あけぼの・広角線

海岸測量　183k172m〜182k272m付近　@20m　5測点

183k172m

183k272m

No.11　No.12　No.13　No.14　No.15

海岸測量　183k272m〜183k330m付近　@5m　7測点

183k272m

183k330m

No.16　No.18　No.20　No.22

No.21

No.19

No.17
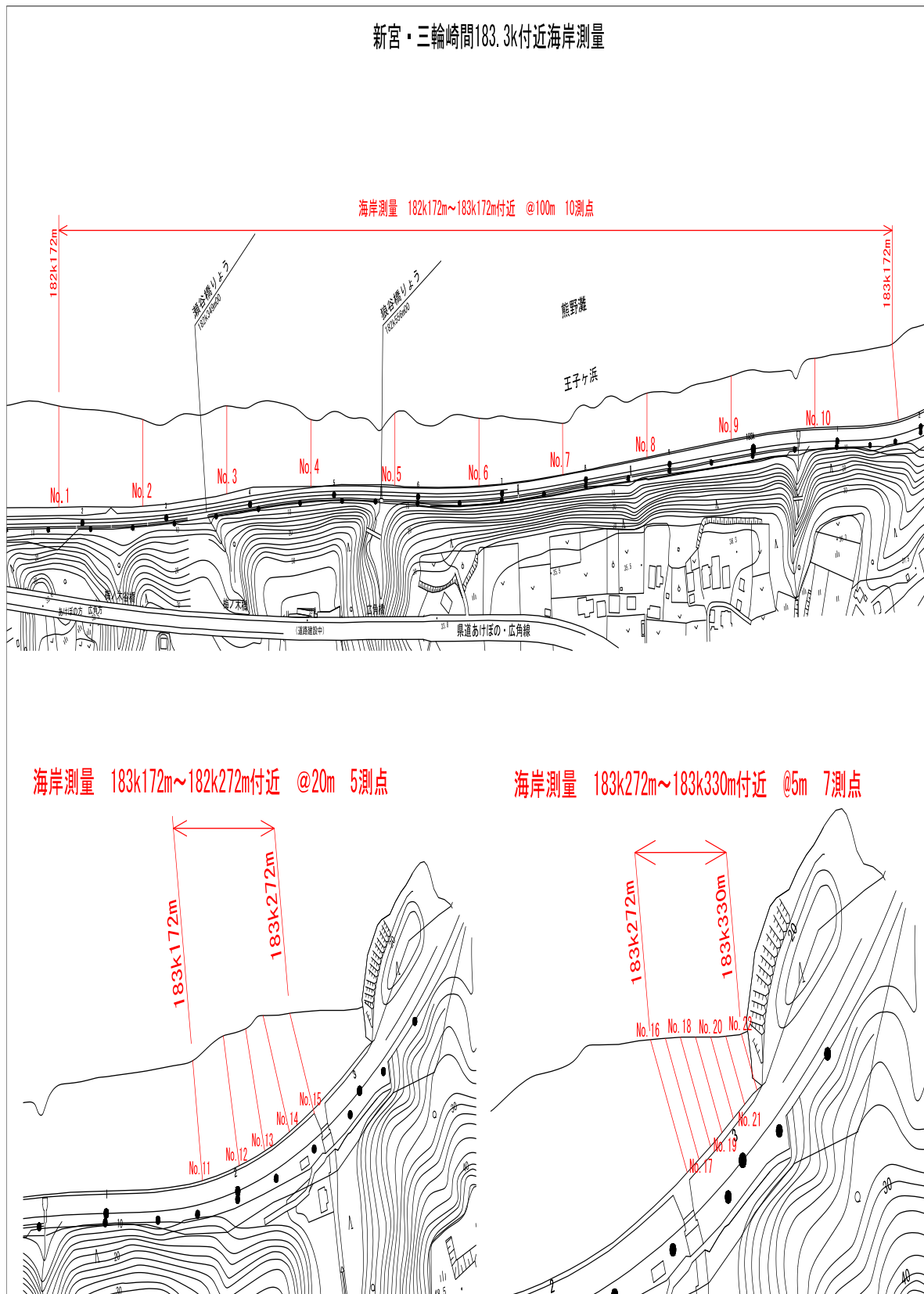
Figure 2.11 Sketch of topographic survey lines

2.3.4 Survey of gravel layer

A. Measurement

Unlike the common beach, the Ojigahama Beach has a cross-sectional configuration where the sand layer covers the gravel layer. At the time of the disaster in 2015, it had been confirmed that the gravel layer covering the surface had disappeared. Subsequently, the sand layer had been subjected to direct wave action. However, the current condition showed that the gravel had restored to normal condition as shown in Fig. 2.12. By assuming that a large amount of gravel restored on the beach, the measurement on the thickness of the gravel layer was thought necessary to be done.

The thickness of the gravel was measured by using a scoop at a point about 7 m from the shoreline, and the excavating depth was measured using a scale. Fig. 2.13 (left side) shows a photograph of gravel on the surface of the drilling site. The gravel covering the surface at the excavation site had a particle diameter of about 7 to 8 cm, and when excavating about 30 cm from the surface, we could confirm that 1 to 2 cm gravel particle exists at the bottom side. The ratio of small gravel increased as drilling progressed further. Although about 60 cm was excavated from the surface, it was not possible to confirm the sand layer existing below the gravel layer as shown in Fig. 2.13 (right side).

Figure 2.12 Natural of beach restoration after 2 years of disaster

Figure 2.13 Surface of excavation site (left), condition after 60 cm excavation (right)

B. Distribution of gravel across the beach

An average particle distribution of the beach surface was measured at the Ojigahama Coast. The measurement was conducted on two lines L1 and L2 on January 31, 2018. The position of each survey line is shown in Fig.2.14. The photographs of the beach surface were taken at intervals of 5 m from the revetment toward the shoreline, and the grain size of the gravel was calculated from the image to obtain the average particle size. The average particle size distribution of L1 and L2 is shown in Figure 2.15, and the photo of the beach surface from the revetment to the shoreline is shown in Figure 2.16. In L1, there was large gravel with an average grain size of 10 cm or more near the revetment, but small gravel with an average grain size of about 1 to 2 cm exists from 5m to 40m, and the grain size increased about 3 to 7 cm from 40 to 90 m.

The average grain size of the gravel near the revetment in L2 was 4.2 cm, which was smaller than grain size at the same point in L1. Furthermore, the average grain size of 2 cm or more was observed from 5 m to 40 m, in which this was larger than the average grain size at the same point in L1. Besides, although it is not shown in Fig. 2.14, the average grain size near the edge of the shoreline was 2.2 cm and 1.9 cm for L1 and L2 respectively. Moreover, it was confirmed that L2 was shorter 10 m than L1, which had a total width of 90 m.

Figure 2.14 Two sampling location of measurement
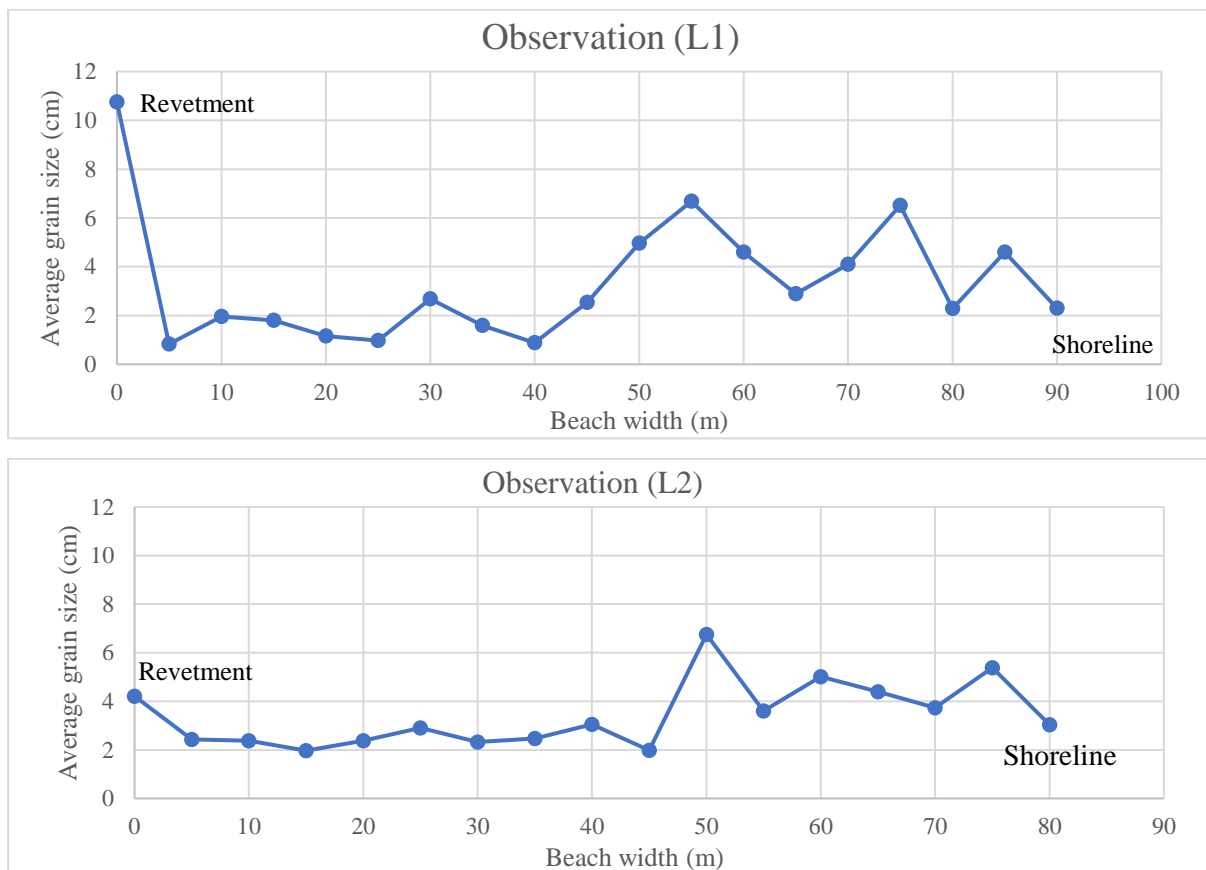
Figure 2.15 Distribution of gravel particle across the beach

5 m

95 m

Top
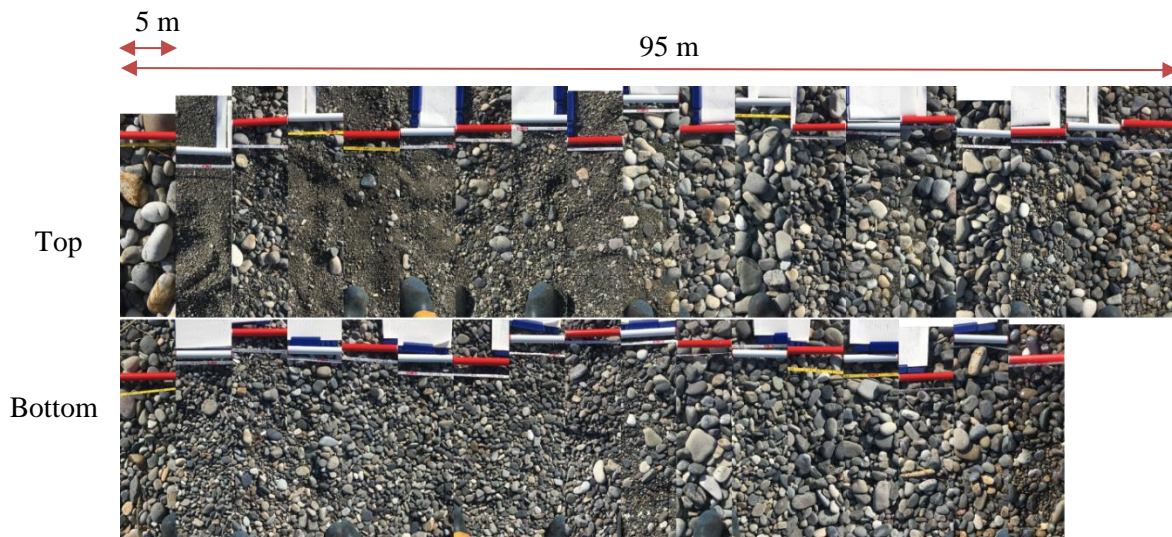
Bottom

Figure 2.16 Top: Photo on L1, Bottom: Photo on L2

C. Cusp formation along the beach

The formation of beach cusp was observed on January 31(Fig. 2.17 left), although the cusp did not exist on the day before. The beach cusp formation is caused by self-organization of the sediment as the result of the hydrodynamics force of the flow/wave [4]. The cusp length and the average particle size of the gravel on the cusps were measured using the same method as the previous term. The average particle size was measured for the cusps formed at points near L1 and L2, respectively. The cusp length was about 10 m, and the difference between the other cusps was not significant. Fig. 2.17 shows the surface of the cusp and area between the cusps. The difference of gravel particles deposited on the surface of the cusp and between the cusps was confirmed. At the middle point of the cusp (a), fine gravels with a particle size of 1 cm or less were deposited, but on the cusp (b), large gravel with a particle size of about 5 cm was deposited.

Figure 2.17 Left: Cusp formation in the winter season
Right: a) the particle between the cusps, b): the particle on the cusp

2.4. Wave Data Analysis in 2016 (Measured Data)

2.4.1. *Weather condition during observation period*

Figure 2.18 to 2.20 shows the trajectory and central pressure of the major typhoons which seems to have affected the sea near Japan during the observation period [5]. In 2016, a large typhoon did not hit the Ojigahama Coast directly, but there was also a typhoon moving in the Pacific while developing, and a typhoon such as Typhoon 1610 that stagnated or strayed in the Pacific Ocean.
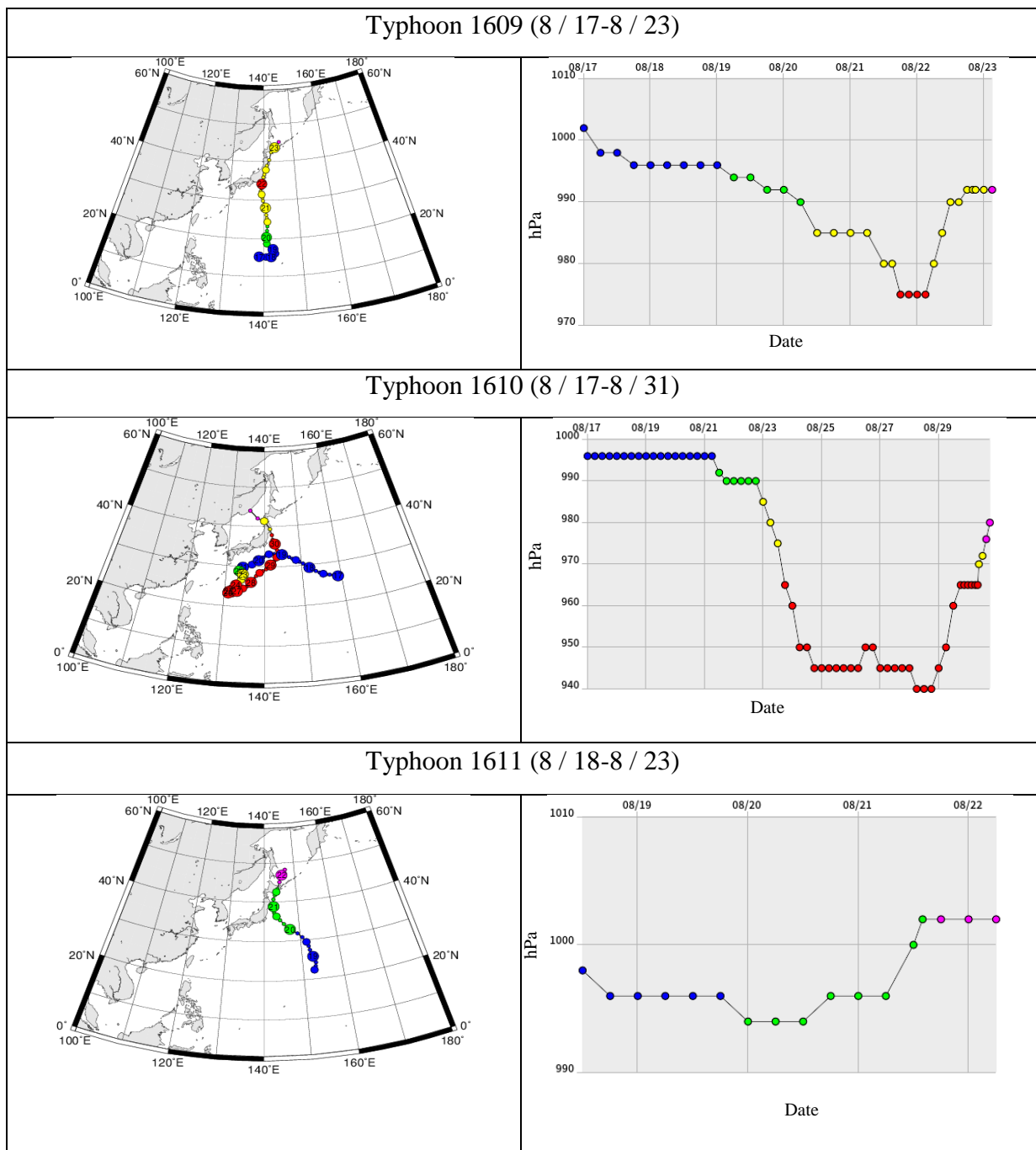
Figure 2.18 Trajectories and central pressure of the typhoon (August)

26

Typhoon 1612 No. (8 / 31-9 / 6)	

Typhoon 1614 No. (9 / 9-9 / 18)	

Typhoon 1616 No. (9 / 12-9 / 21)	

Typhoon 1617 (9 / 23-9 / 29)	
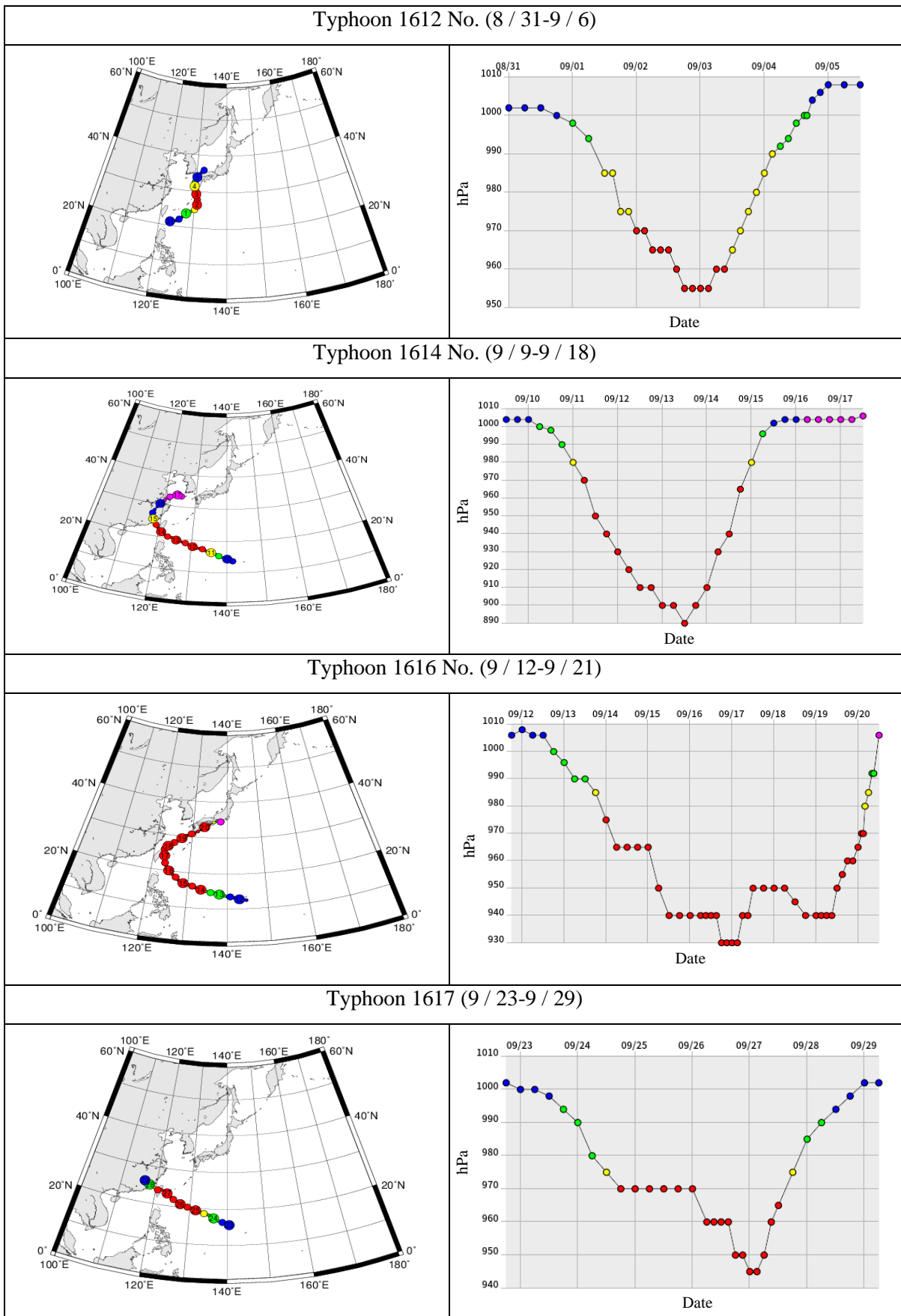
Figure 2.19 Trajectories and central pressure of the typhoon (September)
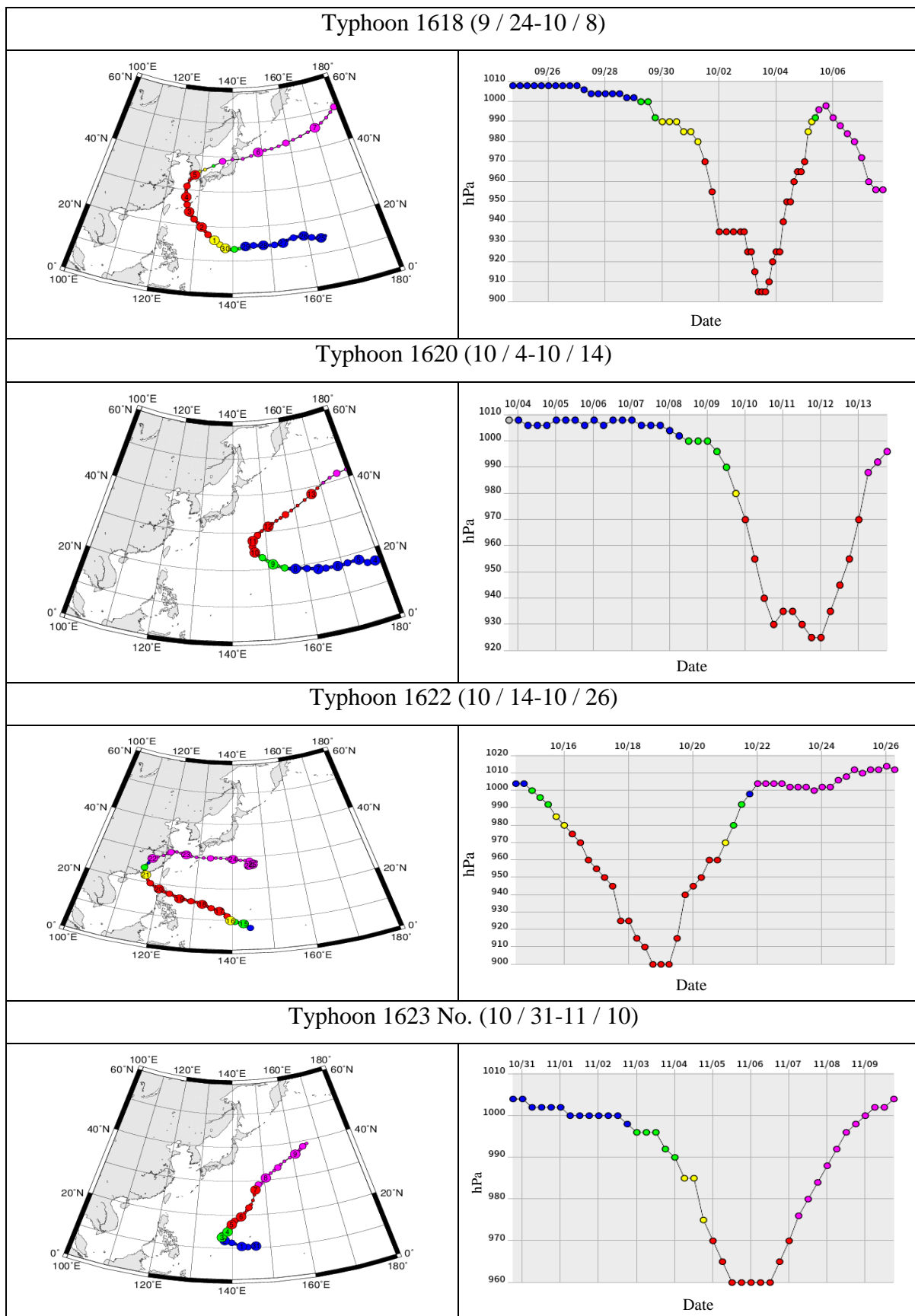
Figure 2.20 Trajectories and central pressure of the typhoon (October-November)

Figure 2.21 shows the data of wind speed and direction of AMeDAS Station in Shingu City [7]. The observation point is shown in Fig. 2.22, which is located in the inland area separated by a ridge from the ocean wave observation point in Ojigahama Coast. In the figure, the solid red line shows the wind speed, and the blue dot shows the wind direction. The wind direction is expressed by 16 directions, in which 1: north-north-east, 2: north-east, 3: east-north, 4: east, 5: east-southeast, 6: southeast, 7: south-southeast, 8: south, 9: south-southwest, 10 southwest, 11: West southwest, 12: west, 13: west-northwest, 14: northwest, 15: north northwest, 16: north. While Fig 2.23 shows the above wind data as a wind map. Therefore, it can be understood that the wind from the Northwest direction (mountainside) was most prominent in the inland area, while the wind from the seaward was excellent in the direction from the East to the Northeast.
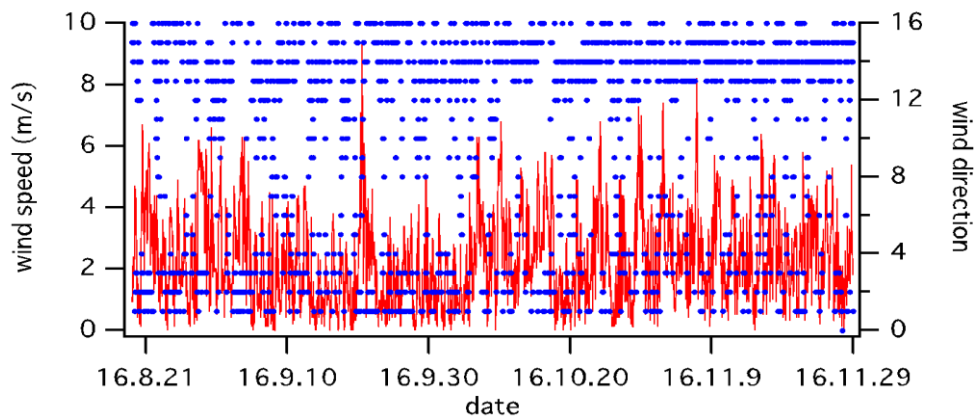
Figure 2.21 Wind speed and direction in Shingu during observation period
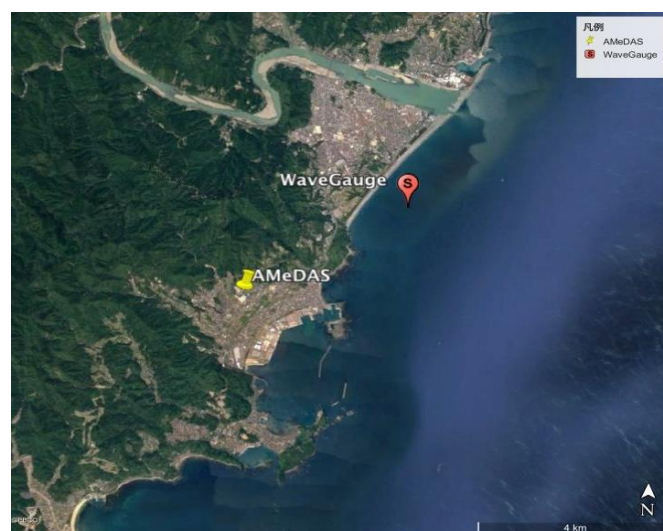
Figure 2.22 Location of AMeDAS Station to wave observation point
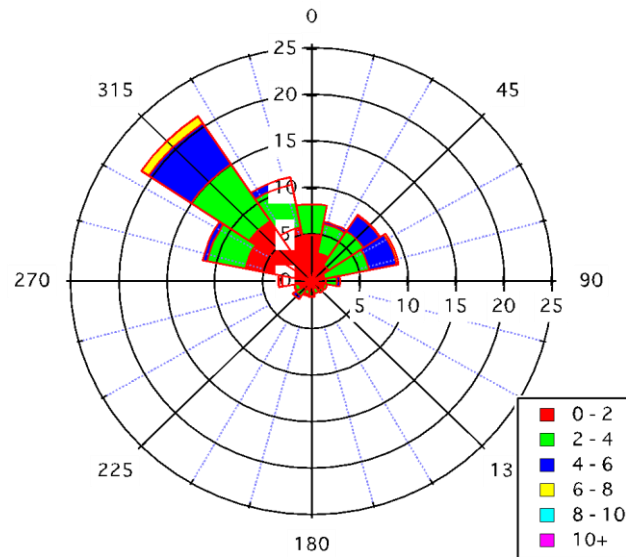
Figure 2.23 Wind map of wind data during observation period

2.4.2. *Wave data processing method*

The flow of wave data processing is as follows.

Step-1: Determine the mean water depth using ultrasonic water level data for 40 minutes and remove the tide trend by the least squares method.

Step-2: Calculate various representative waves (maximum wave, significant wave, mean wave) by wave analysis (zero down crossing method) using the data from which the trend is removed.

Maximum wave : The wave with the largest wave height among the individual waves in the wave group

Significant wave : The average wave height of the highest third of individual wave height

Mean wave : The average the wave height of all individual waves height

Step-3: For the case where the wave height or wave period has an abnormal value, check the raw data, correct and complete data, and recalculate from Step-1. For cases where correction is not possible due to long-term data loss, wave height is calculated using water pressure data if water pressure data is available. If the wave height is small and water pressure data cannot be used, it is considered as "data missing".

Step-4: From the flow velocity data, wave direction (following equation θ is mean wave direction. Here, η is the water level fluctuation, and *u and v* are the flow velocity components that are positive in the east and north directions.

$$\theta = \tan^{-1}\left(\frac{-\overline{\eta v}}{-\overline{\eta u}}\right)$$

Due to data loss, the data of September 20 at 11:40 -12.20 was neglected.

2.4.3. Wave Characteristics

A. Tide

Figure 2.24 shows the temporal variation of the average water depth of each data set for 40 minutes and corresponds to the tide variation. From this, it can be understood that the tide level deviation was about 1.5 m on average at high tide and about 0.5 m at low tide. Figure 2.25 is the value obtained by subtracting the tide level waveform (this is regard to astronomical tide level) reconstructed from the observed tide level in Figure 2.24 by using only component waves with a period of 12 hours or more (this is the tide level deviation). Although errors at the both ends of the calculated astronomical tide were included in the analysis, the tide level deviation showed a rather large value at the time of the typhoon. Although it was about 20 cm at the highest, it could be confirmed that a large tide rise (storm surge) did not occur.
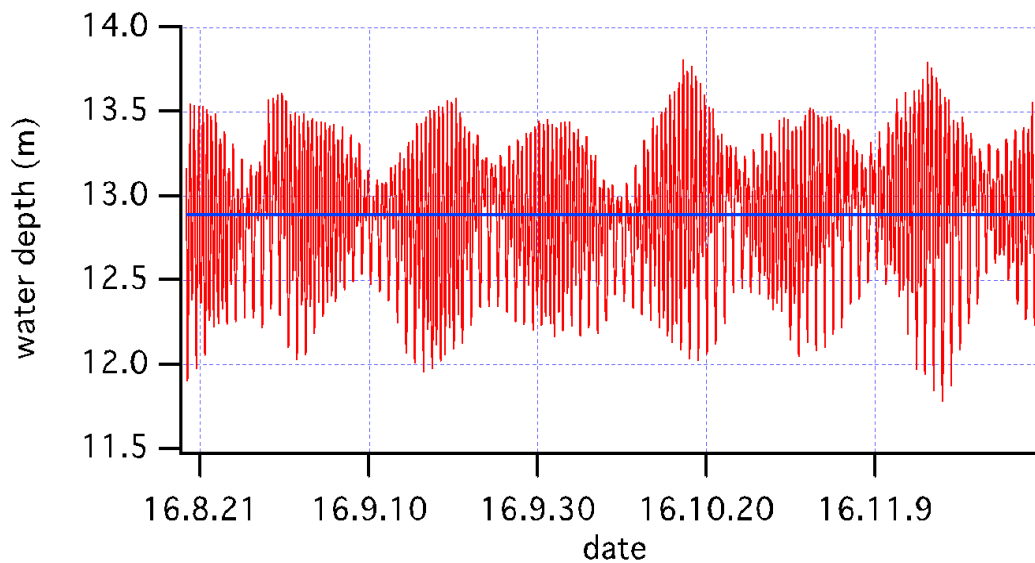
Figure 2.24 Tidal fluctuation during measurement period
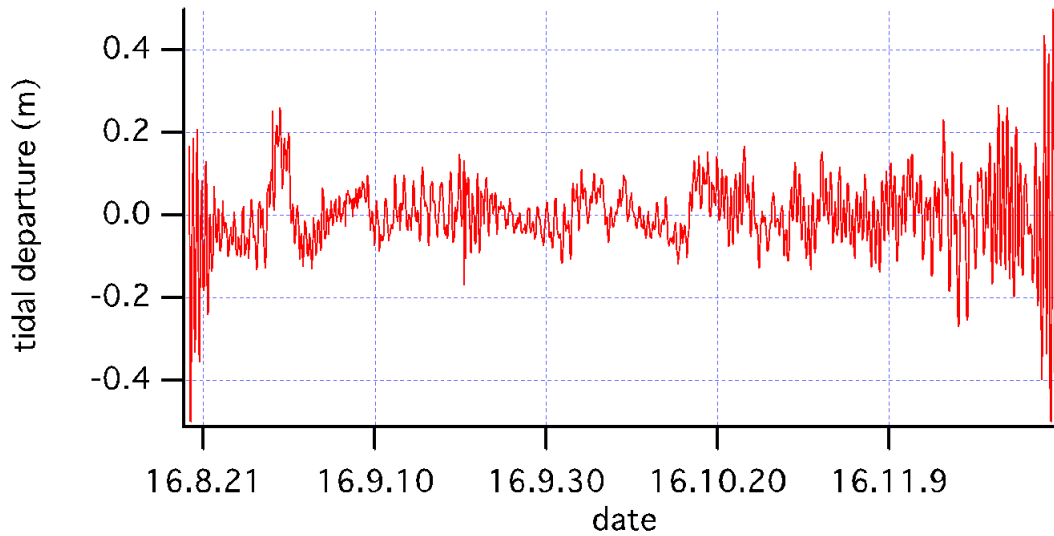
Figure 2.25 Estimated value of tide deviation

B. Wave height and wave period

Figure 2.26 and Fig. 2.27 show the change of wave height and period of the representative waves during measurement period respectively. In the figure, H_{max} and T_{max} indicate the maximum wave, $H_{1/3}$ and $T_{1/3}$ indicate the significant wave, H_{mean} and T_{mean} indicate the wave height and the period of the average wave, respectively. The impact of the typhoon on the coast was not large in 2016. The largest significant wave height during the measurement period was about 3.4 m for significant wave, and 5.9 m for maximum wave height. On the other hand, the significant wave period fluctuated in the range of 5s to 13s.
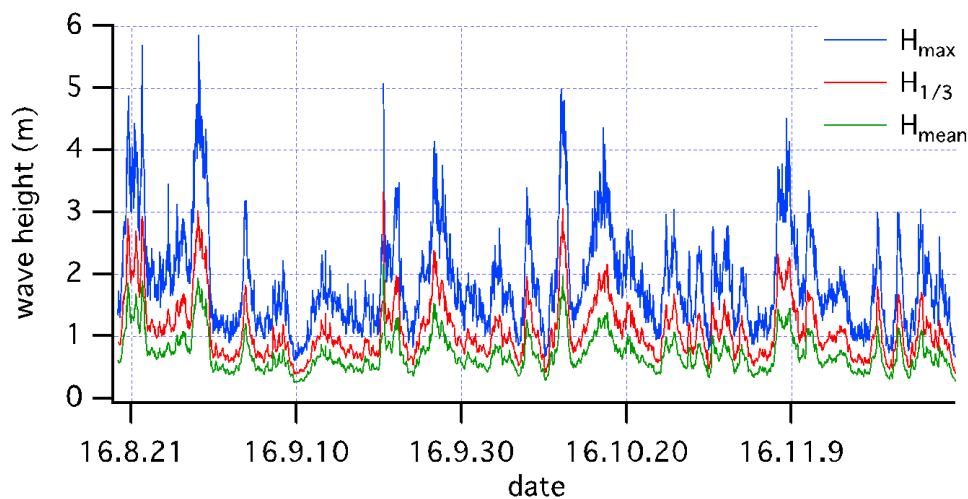
Figure 2.26 Fluctuation of representative wave height during measurement

Figure 2.28 (left) shows the relationship between the significant wave height and the maximum wave height, where is H_{max} is within the range of (1.5 to 2.0) $H_{1/3}$. Figure 2.28

(right) shows the correlation between the significant wave period and the significant wave height. There was a correlation between the wave height and the period in the region where the wave height was large, but the factor was not constant.
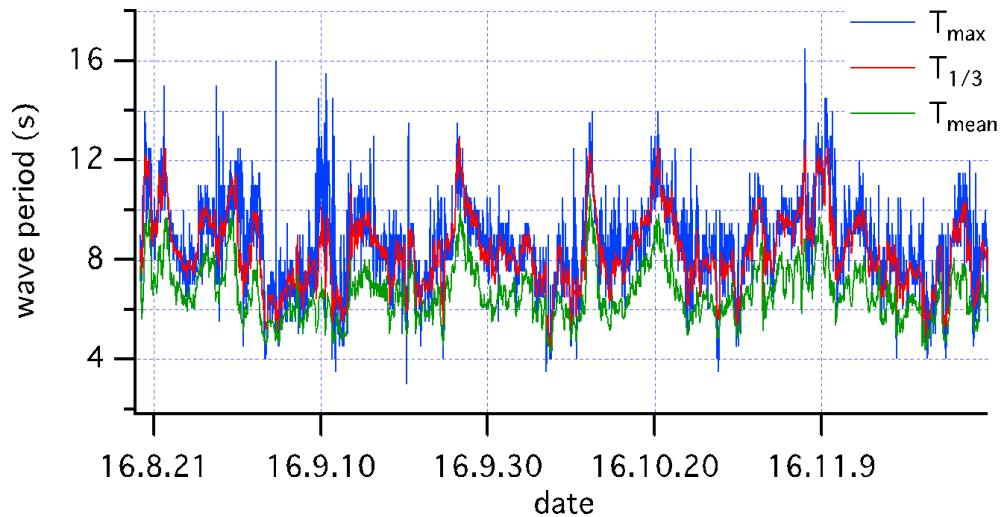
Figure 2.27 Fluctuation of representative wave period during measurement
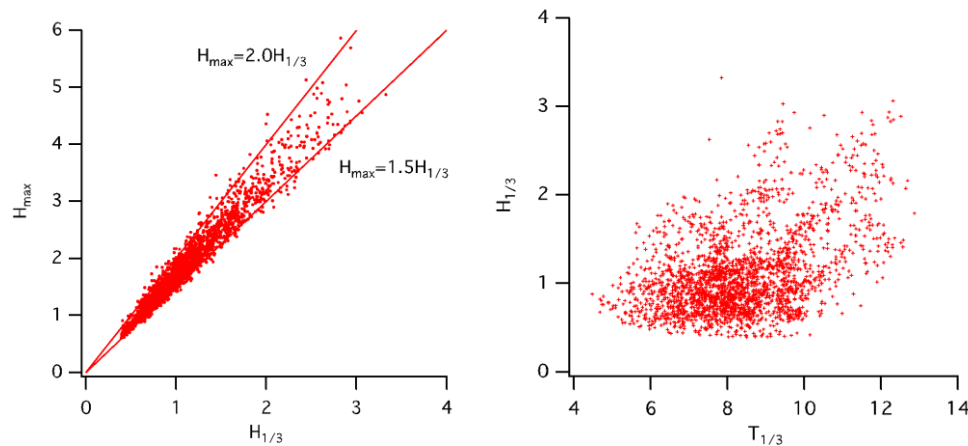
Figure 2.28 (Left) Relationship between H_{max} and $H^{1/3}$, (right) relationship between $H^{1/3}$ and $T^{1/3}$

C. Wave direction

Figure 2.29 shows the change of wave direction (mean wave direction θ) during the measurement period. The definition of the wave direction is the angle measured counter clockwise from the coordinate axis of the east direction of the normal wave incident. The angle between the coastline of Ojigahama and the coordinate axis in the east direction was about 53 °, so the angle of waves incident perpendicularly to the coastline is 90 ° + 53 ° = 143 °. As shown in the figure, the value under 143° represented the wave incident from the south direction of

the coast. Furthermore, the frequency of waves coming from the south of the coast was high, unlike the wind direction in Fig. 2.23.

Figure 2.30 shows the relationship between significant wave height and wave direction. Although the relationship with the wave height was not clear, it can be seen that there were not a few waves incident that came from the south (waves smaller than 143 °) with a large wave height.
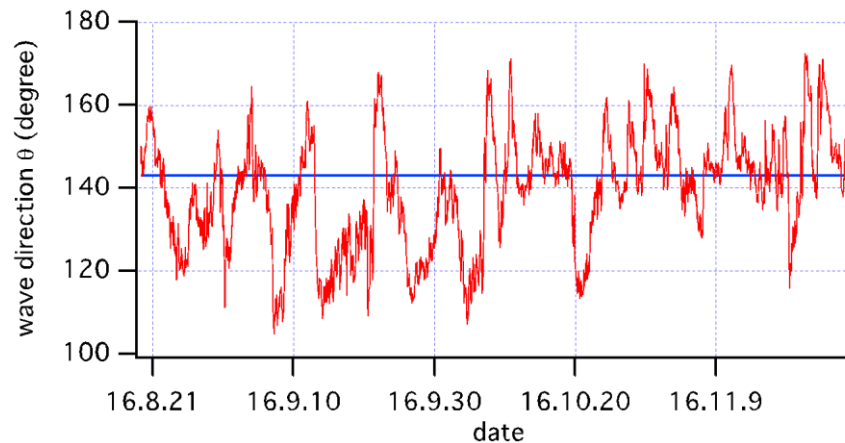
Figure 2.29 Fluctuation of wave direction during measurement period
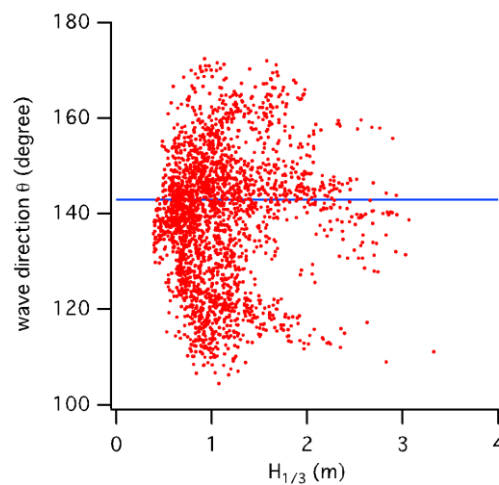
Figure 2.30 Relation of significant wave height and wave duration

D. The comparison between wave data measured and NOWPHAS

The wave gauge of NOWPHAS Owase (Ministry of Land, Infrastructure, Transport and Tourism real-time [6]) is installed on the offshore (water depth of 210 m) at N 33 ° 54 '8.00 ", E 136 ° 15' 3 4.00, Mie Prefecture. It is located about 32.5 km Northeast from Ojigahama Coast as shown in Fig. 2.31. The wave characteristics are discussed with reference to the typhoon's attack status, comparing the preliminary data with measurement data. In Owase station, the

wave direction is defined as the direction in which the waves come in (the same as the wind) as the angle measured clockwise from North (90 ° represents the wave from the east). Hereafter, the definition of the wave direction for Ojigahama measurement values was also adjusted to Owase Station. Therefore, the direction of the wave that entering the coastline at right angles was 127 °. Also, waves with angles larger than this value were waves coming from the South.

Figure 2.31 Positional relationship between Owase wave gauge and measurement wave gauge

Figure 2.32 to Figure 2.35 show the comparison of wave characteristics for both the Owase and measurement data (i.e., remarked by "Shingu") from August to November. Furthermore, the wave characteristics are discussed below, associated with the typhoon routes data in Fig. 2.18 to Fig. 2.20 for each month.

By looking at the August data shown in Fig. 2.32, high waves with a significant wave height of about 3 m and a significant wave period of about 12 s were observed from August 20th to 22nd at Ojigahama. By referring to the route map of the typhoon in Fig. 2.18, this wave was considered to be caused by Typhoon 1609, which moved up from the Pacific Ocean, North of the Izu Peninsula to Tokyo Bay. Similarly, significant wave height of 4 m or more was also observed at Owase. These waves were generated by the tail fin of typhoon on 22nd of August. Furthermore, because of wave refractionthe wave direction at measurement point (Ojigahama Coast) is perpendicular to the shoreline compared to that at Owase.

Also, the wave height of 3 m and a period of about 11 s was observed from August 29 to 30. It was probably due to the typhoon 1610 that had crossed the Pacific Ocean of the Japanese Islands. Figure 2.36 shows the energy spectra of the waves under the influence of the above two typhoons in comparison with the Bret Schneider and Mitsuyasu (B-M) type spectrum.

Subsequently, it is understood that the spectrum on August 29 was bimodal, which were the long-period wave and short-period wave by the local wind coexist.

In Figure 2.33, the significant wave heights of 3 m or more were observed in a short time on September 20. This was probably due to Typhoon 1616, which landed in Kagoshima early on the 20th and reached the Kii Peninsula through the South Coast of Shikoku on that day. Figure 2.37 indicates the wind data of AMeDAS Shingu. On September 20, more than 10 m/s strong wind was blowing from the Southeast and Southwest. Consequently, the wave increased temporarily.

On the other hand, the influence of Typhoon 1617 to the wave was small. It turns out that the typhoon route was far away from Owase and Ojigahama Coast. Although there were many relatively calm periods in September, some typhoons may had passed through the Pacific South Sea, which caused the waves to propogate from Southward (wave direction larger than 127°). Besides, the overall comparison of wave height data of Owase and measurement revealed that the wave height data from measurement was a little smaller. For the wave direction, the fluctuation of Owase data shows longer than measurement data. It could be described that wave refraction effect is significant on the measured wave because the measurement location was in shallow water. However, if the wave direction was larger than the angle of normal incidence at Ojigahama, the wave direction from the south was clear even in Owase, and so the change of wave direction was corresponding well for both Owase and shingu.

In Figure 2.33, a wave height of 3 m and a period of about 12 s was observed from October 11 to 13. It was considered as the effect of Typhoon 1620. At this time, the wave height at the measurement location was larger than the wave height at Owase Station. It could be related to the wave direction, but it was unclear. The typhoon travelled southeast of the Japan Islands, and the wave direction was dominant to the coastline at right angles. On the other hand, the long period waves had been observed around October 20, but the wave direction seems to be influenced by Typhoon No. 1622, in which it showed lower direction than normal wave incident for both measurement and Owase data. While the condition in November was shown in Fig. 2.34, There was Typhoon 1623 in this period, but the impact was not significant to the waves, neither Owase Station nor measurement location.
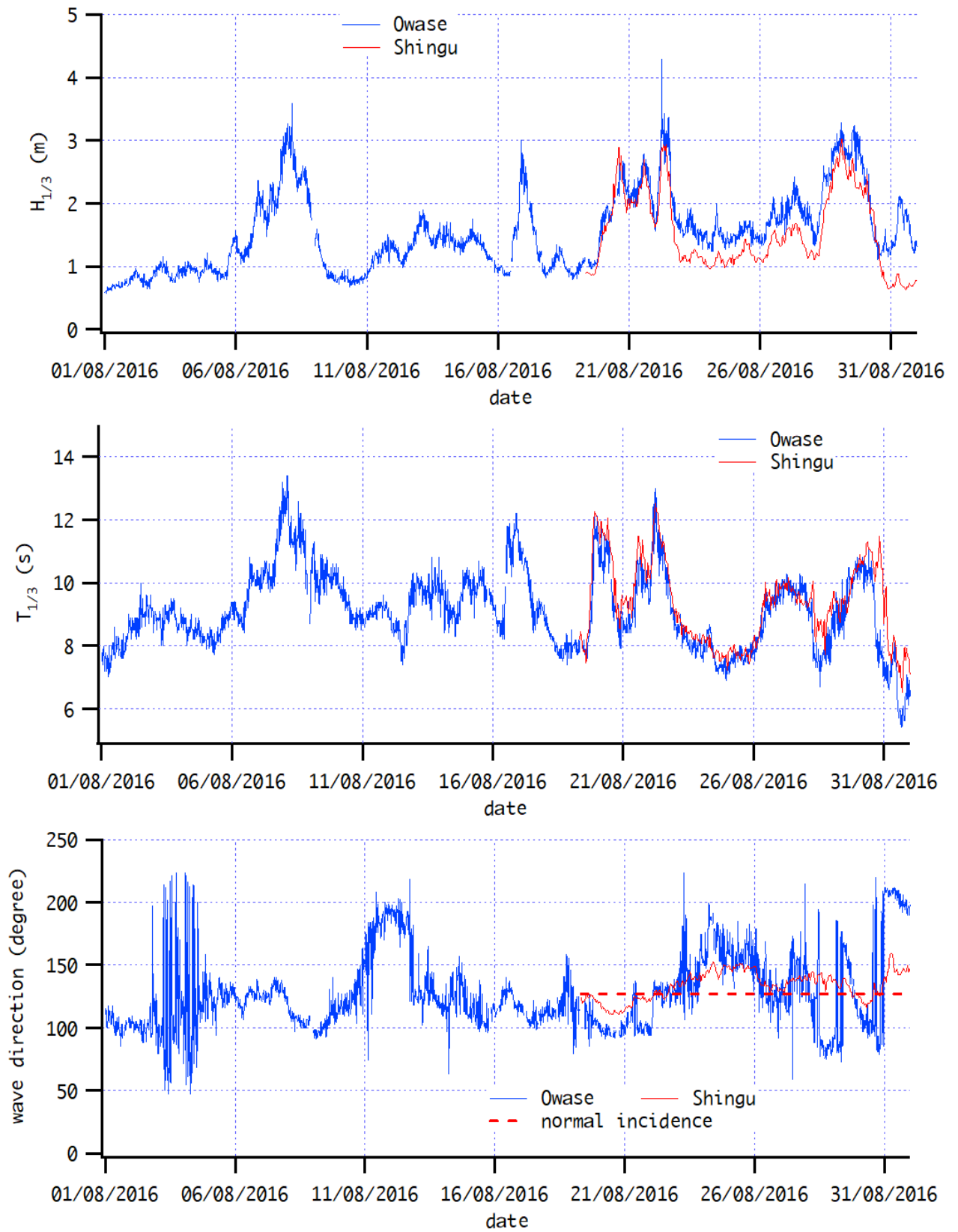
Figure 2.32 Wave characteristics of the August
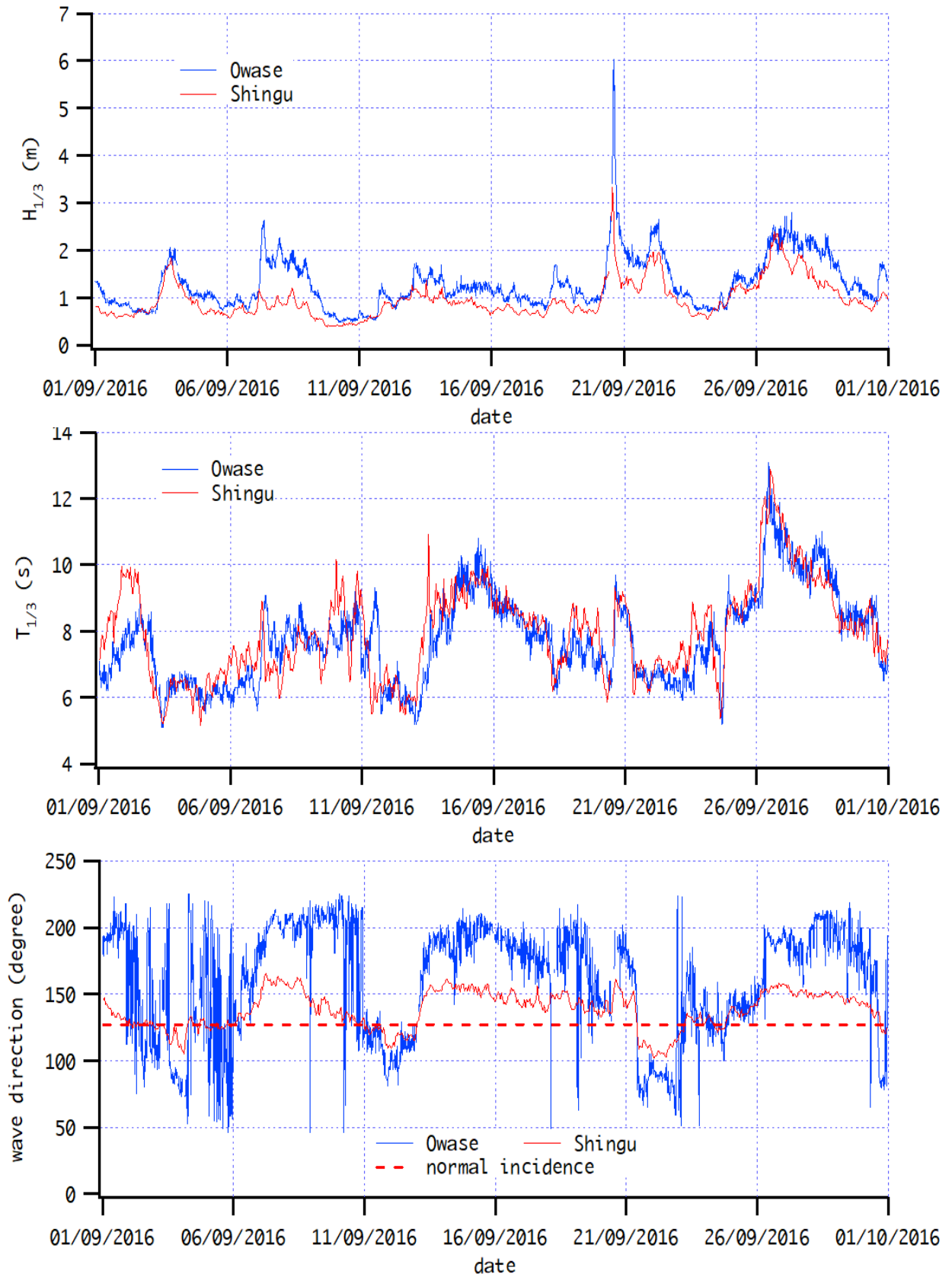
Figure 2.33 Wave characteristics of the September
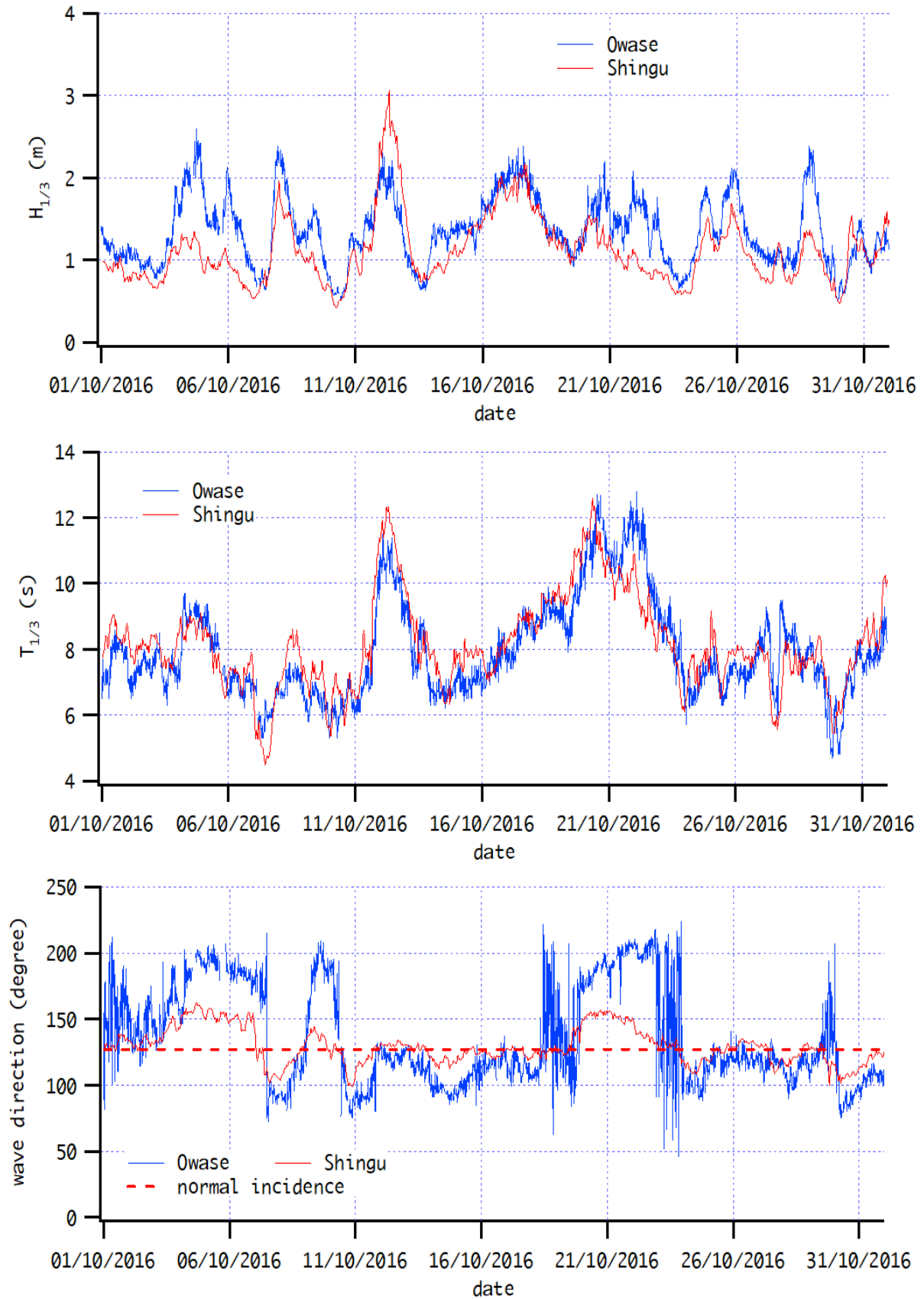
Figure 2.34 Wave characteristics of the October
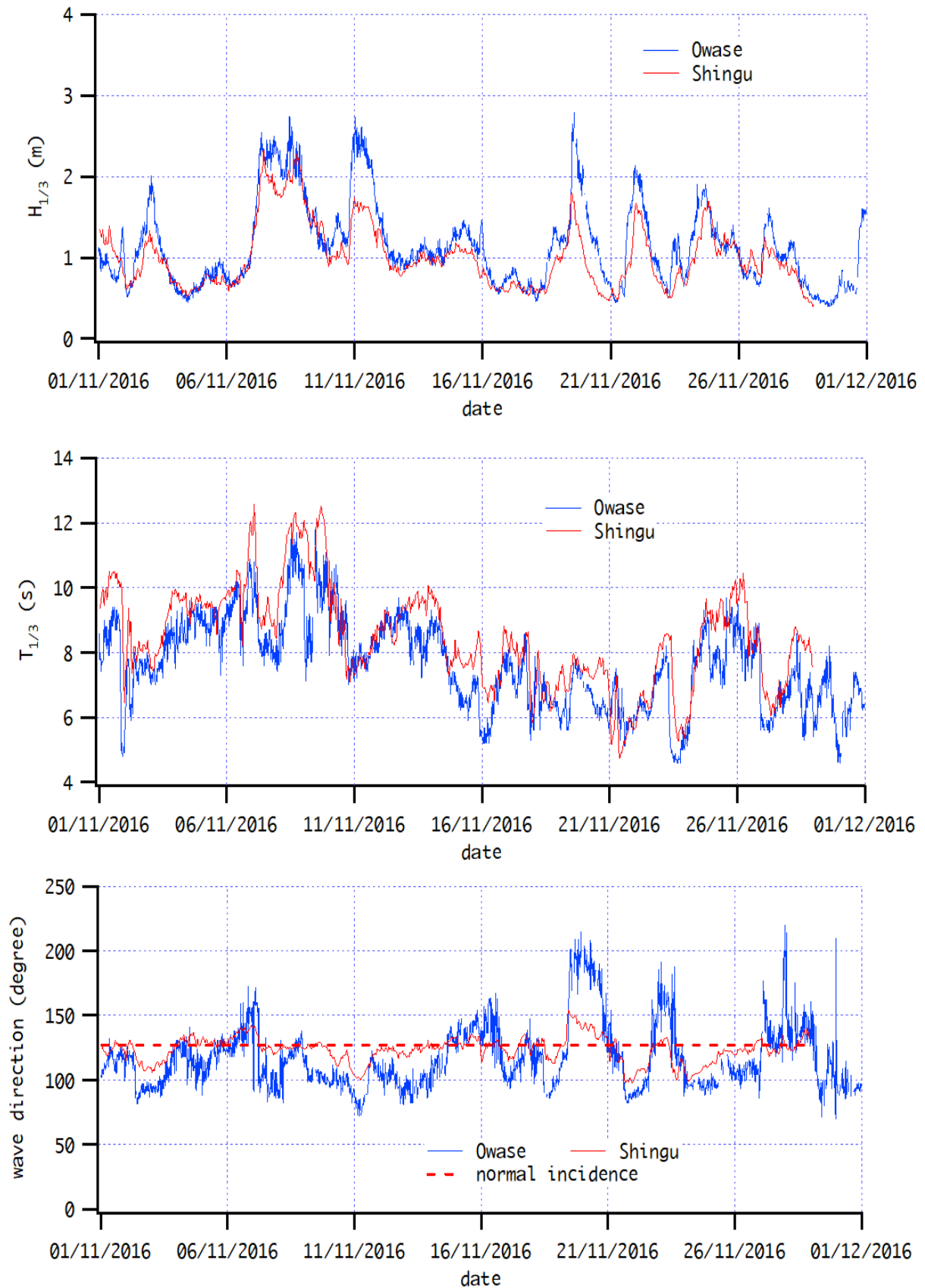
Figure 2.35 Wave characteristics of the November
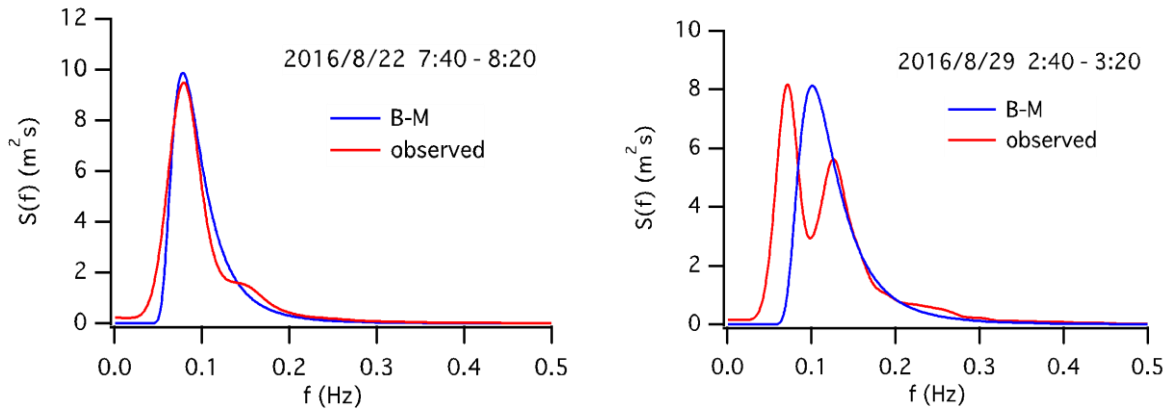
Figure 2.36 Wave energy spectrum of wave data measurement at specified date
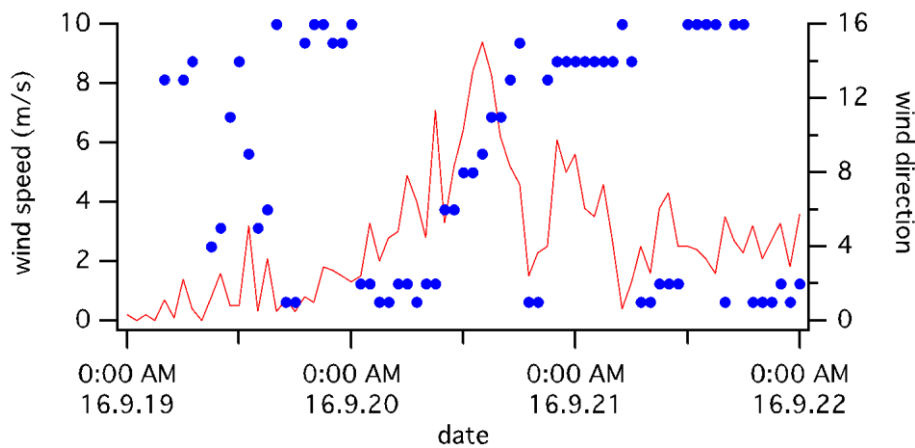
Figure 2.37 Wind data of AMeDAS Shingu (Sept. 19-21)

E. Wave characteristics of Owase during the disaster in 2015

From the comparison in section D, it was found that the waves at Ojigahama and the waves at Owase have some similarities. Therefore, in the following section, a discussion at the time of disaster using the data of the wave and typhoons of 2015 (1st: Typhoon No. 1511 on July 16 to 17, 2015; No. 2 Typhoon No. 1516 on August 21st, 2015) are performed. The damage mechanism is inferred from the wave characteristics at Owase. Figures 2.38 and 2.39 show the change in the pressure and the route map of Typhoon 1511 that caused the first disaster. The typhoon landed in Shikoku and crossed the Chugoku region. Figure 2.40 shows wind data of AMeDAS Shingu before and after the disaster in July. The strong winds were blowing from 16th to 17th of July, and also it can be seen that the wind direction changed from Northeast to South.

Figures 2.41 and 2.42 show the route map and pressure changes of Typhoon 1516 that caused the second disaster. This typhoon was moving Northward in the South-eastern sea of

the Japanese Islands while maintaining its power. Figure 3.43 shows wind data of AMeDAS Shingu before and after the disaster in August, and no strong wind had been observed.
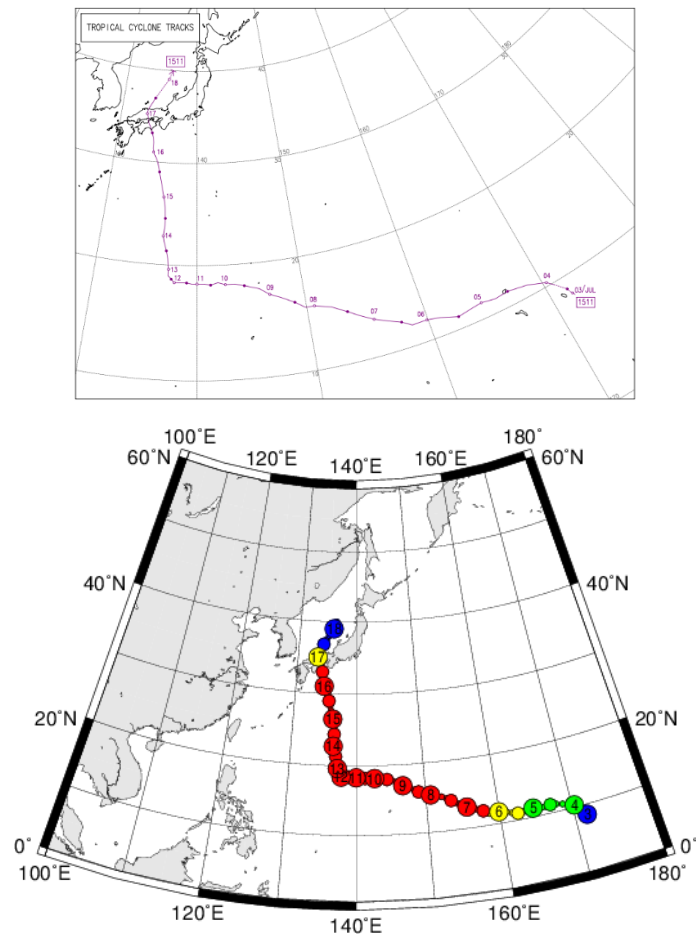
Figure 2.38 The route of Typhoon 1511 (upper: Meteorological Agency [6], lower: digital typhoon [5])
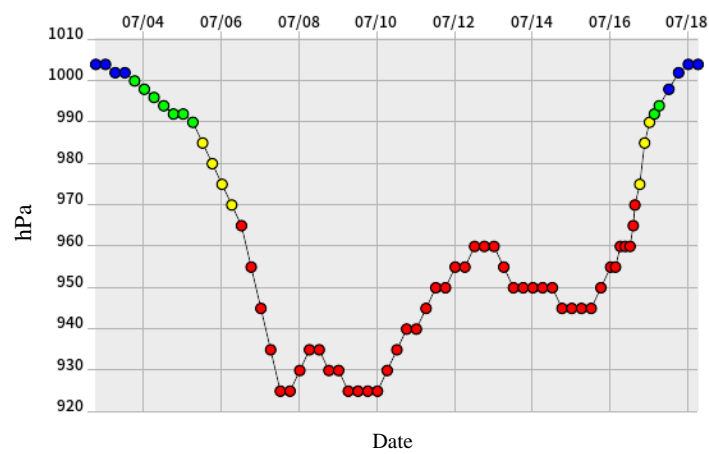
Figure 2.39 The change in central pressure of Typhoon 1511 (Digital Typhoon [5])
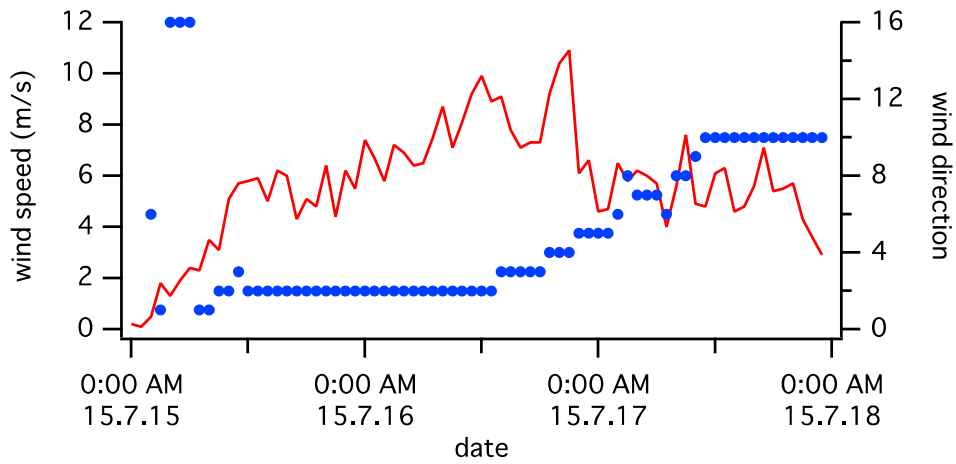
Figure 2.40 Wind conditions during the disaster in July 2015 (AMeDAS Shingu)
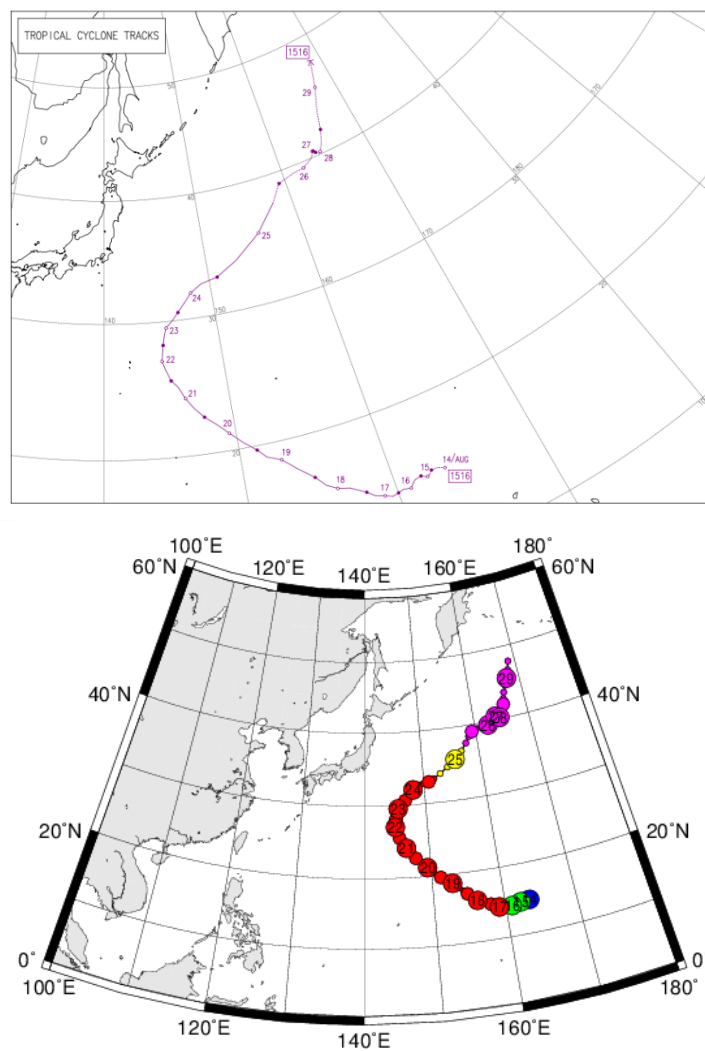
Figure 2.41 The route of Typhoon 1516 (upper: Meteorological Agency [7], lower: digital typhoon [5])
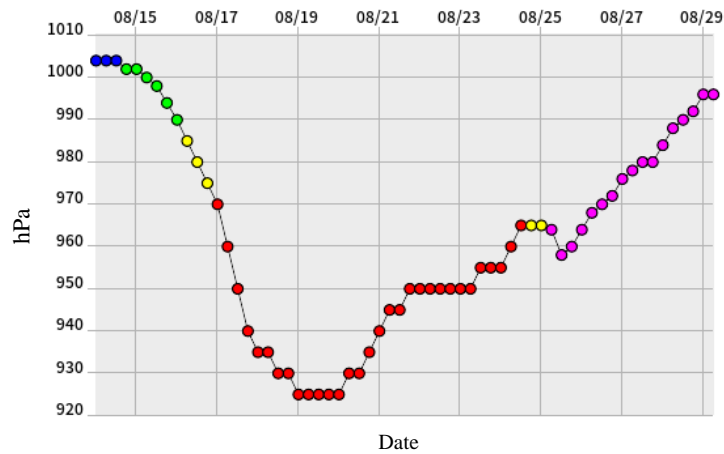
Figure 2.42 The change in central pressure of Typhoon 1516 (Digital Typhoon [5])
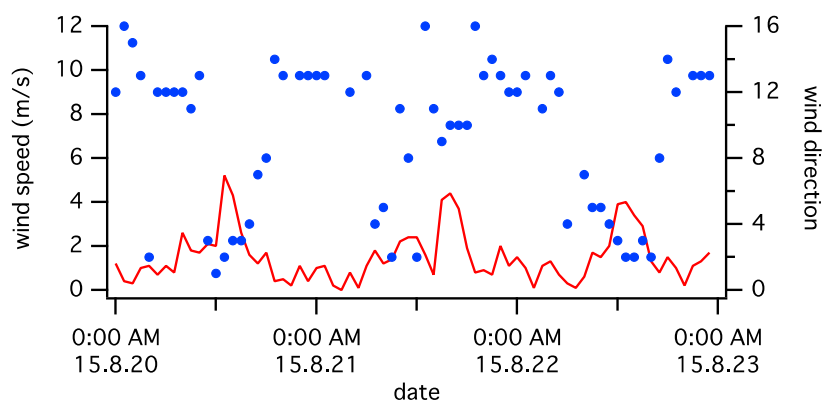
Figure 2.43 Wind conditions during the disaster in August 2015 (AMeDAS Shingu)

Figures 2.44 and 2.45 show the wave characteristics in the period of July 15-17, 2015 and August 20-23, 2015. The upper figure shows the significant wave height and the significant wave period, and the lower figure shows the wave direction. At the time of the disaster in July, significant wave height of up to about 10 m was observed, and it is thought that this wave caused the disaster. As for the wave direction, the S to the SSE direction was dominant. The dashed line in the figure indicates the wave direction angle (127 °) at which waves come at a right angle to the shoreline of Ojigahama. It can be seen that the value was much more larger (Southern) than 127° (the normal of an incident wave).

On the other hand, it is clear that the waves at the time of the disaster in August were relatively small, with a wave height of about 3.5 m, and the wave direction was dominant in the SE (135 °) direction, as the typhoon had passed far from the coast. Although details are still unknown, it is presumed that the damage in August was due to the effects of the damage in July (insufficient recovery of the beach). According to Figure 2.44, the rapid beach erosion in front of the revetment, which was caused by the disaster in July, was due to high sea waves on

the beach. It is thought that it may be because sediment runoff occurred in a short period on the beach at the southern end where there was no sediment.
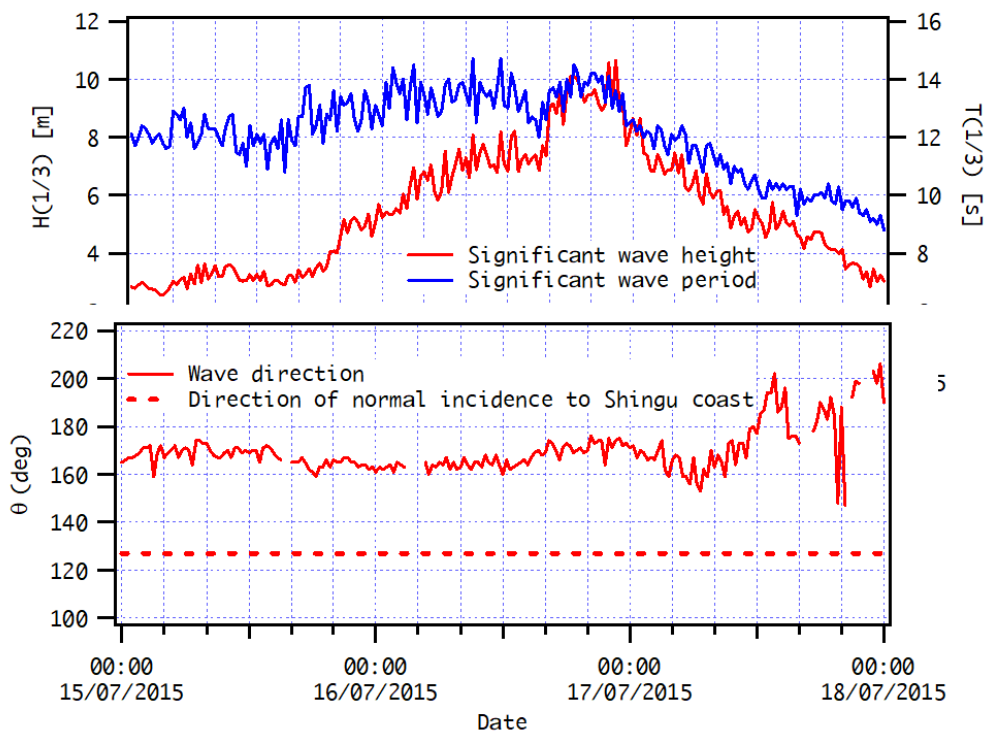
Figure 2.44 Wave characteristics at the time of disaster in 2015 (July)
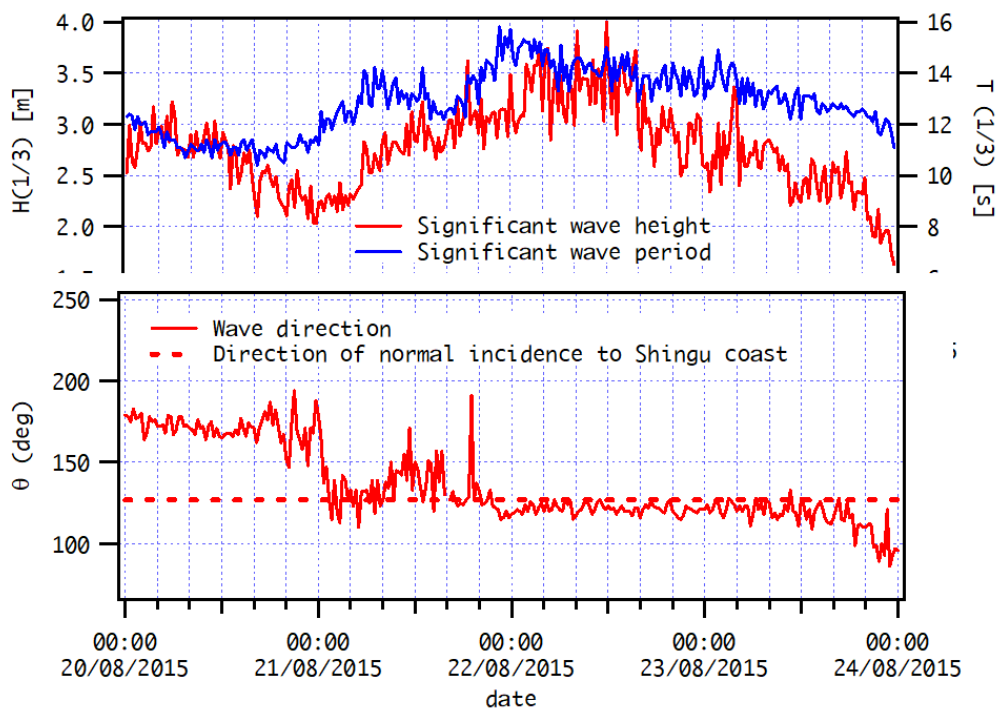
Figure 2.45 Wave characteristics at the time of disaster in 2015 (August)

2.5. Topographic Analysis in 2016

2.5.1. Topographic survey result

Figure 2.46 shows the cross-sectional topography of the 22 survey lines of Fig. 2.11. There were five implementation days: August 8th, September 24nd, October 24th, November 21st, and December 21st. The X = 0 indicates the revetment along the Ojigahama Beach. Figure 2.47 is a three-dimensional display of the topography based on the cross-sectional view of the front of the disaster revetment (line measurement No. 16-No. 22). In the figure, the ground height represents the height from the reference surface (DL). DL at Shingu is about TP-0.9m.

Survey Line No7

Survey Line No8

Survey Line No10

Survey Line No11

Survey Line No12

Survey Line No13

Survey Line No14
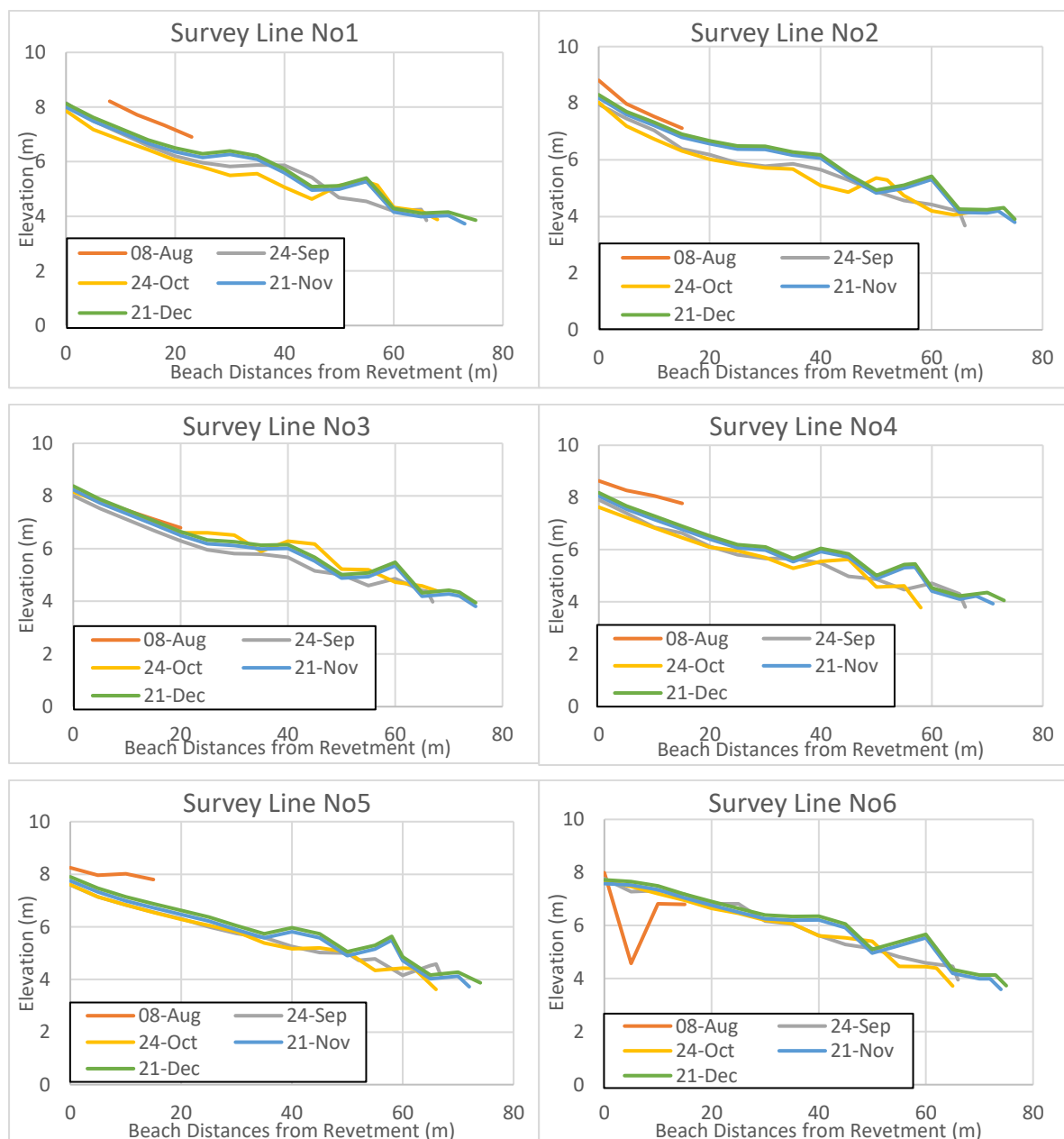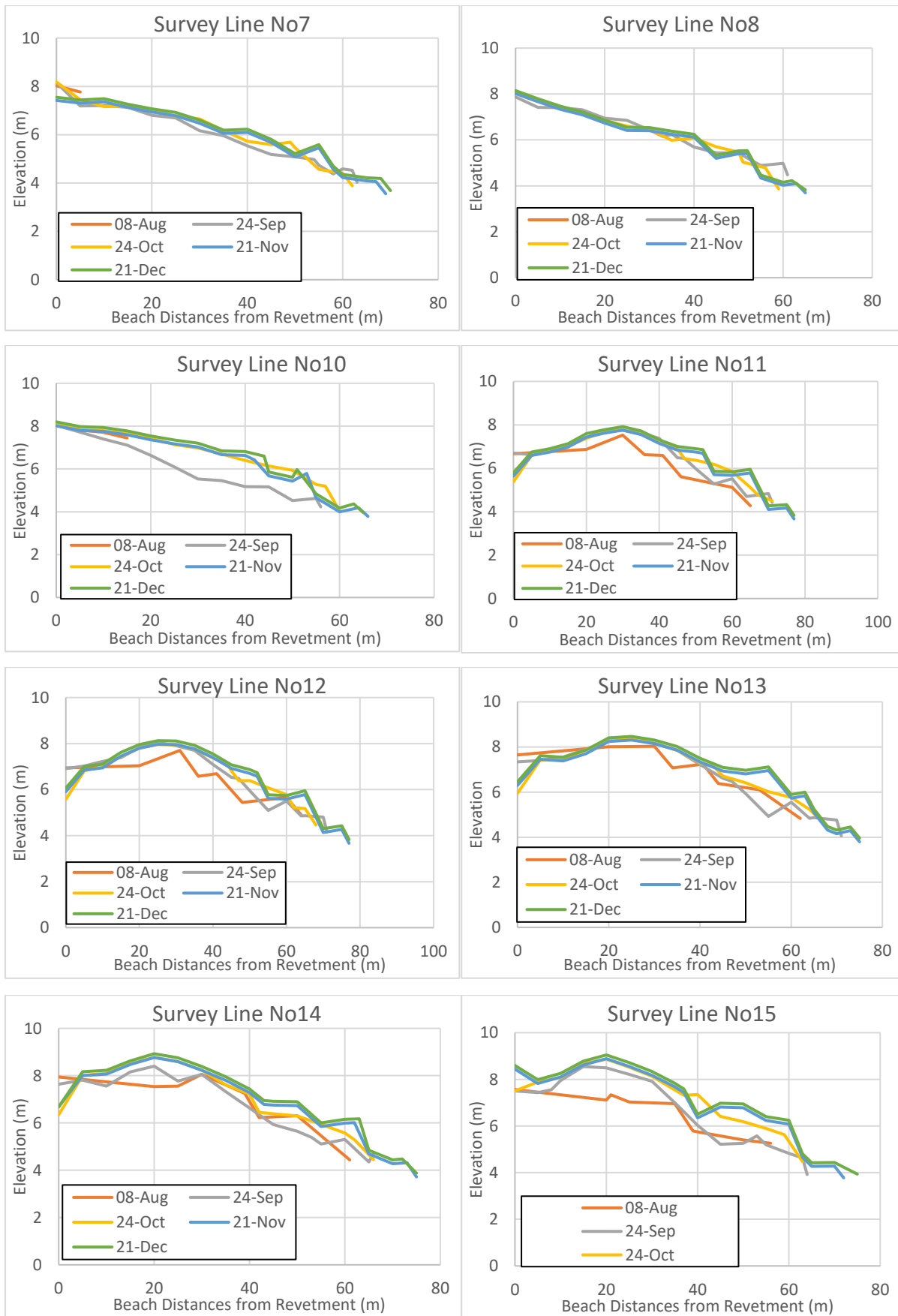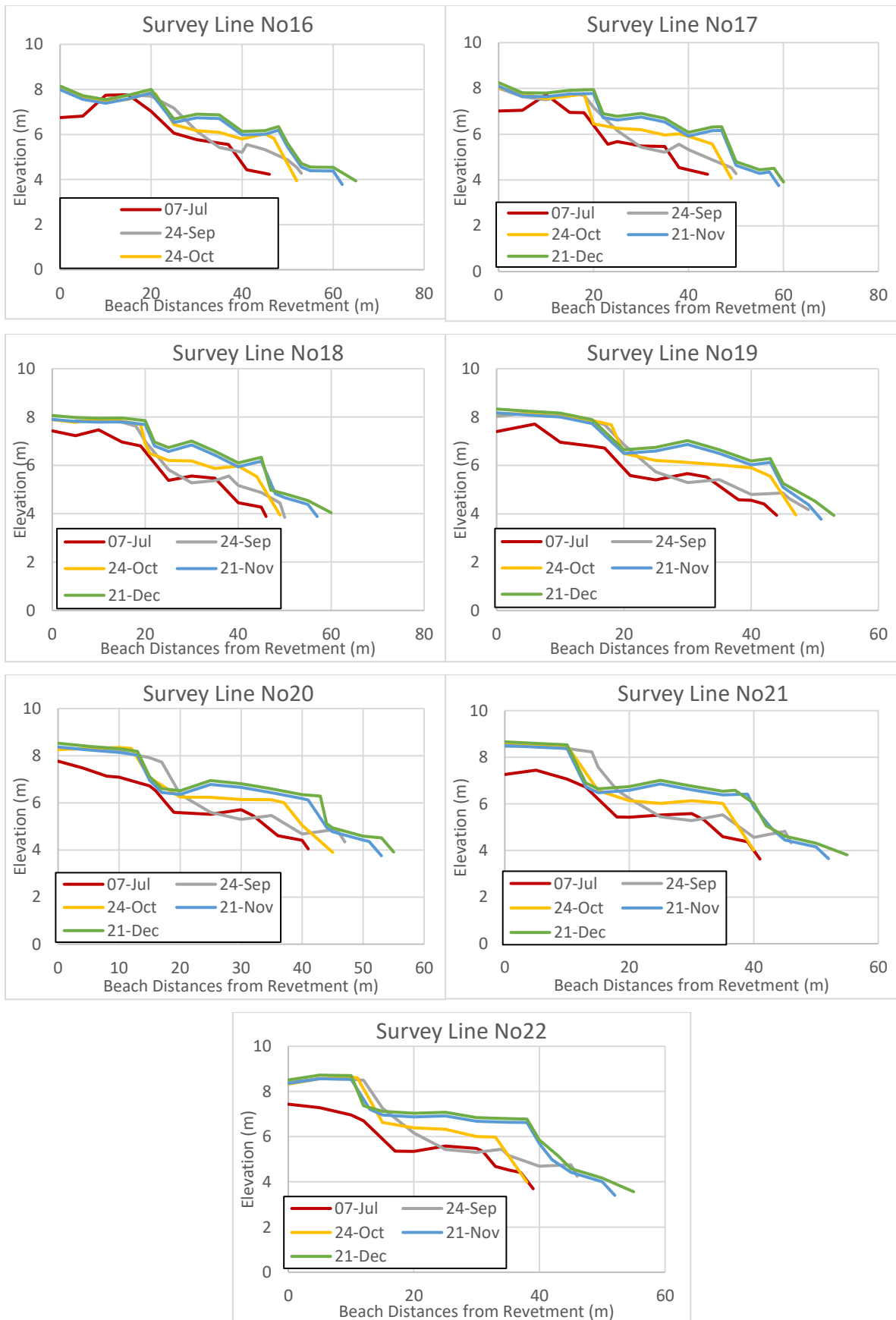
Survey Line No15

Figure 2.46 Cross section of beach topography in 2016
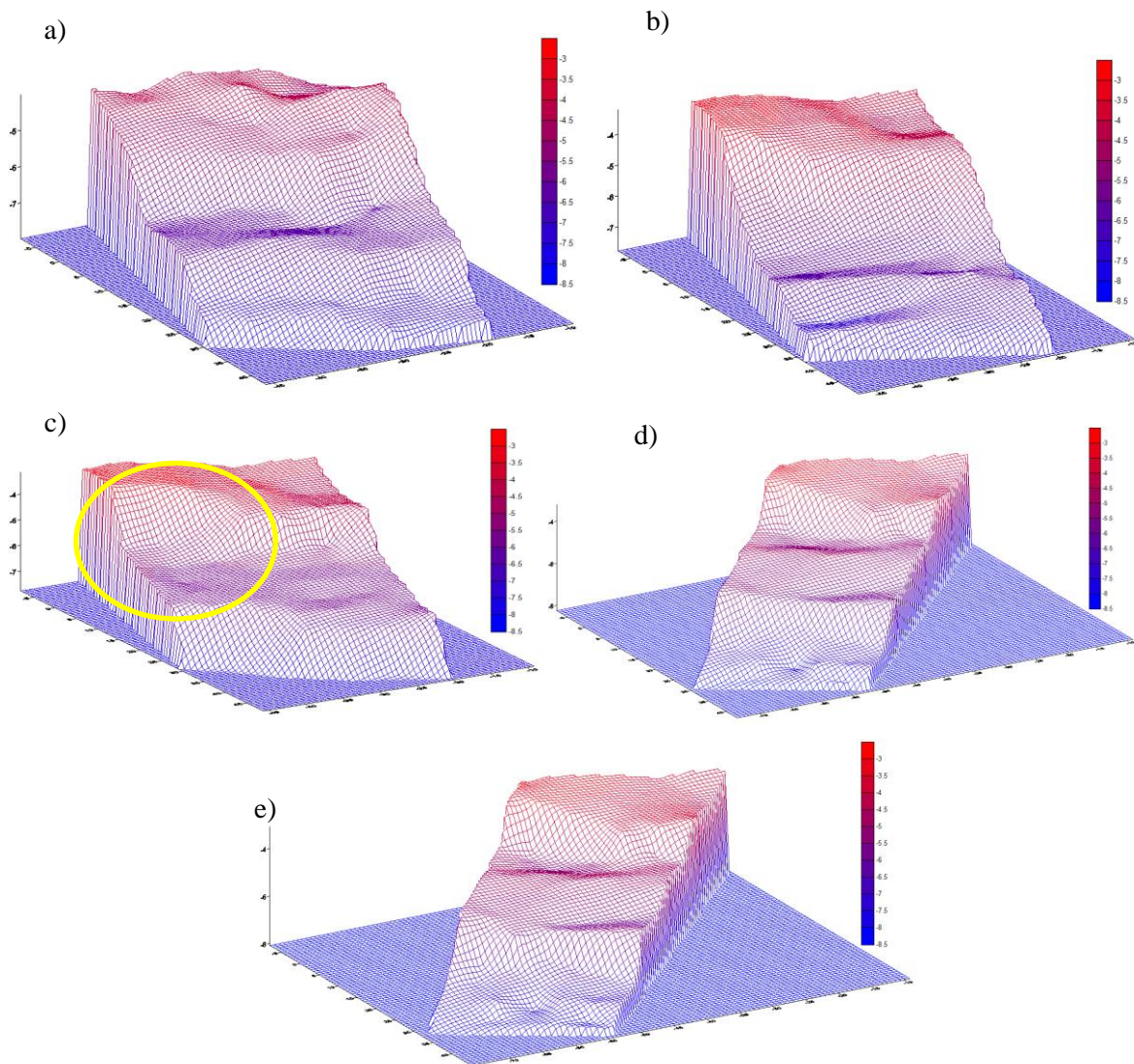
Figure 2.47 Beach topography of survey line No. 16-22 (in front of revetment) : a) July, b) September, c) October, d) November, e) December

2.5.2. Variation of topographic characteristics

The survey data in July and August were unnatural, so those data would not be used in the discussion below. Based on the survey data of September 24th, October 24th, November 21st and December 21st, the topography changes every month is compared and discussed below.

In the whole survey line, the cross sections in November and December were almost unchanged regardless of foreshore and backshore, and it is understood that the beach was stable. On the other hand, the characteristics of topography were various in particular survey lines. The beach topography had a relatively uniform beach gradient on the northern survey line from

No. 1 to No. 10, and the beach slope was about 1/18. While in No.11 to No.15, the topography was convex upward, and the slope on the seaside was as steep as about 1/10. Furthermore, the beach section at the front of the damaged revetment at the southern end from No. 16 to No. 22 had a beach gradient of about 1/10 and the beach width was narrow.

By looking at the topography in September and October, it can be seen that the beach were generally lower than in the condition in November and December. Furthermore, the shorelines were shorter compared to November and December. Especially in front of the damaged revetment, the beach width had decreased considerably in October (Fig. 2.47 c). The characteristics of the wave during September and October contributed to significant change on the topography. The wave in those months had larger wave height compared to the condition in November and December. This tendency was remarkable in the southern lines (No. 16 to No. 22) than northern lines (No.1 to No.10) which did not show significant change on topography.

2.6. Wave Analysis of 2017 (Wave characteristics based on NOWPHAS at Owase)

The comparison of wave data measured at Ojigahama and NOWPHAS wave data in 2016 above in the section (refer to Fig 2.32 to 2.35) shows that the similarity of both data was good enough, despite the wave data measurement was little smaller than NOWPHAS data. In 2017 the measurement of the wave at Ojihama Coast was not conducted, instead NOWPHAS wave data is used in this section. Furthermore, there were six periods that the significant wave height about 5 m or more were observed, which are as follow:

(1) February 23 to 24 : maximum $H_{1/3}$= 5.73 m, $T_{1/3}$= 9.6 s, 187 degrees (2/23, 9:00)

(2) April 10 to12   : maximum $H_{1/3}$= 5.59 m, $T_{1/3}$ = 9.3 s, 128 degrees (4/11, 14: 20)

(3) June 21 to 22   : maximum $H_{1/3}$= 5.23 m, $T_{1/3}$= 9.2 s, - (6/21, 10: 20)

(4) August 7 to 8   : maximum $H_{1/3}$= 4.98 m, $T_{1/3}$= 8.6 s, 177 degrees (8/7, 16: 40)

(5) September 16 to 18: maximum $H_{1/3}$= 5.91 m, $T_{1/3}$= 8.6s, - (9/17, 23: 20)

(6) October 22 to 23: maximum $H_{1/3}$= 10.44 m, $T_{1/3}$= 15.4 s, 175 degrees (10 /23, 0:00)

Among the high wave period above, the case like the disaster in July 2015 occurred in the October period (6) as shown in Figure 2.48, with the significant wave height of 10 m or more and long period wave coming from SSE to S direction were observed. However, the wave height of 7 m or more came about 6 hours from October 22nd 21:00 to 23rd 3:00, which was shorter than at the time of the disaster (22 hours). Figure 2.49 shows the changes in the path

and central pressure of the typhoon in 2017 that produced the high waves [5]. Typhoon 1721 in October was a strong typhoon that passed through the southern area of the Kii Peninsula. Nevertheless, it was clear that the period of high waves observed was short because the moving speed in the sea near Japan was very large.
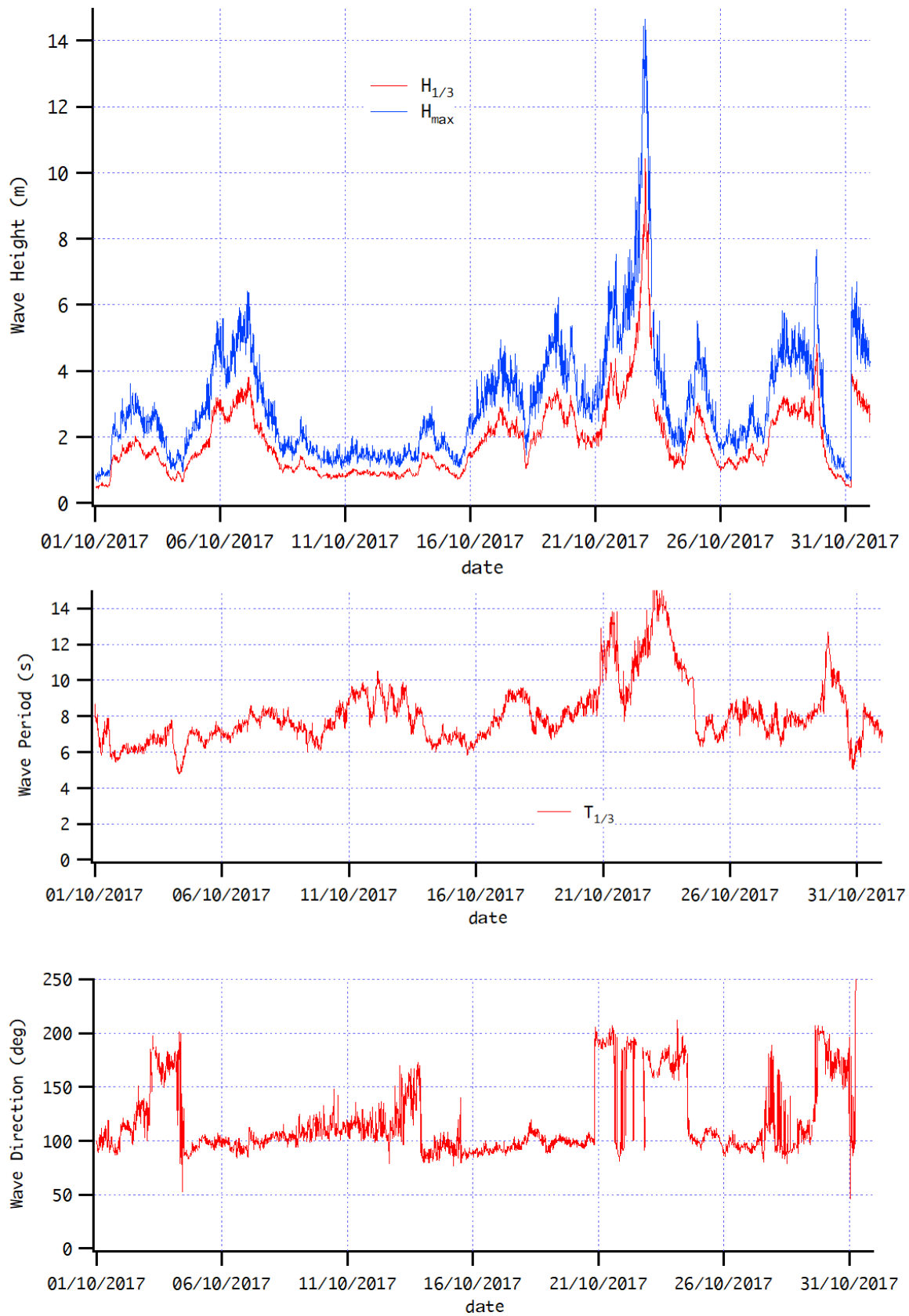
Figure 2.48 Wave characteristics of October 2017

No. Typhoon 1705

No. Typhoon1718

No. Typhoon1721

Figure 2.49 Typhoon route and changes in central pressure [5] (July-October 2017)

2.7. Topographic Analysis 2017

The survey of the beach topography was conducted on the same 22 lines as 2016. There were five implementation days: July 20th, August 22nd, September 25th, October 28th, and January 30th. The position of the survey section is shown in Figure 2.11. From the Figure 2.50

the topography in July, August, and September sections were almost overlapped from the survey line 1 to 10, even with 5 m wave height, the topography change did not occur notably. On the other hand, compared to survey lines 1 to 10, survey line 11 to 22 showed relatively significant topography change, and it can be seen that a large berm was formed especially near the dune.

Focusing on the topography of October 28, one week after receiving the high waves in October, the shoreline side had receded by about 20 m to 30 m from survey line 1 to 10. The shoreline retreat was a little small up to about 20 m up on the survey line 11 to 22, and no significant topography change was found near the revetment. Moreover, in survey line 15-22, although the shoreline was receding, the cross-sectional beach area was increasing as a result of a deposit of gravel on the back side of the beach part.

From the above discussion, it could be deduced that even in waves of about 10 m, if the duration of the high waves is short, erosion near the shoreline will not reach the revetment, and the risk of damage to the revetment will be small. According to the survey results of January 30 which is the topography during the winter season, the topography near the shoreline was restored, and the cross-sectional of the beach area was more extensive than that in July.

Survey Line No5

Survey Line No6

Survey Line No7

Survey Line No8

Survey Line No9

Survey Line No10

Survey Line No11

Survey Line No12

Survey Line No13

Survey Line No14

Survey Line No15

Survey Line No15

Survey Line No16

Survey Line No17

Survey Line No18

Survey Line No19
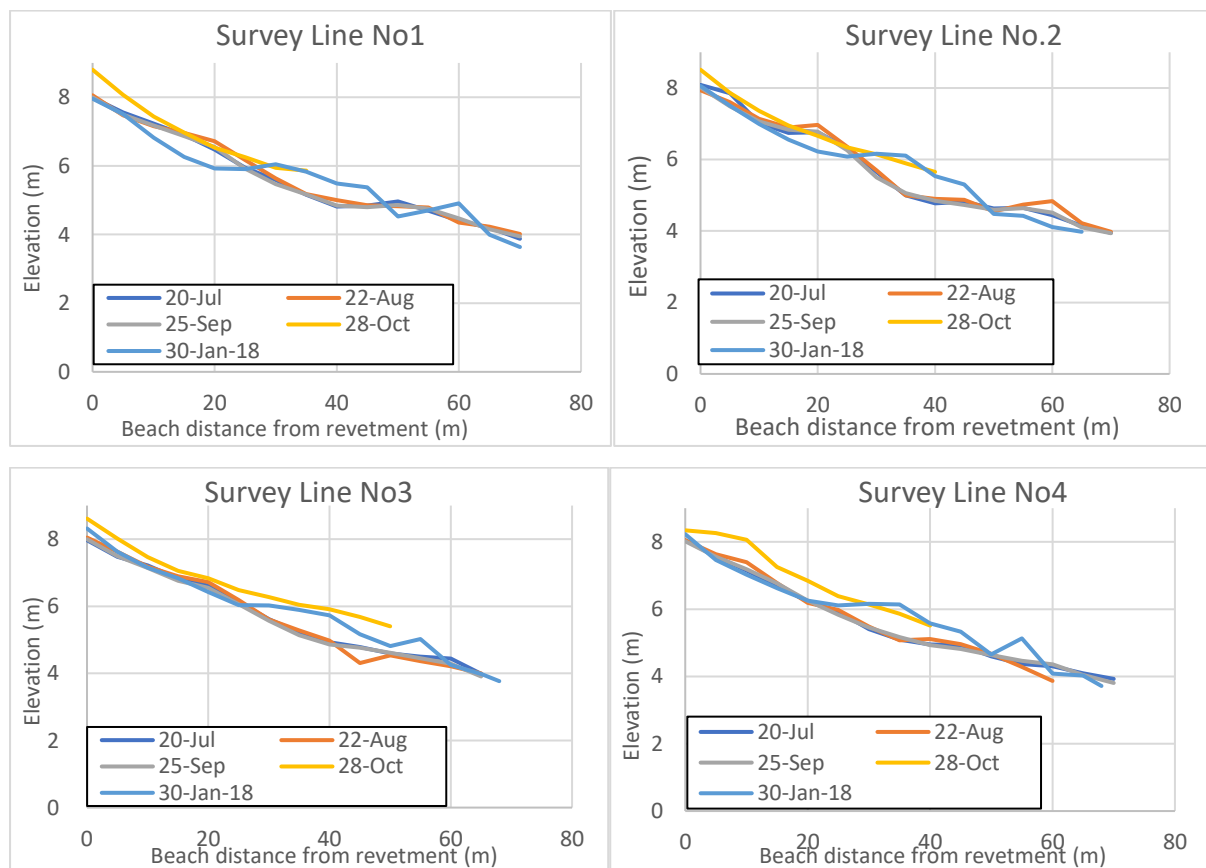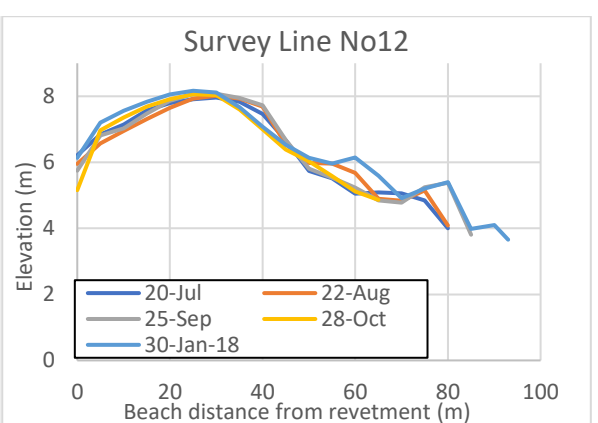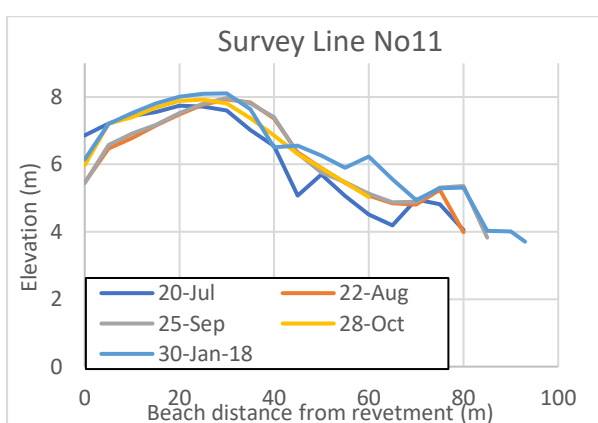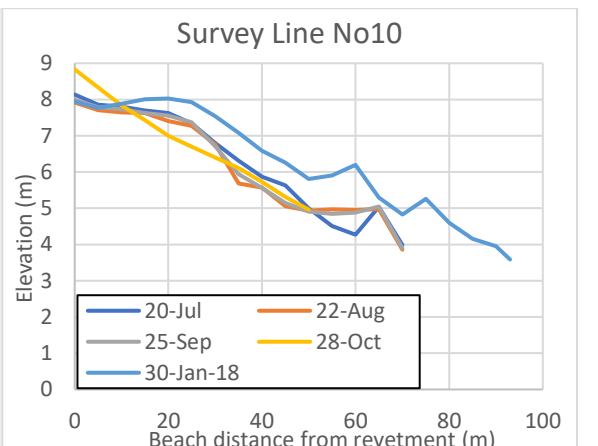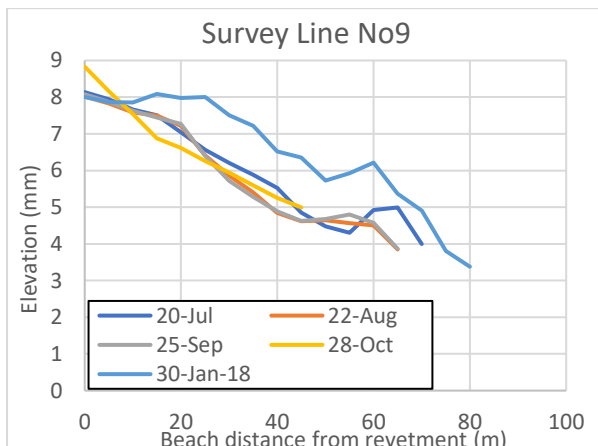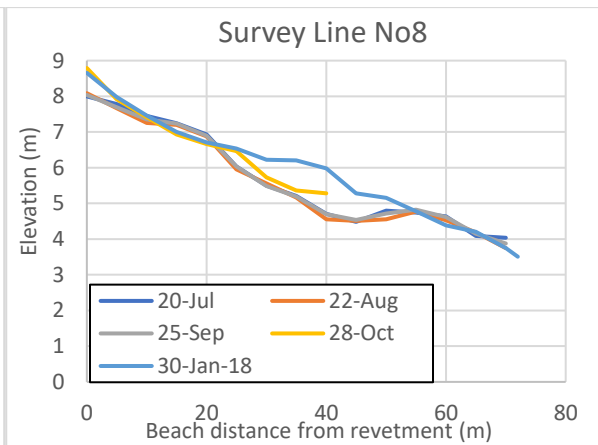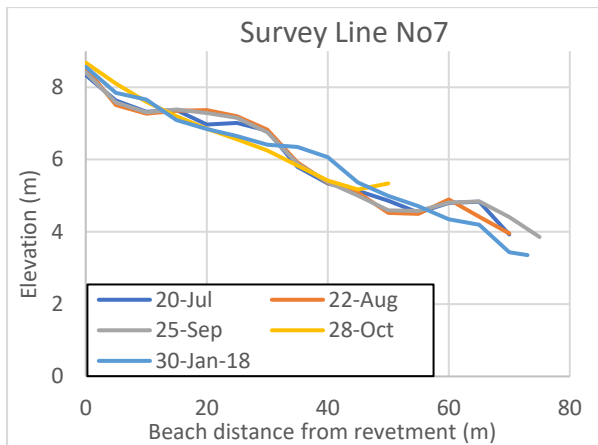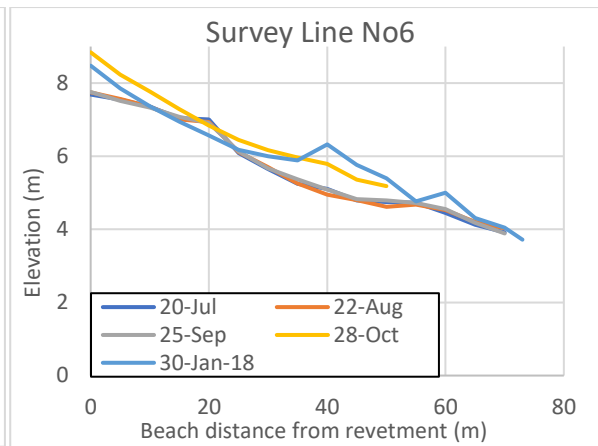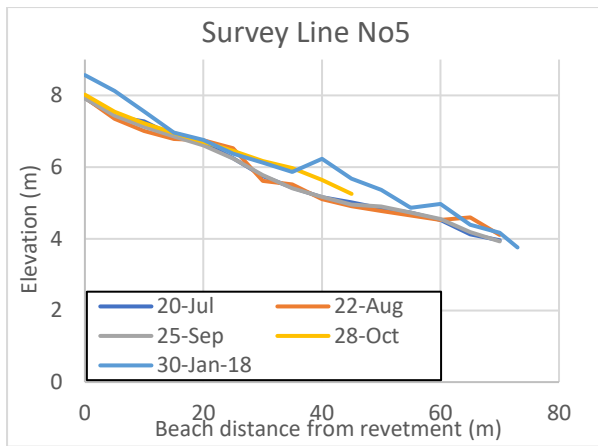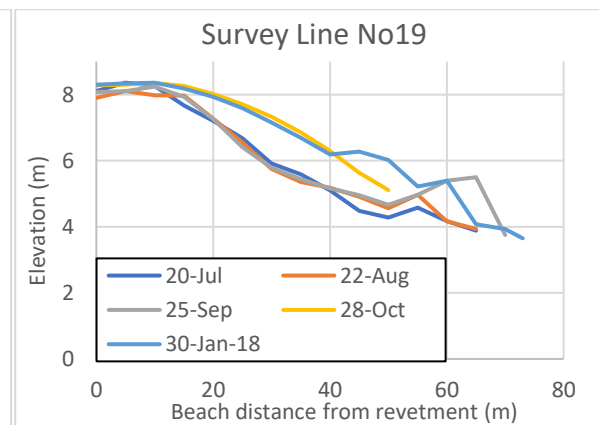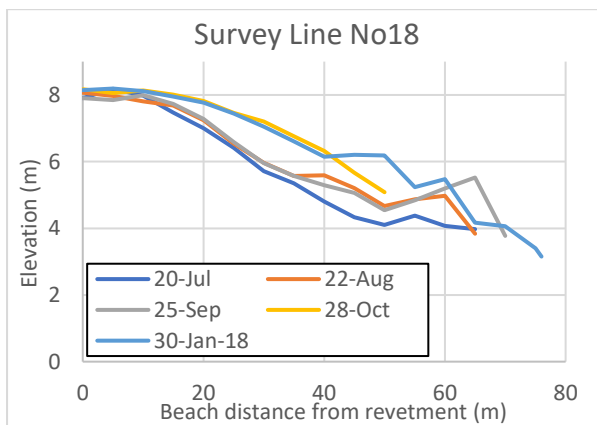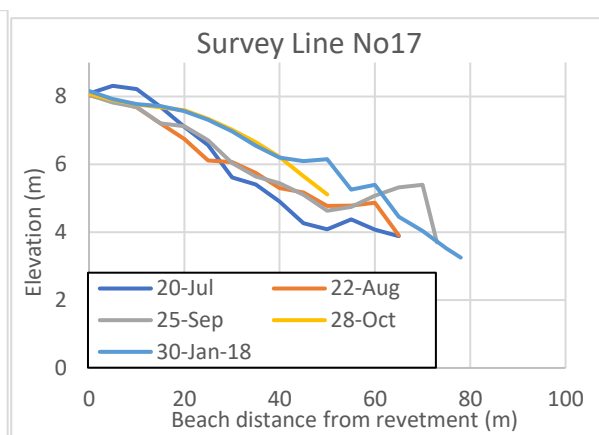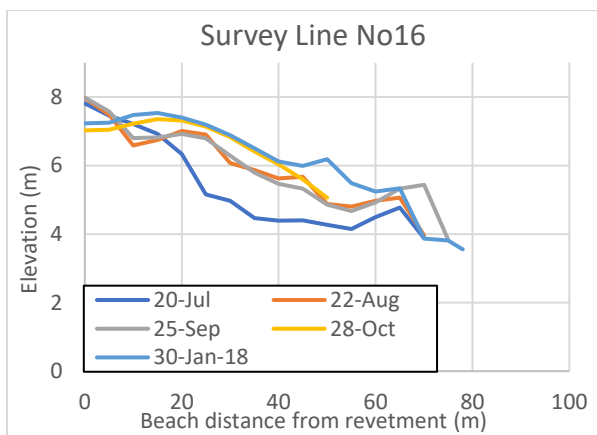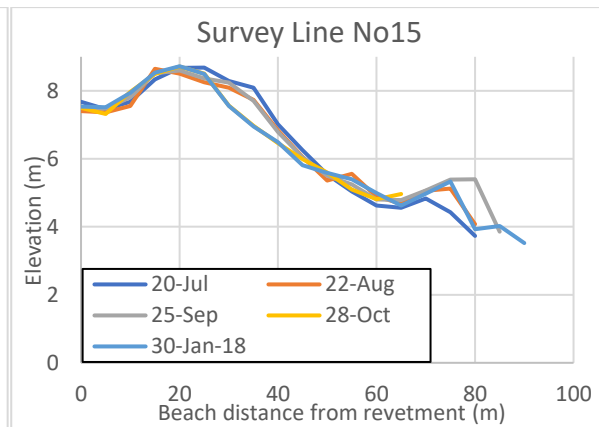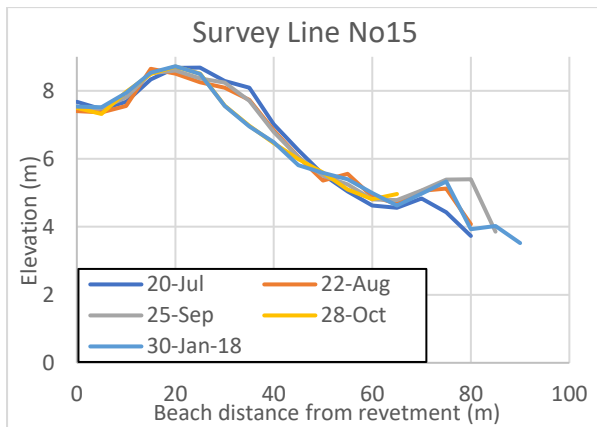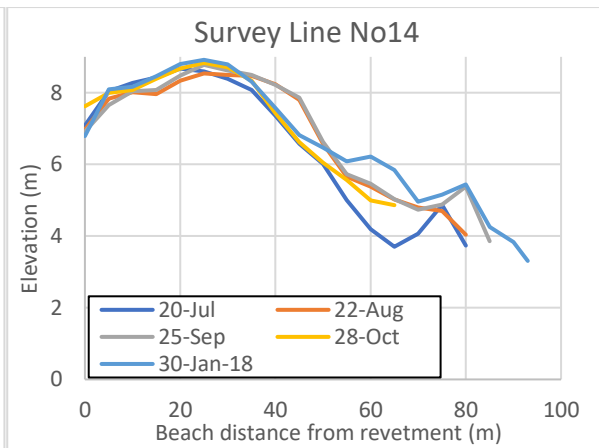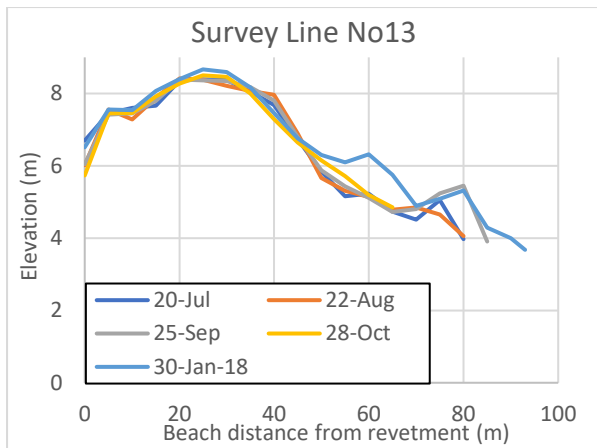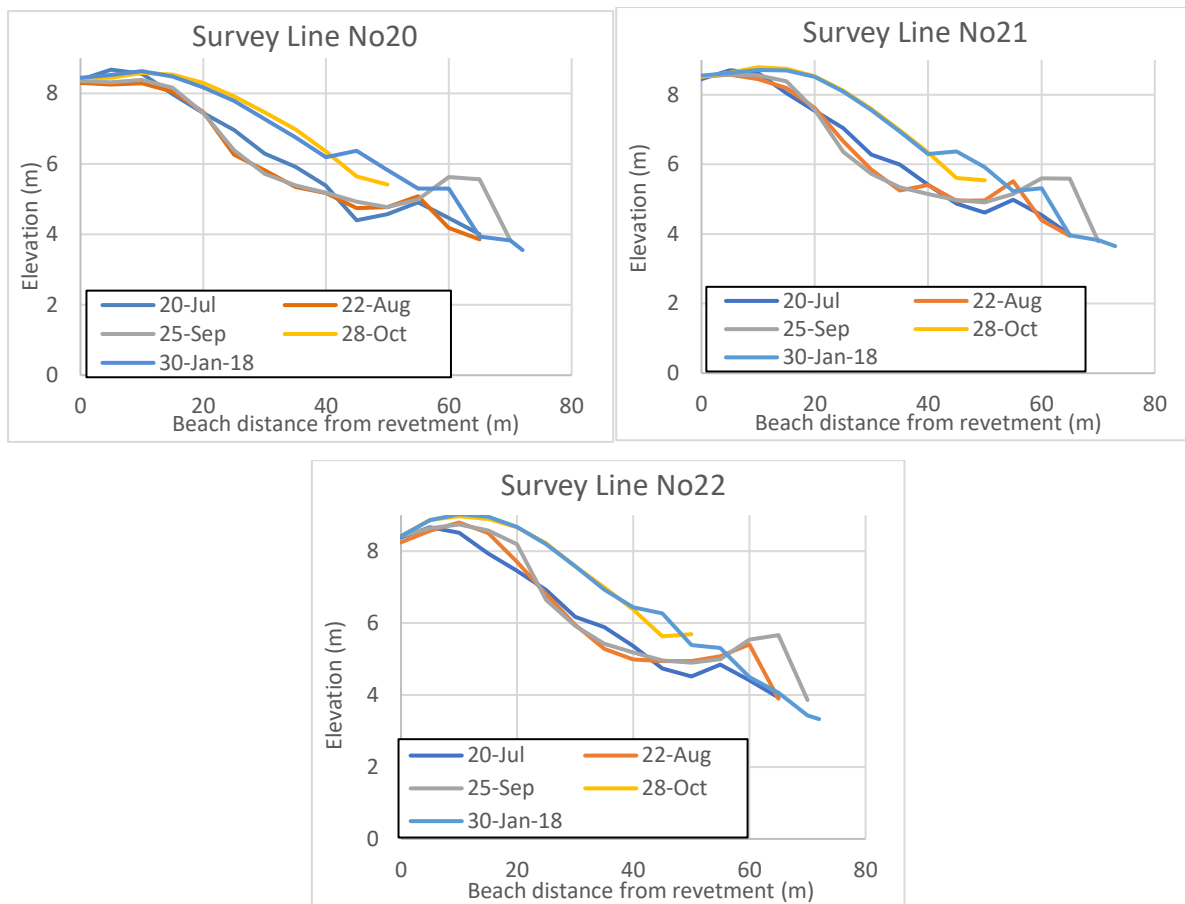
Figure 2.50 Cross section of beach topography in 2017

2.8. Wave Condition in 2018 (Wave characteristics based on NOWPHAS)

There were four incidents that significant wave height of 5 m or more was observed during this year, in which three of them over 10 m. The details period of occurrences as follow:

1) March 21st to 22nd : maximum $H_{1/3}$ = 6.45 m, $T_{1/3}$= 10.7 s, 92 degrees (10:20 pm)

2) August 23rd to 24th : maximum $H_{1/3}$ = 10.8 m, $T_{1/3}$= 13.7 s, 168 degrees (9.20 pm)

3) September 4th   : maximum $H_{1/3}$ = 11.09 m, $T_{1/3}$= 14 s, - degrees (3.40 pm)

4) Sept. 30th to Oct. 1st: maximum $H_{1/3}$ = 10.31 m, $T_{1/3}$= 13.1 s, 198 degrees (9.40 pm)

It was recorded that there were three periods of extreme wave (over than 10 m) which passed through the Osaka Bay with different wave duration, as shown in Fig. 2.51 to 2.53. The maximum significant wave height occurred on September 4th with 11.09 m, 17 s of wave period and 11.5 hours of the wave height over 5 m (see Fig. 2.52). However, the most prolonged duration of the wave over than 5 m occurred in August 23rd to 24th with 22 hours of wave duration. Moreover, it was longer than the case of October 2017 (refer to Fig. 2.48), which had wave height about 10.3 m, 13 s of wave period and 12 hours of the wave over than 5 m. Despite

it had been the longest wave duration for the wave height over than 5 m in past three years, the condition in August did not cause any severe damage like disaster in July 2015, in which the wave at the time of disaster had 32 hours wave duration for the wave over than 5 m (refer to Fig. 2.44).

Figure 2.54 shows the route of the typhoons and the change in the central pressure of the typhoons in 2018. The summer-autumn season in 2018 seems to become the beginning of bad moment to Japanese Coast, where within the period the strong typhoons passed through Japan. Moreover, it was recorded that ten typhoons passed near mainland Japan in 2018, and three of them generated the extreme wave over than 10 m within the period of August to September. The three of the typhoons also made landfall at mainland in Japan. The duration of the typhoons was different between three of them. The Typhoon 1820 and Typhoon 1821 had duration for 6 days and 8 days 6 hours respectively. Those typhoons were sourced at the same location in Ocean Pacific.

Moreover, the trajectory of the typhoons was almost similar between those typhoons, which passed through Osaka Bay. While Typhoon 1824 had the longest duration over the other, which was 9 days 18 hours. The typhoon passed through Osaka Bay and Ise Bay. Furthermore, the typhoon mainly crossed the main lands of Japan.
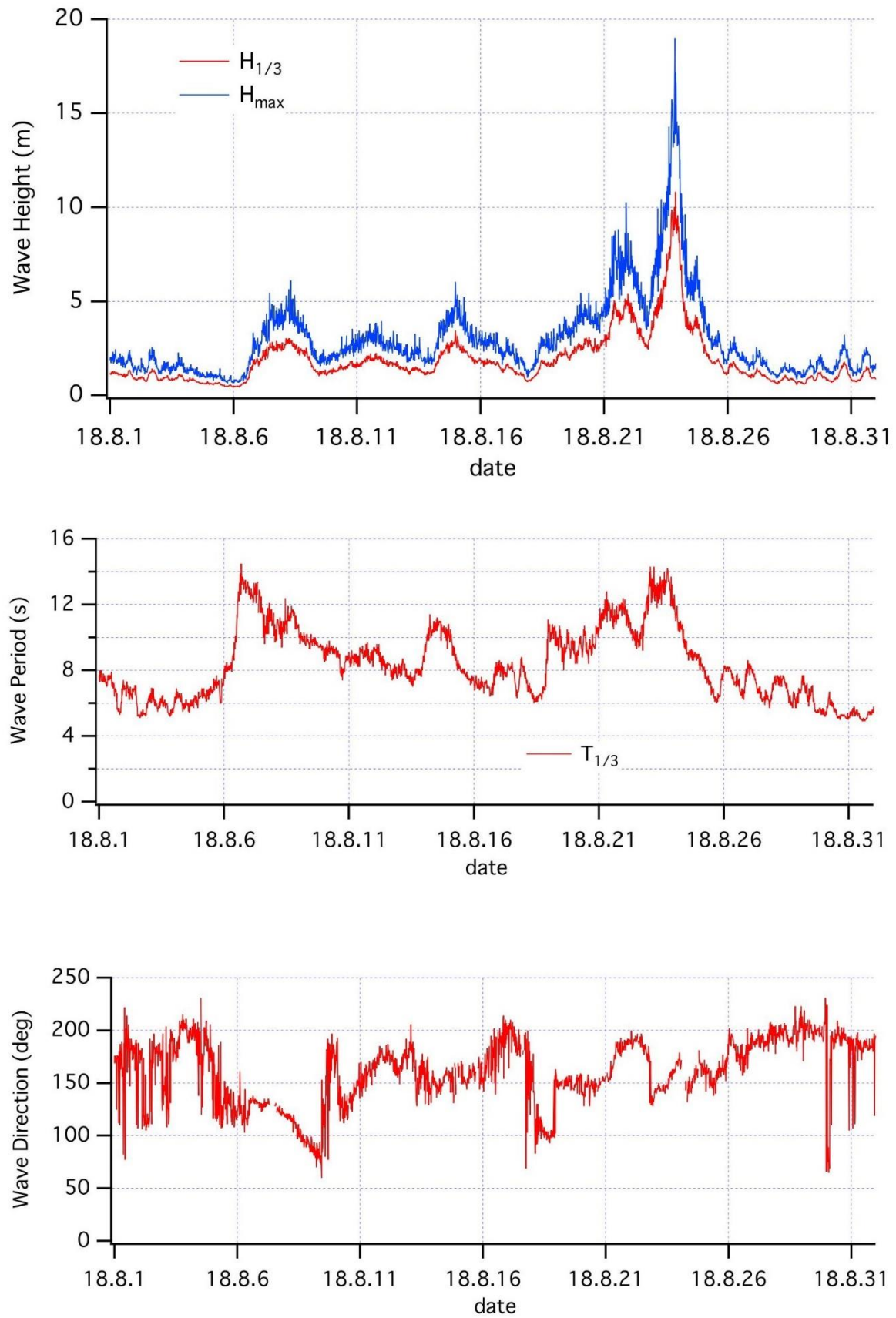
Figure 2.51 Wave characteristics of August 2018
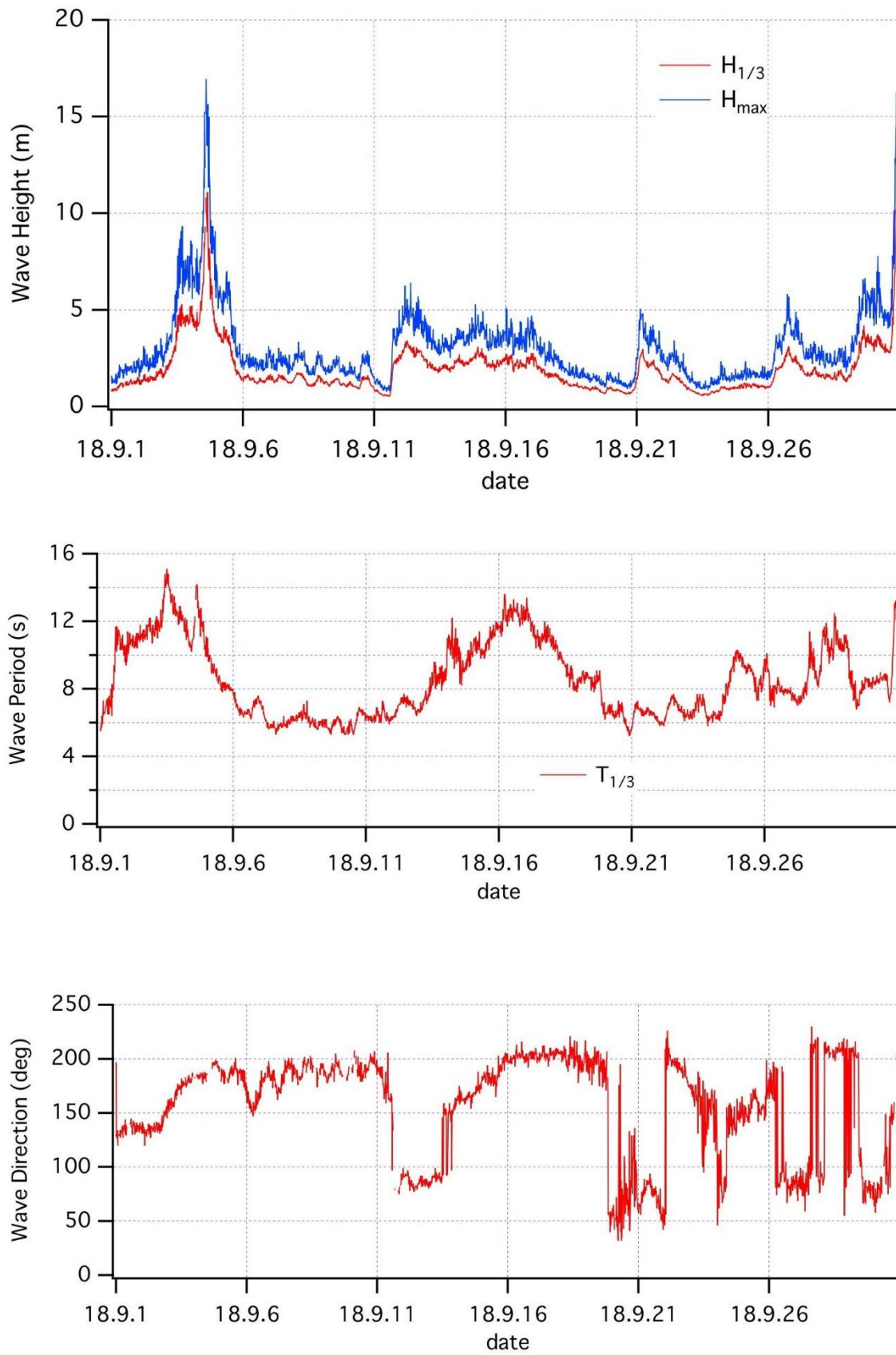
Figure 2.52 Wave characteristics of September 2018
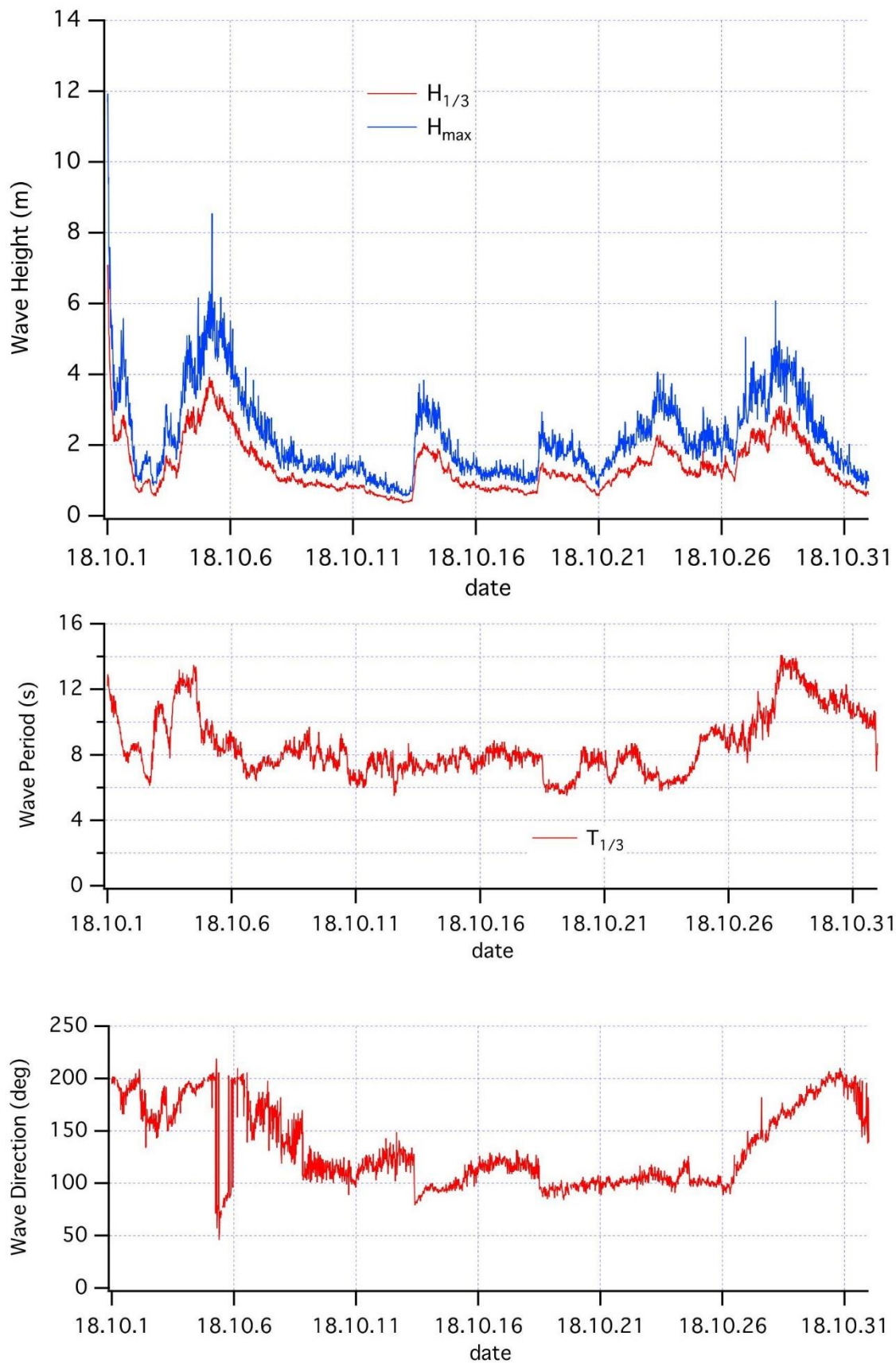
Figure 2.53 Wave characteristics of October 2018

No. Typhoon 1820

No. Typhoon 1821

No. Typhoon 1824

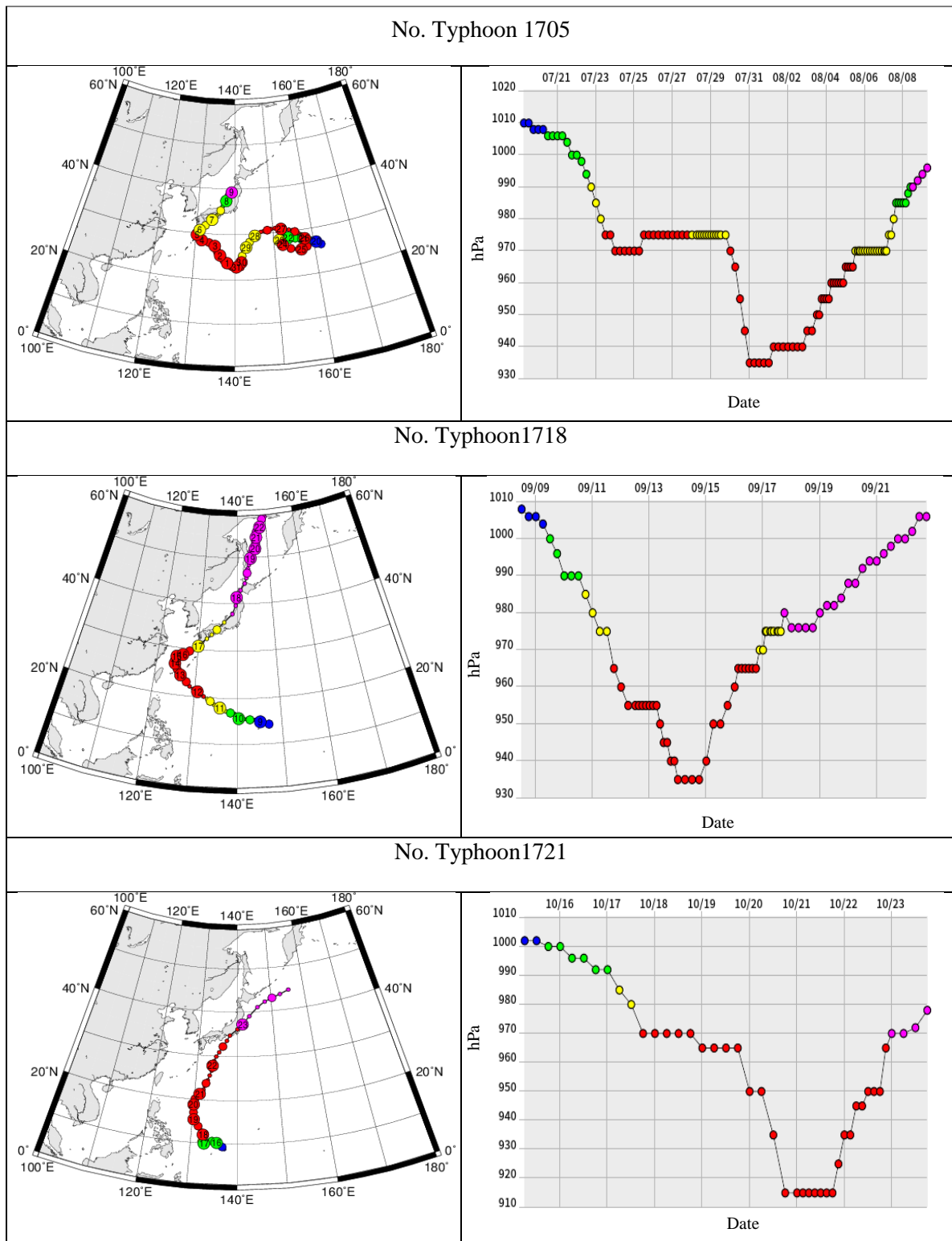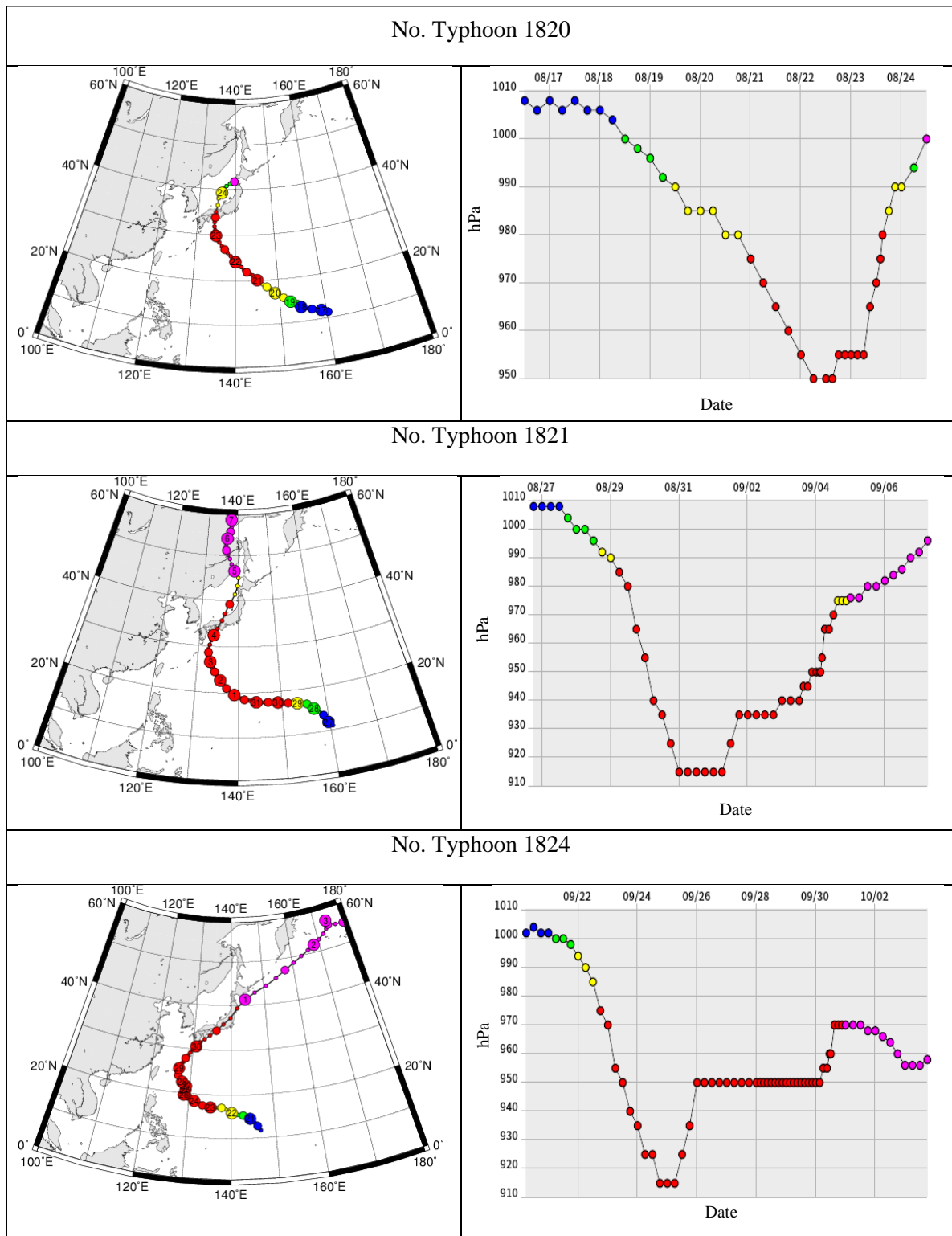Figure 2.54 Typhoon route and changes in central pressure [5] (August-October 2018)

2.9. Topographic Analysis in 2018

The setup of the topographic survey was similar to the previous survey (see. section 2.5.1 or 2.7.1). However, the topographic survey in this year was implemented into four days: July 30th, August 27th, September 7th, and October 31st. These periods were selected correspond to

the event of the extreme wave during the summer-autumn season. Moreover, from these periods, the topographic changes before and after the extreme wave could be observed. The extreme wave remained the impact to Ojigahama Coast. Despite there was no severe damage to the revetment along the coast, the topography was changed significantly due to the extreme waves.

Figure 2.55 describes the topographic change from July, August, September, and October in every section of the survey line. From the survey, line No.1 to No. 8 the topography changed slightly, especially near the shoreline — the elevation of the profiles decreasing by the time of the survey. The impact of the extreme waves on beach topographic in those lines was not significant. On the contrary, the critical change was observed from line No.9 to No.22. Especially in the line No. 9, the impact of extreme waves of the August 23rd and September 4th still did not cause significant change on the profile until right after the extreme wave in September 30th, the shoreline profile retreated 30 m from last profile condition.

The impact of the extreme wave of the August 23rd was seen obviously from line No.10 to No 22. A considerable amount of berm formation had disappeared from the beach, and it was remaining unknown where the gravel berm was transported. As the effect of the disappearance of gravel berm (huge erosion), the shoreline retreated, and the slope became steeper. Average shoreline retreat along the line of 10 to 22 was 25 m. While the impact of the extreme wave on September 4th also affected to the beach topographic in line No.10 to 22. Although the impact was not severe as the impact on August 23rd, however, the shoreline keeps receding and profile elevation lower than prior condition. The average shoreline receded in line 10 to 20 was about 12 m.

A prominent change was seen in the southern end of the beach (line No.19 to 22). The shoreline receded about 45 m after two times the extreme waves (August 23rd and September 4th) hit the coast. Since then, the width of the beach became short; it reached only about 25 m from the revetment. This condition became worse when the last extreme wave (September 30th) in this year hit the coast. The shoreline continues to retreat for most of the lines, except in the southern end of the beach which was found to be very small compared to the impact of the prior extreme wave. Since the beach width remained only 25 m from the revetment to shoreline, a short-term action must be done to encounter the issue in the southern side of the beach; otherwise, the shoreline will be gone if at least extreme wave like August 23rd attack this side again. For long-term action is also vital to be solved, considering the typhoon is a yearly issue that will always arise.

Survey Line No.1

Survey Line No.2

Survey Line No.3

Survey Line No.4

Survey Line No.5

Survey Line No.6

Survey Line No.7

Survey Line No.8

Survey Line No.9

Survey Line No.10

Survey Line No.11

Survey Line No.12

Survey Line No.13

Survey Line No.14

Survey Line No.15

Survey Line No.16
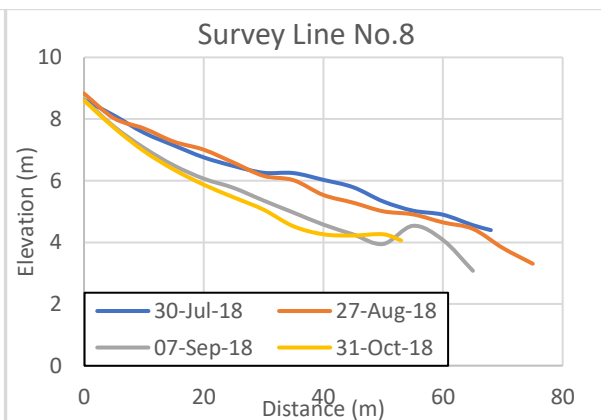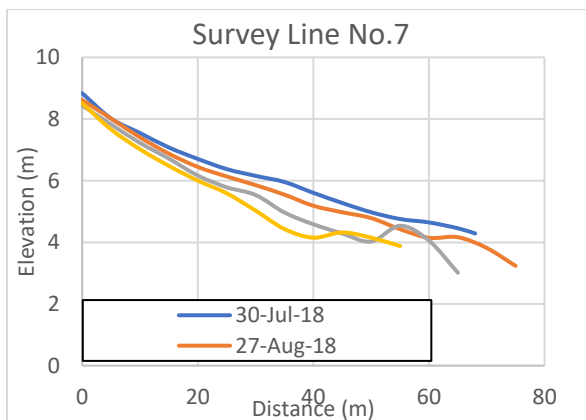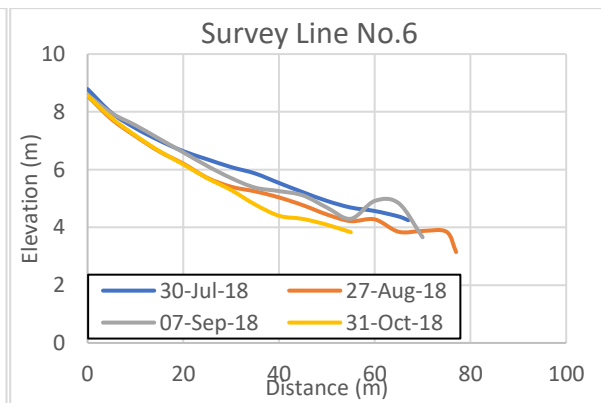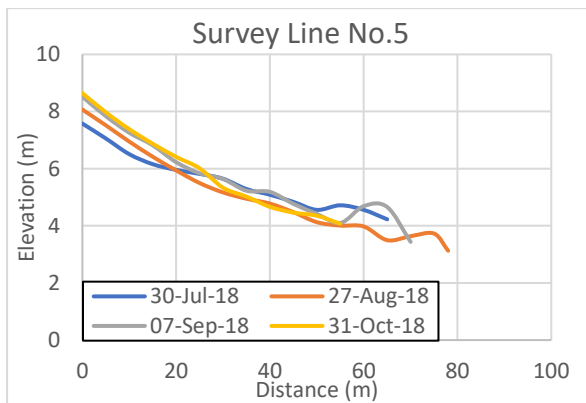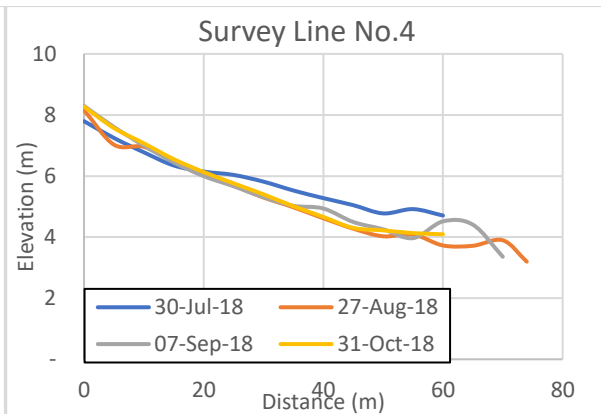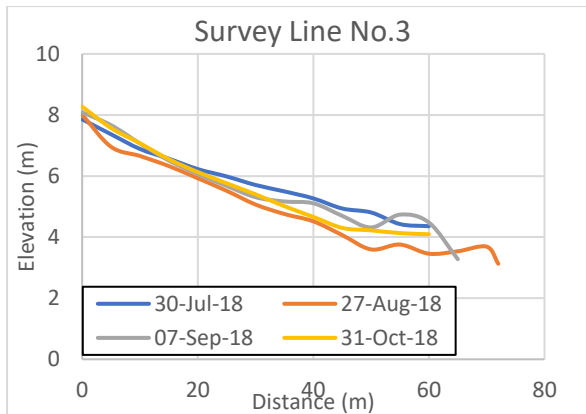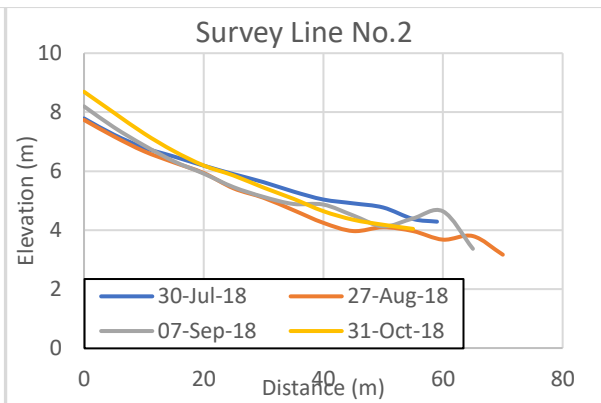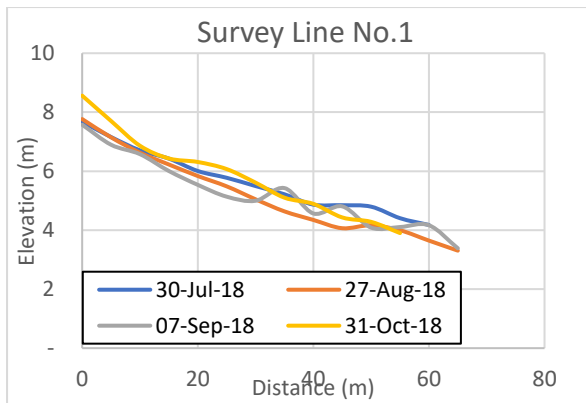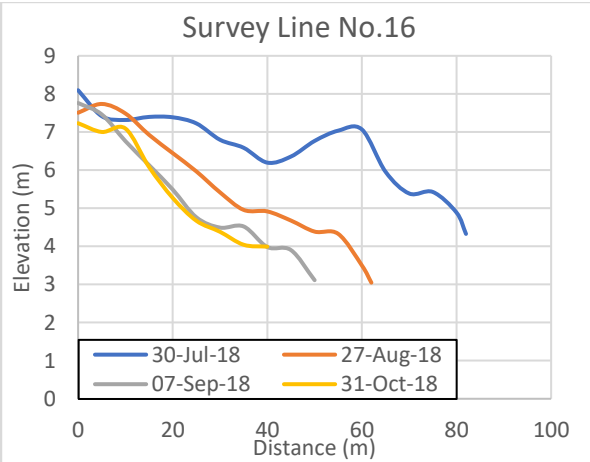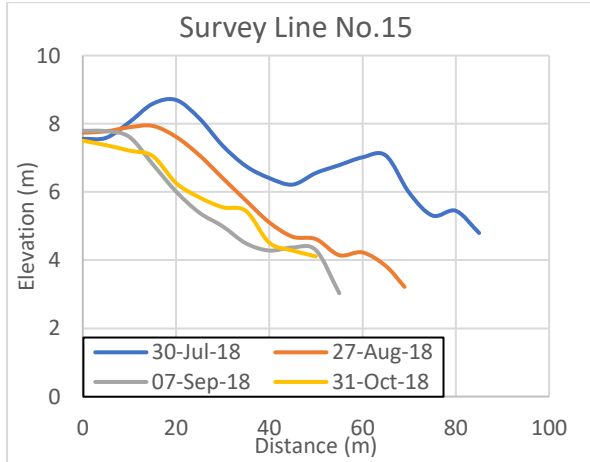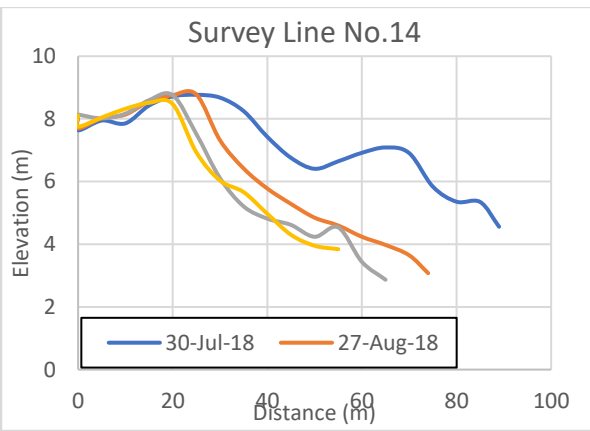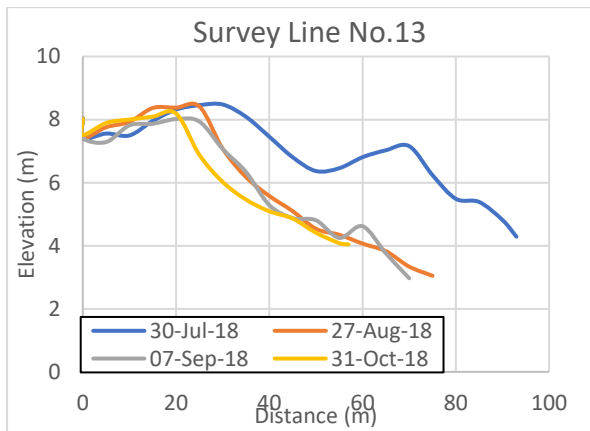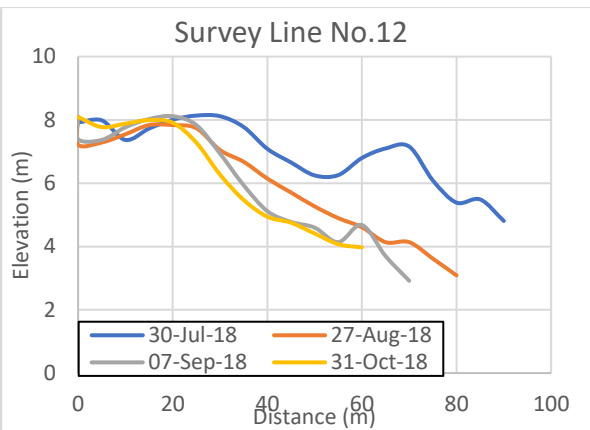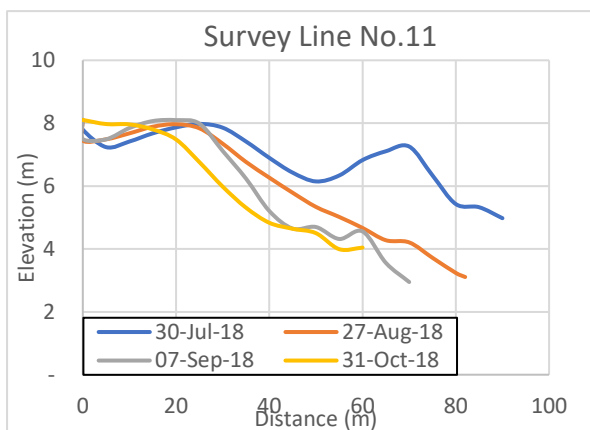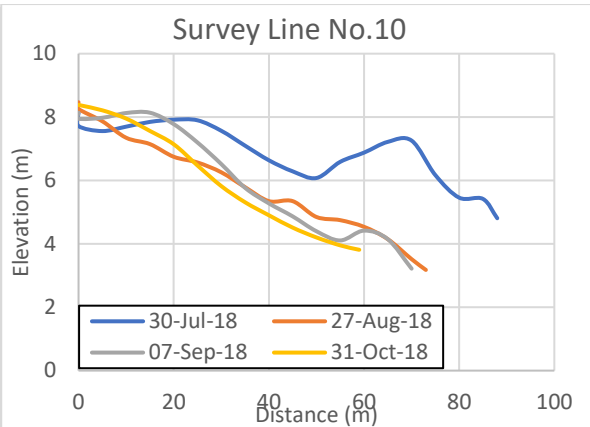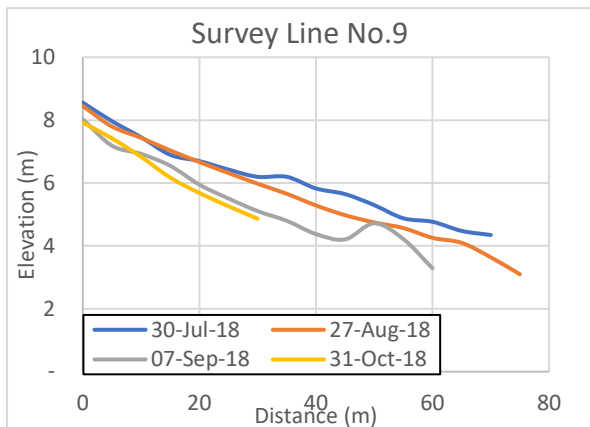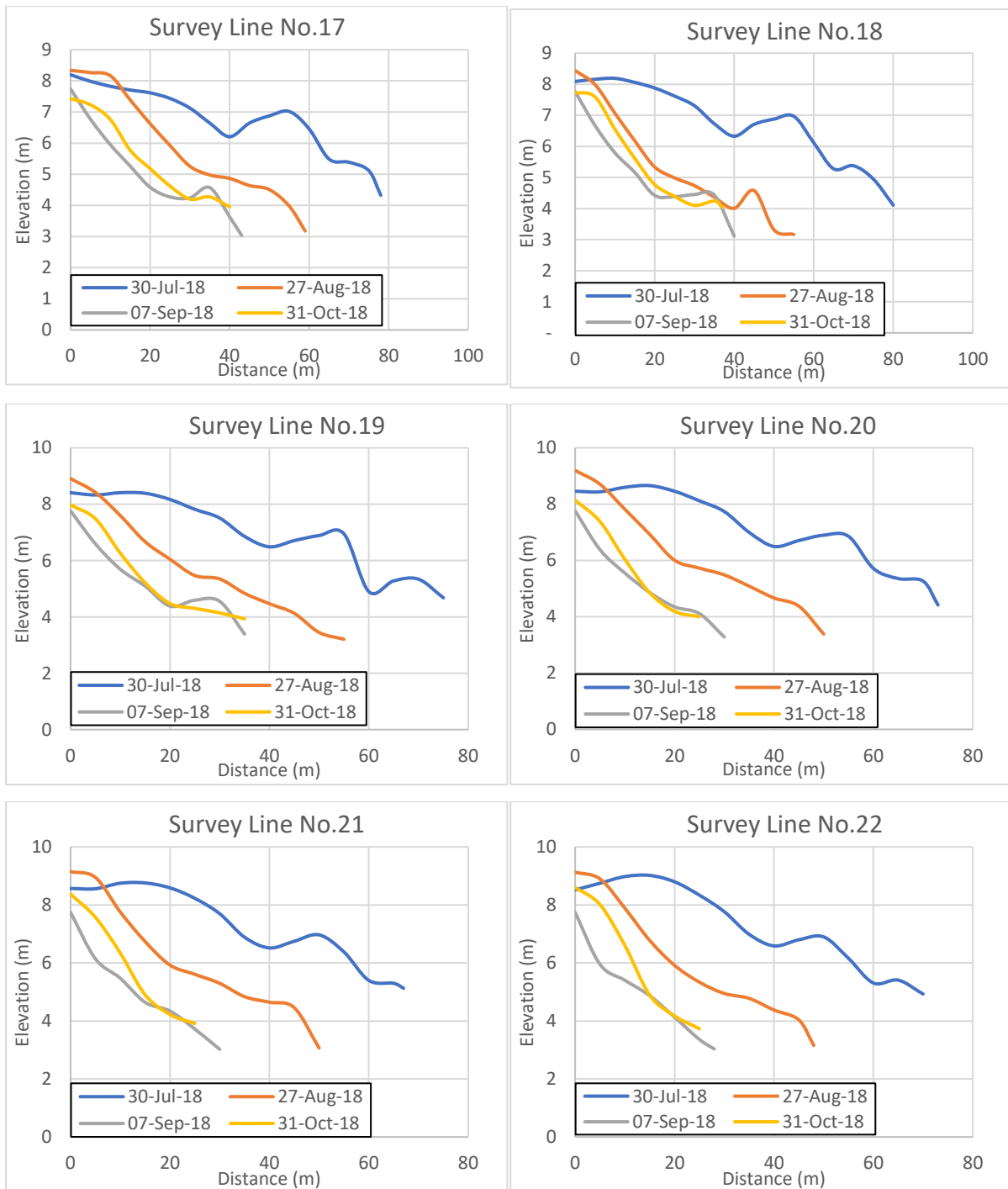
Figure 2.55 Cross section of beach topography in 2018

2.10. Conclusions

Based on the result of field study that had been done since 2016 to 2018 in Ojigahama Coast, there are several important points that need to be highlighted to understand the characteristic of the beach and the wave itself. Thereby, the following conclusions are separated according to the year of measurement, as follows:

<u>Wave Condition</u>

1. The condition of waves that attack Ojigahama from summer to autumn fluctuates due to the influence of typhoons that strike Japan nearer than local winds. The wave direction is often southerly to the direction perpendicular to the shoreline. In 2016, there is no approach of a large typhoon, so no high waves or storm surges that caused significant beach deformation are observed.

2. As a result of comparing with the Owase data, the wave height from Owase corresponds to the wave height from direct measurement, although the fluctuation was a little smaller. As for the wave direction, the fluctuation data of Owase is larger than a direct measurement. It is understandable because the Owase station is located offshore, but at Ojigahama located in the shallow water area, the fluctuation gap between those both data in term of of the wave direction is large due to the effect of refraction.

3. During October 2017, over 5 m to 10 m significant wave height, which is similar to disaster in July 2015 is observed. Duration of the wave is 10-12 hours which is smaller than the event in 2015 (40 hours). However, erosion on the backside of the beach (revetment) is not found. There are still some unknown factors that might reveal the reason behind the different condition between 2015 and 2017.

4. It is recorded that there are four incidents where the significant wave height is over than 5 m in 2018. Moreover, three of the wave conditions are about 10 m, and it happens in a short range of time. It has been the highest occurrence of high wave in Owase since the last three years of field study. Furthermore, the duration of the wave are different each other, and none of the four incidents has the wave duration more than 32 hours (total duration for the wave over than 5 m) like the disaster in July 2015. Therefore, there is no severe damage is found near the revetment; however, the topography changes significantly due to the four incidents.

5. There are ten typhoons incident that passes near the mainland in Japan, and three of them conduces the extreme wave over than 10 m from August to September. The longest

duration of the typhoon is nine days and 18 hours, which pass through the Osaka Bay and Ise Bay. Typhoons No. 1820 and No. 1821 have the duration for six days and eight days, 6 hours respectively. Furthermore, the source of the typhoons come from the same territorial, which is the South of Ocean Pacific.

Topography Condition

1. It was estimated that the first damage to the revetment that occurred in July 2015 was caused by a high wave (over 10 m significant wave height at the tail end) caused by Typhoon No. 1511 that came from the south. Rapid beach erosion in the front of the revetment occurs in a short period due to the high waves that come in from the south that move large amount and rapidly toward the north (coastal direction). Furthermore, the wave height was relatively small at around 3.5 m at the time of the second disaster, it is speculated that the disaster in August is due to the effects of the disaster in July (insufficient recovery of the beach, etc.).

2. The seabed cross section in the southern part of Ojigahama is a steep slope of about 1/10 with the depth of about 7-8m, and a gentle slope of about 1/150-1/140 at a depth of 8-9m or less is there. The sediment is very fine sand with a depth of less than 6 m where the gentle slope of the seabed is less than 0.2 m, and the foreshore is a mixture of fine sand and gravel.

3. The topography of the southern end of Ojigahama, which has many components of coral, is steeper in the foreshore than in the central area, and the topography is more variable. Therefore, the influence of the high waves at the typhoon season tended to appear prominently on the south coast where the grain size is large forming the beach.

4. The topography change in the foreshore (near the middle section of survey line) does not occur notably with the wave height of about 5 m. On the other hand, the survey line 11 to 22 shows relatively large topography change compared to the survey line 1 to 10, and in particular, a large balm is formed near the shoreline.

5. The shoreline has retreated about 15-20 m after the high wave attack in October. It is found that the erosion near the shoreline does not reach the revetment and the risk of damage to the revetment does not increase even if the wave height is about 10 m, but the duration of the high wave is too short of causing the damage.

6. The topography of Ojigahama beach is changed significantly during extreme wave attack. The most severe impact is located in the southern end of the beach (survey lines No. 19 to 22). Moreover, the shorelines recede about 45 m after two incident of extreme wave attacks

(August 23rd and September 4th). Since then, the shorelines become short; it only remains a width of 30 m from the revetment

7. Based on the observation of wave effect to the topography, it could be deduced that for the wave up to 5 m with wave duration more than 10 hours could cause the shoreline retreat about 15-20 m in one incident. Moreover, it could be a serious problem if such as wave condition above (up 5 m with wave duration more than 10 hours) happen at least three times in a short time without sufficient beach recovery, the same disaster like in 2015 could be repeated in Ojigahama Beach (i.e., the normal width is 70-80 m; the shorelines retreat about 15-20 in every extreme wave attack).

References

1) Ito, D., and Kenji, K. (2014). "Cause of Sinking-Back and Measures of Shin-etsu Line Coast Revetment", *Journal of Japan Railway Facilities Association,* Vol. 52, No. 8, pp. 604-606. [In Japanese]

2) Kosuke, M. (2017). "Roadbed Subsidence Measures Affected by Water Level Fluctuation at Sea Level", *Journal of Japan Railway Facilities Association*, Vol. 55, No. 2, pp. 144-146. [In Japanese]

3) Keita, Y. (2016). "Countermeasures for Maintenance and Management of Coastal Revetment", *Proceedings of the Annual Conference of the Institute of Civil Engineers*, VI-099. [In Japanese]

4) Werner, BT., and Fink, TM. (1993). "Beach cusps as self-organised patterns", *Science,* 260, 968-971

5) National Institute of Informatics (2018). Digital typhoon: typhoon image and information. Retrieved from http://agora.ex.nii.ac.jp/digital-typhoon/

6) Real-time NOWPHAS (2018). Wave data download. https://nowphas.mlit.go.jp/pastdata_select/

7) Japan Metrology Agency (2018) Various data and materials, http://www.data.jma.go.jp/fcd/yoho/typhoon/index.html

Chapter 3

2D Experiment: Cross-Shore Morphodynamics of Composite Sand-Beach

3.1. Introduction

Composite sand-gravel beaches are found in many coastal systems worldwide. The beach is composed of gravel in inter- to supra-tidal swash zone and sand lower to sub-tidal surf zone [1]. The beaches can be found both in a natural condition and in the design beach construction [2]. A number of reports and studies have been published regarding the degradation of the beaches and in some instances of severe cutback [3] and breaching [4].

Larson and Kraus [5] and Pontee et al. [6] studied about the cross-shore variability of composite sand-gravel beaches, in which they found that a composite sand-gravel beach was distinctly different to that of sand beaches. It was also different to the other forms of coarse-grain beaches (mixed beaches and pure gravel beaches) regarding profile shape, profile response to hydrodynamic forcing, sediment characteristics and sediment distribution.

Mixed beaches and composite beaches are also found when beach nourishment schemes use materials that are significantly different to the indigenous one in size and distribution. The beach nourishment are often selected rather than hard coastal protection particularly in areas used for coastal recreation. Also, the gravel beach has been proposed as an engineering solution to mitigate erosion[7].

The morphodynamic response of the beach is determined based on the composition and cross-shore distribution of beach sediment. Pontee et al. [6] showed on their field study that the composite sand-gravel beaches differ significantly from pure gravel or mixed sand-gravel beaches where sand and gravel are spatially separated in the cross-shore profile. Composite sand-gravel beaches have coarse steep swash zone that changes abruptly into a low gradient sandy beach in the inter-tidal to sub-tidal zone [4].

On the contrary, sandy beaches have gentler cross-shore slopes and wide but shallow surf and swash zones. Meanwhile, higher energetic wave uprush and lower back-wash lead net onshore transport for gravel beaches [8][9]. As a result, composite sand-gravel beaches are formed due to sediment sorting across the profile where gravel accumulates at the supra-tidal and upper inter-tidal region of the profile while sand accumulates at the lower inter-tidal and sub-tidal regions [10]

In the present study, along with the literature above, laboratory experiments in a 2D wave flume were performed to gain deeper understanding about composite gravel-sand beach morphdynamics. In the 2D experiment, equilibrium profiles for normal, storm and post-storm waves were investigated, and the effect of gravel on the profile change was discussed by comparing the results of three cases with different wave condition.

3.2. Experimental Condition

A 2D experiment was carried out in a wave flume at Hydraulic Laboratory of Osaka University. The experimental set up is shown in Fig.3.1 Most of the parameters of experiment are considered based on actual condition in Ojigahama Coast, Wakayama Prefecture, Japan. This study was triggered by the severe beach erosion at Ojigahama, a typical composite sand-gravel beach, caused by a Typhoon in 2015. Nevertheless, the objective of this experiment is not to reproduce the actual condition, but rather study the morphodynamic response to waves by adopting parameters (wave) and characteristics (grain size) of Ojigahama beach as one of examples of composite sand-gravel beach. Thus, a field study was carried out to obtain primary data (e.g. wave data, sediment sampled at beach and underwater) before designing the experiments. A geometric scale 1/100 was used in the experiment. Based on the field data, median grain sizes (D_{50}) of sand and gravel were 0.18-0.2 mm and 17-23 cm, while the grain size (D_{50}) used in the experiment for sand and gravel were 0.15 mm and 2.3 mm respectively. To scale down the sand grain size without scale effect is usually difficult.
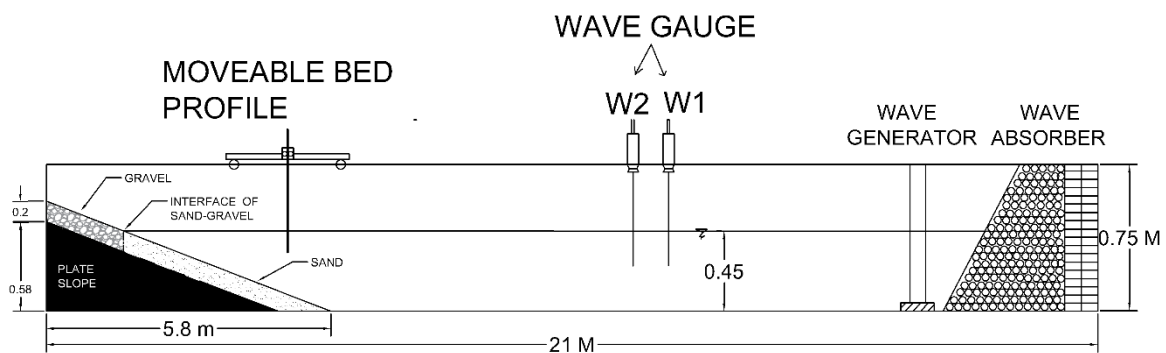
Figure 3.1 Sketch of experimental set up in 2D wave flume

The wave parameters in case-T1 and case-T2 were determined based on combining wave data measurement (three months) and nearby wave data station. The normal wave condition observed was 3-4 meters (H_s) and 10s (T_s), while the storm wave was 13-14 meters (H_s) and 14s (T_s). The case-T3 was designed as additional condition, by expecting worse scenario than the actual condition on the field. The wave duration was different for each case (4-8 hours); it depends on how long equilibrium beach profile would be formed (i.e. 1-hour wave = 3260 waves). In addition, the water depth and slope used

in the experiment was 0.45 m and 1/10 respectively. Detailed parameters in the experiment are shown in Table 1.

Table 3.1 Wave parameters of 2D experiment

Case	Wave	Normal wave		Storm wave		Post-storm wave	
		H (m)	T (s)	H (m)	T (s)	H (m)	T (s)
T1	Irregular	0.04	1	0.11	1.4	0.04	1
T2	Regular	0.028	1	0.07	1.4	0.028	1
T3	Irregular	0.06	1	0.16	1.4	0.06	1

The authors realize that not all the parameters on the field could be scaled similarly and perfect with the experiment. There would be scale-effect issue which might affect the experimental results. Consideration of the scale-effect of each parameters (e.g. sand, gravel, wave height, wave period, wave duration, etc.) and scale-effect combination of the parameters are important, but it needs comprehensive or specific study to discuss deeply about that. This research aims at clarifying the general characteristics of the beach response under experimental circumstances**.**

3.3. Equipment and Setup

Three wave gauges were used to record instantaneous water surface displacement η (t). Two wave gauges were located at 7 m and 7.3 m away from the wave maker, and the other one was used to record wave distribution along the beach with 30 cm interval by using a trolley. The beach profile was measured at 2 cm interval by an optical bottom profiler. The profiler was placed on a trolley and moved manually.
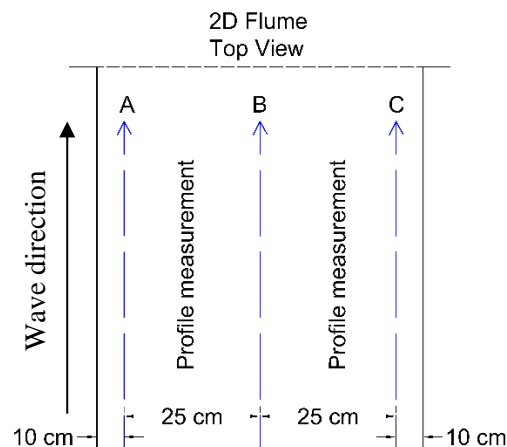
Figure 3.2 . Lines of profile measurement

The experiments were carried out for three cases with different wave condition such as the normal, storm and post-storm that were applied in this order in each case. The case-T1 is an irregular wave case, which represents actual storm wave condition near Ojigahama Coast. The case-T2 is a regular wave condition in which the wave energy is set to be equal with case-T1 (irregular). While the case-T3 is a case with extreme irregular wave condition. The spectrum of the irregular wave (i.e. case T1 and T3) used in the experiment was Modified Bretschneider-Mitsuyasu [11] (see Eq.3.1). For each case, the profile was measured every 30 minutes in three parallel sections of the beach, namely; A, B and C as illustrated in Fig. 3.2.

Measuring profiles on three sections allowed us to obtain detailed condition of profile change side by side. After measuring the final profile, vertical sampling of sediments was carried out to assess the mixture ratio of sand and gravel. The 12 samples were taken along the wave flume for each wave condition except in the normal wave condition, because the mixture (sand and gravel) did not occur during the normal wave condition.

3.4. Results and Discussions

3.4.1. Profile response to the waves

The profile response will be discussed based on the experimental results according to the order of wave condition. The profile response was observed under normal, storm and post-storm wave conditions. The time duration of each wave condition was determined as the time until the profile almost reached the equilibrium state [12]. The profile was measured continuously throughout the experiments of three wave conditions without re-shaping the beach profile. The profile in section B (Fig. 3.2) was selected for discussion in this section and the profiles at the other sections will be used for the analysis of net sediment transport rate.

Figure 3.3 illustrates the successive response of the beach profile for the three different wave condition in case-T1. The wave duration for normal, storm and post-storm were 4 hours, 5.5 hours, and 4 hours respectively. In normal wave condition, the beach profile changed rapidly in the first 30 minutes, showing the erosion along the nearshore area and formed a berm on the top of the beach. In the remaining time, the profile was changed slowly. While in the storm wave condition, the profile was eroded gradually in every 30 minutes and the erosion became considerable at the final state (i.e., equilibrium state). This enormous erosion may be strongly related to the wave uprush and downrush near the waterline. The downrush was stronger than uprush and carried fine sediment away to the bottom, causing the steep slope (see Fig.3.3). Furthermore, high berm was formed on the top beach, which was mainly composed

of gravels. The height of the berm increased progressively during 4 hours (i.e. 40 hours in the real condition) of storm wave generation. The formation of the berm indicates the onshore sediment (i.e. gravel) transport occurred even under storm wave condition.
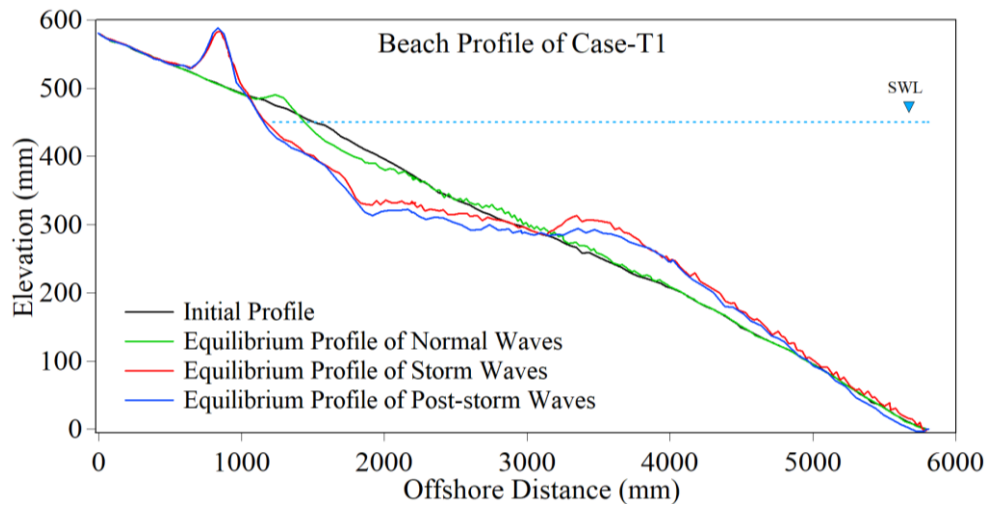
Figure 3.3 Profiles evolution in case-T1 under different waves conditions

In the post-storm wave condition, the profile changed slightly until the final state after 8 hours. It was expected that the profile recovered to the profile of normal wave condition, but in fact the profile kept scoured and did not recover. The steep profile in sub-aerial to the nearshore area and the flat profile in the offshore area might be major factors that restrains the recovery of the beach.

Karunarathna et al. [1] support this statement in his survey study on a cross-shore profile of composite sand-gravel beaches, and concluded that a composite sand-gravel beach might become unstable due to sub-aerial profile cutback during storms and sandy beach is destabilized due to beach lowering. As the result, it makes more difficult for the upper foreshore of a composite sand-gravel beach to recover from an erosive event than for a sandy beach.

Figure 3.4 describes the evolution of profiles in case-T2, in which regular wave was used for the comparison. In order to compare with case-T1, the total wave energy of this case was designed to be equal with case-T1. The Modified Bretschneider-Mitsuyasu spectrum is expressed by Eq. (3.1), and the total irregular wave energy E_I is given by Eq. (3.2), where H_s and T_s represent the significant wave height and period, respectively. On the other hand, the energy of the regular wave E_R with wave height H is given by Eq. (3.3). From equation $E_I=E$ the relationship between H_S and H is obtained as Eq. (3.4). The duration of wave generation was smaller than case-T1, which were 3, 4 and 2 hours for the normal, storm and post-storm

waves respectively. As the first wave generated, the normal wave created erosion nearshore and very small berm on beach face, which is similar behavior to case-T1.

$$S(f) = 0.205\ H_s^2 T_s^{-4} f^{-5} \exp\left(-\frac{0.75}{(T_s f)^4}\right)$$ Eq. 3.1

$$E_I = \rho g \int_0^{+\infty} 0.205 H_s^2 x^{-5} e^{-0.75 x^{-4}} dx = 0.068\ \rho\ g\ H_s^2$$ Eq. 3.2

$$E_R = \frac{1}{8}\rho g H^2$$ Eq. 3.3

$$H = \frac{H_s}{1.36}$$ Eq. 3.4
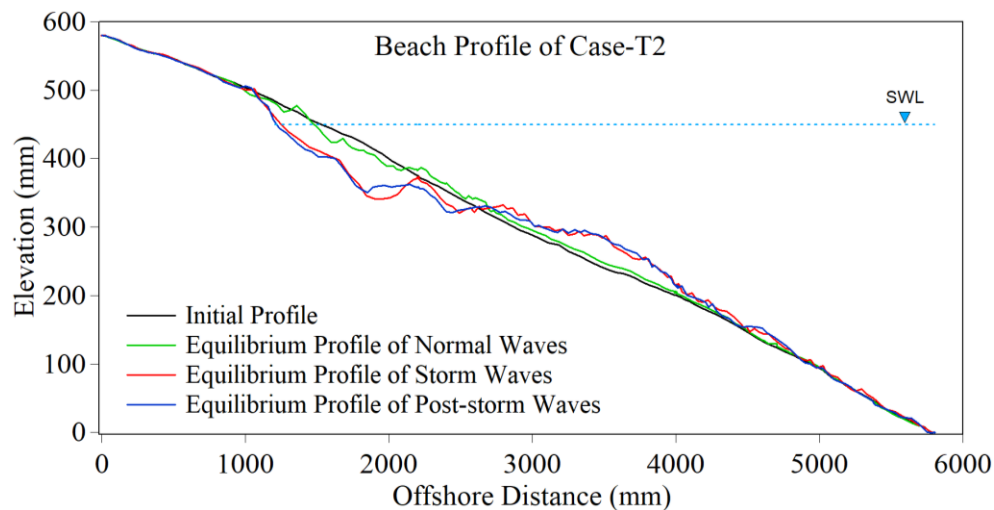
Figure 3.4 Profiles evolution in case-T1 under different wave conditions

In the storm wave condition, the profile changed rapidly in the first 30 minutes and reached gradually to the equilibrium state. There are two significant differences between T1 and T2 cases in terms of profile response to the storm wave. The first is that there was no berm formation on the beach face in case-T2. The second is that the erosion area of case-T2 was less than case-T1 by looking at the final profile. These differences might be affected by beach profile and wave characteristics during wave action. In the post-storm wave condition, there was no critical response of beach recovery to the wave. The beach recovery was found to be small.

For the last case of this experiment, case-T3 was designed to meet extreme condition on the field under irregular waves. In this case, wave durations were 2, 4 and 8 hours for normal, storm and post-storm wave conditions, respectively. Like other cases in this experiment, the normal wave with 6 cm significant wave height created the erosion nearshore. Furthermore,

the profile became eroded extremely at the final state of storm wave. The storm wave also induced the formation of the berm on the top of the beach with gradual increase. The response of the profile was almost similar to case-T1. The profile was getting steeper nearshore as the result of the strong backwash and forming the flat part offshore. High offshore bar and troughs were also formed. This offshore bar contributed to cause wave breaking which may affect the profile response. In the post-storm wave condition, small recovery was identified only at the offshore bar area.
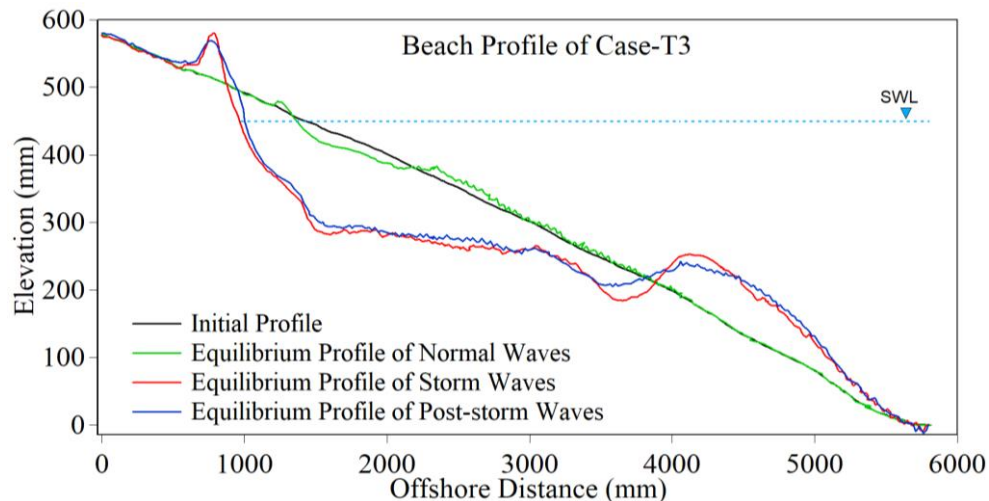
Figure 3.5 Profiles evolution in case-T3 under different wave condition

Based on the discussion of profile response over three cases above, the response of the profile to waves shows similar characteristics such as unexpected erosion occurs during normal wave condition which is started from sub-aerial zone (dry-wet zone), the formation of the steep slope as the result of strong backwash current, and low recovery response under post-storm wave. The typical composite sand-gravel is very vulnerable to wave, especially in the sub-aerial zone (dry-wet zone). This zone is also the zone in which the shoreline separates the gravel and sand. The sub-aerial zone is critical even for the normal wave, in which under the normal wave conditions the berm (i.e. contained only gravel) is formed on the top the beach, like in the of case-T1 and case-T3.

The formation of the berm might contribute to the change of the wave and current propagation. The formation of the berm also induced by strong up wash current. The case-T1 and case-T3 have both upwash and backwash current, which might be same in the magnitude. While in the case-T2, the magnitude of upwash current seems to be lower than backwash current, as the formation of the berm could not be formed of top of the beach. The backwash current seems to dominate in the sub-aerial zone over the three cases. The strong backwash

current leads to the formation of the steep profile as it pulls down the amount of gravel from the beach top to the sea. In which at that circumstance, the shape roughness of gravel has a role in accelerating the erosion of the sand layer (i.e. substantial contact/interaction between gravel and sand fractions). The steeper profile is formed, the stronger the backwash current is generated. This condition could be worst under the storm wave, as higher the berm formed and the erosion becomes more extensive, which followed by steeper profile formation. The post-storm wave condition could not fully recover the beach due to the steep beach slope.

3.4.2. Shoreline retreat

Shoreline change was analyzed to study the response of shoreline. The shoreline retreat was evaluated by comparing the profiles between the initial and the final state at the waterline as illustrated in Fig. 3.6. The shoreline change was analyzed in every 30 minutes which indicated by dotes mark in Fig.3.7. The duration of shoreline change measured was correspond to the wave durations of each case. The durations of case-T1 were 4, 5.5, and 4 hours, case-T2 were 3, 4 and 2, while case-T3 were 2, 4 and 8 hours for normal, storm and post-storm wave condition respectively.
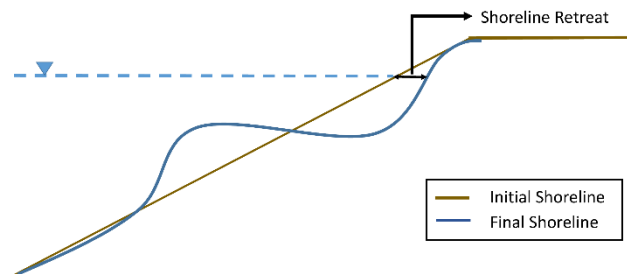
Figure 3.6 Illustration of shoreline retreat

Figure 7 exhibits that the shoreline started to retreat under normal wave condition and continued receding until the final condition The shoreline declined drastically during storm wave condition. In post-storm wave condition the shoreline did not recover (i.e., irreversible state) due to formation of steep slope as the result of considerable erosion onshore. This statement prevails in all the cases. However, the magnitudes of shoreline retreat at the final condition (i.e., post-storm) were different for each case, which are 290 mm, 270 mm and 420 mm for the case-T1, T2 and T3, respectively. Based on this information (i.e. shoreline retreat calculated), countermeasure work could be proposed at the specific impacted area of shoreline recession to prevent from severe problem.
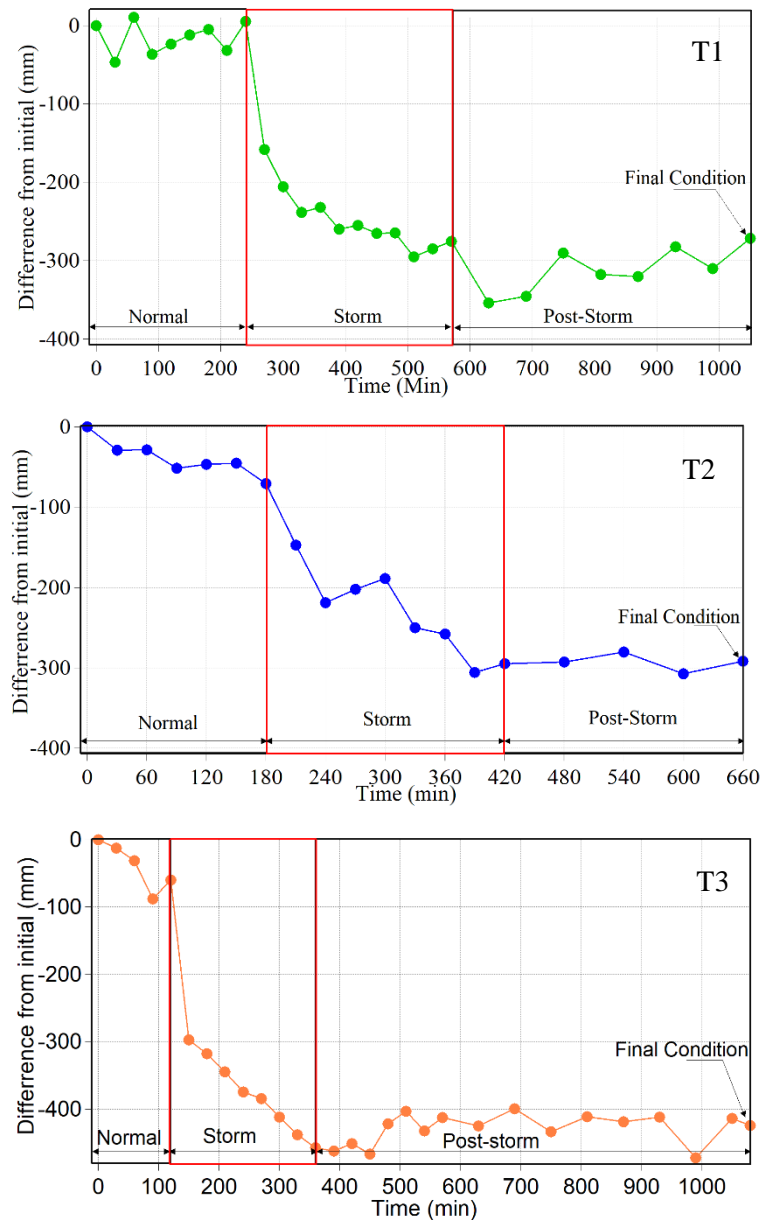
Figure 3.7 Shoreline change during waves sequences for case-T1, T2, and T3

3.4.3. Net sediment transport rate

The average rate of on-offshore sediment transport can be estimated from the beach profile change as shown in Fig. 3.8, we consider conservation of sediment in the normal shore section. Q denotes net sediment transport integrated vertically, q_z denotes suspension or deposit flux from/to the bottom (positive suspension)[13].

$$\frac{\partial c}{\partial t}\Delta x h = Q - \left(Q + \frac{\partial Q}{\partial x}\Delta x \right) + q_z \, \Delta x \qquad \text{Eq. 3.5}$$

Under steady-state condition: $\frac{\partial c}{\partial t} = 0$,
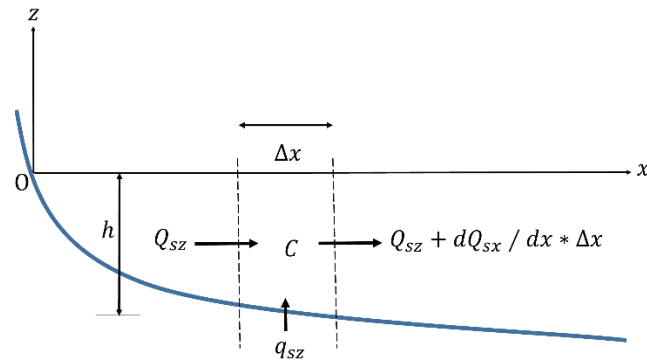
Figure 3.8 Illustration of net sediment transport rate

$$q_z = \frac{\partial Q}{\partial x} \qquad\qquad\qquad \text{Eq. 3.6}$$

q_z can be related to $\partial h/\partial t$ as in $(1 - \lambda)\ \partial h/\partial t = q_z$, where λ is the porosity and has value of $0.3\sim0.4$.

$$\frac{\partial h}{\partial t} = \frac{1}{(1-\lambda)}\frac{\partial Q}{\partial x} \qquad\qquad\qquad \text{Eq. 3.7}$$

Therefore, the net sediment transport rate Q over a time duration Δt of wave action is evaluated from the bed elevation change Δh during the same period by:

$$Q = (1 - \lambda)\sum_0^x \frac{\Delta h}{\Delta t}\ \Delta x \qquad\qquad\qquad \text{Eq. 3.8}$$

In which x is positively seaward, zero means the shoreward limit of beach deformation. From Eq.3.8 the spatial distribution of sediment transport rate $Q_{(x)}$ can be obtained. Figure 3.9 shows an example of accretion and erosion beach type with the distribution of sediment transport.
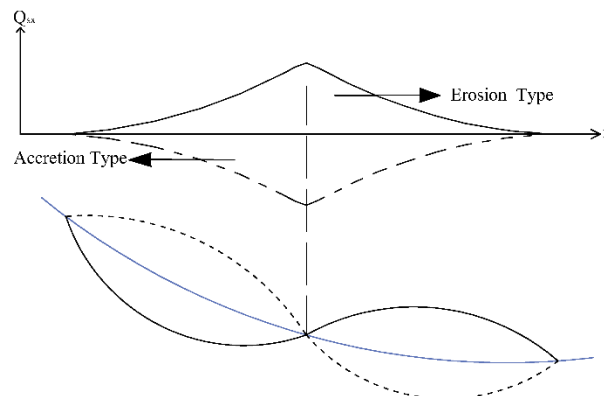
Figure 3.9 Beach type along with distribution of sediment transport

In the evaluation of net sediment transport rate, average beach profiles of three sections were used (see Fig. 3.2), because the cross-shore sediment transport is not always the same in each section due to sidewall effect of the flume. By calculating sediment transport rate distribution, a classification of "equilibrium transport rate distribution" can be determined. Larson and Kraus [14] were classified the equilibrium transport rate distribution into three main types as follows;

a. Erosional (Type E); transport directed offshore along the entire profile.
b. Accretionary (Type A); transport directed onshore along the entire profile.
c. Mixed accretionary and erosional (Type AE); transport directed onshore along the seaward part of the profile and transport directed offshore along shoreward part of the profile

Figure 3.10 shows the spatial distribution of net transport rate Q of case-T1. Positive values of Q indicate the net transport toward the offshore-direction, while negative Q means the onshore direction. As it is seen in Fig. 3.10 (a to b), the offshore sediment transport is generally predominant nearshore. The maximum net sediment transport occurs at the first 60 minutes then decreases gradually with time. In the normal wave condition, the offshore sediment transport is dominant in the first 120 minutes, and in the rest of 2 hours, the sediment is moved slightly toward the onshore direction.

In storm wave condition, the net sediment transports are divided into two directions. The sediment transport dominates in the offshore direction although a minor onshore transport takes place as a result of the formation of gravel berm on the beach face. On the other hand, onshore sediment transport initiates in the first 60 minutes of the post-storm condition. Right after 60 minutes, the sediment moves offshore inconsistently with time. The classification of the equilibrium rate of case-T1 was identified as Type AE.

Figure 3.10 (d to f) reveals that the case-T2 has different characteristics than case-T1. In terms of classification of equilibrium transport rate, figure (d) and (f) are classified as Type AE, while figure (e) is Type E. In the figure (d), the maximum transport rate in the first 60 minutes is almost half of the rate in storm wave condition (figure (e)) in the same period. The transport rate under storm condition is decelerated with time after prominent rate in the first 60 minutes. The location where the sediment transport rate shows the peak in case-T2 and T1 during 60 minutes is slightly different. On the other hand, in the post-storm condition of case-T1, case-T2 exhibits similar characteristics. Figure 3.10 (f), indicates that in the first three hours,

offshore transport rate was predominant, and then at the last hours, the sediment tends to move onshore.
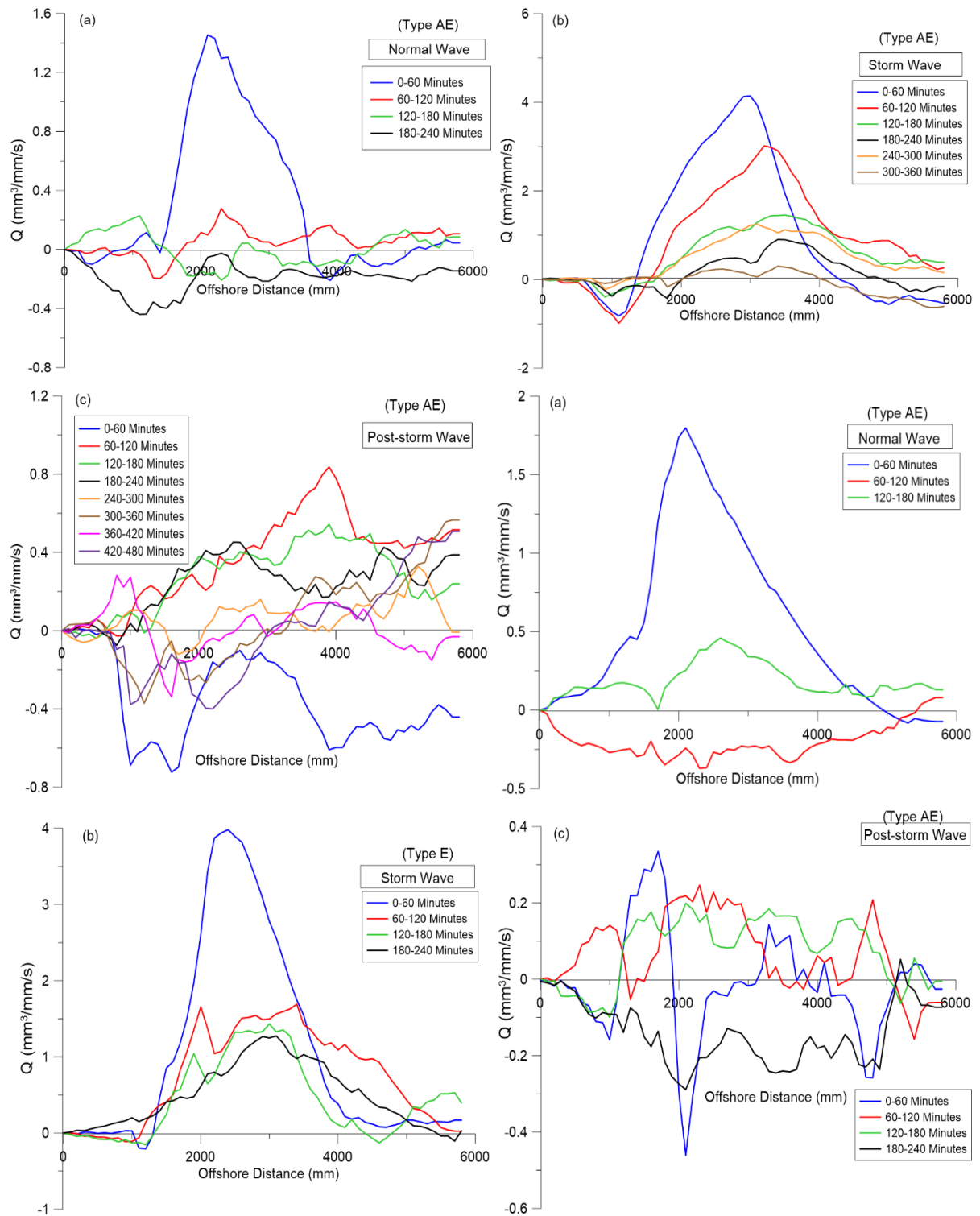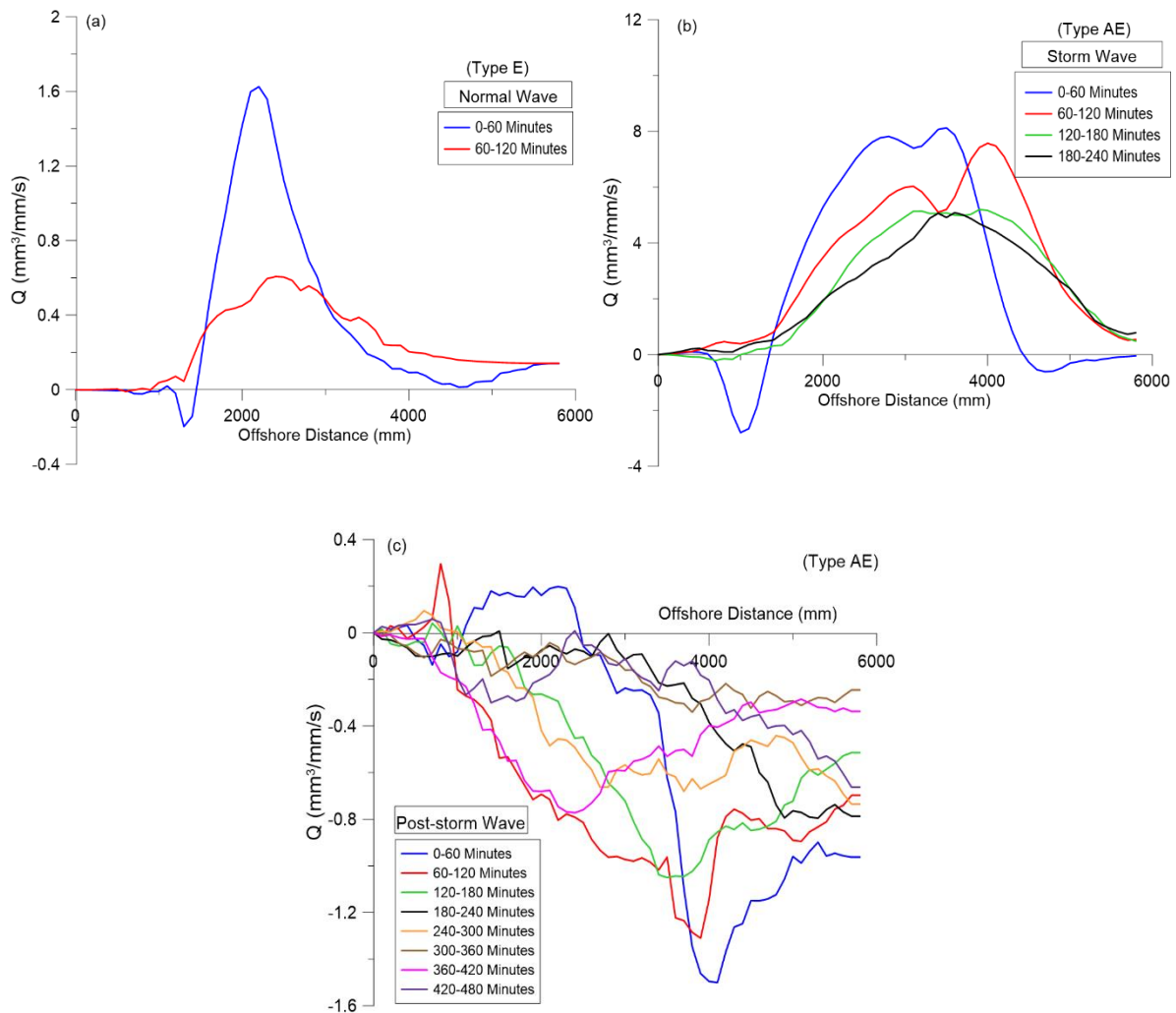
Figure 3.10 Net sediment transport based on wave sequences for case-T1 (a to c), case-T2 (d to f) and case -T3 (g to i)

In the case-T3, under normal wave condition, offshore transport rates are still dominant as seen in Fig.3.10 (g to i). However, with the highest wave height among the other cases, it does not produce the highest transport rate as well. The highest transport rate under normal wave condition among the cases is seen in case-T2 (Fig.3.10 g) with H=2.8 cm. In the storm condition, although offshore transport is dominant, a small onshore rate as the result of berm formation on foreshore, which classifies the equilibrium transport rate into Type AE. For the same reason, it is classified into Type AE for the post-storm condition. Despite onshore transport are prominent, a small offshore transport occurs during short periods. The transport rate is inconsistent during the time due to low recovery response of the profile (Fig. 3.5).

3.4.4. Sand-gravel mixture analysis

Sand-gravel mixture analysis is done based on data of sediment sampling. Sediment sampling was conducted in the experiment for two cases only, case-T1 and T2. For both cases, the samples were taken from different locations, depending on the location of the mixture.

However, the number and interval of each sampling were the same, which are 12 samples and 10 cm respectively, with the diameter of the pipe is 5 cm. Principally, the purpose of the sediment sampling is to estimate the ratio and thickness of the mixture, along with mixture layers of beach profile.
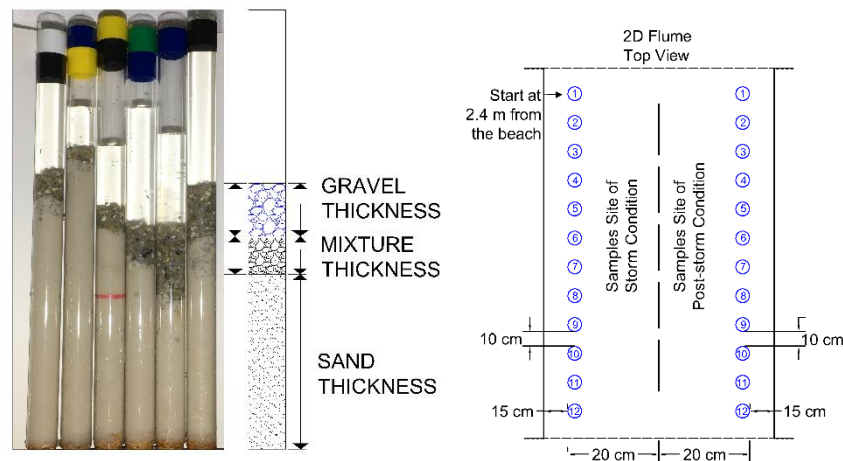
Figure 3.11 Cores of sediment samples and Sketch of samples location

Figure 3.11 describes the definition of thickness of mixture, which is defined as a length of the layer in which gravel and sand coexist. The mixture ratio was measured by normalized dry weight fractions of gravels W_G and sand W_S of the mixture layer. Equation 3.9 defines the mixture ratio R_M.

$$R_M = \frac{W_G}{W_S}$$
Eq. 3.9

A significant interaction occurs between waves, sand, and gravel. As a result, a great mixture of sand and gravel was found under storm and post-storm wave conditions. Storm condition initiates significant influences to mixture fractions as the result of high wave energy. However, the post-storm condition could also determine whether the mixture will be higher or lower depending on the shape of the beach profile and wave characteristics. The existence of mixture area may affect significantly to bed load transport and seabed profile change. [15]

Figure 3.12 describes the mixture area of the beach under irregular wave (case-T1). The mixture area is flanked by surface and interface layers, in which surface layer is composed of very few gravels and interface layer is the boundary of mixture area to the sand layer beneath. The mixture area was measured at the final state of each wave conditions. The formation of mixture area was triggered by strong backwash under storm condition which pulled down the gravel from the beach face to the nearshore [16]. Furthermore, the troughs in the interface profile for storm wave conditions was created as the impact of plunging breaker. In the troughs, the

mixture thickness became higher as the sand-gravel was slammed deeper into the sand layer. While in the post-storm wave condition, the mixture materials dwindled due to little backwash to the offshore.
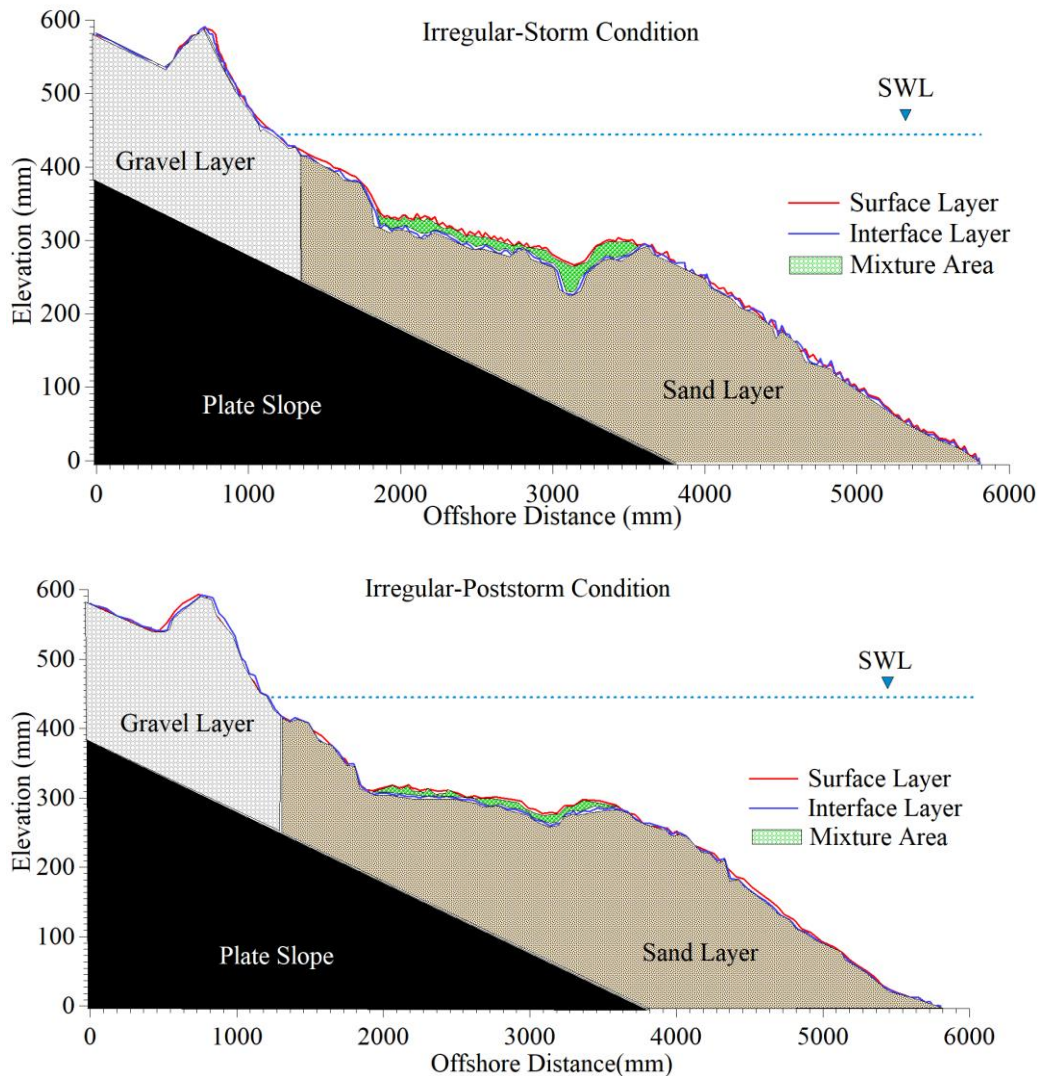
Figure 3.12 Beach mixture profile of case-T1

Figure 3.13a shows the comparison of the mixture ratio and mixture thickness. It is shown that both the ratio and thickness of the mixture in the storm condition is higher than a post-storm condition. The mixture ratios varies in the range of 10 to 25% of gravel fractions in storm condition. McCarron et al. [15] revealed that a sediment mixture containing 15% gravel could reduce transport rate by more than 66% compared to pure sand. Therefore, it is believed that the lower ratio produced in post-storm condition is influenced by decreasing transport rate as the result of the higher mixture in storm condition. The correlation between the mixture ratio and thickness of mixture and ratio are shown in Fig. 3.13b. As the thickness of mixture

increases, the mixture ratio also increases. The correlation between ratio and thickness for both wave conditions are in good agreement.
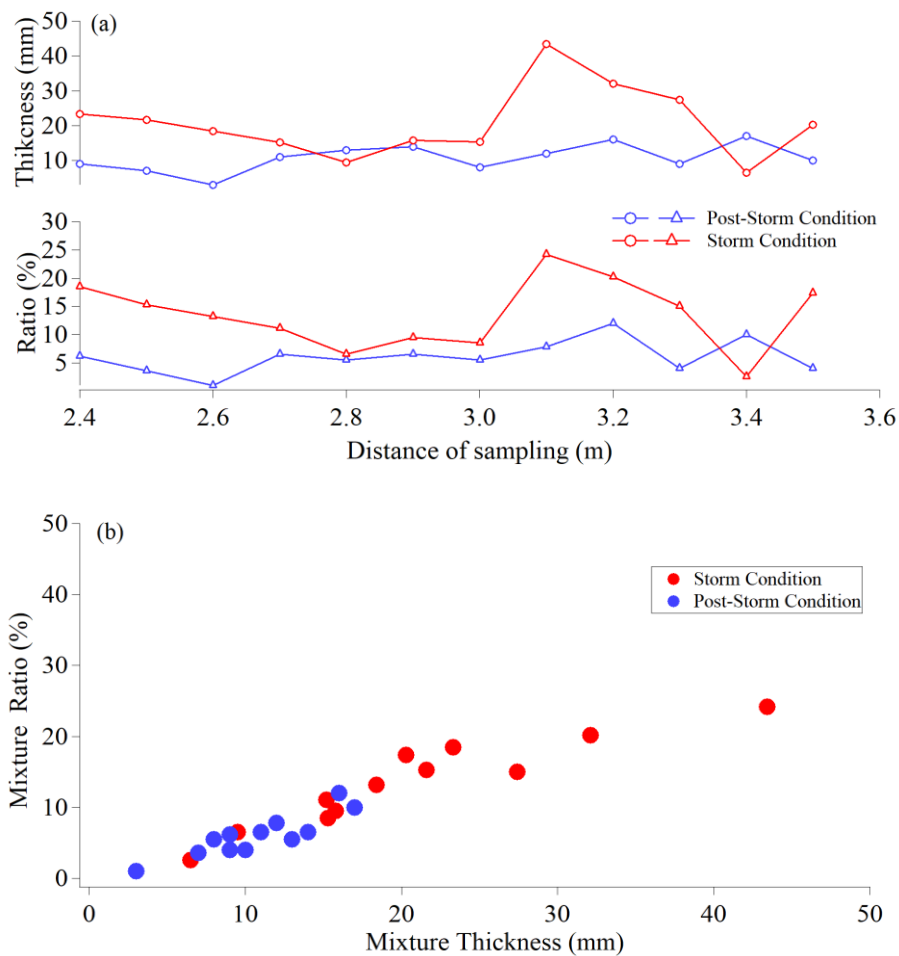
Figure 3.13 comparison (a) and correlation (b) of mixture thickness and ratio in case-T1

On the other hand, case-T2 exhibits a bit different characteristics and behavior. In this case, the mixture occurred nearby the waterline with a distance shorter than case-T1 as seen in Fig. 3.14. A different location and area of the mixed material depends on wave characteristics and shape of a beach. As mentioned above, case-T2, which used regular wave, generate the same waveform with time, as the result, the beach profile produced in this condition will be different from the profile in case-T1 with irregular waves.
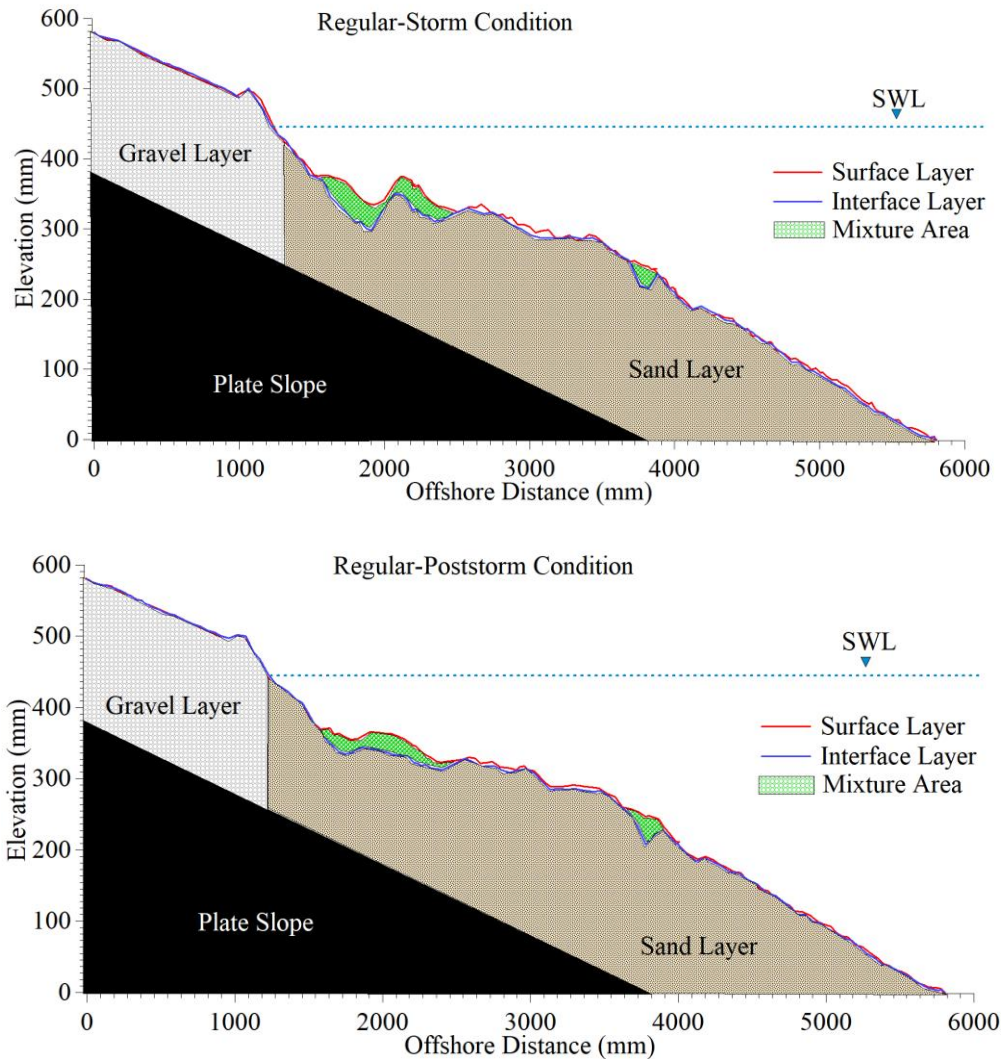
Figure 3.14 . Beach mixture profile of case-T2

Similar to case-T1, the storm condition is still predominant in enhancing mixture as shown in Fig.3.15a. The correlation shown in Fig. 3.15b reveals that comparison between both wave conditions is slightly different but consistent. Furthermore, the mixture thickness in case-T2 is higher than case-T1 in average, about 21.64 mm and 20.7 mm respectively. The mixture ratio in case-T2 is lower than case-T1, which are 12.9% and 13.5% for case T2 and T1 respectively.
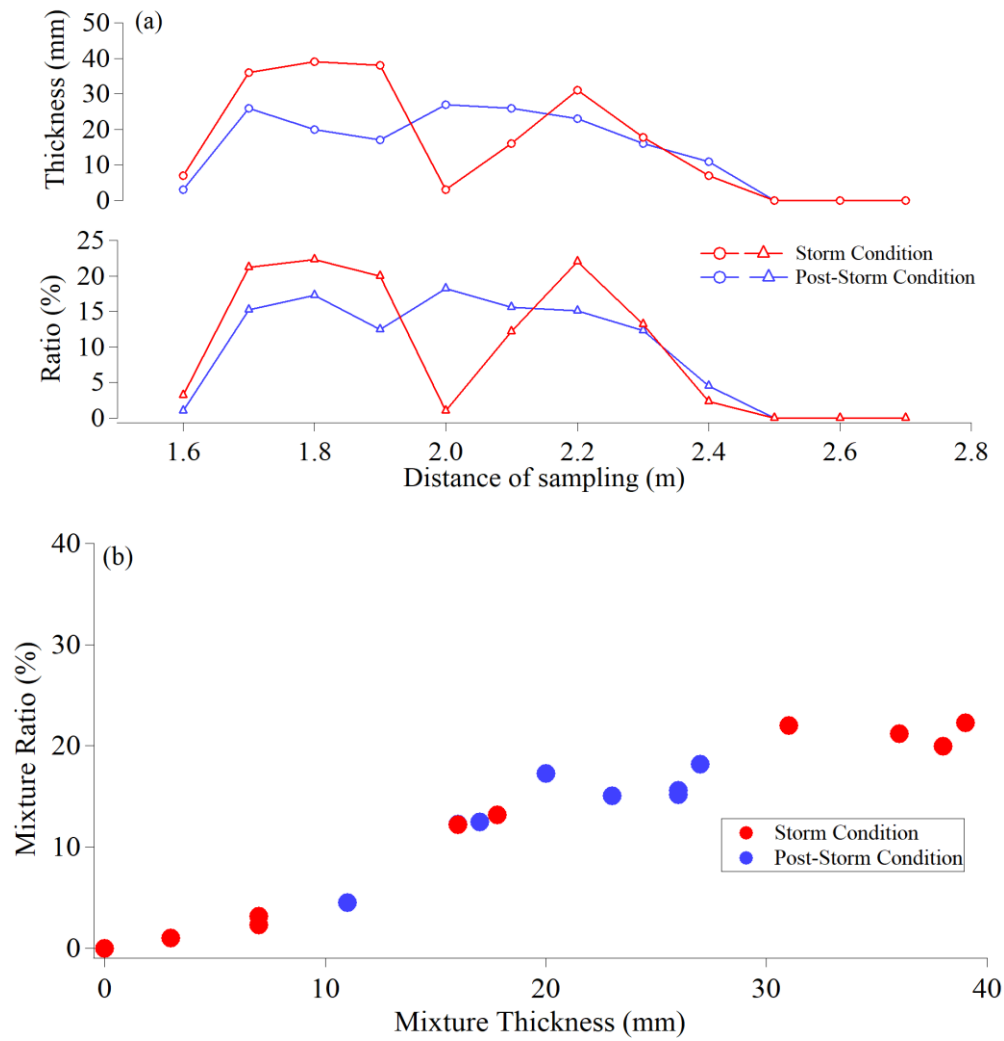
Figure 3.15 comparison (a) and correlation (b) of mixture thickness and ratio in case-T2

3.5. Conclusions

In this chapter, morphodynamics of a composite gravel-sand beach is studied through 2D experiment. The response of the beach profile to the normal, storm and post-storm waves were tested for three cases. The significant findings in the experiments are as follows:

1. The beach profiles under irregular wave cases (case T1 and T3) behave similarly, in which the profile form steep slope nearshore and berm on the beach face. The recovery of the beach by post-storm wave is prolonged. While the profile in regular wave case (case-T2), despite a steep slope is formed, there is no berm formed on the beach face.

2. For all the cases, the shoreline started to retreat under normal wave condition, and continued receding until the final state. Also, the shoreline did not recover due to the formation of steep slope as the result considerable erosion.

3. In terms of sediment transport rate, significant transport rate occurs during the first 60 minutes and decreases gradually with time. Transport rates in the post-storm conditions are discovered to be inconsistent every hour (i.e. in terms of transport direction) due to the low recovery response of beach.

4. The ratio and thickness of the mixture are predominant in storm wave condition rather than post-storm wave condition. Furthermore, the correlation between ratio and thickness of the mixture are in good agreement, as the mixture thickness increases, the mixture ration also increases.

References

1) Karunarathna, H., Horillo-Caraballo, J., Ranasinghe, R., Short, A., and Reeve, D. (2012). "An Analysis of Cross-Shore Beach morphodynamic of a Sand and a Composite Sand-Gravel Beaches," *Marine Geology*, Vol. 299-302, pp, 33-42.

2) Hicks, BS., Kobayashi, J., Puleo, JA., and Farhadzadeh, A. (2010). "Cross-Shore Transport on Gravel Beaches," *Proceedings of 32ⁿᵈ International Conference on Coastal Engineering*, ICCE, sediment.43, 1-9.

3) Chadwick, AJ., Karunarathna, H., Gehrels, R., Massey, A., CO'Brien, D ., Dales, D. (2005). "A New Analysis of the Slapton Barrier Beach System," *Maritime Engineering,* 158, 4, 147-161.

4) Carter, RWG., and Orford, JD. (1993). "The Morphodynamics of Coarse Clastic Barriers and Beaches: A Short and Long Term Perspective," *Journal of Coastal Research*, Vol.15, 158-179.

5) Larson, M., and Kraus, NC. (1994). "Temporal and Spatial Scales of Beach Profile Change, Duck, North Carolina," *Marine Geology*, Vol. 117, 75-94.

6) Pontee, NI., Pye, K., and Blott, SJ. (2004). "Morphodynamic Behaviour and Sedimentary Variation of Mixed Sand and Gravel Beaches, Suffolk, UK," *Journal of Coastal Research*, Vol. 20(1), pp, 256-276.

7) Muir-Wood, AM. (1970). "Characteristics of Shingle Beaches: The Solution to Some Practical Problems," *Proceedings International Conference on Coastal Engineering*, ASCE, 1059-1075.

8) Carter, RWG., and Orford, JD. (1984). "Coarse Clastic Barrier Beaches: A Discussion of the Distinctive Dynamic and Morphosedimentary Characteristics," *Marine Geology*, Vol. 60, pp. 377-389.

9) Carr, AP. (1983). "Shingle Beaches: Aspects of Their Structure and Stability. Shoreline Protection," *Proceedings of Shore Protection*, A conference organized by the Institution of Civil Engineers, University of Southampton, Thomas Telford, 69-76.

10) McLean, RF., and Kirk, RM. (1969). "Relationship between Grain Size, Size-Sorting, and Foreshore Slope on Mixed Sand- Shingle Beaches. New Zealand," *Journal Geology Geophysics*, 12, 138-155.

11) Goda, Y. (1985). *Random Seas and Design of Maritime Structures*, University of Tokyo Press, pp. 25.

12) Dean, RG. (1991). "Equilibrium Beach Profiles: Characteristics and Applications," *Journal of Coastal Research*, Vol. 7(1), 53-84.

13) Aoki, S. (2015). Sediment Transport and Beach Deformation, Lecture note 1-65

14) Larson, M., and Kraus, NC. (1989a). *SBEACH: Numerical Model for Simulating Storm-Induced Beach Change, Report 1: Theory and Model Foundation, Technical Report CERC-89-9*, US Army Engineer Waterways Experiment Station, Coastal Engineering Research Center, Vicksburg, MS.

15) McCarron, C., Howard, N., Van Landaghem, K., Baas, J., and Amoudry, LO. (2016)." Sediment Transport and Bedform Morphodynamics in Sand-Gravel Mixtures," *MARID Conf V*, New South Wales, UK.

16) Muhajjir, Suga, H., and Aoki, S. (2018)."Transportation of gravel on the Upper Part of the Sandy Beach," *Proceeding 28th International Offshore and Polar Eng Conf*, Sapporo, ISOPE, 1098-6189.

Chapter 4

3D Experiment: Longshore Sediment Transport of Composite Sand-Gravel Beach

4.1. Introduction

Longshore sediment transport (LST) has been studied widely among coastal engineers. The process that transport the materials within surf zone, directed parallel to the coast, which is involved by wave, beach, fluid, current characteristics of particular coast. This process also plays a role in maintaining the stability of the beach. Although it is a part of the natural process, not least of the cases is an act of human interference such as the groin, breakwater, jetty, etc. Sometimes by constructing structure adjacent to the coast could cause the severe alteration of the natural process in the beach system (beach erosion). However, these things could be prevented if we truly understand how to manage the coastal zone appropriately. There have been several studies which work specifically on longshore sediment transport[1)2)3)]. Nevertheless, most of their studies are limited to the case of sandy beach only.

Recently, development of beach protection has approached to a new phase, where the gravel beach has turned up into elemental part to encounter beach erosion issues [4)].The gravel beach could be found both in natural condition and in artificial beach design[5)]. Jenning and Shulmeister[6)] classified the scheme for gravel beach based on characteristics distribution into three types; pure gravel (G), mixed sand-gravel (MSG), and composite sand-gravel (CSG). Pontee et.al[7)] revealed that the response of those beaches to wave is obviously disparate in each type, especially in terms of profile response, characteristics and distributions of sediment. Hence, it is pivotal to understand and differentiate the characteristics of object beach (beach type) that we want to study about, so the approach methodology could handle suitably.

One of beach type concerned in this study is composite sand-gravel beach (CSG). The beach is composed of gravel in inter-to supra-tidal swash zone and sand lower to sub-tidal surf zone[8)]. Since the last two decade, the number of researches study on gravel beaches used in coastal protection have been widely increased, especially for pure gravel beach (G) and mixed sand-gravel (MSG)[9)10)11)12)]. However, the study on composite sand-gravel (CSG) is still limited in term of laboratory study. Therefore, in this chapter, we are attempting to expand the study of composite sand-gravel beach from the previous chapter by conducting the experiment in a 3D wave basin.

The purpose of study in this chapter is to observe the longshore sediment transport process of CSG beach under storm wave and identify the distribution of colored gravel along and across the beach which has an output of trajectory scheme of gravel movement (i.e., colored gravel is used as a tracer in this experiment). Furthermore, the topography response to storm wave associated with the nearshore current will be discussed in advance.

4.2. Experimental Condition

A 3D experiment was carried out in the wave basin at Hydraulic Laboratory of Osaka University. The sketch and condition of the experiment could be seen in Fig. 4.1. Like in the previous study (i.e. 2D experiment in chapter III), some of the parameters in this experiment are considered based on the actual condition in Ojigahama Coast,Wakayama Prefecture, Japan, especially the parameters at the time of beach erosion as the impact of storm wave generated by typhoon in 2015.
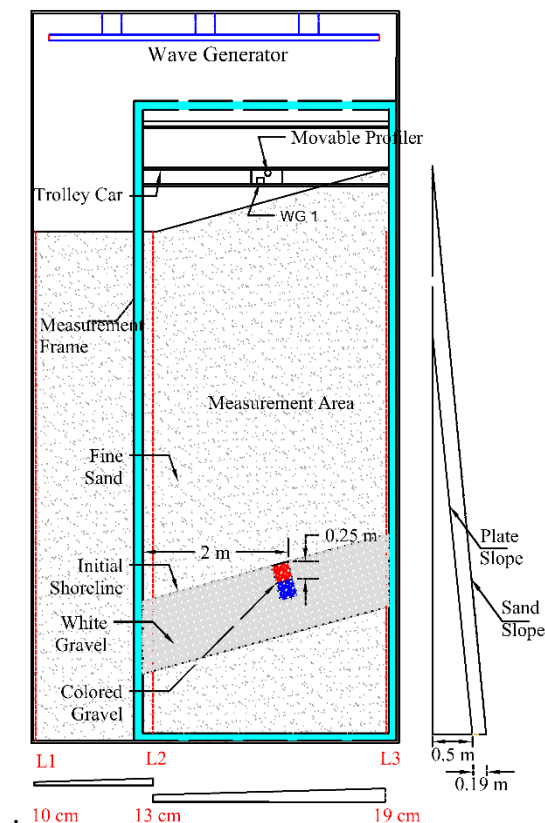
Figure 4.1 Sketch of 3D experiment with oblique beach (15°)

Two cases of the experiment were carried out in the 3D wave basin with 10 m length, 5 m width, and 0.6 m depth with geometric scale of 1/100. In this experiment, two types of material were used for sediment, which was sand with $D_{50} = 0.2$ mm, and three colored gravels: red, blue and white with the same grain size $D_{50} = 2.3$ mm. To create equilibrium profiles, the

regular storm waves were generated with incident wave height H=14 cm and wave period T = 1 s. The beach was designed oblique (15°) to the wave incidence with a slope of 1/10 for all the cases.

4.3.   Equipment and Setup

The equipment used in this experiment was almost the same as in the 2D experiment. A wave gauge and a velocity meter *ACM 200-A* were used to measure the wave height and current velocity distribution. The optical bottom profiler was also used to measure topography.

In the experiment, two cases were tested to investigate the movement of colored gravels. The beach was initially built by the sand, and then the white gravel was placed on beach face by replacing the sand with gravel keeping the slope 1/10. In addition, the colored gravels with total weight of 6 kg (2.52×10^{-4} m^3) for each color were used. The colored gravels were placed in the square area of 25 cm x 25 cm on the beach face at a specific position, which was 2 m distant from the left end of measurement frame (See Fig. 4.1). The colored gravels were buried by replacing white gravel and to be level with white gravel. In determining the position of the colored gravels, a preliminary experiment was carried out, in which current measurement was also done. On the beach designed oblique to the wave direction, complex current system was generated especially in a closed wave basin. Details preparation figures could be seen in Fig. 4.2

The experiment was carried out for two cases (E4) and (E5). The difference condition between case E4 and E5 are only in the water depth, which are 40 cm and 42.5 cm respectively. For both cases, the wave was generated for 90 minutes with measurement of beach topography at 30, 60 and 90 minutes after wave generation. The measurement of wave height and current velocity were also conducted every 30 minutes. The measurement was done along the nearshore line parallel to the wave maker with interval of 30 cm. Beach topography was measured every 30 minutes on 22 lines with 20 cm interval. After 90 minutes, sampling gravels was done to analyze the distribution of colored gravels around the beach. By applying the grid method to sampling area, the distribution was quantified over the grid area. The area of each grid was 25 x 25 cm same as the size of the initial colored gravels. For each grid sample, the gravels of red, blue and white mixed were separated manually and measured the volume.

Take out the sand part in the beach face	Replace sand with white gravel in the beach
Square design of colored gravels	Top view of beach face
Final preparation (front view of wave gen.)	Filling the water for preliminary test
Installation of the instruments	Preliminary test

Figure 4.2 The preparation and set up of the experiment

4.4. Results and Discussions

4.4.1. Beach profile response

The response of the beach to storm wave is discussed through profile sections (i.e., cross and long section) analysis. Figures 4.3 and 4.4 describe the topographic conditions of case E4 and E5 during 90 minutes wave generation. The topographic measurement was done every 30 minutes. The representative profiles in the long section and cross section were analyzed to evaluate the details condition of the topographic profile. There were two profiles selected for each of section, which namely L I, L II for Long Section I, Long Section II and C I, C II for Cross Section I, Cross Section II, respectively. The zone section selected had different reasons, in which the long-section zone was based on the significant effect on the beach profile and wave breaking zone, while the cross-section zone was based on the location of colored gravel set up (i.e., details about the grid area will be discussed in the next sub-section).

Figure 4.3 shows the case of E4, in which it could be seen that the design of 15° oblique beach to wave source (wave generator) was created well adequate, which was indicated by topographic contour at 0 minutes. As the beach design was ready, the experiment started by generating a storm wave with 14 cm wave height and 1 s wave period every 30 minutes. Immediately after 30 minutes, the beach profile was changed significantly, however, in the remaining time, the change was small. In the long section I, the elevation along the beach decreased at the first 30 minutes, the decrease in elevation was getting more significant from the right side to the left side (3000 to 0 mm). At the final condition (90 minutes), the decrease in elevation along beach could be estimated at L I, in which it found that the average of elevation decrease was about 6 cm. While, in the long section II, the significant erosion occurred at the point of 2.5 m in first 30 minutes. This erosion led to decrease in elevation was about 8 cm from initial profile or half of sand layer thickness. However, the sand lost from erosion area was transported mainly to left side area (at point 500 – 0 mm), subsequently, deposited there in the level of 4-6 cm above the initial profile.

On the other hand, from cross-section view, considerable erosion was also observed in the first 30 minutes from the beach face to nearshore, and this occurred at both section of C I and C II. The erosion that started occurring from the beach face was influenced by grind-effect of the gravel shape associated with strong backwash current. Some of the gravel from the beach was dragged down to nearshore due to backwash current. During the dragging process, the shape of the gravel plays a critical role in erosion. The shape of gravel accelerated the erosion

process nearshore due to the strong friction forces between gravel and sand layer. Furthermore, the sand lost from erosion formed the high offshore bar about 5 cm above initial profile, which was observed in section C I. However, the offshore bar was not found in section C II, the sand lost in nearshore spread evenly across the offshore side. Overall, the response of the beach profile to wave occurred significantly in first 30 minutes wave. Longshore sediment transport was predominant in breaker zone (nearshore), while cross-shore sediment transport mostly took place from the beach foreshore to nearshore.

In the second case (E5), the design of oblique beach was better than case E4. It is essential to notice that the better design of the beach, the closer and similar phenomena it will get from the real condition. As it is seen in Fig. 4.4 at 0 minutes, the contour line indicated that the slope and angle of the beach from bottom to the upper part of the beach was created nicely. Thus, the result of case E5 was expected to be clearer and more distinct. In the case of E5, the water depth was set to be higher 0.25 cm than case E4. As the water depth was increased, the breaker zone was moved slightly landward as depicted in Fig.4.4 at 30 minutes condition of topographic figure. The breaker zone was indicated with low-level contour (+280) around 2.5 to 3 m cross-shore distance. The movement of the breaker zone would influence the response of the beach profile to wave as well.

In C I and C II, the profile response to wave was distinctly different compared to case E4. Without losing much sand or gravel from the beach, the offshore side gained sand supply that deposited across the offshore side. Thus, this might indicate that the deposited sediment was supplied by a longshore current which brought sediment. Like in the case of E4, the phenomenon significantly happened in the first 30 minutes. While, in L I and L II, there were increases in the elevation almost along the section of profile beach, except L I which showed a decrease in the elevation at the left side of the beach (1000 to 0 mm). The increasing indicated that there was a supply of sediment from other side either cross shore or longshore.

If we look at both long section L I and L II graph in Fig. 4.3 and 4.4, respectively, there was significantly different in the changing of profile elevation. In Fig. 4.3 at L 1 and L2 graphs, it described decreasing elevation (eroded) in almost along the section, vice versa the increasing elevation (deposited) occurred in almost along section as shown at L I and L2 graphs in Fig.4.4. The decreasing elevation could mean that the intensity of wave and current motions were high at this section, so the sediment was transported simultaneously and continuously by wave and current until reached out the calm water and deposited the sediment. On the contrary, increasing

elevation at L I and LII means that the intensity of wave and current motions were low (calm water) at this section, so then the sediment would be deposited quickly at this condition.
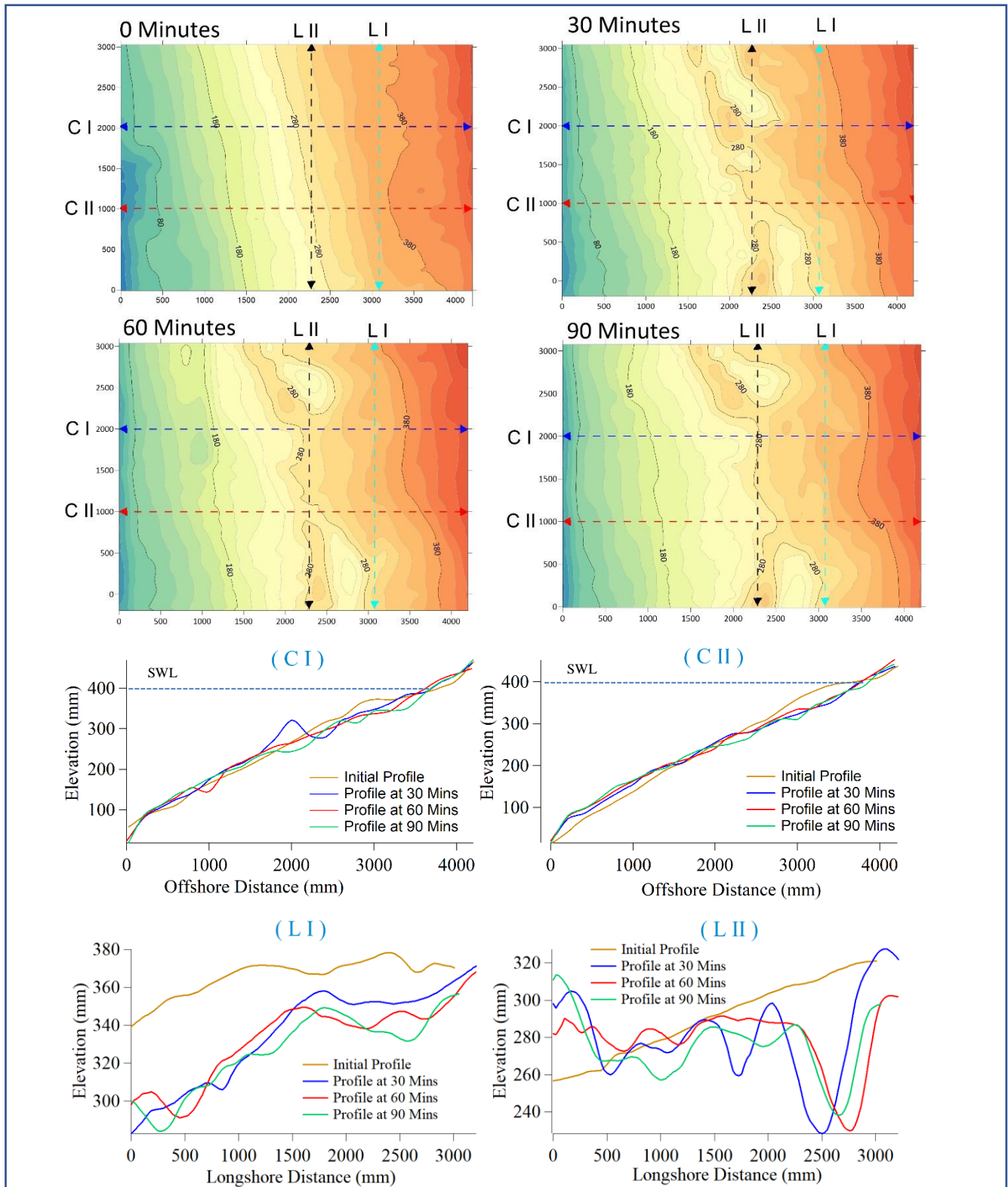
Figure 4.3 Representative sections of topography of case E4
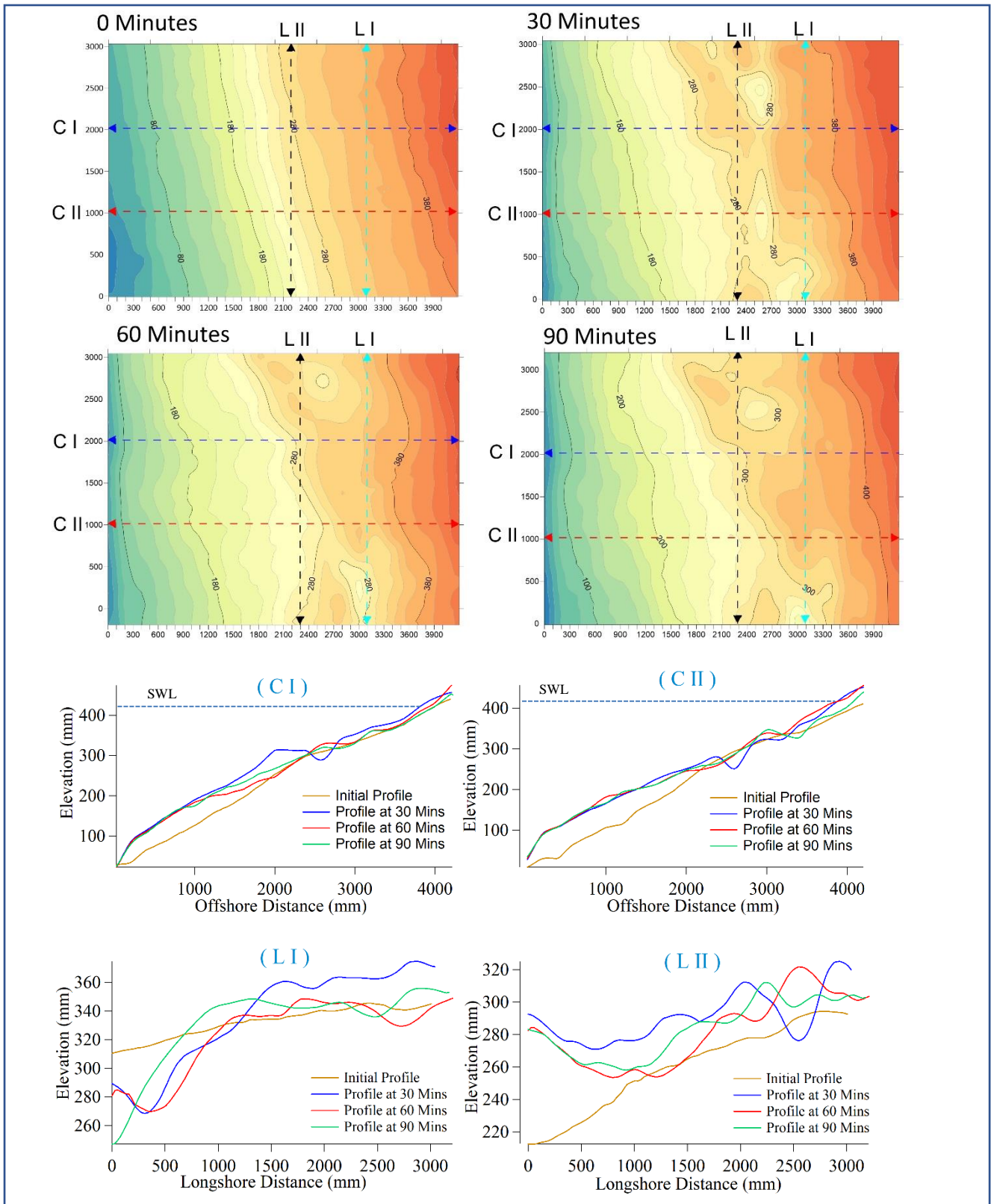
Figure 4.4 Representative sections of topography of case E5

4.4.2. Current and wave condition

The wave and current data were measured simultaneously at two periods: at the initial and final condition. The initial condition means that the measurement was done at the first 3 minutes of wave run, while the final condition means at the last 3 minutes of wave run. The purpose of doing two periods of measurement was to observe the influence of topographic change to wave and current. Figure 4.5 shows the sketch of wave and current measurement. The measurement could not be done parallel to shoreline due to the limitation of the experiment. This typical wave basin is set to conduct beach profile measurement where the beach design perpendicular to the wave, as well as the frame instrument was set-up.

Furthermore, the frame which supported the trolley instrument (profiler) was weighty, so it was tough to set the frame itself parallel to the shoreline. Therefore we defined this condition as the limitation of the experiment. The orange dash line indicates measurement-line, which had 10 points with 30 cm interval. The measurement of current and wave were done simultaneously for about 100 waves (or about 3 minutes) for each point, and then the measurement moved periodically from one point to the other points after about 3 minutes measurement.

The location of measurement-line was selected based on the preliminary test, which initially had three measurement-lines. After several preliminary tests, the author selected only one measurement-line, considering the effectiveness of data used and time efficiency of measurement. The unselected measurement-line did not have a significant impact on analysis. Furthermore, the purpose of this measurement was to obtain the current velocity and wave data as close as possible to the coast, despite coincidentally at the same location to wave breaking zone. The measurement-line selected was located 2.75 m (nearshore) from the wave generator. For the current measurement, X and Y indicate the direction of current propagate. In X direction, (+) indicates that the current moves to the left side of the beach, (-) means that the current moves to the right side (if we look from beachfront view). While in the Y direction, (+) indicates current moves to the upside of the beach, (-) means the current move down the side of the beach.
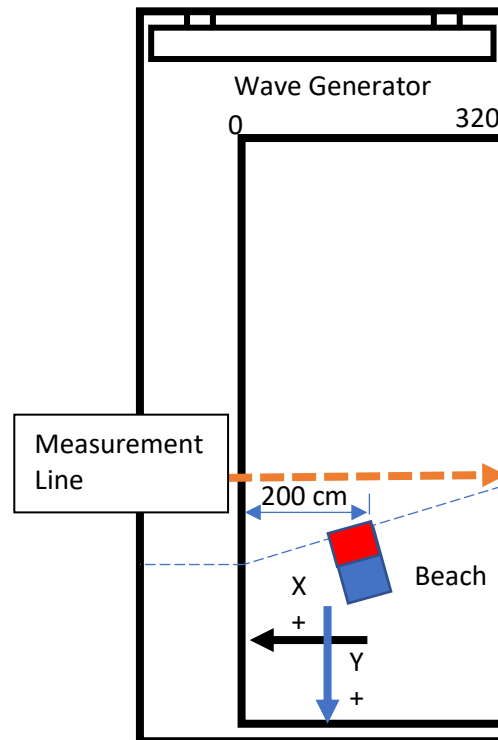
Figure 4.5 Sketch of measurement in 3D wave basin

Figure 4.6 describes the average current velocity in a certain period in X and Y directions. The current in X direction was expected to be higher than the Y direction since the oblique beach was built. Thus the longshore current could be developed successfully. The velocity in the grid area was used to analyze the distribution of gravel through "gridding method," which would be discussed in details the next section. In the X and Y direction, there was an interval time between the measurement of initial and final condition, which was 24 minutes. In between these periods, the topography changed rapidly at a specific location, especially at in the first 30 minutes, so the topography change contributed to either increase or decrease in current velocity in a particular area as well.
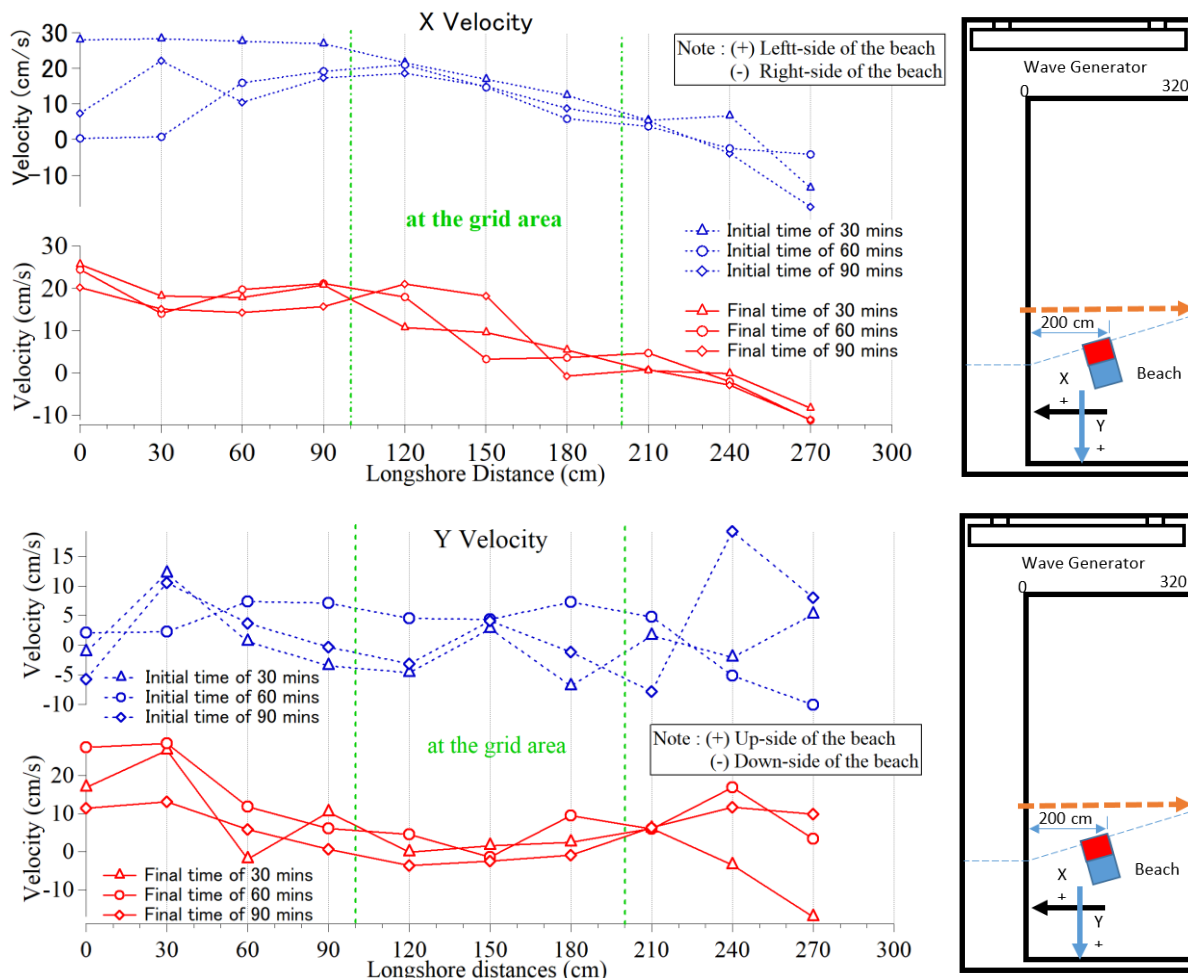
Figure 4.6 Fluctuation of current velocity of case E4

In the current velocity of X direction, the velocity at the initial time of 30 minutes indicated the highest values over the other period of measurement. Moreover, the X velocity increased from the right side to the left side of the beach (2.7 to 0 m) at the initial time of 30 minutes. Despite there was the decreasing velocity of on the left side of the beach (0.9 to 0 m) at the initial time of 60 and 90 minutes, the overall velocity pattern of the current was stable adequate, including in the grid area. On the other hand, the measurement at the final conditions (i.e., 30, 60, 90 minutes) indicated little difference with in the initial condition, especially in the grid area where the current velocity fluctuated significantly by the time compared to another side (i.e., right and left side of the beach).

In the current velocity of Y direction, the current tends to move upside of the beach rather than the downside of the beach during the whole time of wave run, which was indicated by the positive value of velocity. In term of the condition of the measurement period between initial and final condition, there was a different pattern between them. In the initial condition of measurement, at some points (0.6 to 2.1 m) the current velocity increased significantly from

30 to 60 minutes, then decrease a little bit in 90 minutes. While, in the final conditions of the measurement, the current fluctuation was not clear at the first 30 minutes, however, the current velocity along the beach decreased from 60 to 90 minutes conditions. From both measurement conditions (initial and final), it appeared that current velocity on the left side of the beach (0.9 to 0 m) had a higher magnitude compared to the other side. This might be because of the well-developed of the oblique wave which accumulated the current velocity from the right side to left side became higher.

Figure 4.7 shows the current velocity of case E5. Unlike in the previous case, the current velocity of X-direction increased slightly every 30 minutes of initial measurement. Besides, the current magnitude also increased from the right side to the left side of the beach. While the pattern of current velocity in the final time (30, 60, 90 minutes) was almost similar to the initial conditions. The velocity tends to increase in every 30 minutes. Despite of any random decline in some points, the overall current velocity showed the increasing of current velocity from the right to the left side of the beach. Both periods of measurement showed the similarity of current behavior in responding to the topography change. Furthermore, it also indicated that the longshore current developed appropriately.

While in the Y direction, the velocity declined at 60 minutes for both initial and final condition, then in the 90 minutes the current velocity increase into the level between 30 and 60 minutes of measurement condition. In the right side of the beach (2.1 to 2.7 m), the magnitude of current velocity seem high and abnormal, and this could be due to sidewall-effect that located precisely at right end side of the beach. Furthermore, the positive values on the graph indicated that at this location the current move toward the beach was predominant.
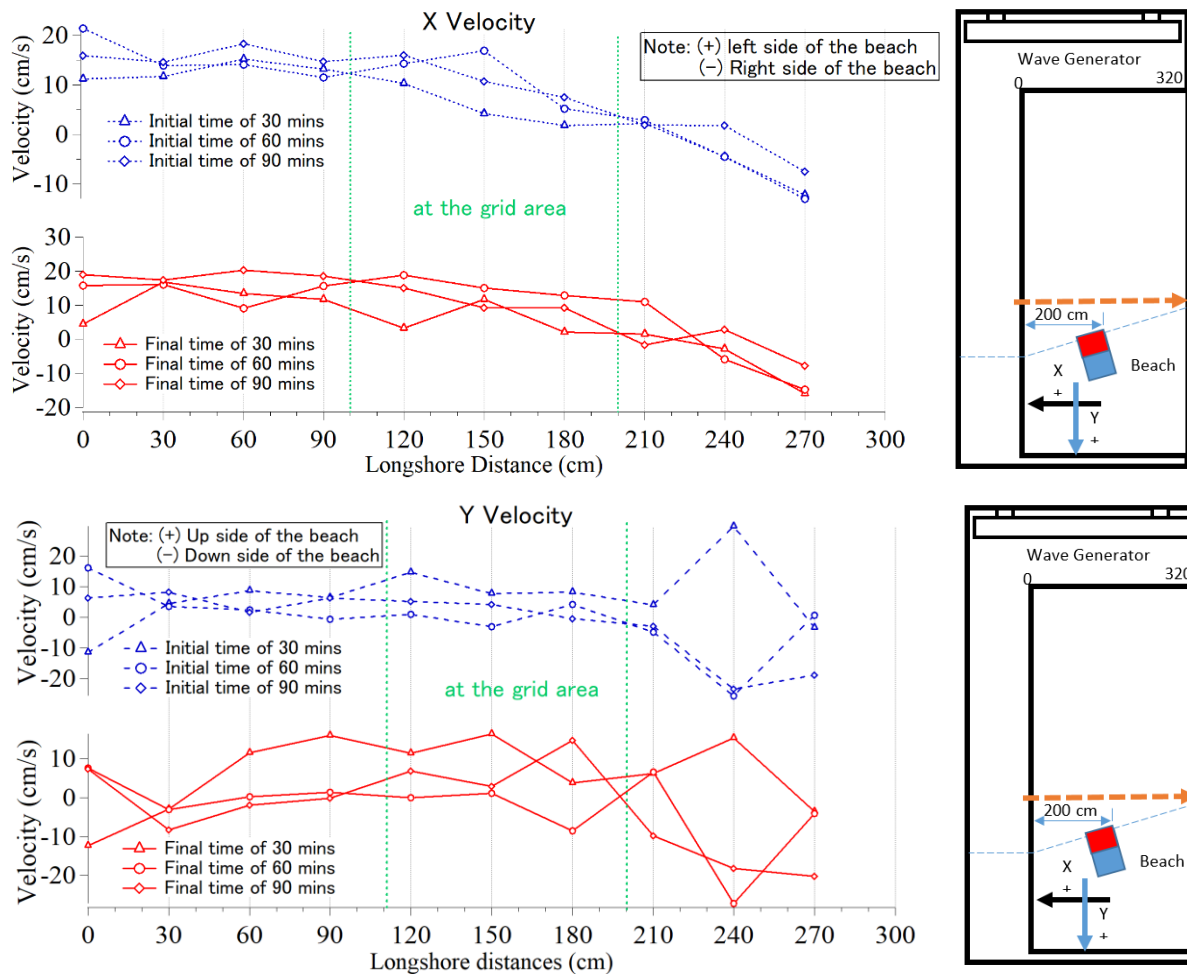
Figure 4.7 Fluctuation of current velocity of case E5

Figure 4.8 shows the distribution of wave height along the beach for case E4. The height of waves on the left side (0.6 to 0 m) of the beach was higher than the middle of the beach to the right side of the beach, except last two points of wave measurement on final time of 30 minutes (2.4 to 2.7 m). The waves in the middle to the right side of the beach were quite stable with a wave height of 7-9 cm. There were different level between the initial and final time of measurement, and this might be due to the effect of topographic change during measurement.

On the other hand, with the higher water depth and the same of the location of wave measurement, case E5 revealed the increasing of wave height in same of the location of case E4 (i.e., on the left side of the beach at 0.6 to 0 m) as shown in Fig.4.9. Moreover, in some other points of measurement, the wave height of case E5 were higher than case E4. Furthermore, unlike case E4, the heights of the waves in the first 30 minutes condition were not dominant, even mostly it becomes the lowest wave height condition. The wave reached the maximum condition in 60 minutes, and then the wave condition decreased in 90 minutes. Therefore, based

on the comparison of two cases, it could be deduced that the increase of the water depth might be contributing to the increase of wave height, regardless of the different topography conditions.
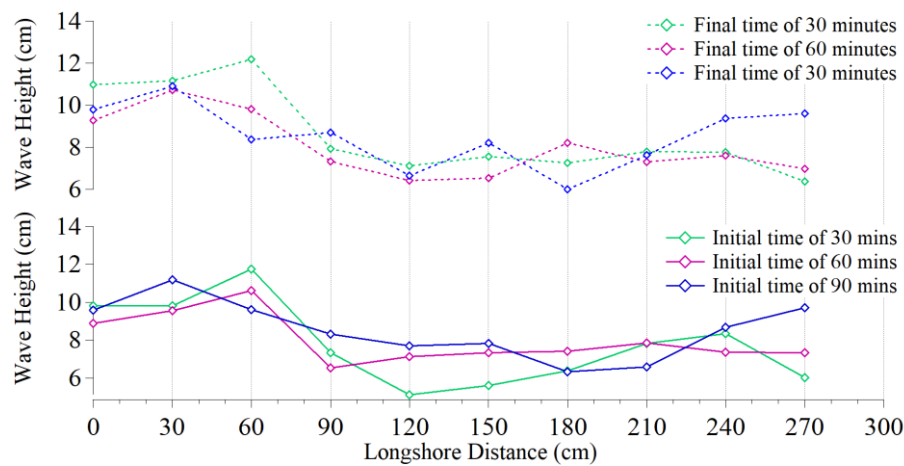
Figure 4.8 Wave height distribution of case E4
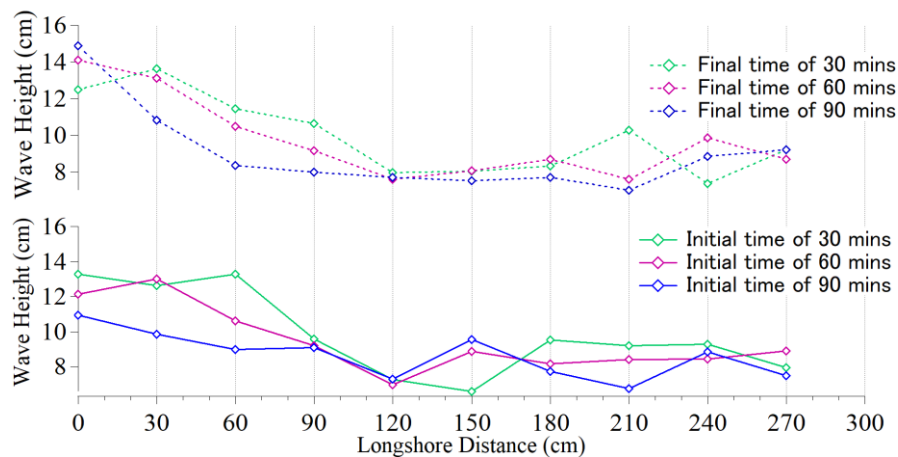
Figure 4.9 Wave height distribution of case E5

4.4.3. Shoreline change

Figure 4.10 shows the shoreline change in the case E4 every 30 minutes after wave generation. Determination of shoreline is based on the topography measured every 30 minutes. The shorelines of 0, 30, 60, and 90 minutes are overlaid in this figure. The contour line with gradation in the figure indicates the final topography map after 90 minutes. In the figure, the blue line indicates the position of the initial shoreline. The elevation of initial shoreline (water line) was at the level of 400 mm. After 30 minutes of wave generation, the shoreline advanced slightly about 10-15 cm on average along the beach. After 60 minutes, the shoreline retreated almost to the same level of initial shoreline. Whereas, after 90 minutes, the shoreline advanced again close to the shoreline after 30 minutes. Furthermore, the erosion took place in the

nearshore area, which indicated by orange-circle. The erosion occurred due to the high intensity of wave plunging at this area.
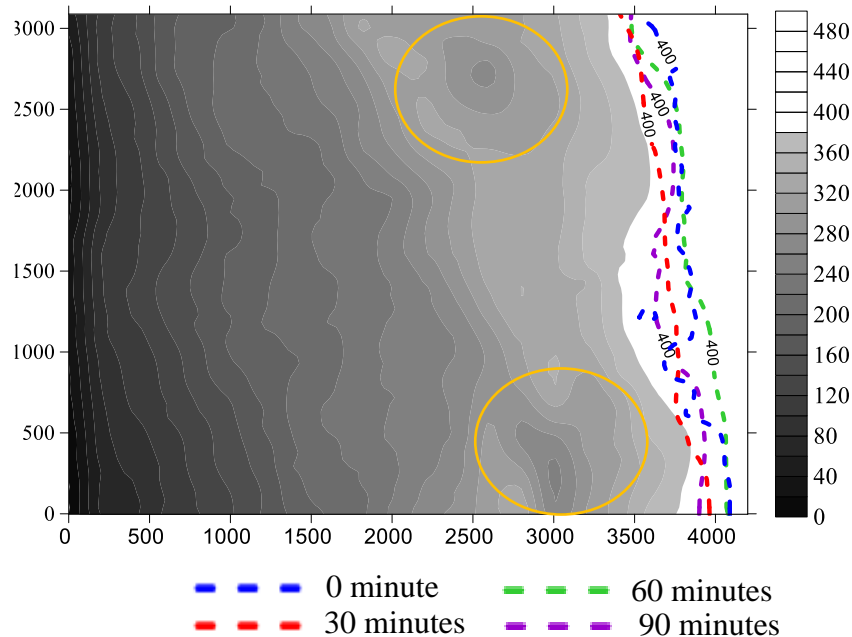
Figure 4.10 Shoreline change and final topography retreat of case E4

Figure 4.11 shows the shoreline change in E5 case. As the water depth was 2.5 cm deeper than the case E4, the elevation of initial shoreline corresponds to the elevation of 425 mm. The initial shoreline in the case E5 advanced a few centimeters in the first 30 minutes and kept moving offshore until 60 minutes after wave generation. However, after 90 minutes, the shoreline retreated slightly and resided between the shoreline of 30 and 60 minutes. On the other hand, the nearshore erosion (orange-circle) seems to move lower back than the case of E4.

As seen in the shoreline change in Figs. 4.10 and 4.11, the topography did not reach the equilibrium even after 90 minutes. This may be due to the oblique incidence of the wave and complicated interaction between the current system in the basin and the beach topography. One of the factors that might influence the topography and shoreline change is the change in wave breaking and associated with the current system. In every 30 minutes, the breaker zone may be changed, which subsequently lead to different position of the swash zone and the current system as well. Furthermore, the effect of increasing water depth was not very clear in shoreline change and final beach topography.
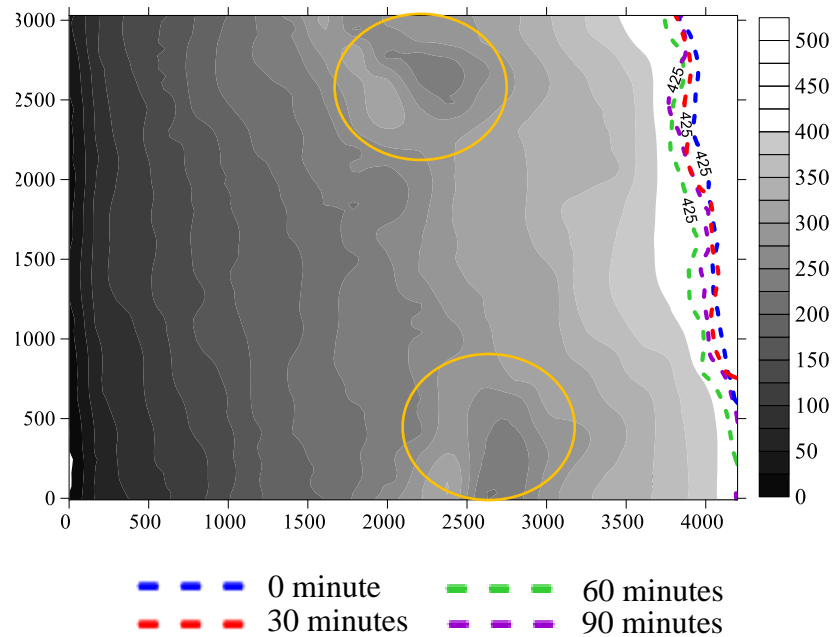
Figure 4.11 Shoreline change and final topography retreat of E5 case

4.4.4. Distribution of colored gravels

As shown in Fig. 4.12, colored gravels were sampled in the grids of 25 x 25 cm. The total area of sampling is 0.94 m^2, which consists of 15 grids. The grids are divided into three sections, namely Upper, Lower, and Toe, which represent the location of distribution along the beach. The location and number of the grid were considered based on the preliminary experiment. Furthermore, the distribution of colored gravel was obtained for each color after 90 minutes of wave generation. Based on the results, a trajectory of gravel transport could be discussed.

Figure 4.13 shows the final results of the distribution of colored gravels over the grid in the case E4, in which the initial shoreline was just between Lower and Toe parts of the grids. The colored gravels were transported continuously alongshore and cross-shore during wave generation. The total transported volume of red gravel was greater than blue gravel. The ratios of blue and red gravels which was transported offshore out of the grid area were 62.2 % and 81.4 % respectively, in the total gravels moved from the original grid. Thus about 37.8% of red gravel and 18.6 % of blue gravel remained in the grid area. The red gravel located lower part of the original gravel area was mainly transported and accumulated offshore.
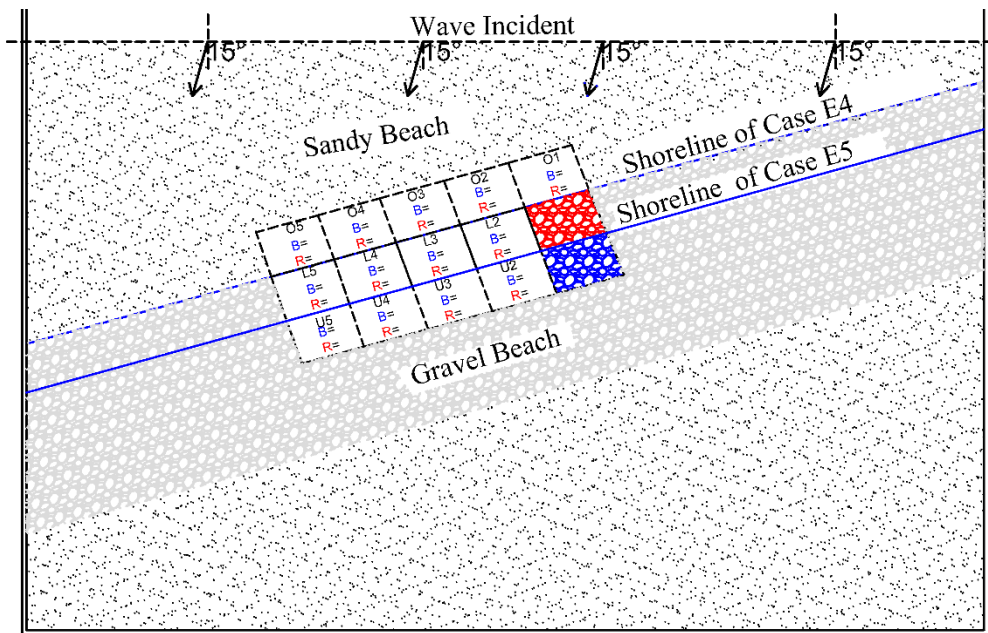
Figure 4.12 Illustration of sampling area
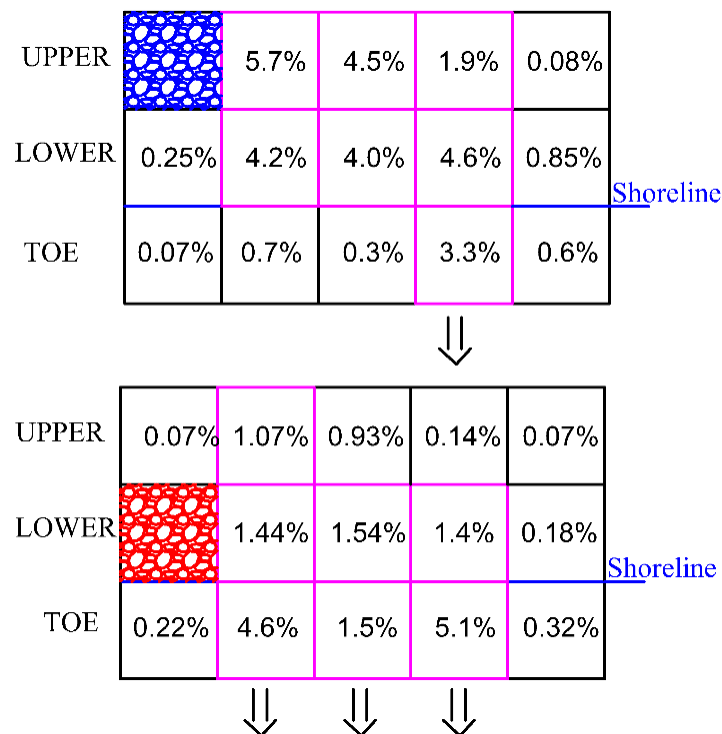
Figure 4.13 Scatter distribution of blue and red gravels in the case E4

In order to investigate the trajectory of gravel transport, the results of colored gravel distribution, distribution of current velocity, and topographic change were employed. The pink color on the grid in Fig.4.13 indicates grids with a high concentration of colored gravels. From the figure, the trajectory of gravel transport could be traced roughly and the arrows in the figure imply the main out flow of gravels from the grid area.
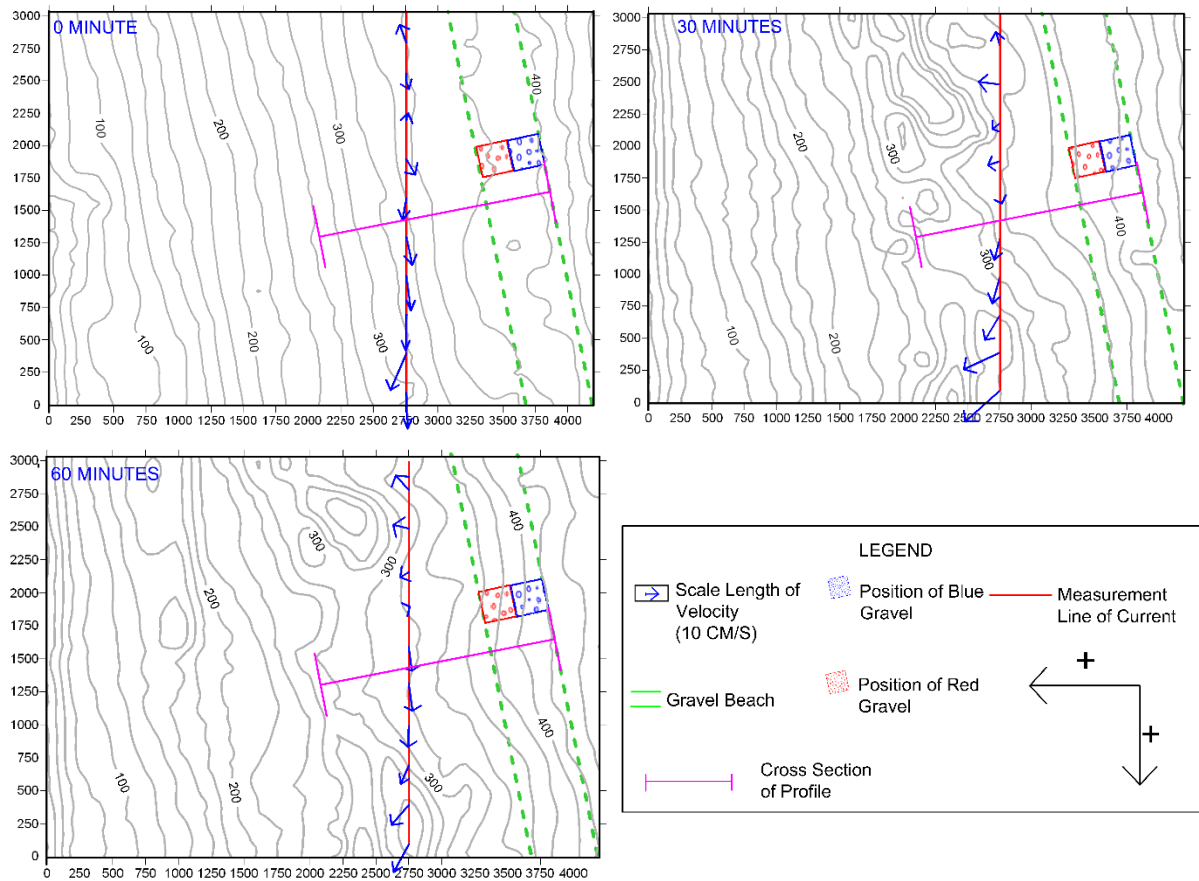
Figure 4.14 Topography and current magnitude in the case E4

Figure 4.14 shows topographic change and averaged current velocity distribution on the indicated line every 30 minutes. From these figures, the current direction in the nearshore region of the grid area tends to be downward (to the bottom axis) because of the oblique incidence of waves. Moreover, the current magnitude is getting greater downward. Although this implies that gravels could be transported mainly longshore, nevertheless the major direction of the gravel movement is offshore, as shown in Fig. 4.13. Figure 4.15 shows the change of the cross-sectional profile along the line indicated by a pink line in Fig.4.14. From the figure, it is found that the profile is getting steeper with time. The formation of the steep profile was due to strong backwash current simultaneously with the roughness effect of gravel shape to the sand layer, which accelerated the erosion process rapidly.

From this profile result, it could be explained how the gravel transport offshore dominantly instead of longshore. Besides, Fig. 4.16 shows the final condition of case E4, in which from the figure it is seen that the gravel spread along nearshore (left side). Therefore, by observing Fig. 4.14 and 4.15, it could be concluded that the gravel transport took place in two directions, which were toward offshore and longshore respectively. When the gravel transported toward offshore from the beach face, the gravel was pulling down to nearshore due

to a steep profile associated with strong backwash current, and then in the nearshore, the gravel transported following longshore current developed due to oblique wave incident.
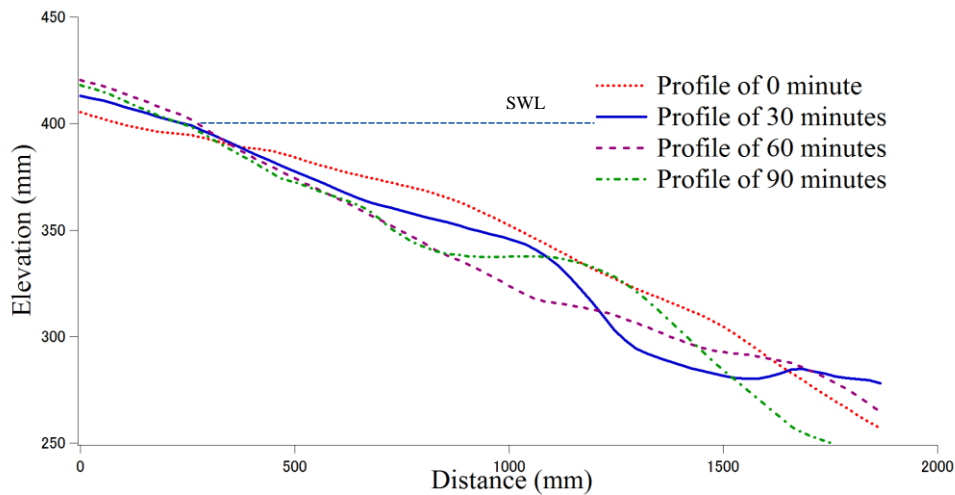
Figure 4.15 Cross-sectional profile in the case E4
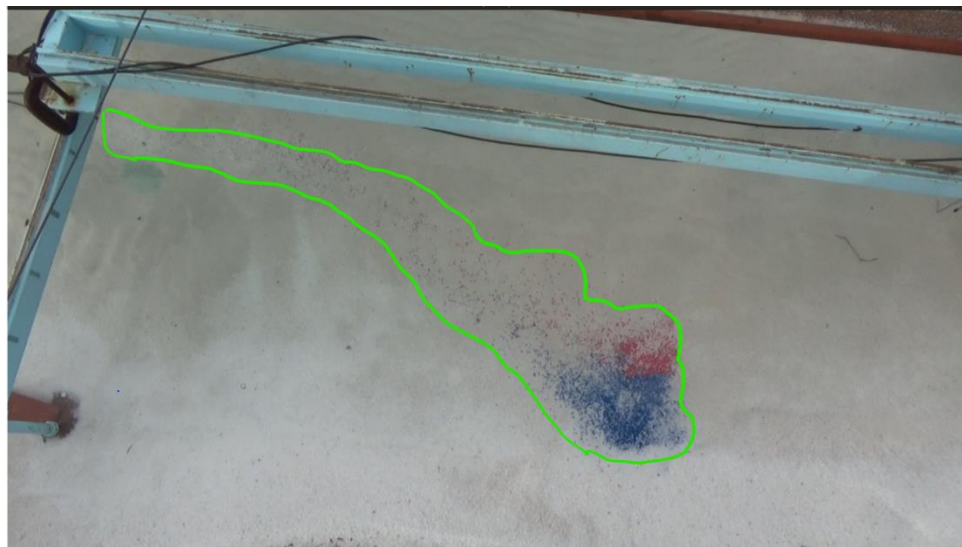
Figure 4.16 Gravels transported in two directions; toward offshore and longshore in Case E4

In the case E5 with a water depth of 42.5 cm, the shoreline is moved up 25 cm from the prior case to the top of the red gravel. As shown in Fig. 4.12, the difference in the shoreline level led to little change in the transportation of colored gravels. In contrast to the case E4, the total transported volume of blue gravel was higher than red gravel. The ratios of blue and red gravels which was transported offshore out of the grid area were 75.6 % and 82 % respectively, in the total gravels moved from the original grid. Thus most of the moved gravels accumulated outside the grid area and 24.4% of blue gravel and 18% of red gravel remained in the grid area. The main trajectory of gravel transport is shown in Fig. 4.17. Similar to the case E4, the dominant direction of the gravel movement is considered offshore as indicated by the arrows.

UPPER		1.96%	0.45%	0.03%	0.04%	Shoreline
LOWER	3.85%	6.34%	1.6%	0.13%	0.02%	
TOE	1.04%	5.6%	3.1%	0.24%	0.02%	

UPPER	0.92%	0.18%	0.12%	0.10%	0.05%	Shoreline
LOWER		4.34%	2.72%	1.9%	0.02%	
TOE	2.93%	3.3%	1.04%	0.33%	0.03%	
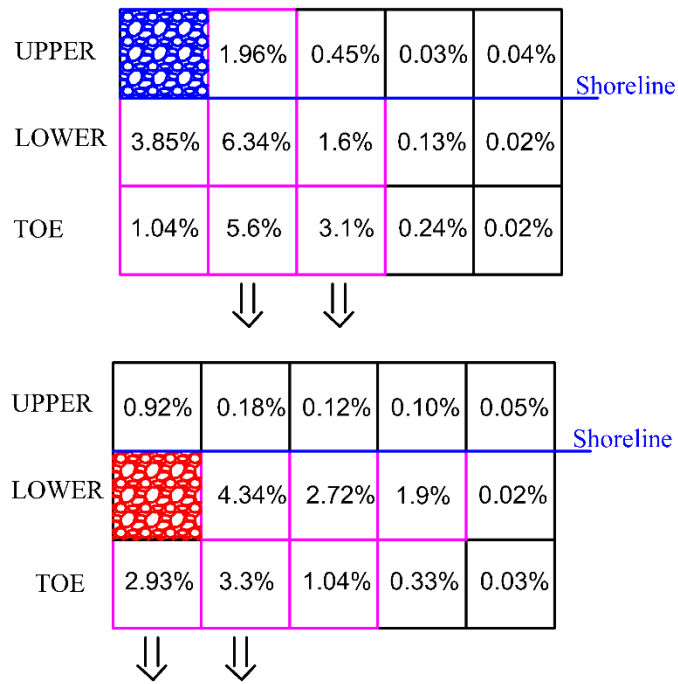
Figure 4.17 Scatter distribution of blue and red gravels in the case E5
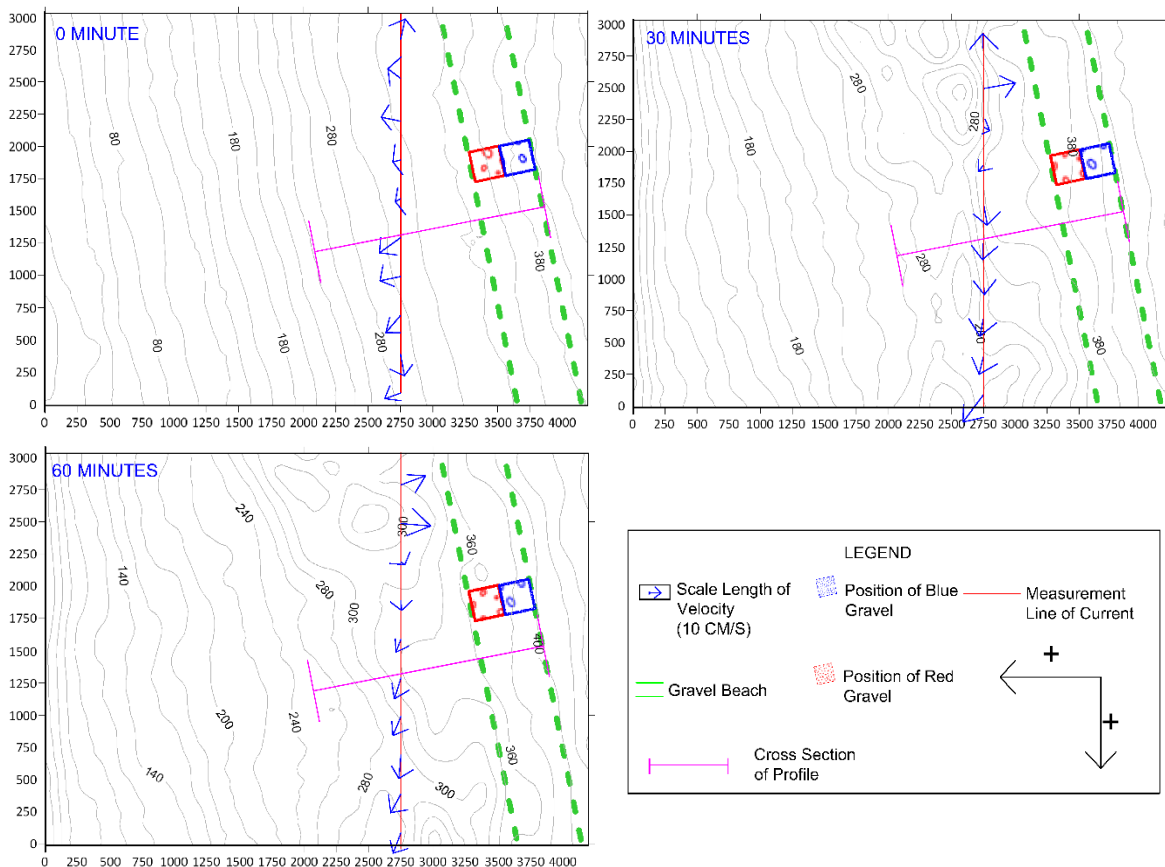
Figure 4.18 Topography and current magnitude in the case E5

Figure 4.18 shows topographic change and averaged current velocity distribution for the case E5. Although the current direction at 30 and 60 minutes is almost downward, the current at 0 minutes is slightly different, where the current direction is predominantly offshore. Figure

4.19 shows the change in cross-sectional profile. In this case, although the profile at initial condition is steeper than others, there is not significant difference in steepness. With such slope steepness, it would be easy for backwash current to pulled down the gravel to nearshore. Thus, the final condition of case E5 could be seen in Fig.4.20. There was not so much difference of gravel movement, the pattern looks similar with case E4.
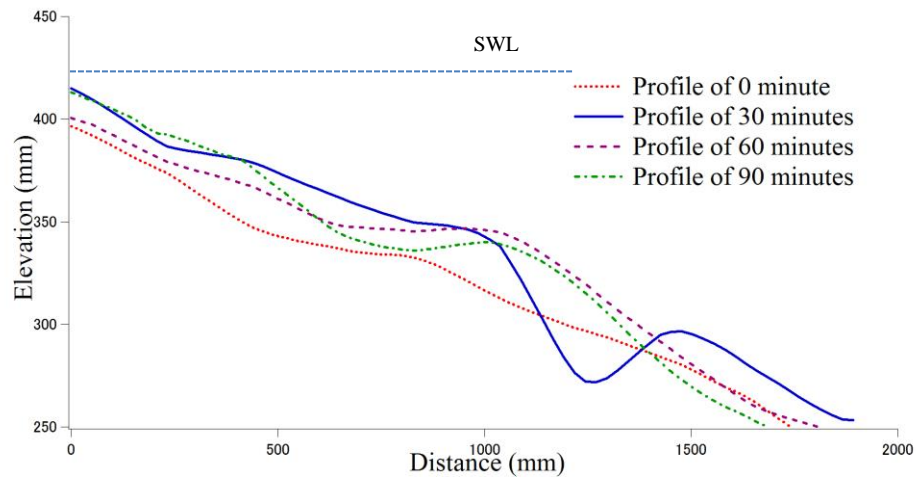
Figure 4.19 Cross-section profile in the case E5
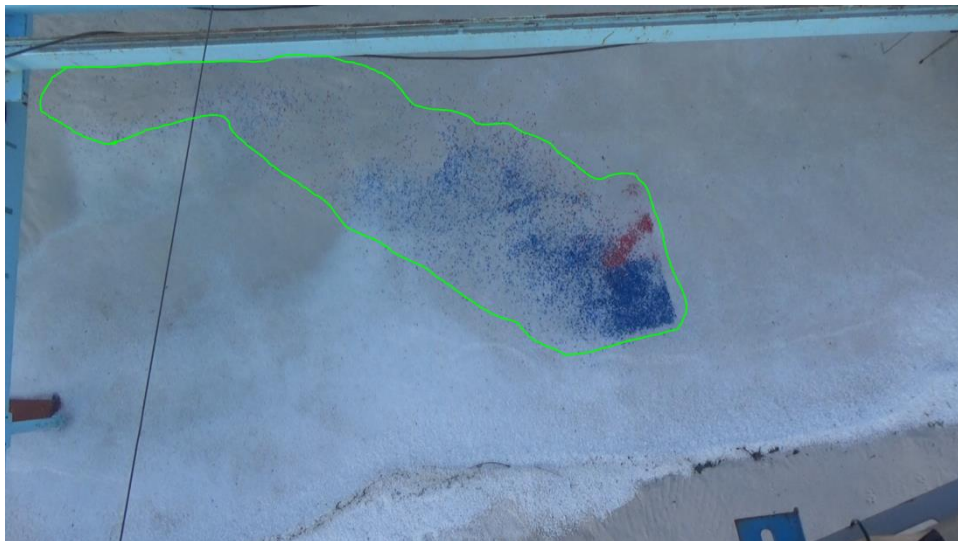
Figure 4.20 gravels transported in two directions; toward offshore and longshore in Case E5

4.5. Conclusions

In this chapter, the movement of the gravel in an oblique condition of wave incidence was investigated under erosive wave condition. The distribution of colored gravels was used along with the results of nearshore current velocity, wave height, and topographic change. Findings in 3D experiments are summarized as follows:

(1) The increase in the water depth led to the different response of topography (profile) change, especially the breaker zone. The breaker zone moves forward toward the beach as the water depth is increased. Consequently, it affects the difference of wave height produced around the breaker zone.

(2) The longshore current is generated successfully nearshore, although the current could not reach the beach area. This phenomenon is proved by the result of X and Y current velocity which indicate the dominant direction movement. The velocity in X direction is little higher than Y direction, which means that either longshore or cross-shore transport (back swash) have almost the same power to transport the sediment.

(3) The colored gravels are transported in two steps; first, the gravels moves seaward as the effect of steep profile formation that associated with strong backwash current, secondly, when the gravel reaches nearshore, the gravel would turn to the left side of the beach in following the longshore current developed.

(4) The difference in water depth enhanced the movement of the upper gravel, but the influence on the characteristics of the movement is not very significant.

(5) The shoreline change along the coast is desperate by the time. The shoreline do not retreat continuously as the wave duration increases, in which it is due to the different topography changing in every time.

References

1.) Komar, PD. (1998). *Beach Processes and Sedimentation 2nd Edition*, Prentice-Hall, New Jersey, 544 pp.

2.) Schoonees, JS., and Theron, AK. (1993). "Review of the Field-Data Base for Longshore Sediment Transport", *Coastal Engineering*, 19, 1-25.

3.) Fredsøe, J. (1993). "Modelling of Non-Cohesive Sediment Transport Processes in the Marine Environment", *Coastal Engineering*, 21, 71-103.

4.) Ahrens, JP. (1990). "Dynamic Revetments," *Proceedings of 22nd International Conference on Coastal Engineering*, ASCE, 1837-1850.

5.) Hicks, BS., Kobayashi, J., Puleo, JA., and Farhadzadeh, A. (2010). "Cross-Shore Transport on Gravel Beaches," *Proceedings of 32nd International Conference on Coastal Engineering*, ICCE, sediment 43, 1-9.

6.) Jenning, R., and Shulmeister, J. (2002). "A Field Based Classification Scheme for Gravel Beaches", *Marine Geology*, 211-228.

7.) Pontee, NI., Pye, K., and Blott, SJ. (2004). "Morphodynamic Behaviour and Sedimentary Variation of Mixed Sand and Gravel Beaches, Suffolk, UK," *Journal of Coastal Research*, Vol. 20(1), pp, 256-276.

8.) Karunarathna, H., Horillo-Caraballo, J., Ranasinghe, R., Short, A., and Reeve, D. (2012). "An Analysis of Cross-Shore Beach morphodynamic of a Sand and a Composite Sand-Gravel Beaches," *Marine Geology*, Vol. 299-302, pp, 33-42.

9.) Masselink, G., Russell, P., Blenkinsopp, C., Turner, I. (2010). "Swash Zone Sediment Transport, Step Dynamics and Morphological Response on a Gravel Beach," Marine Geology, Vol. 274, pp. 50-68

10.) Masselink, G., Russell, P., Blenkinsopp, C., Turner, I. (2010). "Swash Zone Sediment Transport, Step Dynamics and Morphological Response on a Gravel Beach," Marine Geology, Vol. 274, pp. 50-68

11.) Dyksterhuis, PL. (1998). *Cross-Shore Sediment Transport on Mixed Sand and Gravel* (Master Theses). University of British Columbia, Vancouver, Canada

12.) Dawe, IN. (2006). *Longshore Sediment Transport on a Mixed Sand and Gravel Lakeshore* (Doctoral Dissertation). University of Canterbury, Christchurch, New Zealand

Chapter 5

2D Experiment: A Gravel Nourishment on the Sandy Beach

5.1. Introduction

Coastal hazard like storm surge is often a year-round concern for the people who are living around the coast, generating impacts such as flooding, landslide/cliff collapse, and beach erosion. During a storm, the beach system could be changed dramatically due to significant loses of sediment from the foreshore which also is indicated as beach erosion. To deal with a year-round issue such storm surge, which affected to coast area, development of coastal protection is necessary.

In the past two decades, beach nourishment method appeared to offer the solution on eroding coastline problem. Beach nourishment is often least expensive, and it provides a natural seaside environment for coastal communities, even for the animal and vegetation habitat which living around the coast [1]. The approach method based on an artificial addition of sediment of suitable quality to a particular requirement area. Beach nourishment could be applied in many types of beach such as sandy beach, gravel beach or mixed sand-gravel beach.

Several studies have been conducted regarding beach nourishment [2,3,4,5]. Kumada et. al [6,7] had developed a study of gravel nourishment on a sandy beach. The study revealed that gravels friction has better stability than sand material. Yoshioka et. al [8] on a study of beach nourishment using coarse material found that the gravel movement was slower than sand, and the gravel was selectively deposited in the foreshore zone. The research also found that shore protection using the gravel could be achieved with less volume, compared to sand. Therefore, gravel nourishment could be more effective and economically benign option for the long-term project of shore protection

In this study the author is attempting to develop gravel nourishment scheme by conducting two series of experiment separately. In the first series, the gravel is nourished on the upper part of the sandy beach with small and large volume as seen in Fig. 5.1, and in the second series, the gravel is nourished in the offshore with various volumes as seen in Fig. 5.2. The offshore gravel nourishment is a new scheme for shore protection on the sandy beach. Hence, the effectiveness of both schemes is discussed separately through profile result.

5.2. Experiment Setup

The experiments were prepared separately in two series tests. The experiments were conducted in a 2-dimensional (2D) wave flume at Hydraulic Laboratory of Osaka University. The set-up of first and second series experiment could be seen in Fig. 5.1. Details of parameters for the experiment are described in Table 5.1. Median grain size (D_{50}) sand and gravel was 0.15 mm, and 2.3 mm for both experiments series and the water depths were 0.45 m and 0.4 m for the first and second series, respectively.
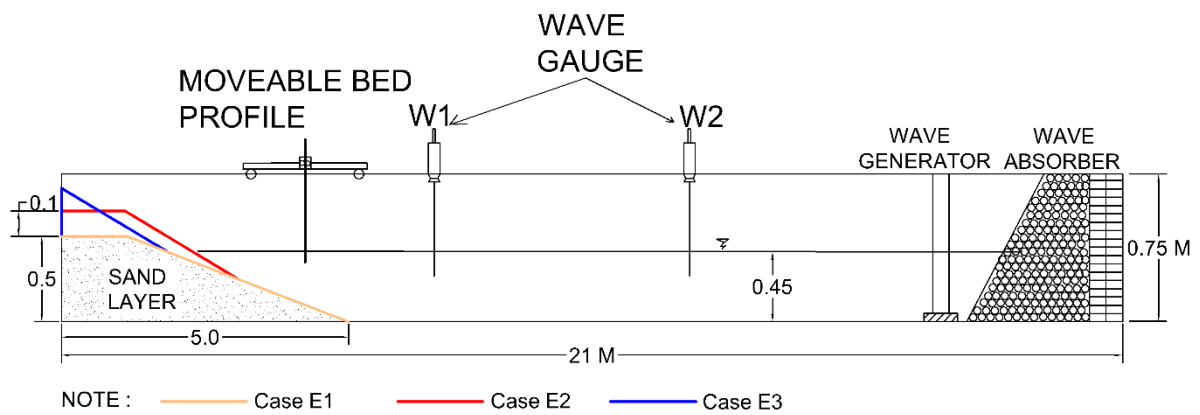
Figure 5.1 Sketch of experimental set up of 1st series
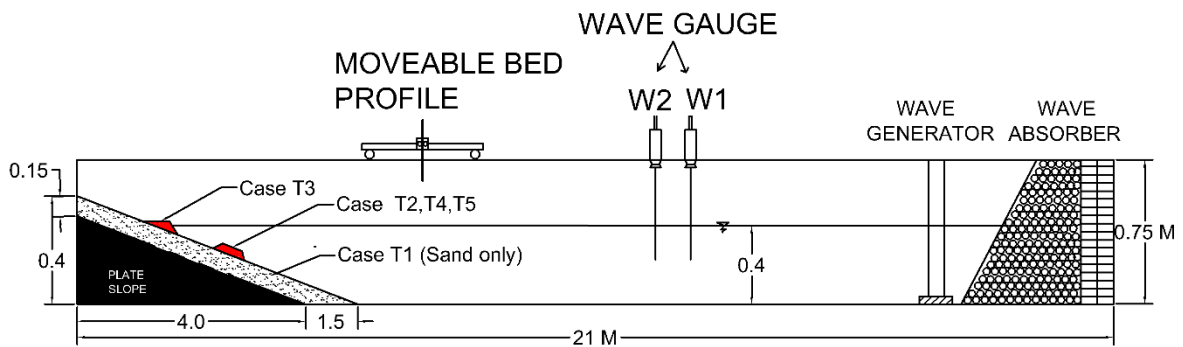
Figure 5.2 Sketch of experimental set up of 2nd series

Table 5.1 Parameters of experiment

Case	Accretive wave (A)		Erosive Wave (B)		Post-storm Wave (C)		Slope		Water Level (m)	Gravel Volumes (m³)
	H(m)	*T(s)*	*H(m)*	*T(s)*	*H(m)*	*T(s)*	*Sand*	*Gravel*		
1st experiment series										
E1	0.05	2	0.14	1	0.05	2	1/10	-	0.45	-
E2	0.05	2	0.14	1	0.05	2	1/10	1/7	0.45	0.09
E3	0.05	2	0.14	1	0.05	2	1/10	1/7	0.45	0.02
2nd experiment series										
T1	0.03	1	0.1	1.4	-	-	1/10	-	0.4	-
T2	0.03	1	0.1	1.4	-	-	1/10	-	0.4	0.01
T3	0.03	1	0.1	1.4	-	-	1/10	-	0.4	0.01
T4	0.03	1	0.1	1.4	-	-	1/10	-	0.4	0.0035
T5	0.03	1	0.1	1.4	-	-	1/10	-	0.4	0.007

5.2.1. Equipment and cases of the first series experiment

Two wave gauges located at 7 m and 18 m away from the wave-maker were used to record instantaneous water surface displacement η (t). The beach profile was measured at 2 cm interval by an optical bottom profiler. The profiler was placed on a trolley and moved manually. The experiment consists of three cases with different wave condition such as accretive (A), erosive (B) and post-storm (C) that was applied in the sequence of each case. The accretive wave is also known as normal wave, erosive is known as destructive wave or storm wave, while the post storm wave is the normal wave which has a role to recover the beach profile from the storm wave. The first case (E1) is the case without gravel, which means the experiment using only fine sand as primary material with the slope of 1/10, i.e., 5 m length and 0.5 m height. The second case was the case with a large volume of gravel (E2). The gravel material was built-up on the sand layer with the slope of 1/7 as shown in Fig.5.1. The third case (E3) used a smaller volume of gravel than (E2) with the same slope. For each case, the profile was measured every 10 minutes after stopping wave generation. The total time of the wave generation was 60 minutes. Also, after measuring the final profile (60 minutes), vertical sampling of sediments was carried out to assess the mixture ratio of sand and gravel distribution. The 14 samples were taken along the wave flume except for the cases of the accretive wave for both cases E2 and E3, since there was no mixture at all in this condition.

5.2.2. Equipment and cases of the second series experiment

Two wave gauges were used to record instantaneous water surface displacement η (t). The wave gauges were located at 7 m and 7.35 m away from the wave maker. The beach profile

was measured at 2 cm interval by an optical bottom profiler. The experiment consists of five cases and two wave conditions such as accretive and erosive, which are generated in order of each case. The first test in the experiment was case-T1, which only use sand (without nourishment). Case-T3, gravel nourishment was built with 0.01 m^3 at the foreshore, while case-T2, T4, and T5 were built in the offshore with the volume of 0.1, 0.0035, and 0.007 m^3 gravel respectively. Gravel nourishment was built-up on sand layer after accretive wave condition, with the intention that gravel nourishment effect in erosive wave could be observed. It prevails for all the cases in this series of the test. Furthermore, in this experiment, the profile was measured every 20 minutes after stopping wave generation. Besides, image analysis was done by capturing some photos in every 20 minutes to observe the distribution of gravel nourishment in erosive wave condition.

5.3. Results and Discussions

5.3.1. Profile response of the waves

The profile result will be explained according to the order of the wave conditions, which are accretive and erosive wave conditions.. Duration of the wave generation is considered as the profile reached equilibrium state (Dean) [9]. The profile discussions in this section are done based on the series of the experiment

A. First series experiment
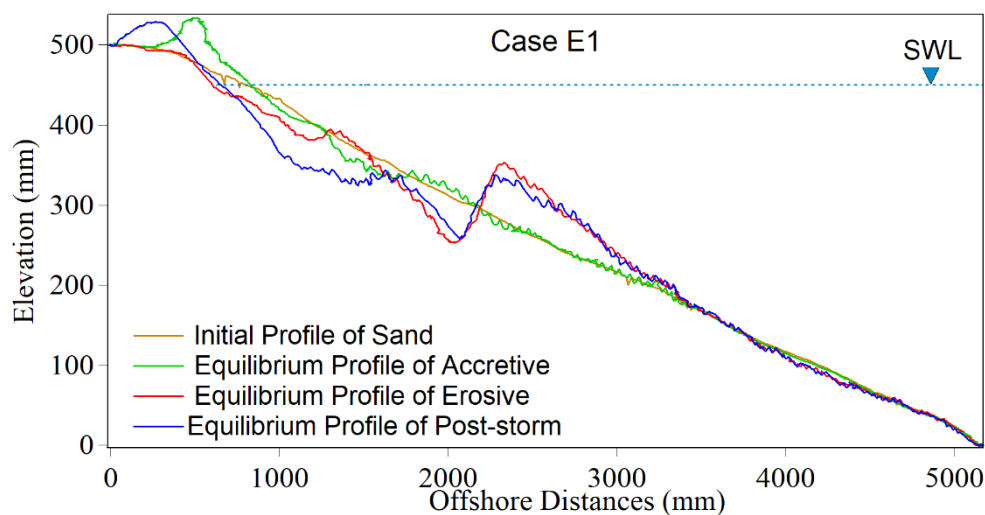
Figure 5.3 Profile evolution in case-E1 under different wave condition

As the first case of the experiment, case-E1 used sand material only without any nourishment process. By having such this case, so then a comparison of the profile evolution with-without nourishment could be discussed. Figure 5.3 illustrates the profile evolution based

on the changing of wave condition. In accretive wave condition, a high sand berm formed in the foreshore and a small erosion in the nearshore. While in erosive wave condition, the profile was changed rapidly in the first 10 minutes and at the equilibrium state, the beach became eroded significantly in offshore and small part along nearshore. Furthermore, the erosion in the nearshore area became considerable during the post-storm condition and formed high berm on the top of the beach. The recovery in this state was not sufficient, where the offshore bar not was eroded nor migrated to the foreshore.
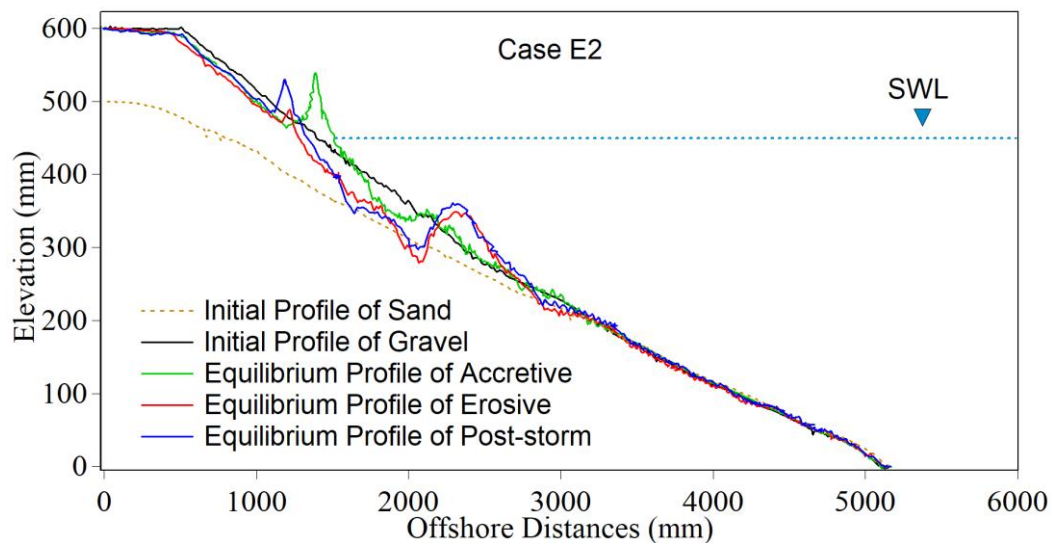
Figure 5.4 Profile evolution in case-E2 under different wave condition

In case-E2, a large amount of gravel nourishment (0.09 m^3) was placed on top of the sandy beach layer. Figure 5.4 shows the profile evolution of case-E2. From the figure, the initial condition of sand and gravel layer could be identified by brown dash-line and black line respectively. In the accretive wave condition, after 60 minutes wave generation, a high gravel berm formed on the beach face followed by small erosion nearshore. While an erosive wave caused considerable erosion from nearshore to offshore and formed high bar about 50 cm (measured from the initial profile at the same point). In same time of erosion period, a high berm, which formed in accretive wave, disappeared. At this condition, it was found that the suspended transport experienced on sand material, while bed load transport on gravels.

Furthermore, there was unique discovering at this state, the gravel layer that designed on the top sand layer, protected the sand layer beneath from direct wave attack, so the sand layer would not experience a great exposure of erosion on the sand layer (i.e., explicitly, it reduces volume of sediment transport). In post-storm condition, the recovery process of the beach was found to be slow. The profile was changed slightly and increased berm high.

In case-E3, the profile response to waves was almost similar to case-E1. In Accretive wave condition, the formation of berm occurred on top of beach face, and slight erosion nearshore. While, in the erosive wave condition, significant erosion took place in offshore which formed a high bar. The bar shape in the case was steeper than case-E1, which might cause the wave plunging in this case was more destructive to the profile than case E-1. Furthermore, the profile was getting steeper in nearshore as the result of strong backwash and carried mostly fine sand away to the bottom troughs. The erosion was also found in the beach face area as the result of the erosive wave. This beach erosion caused the shoreline retreat for some distances.
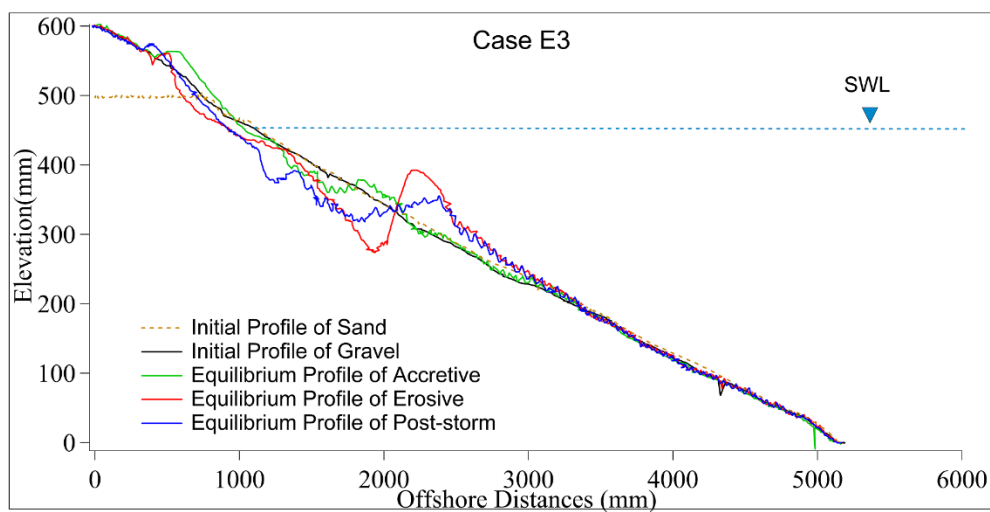
Figure 5.5 Profile evolution in case-E3 under different wave condition

The gravel nourished and designed to protect the beach from the erosion was not sufficient. The placement of gravel nourishment at this position (refer to Fig.5.6) was presumed to be inaccurate and unstable which led the design easy to fail. For future work, the down-edge of gravel nourishment is suggested to be extended lower under the water (sub-aqueous zone) for some centimetre (in this design) to avoid instability and failure of nourishment work. While in the post-storm wave condition, the recovery seen from the initial profile with a deep trough. The offshore bar was diminished and spread over nearshore. The deformation of the bar could be an essential factor to determine how the beach recovery works under post-wave condition.
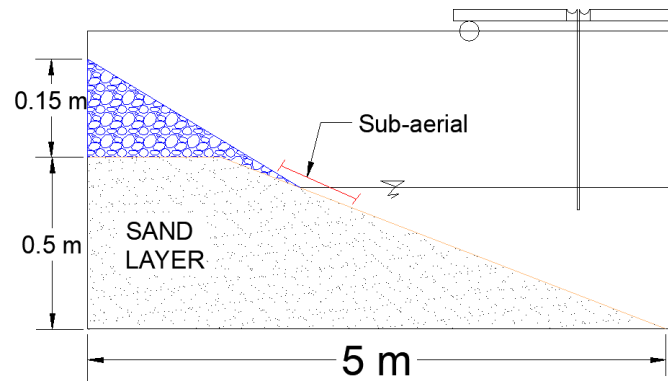
Figure 5.6 Gravel nourishment design of case-E3

B. Second series experiment

In the second series of the experiment, the wave conditions used were accretive and erosive. The focus on this experiment was specified in the effectiveness of gravel nourishment against the erosive wave. As the first case in this experiment, case-T1 represented sandy beach without any nourishment works on it. Figure 5.7 illustrates the profile evolution under the accretive and erosive wave. The profile in accretive wave did not change much during 60 minutes, while immediately after the erosive wave height was increased, the profile changed rapidly in the first 20 minutes. The offshore bar was formed with a deep trough and the shoreline retreated away which followed by erosion along nearshore.
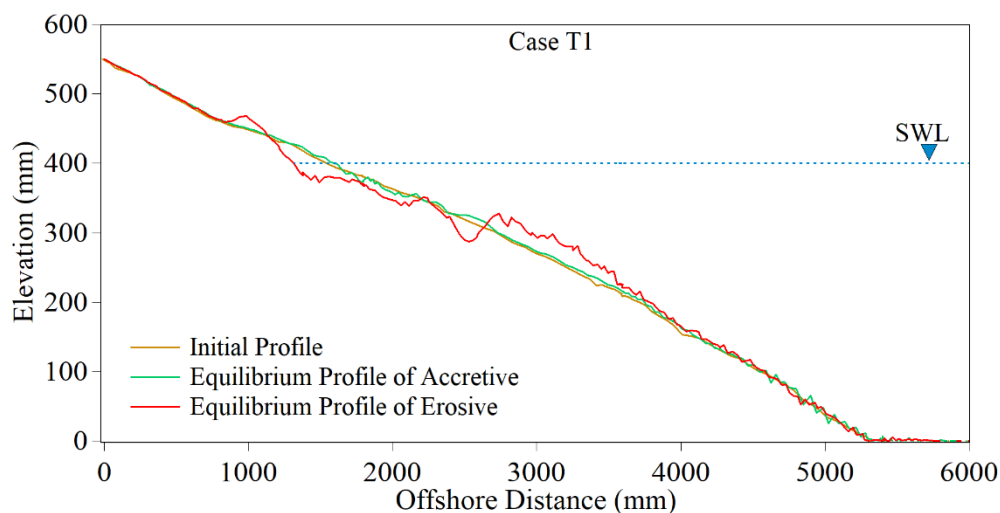
Figure 5.7 Profile evolution in case-T1 under different wave condition

In case-T2, 0.1 m^3 gravel nourishment was placed 68 cm away from the initial shoreline. The nourishment was designed after the accretive wave condition. This set up prevailed to the cases of T4 and T5 as well. The profile response to accretive wave was slightly small. A minor erosion was found along nearshore as shown in Fig. 5.8. In the erosive wave condition, the gravel nourishment was wiped out and spread along nearshore to beach face (refer to Fig. 5.26).

An offshore bar and erosion along nearshore were formed as the result of the wave attack. Furthermore, the shoreline retreat was slightly smaller than case-T1 (without nourishment), the gravel nourishment was trusted contributes to shore protection. The gravels which wipeout along nearshore to beach face during wave run was able to be armor for the sand layer beneath and protect the shore from severe receding. Details about the distribution of gravel nourishment will be explained in the next section.

In case-T3, with the same volume of case-T2, the gravel nourishment was set up in the beach face area as shown in Fig. 5.2. The nourishment was done after accretive wave condition as the other cases. From Fig. 5.9 it can be seen that the shoreline receded a little bit in after accretive wave condition. Furthermore, apart from the area of shoreline retreat was fill-up by gravel nourishment. The gravel nourishment was not able to protect the beach from erosion. The nourishment area collapsed and dispersed adjacent swash zone (refer to Fig. 5.26). A thin gravel layer remained after the first wave (20 minutes) could not able to restrains the next wave hit. As a result, the shoreline receded for couple centimetres in the final state. Moreover, the offshore bar was formed with a deep trough as case-T1, but with less volume of sand along the offshore (by looking at profile result). The response of profile in this case is similar to case-E3 in the first series experiment. The location of nourishment for both of the cases (case-T3 and case-E3) were set up in the beach face. Both of nourishment works were not suitable to use in protecting the beach from erosion.
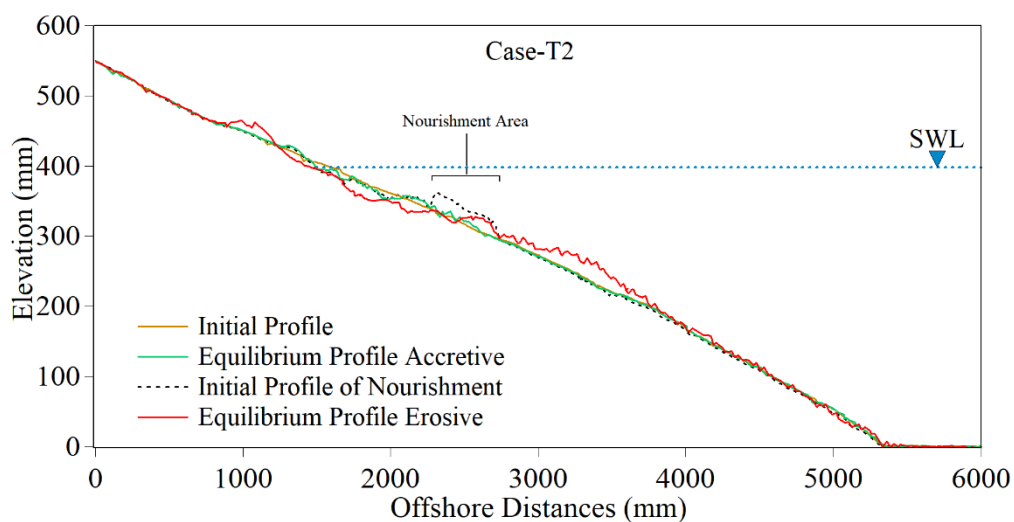
Figure 5.8 Profile evolution in case-T2 under different wave condition
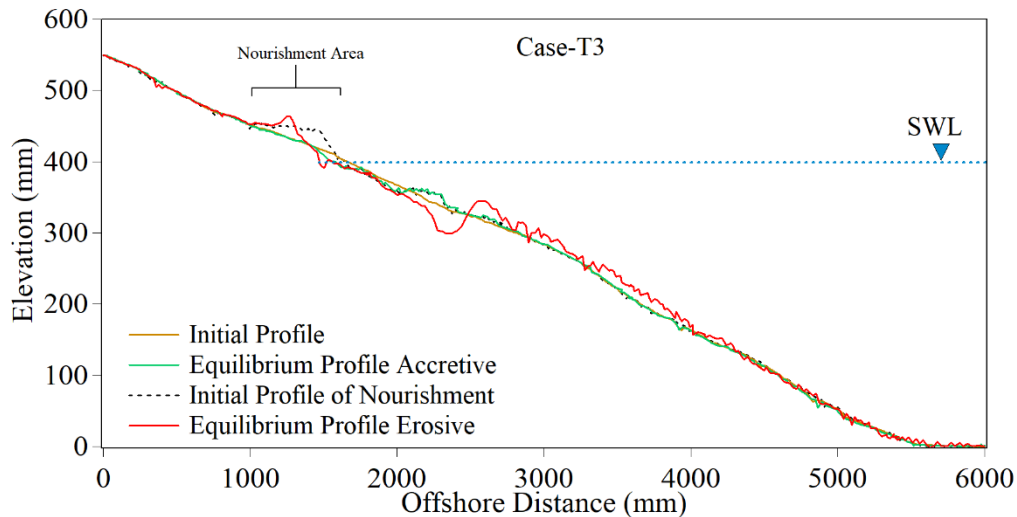
Figure 5.9 Profile evolution in case-T3 under different wave condition
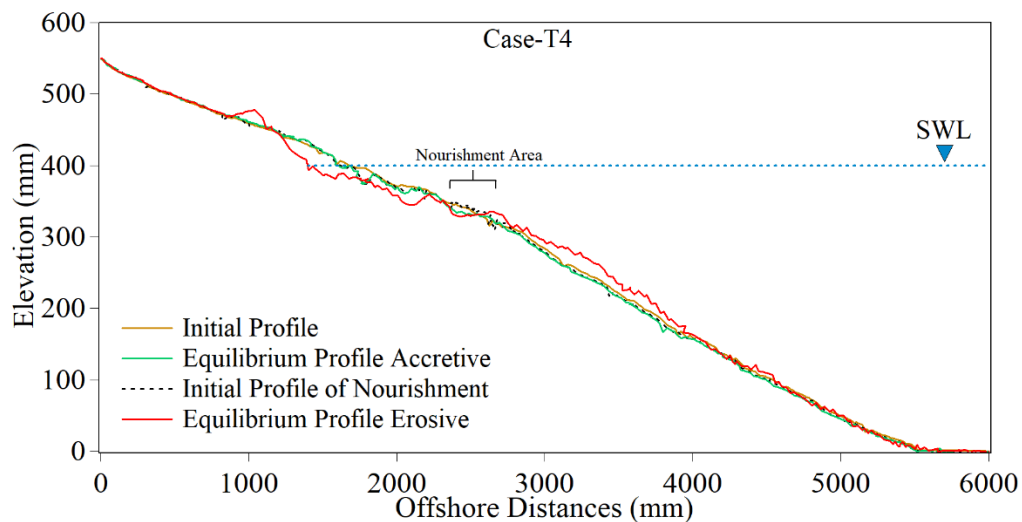
Figure 5.10 Profile evolution in case-T4 under different wave condition

In case-T4, the nourishment volume used was 0.0035 m^3. By looking at Fig. 5.10, the response of profile to the wave was not significant. The erosion was still considerable on beach face, and it spread along the nearshore area. This phenomenon is similar to case-T1, Fig.5.11 reveals that for both cases produced high steep beach profile. It may be strongly related to the wave uprush and down rush near the water line. With such profile shape, the down rush could be stronger than uprush. As a result, it carried fine sediment away to the bottom of the offshore. On the other hand, the protected area was discovered only adjacent nourishment-works. The profile evolution adjacent nourishment-works was quite low, compared to the other cases in the same position. Moreover, there was no high bar formed in offshore.
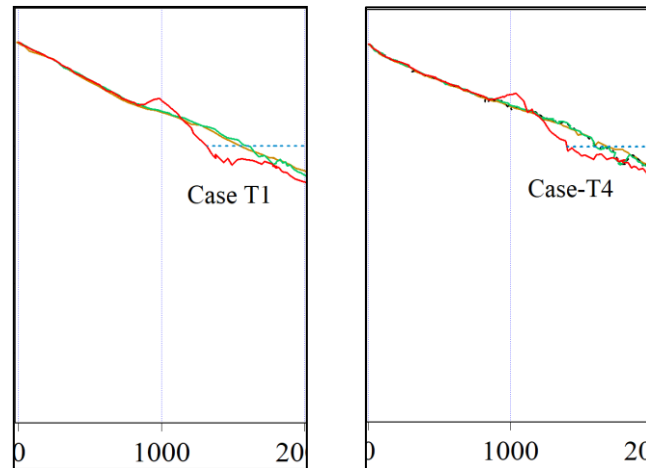
Figure 5.11 Comparison steep beach profile between case-T1 and case T-4

In case-T5, with nourishment volume was twice than case-T4, the effect after nourishment-work was sufficient to protect nearshore to offshore from erosion. However, the problem came over the beach area which erosion took a place. Therefore, based on the profile result of five cases, it could be deduced that the nourishment-work is conditional. It depends on what location is required a protection the most. If we prefer to protect the beach area, case-T2 and case-T3 could be the option, case-T5 is fit for nearshore-offshore protection. Whilst, case-E2 is quite compatible to protect the beach-nearshore area for long periods, however it will change characteristic of the beach from sandy beach to gravel beach and it requires huge amount of gravels material (i.e. increase on the budget as well).
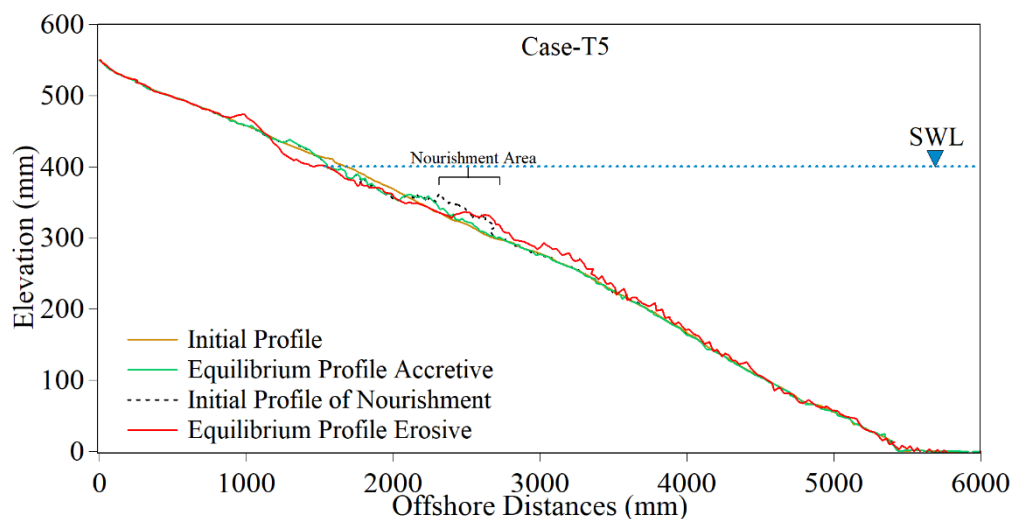
Figure 5.12 Profile evolution in case-T4 under different wave condition

5.3.2. Shoreline retreat

In this section, the shoreline change was discussed by comparing profiles between the initial and final state at the waterline as illustrated in Fig. 5.13. The duration of shoreline measured was corresponding to the wave duration of each series of the experiment.
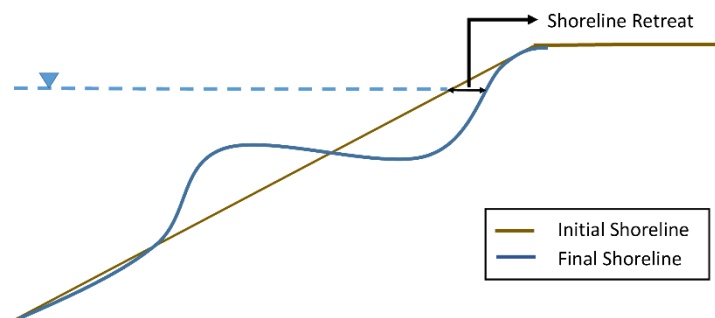
Figure 5.13 Illustration of shoreline retreat

A. First series experiment

In this section, the shoreline was measured every 10 minutes which indicated by a doted mark in the figure below. Figure 5.14 shows the mobility of shorelines of the cases in responding to wave change started from accretive, erosive, and post-storm. Positive and negative values on the graph indicate the shoreline advance and retreat respectively. By comparing all cases, the case E3gives the unfortunate result over all cases, while case E2 on the contrary. In the case of E3, the shoreline retreated immediately after 10 minutes, even with accretive which categorized small wave. This condition continued until the shoreline receded 192 cm from the initial position at the final state. The post-storm wave did not give the proper response to recover the beach from shoreline receding. The recovery state was found to be low in this case. This could be due to the steep profile formed in the nearshore.

Vice versa, the case E2 shows a promising result over the others. The shoreline tends to move forward (advance) 120 cm during an accretive wave. In the erosive wave, the shoreline receded rapidly in the first 10 minutes and became low in the remaining time. It reveals that the gravels nourishment built in case E2 was successfully implemented. The gravel in this case is capable of reducing shoreline receding (beach erosion) during extreme wave attack.

Furthermore, the beach recovery (post-storm state) seems to work favorably in this case. The shoreline tends to move back almost into the initial condition (i.e., indicated by blue dash-

line at 0 points). While the case E1 describes a similar pattern with case E2, but with the lower rate for all wave conditions.
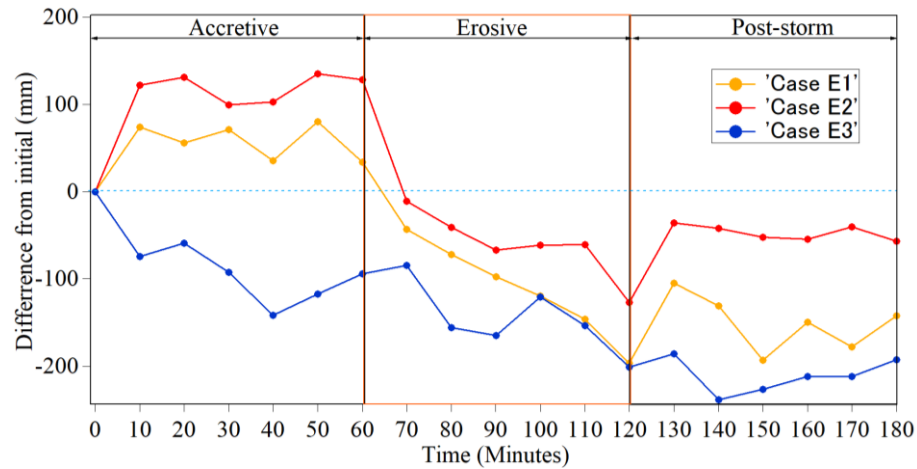
Figure 5.14 The comparison of shoreline change of first series experiment

B. Second series experiment

The shoreline measurement in the second series experiment was different. The shoreline change was estimated after nourishment done (after accretive wave). The effectiveness of nourishment was considered based on which cases provided the optimum result against shoreline retreat. Figure 5.15 describes the comparison of shoreline change overall the cases. From the figure, it is seen that case-T5 gives a preferable result than the other cases. Immediately after nourishment, the beach could hold back the shoreline from the wave attack which might cause severe shoreline recession like the others cases (e.g., Case-T1 to T4). Case-T5 adequated to protect the shore in almost 60 minutes wave before it receded at the last moment with a minor number. However, these results prevail only for shore protection, neither nearshore nor offshore.
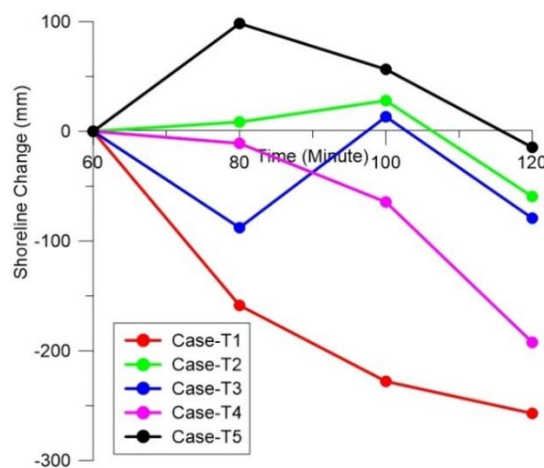
Figure 5.15 The comparison of shoreline change of second series experiment

5.3.3. *Net sediment transport rate*

Net sediment transport was evaluated by comparing beach profile change every 20 minutes. By using a conservative mass equation (see Eq.3.8 in Chapter 3) sediment transport could be estimated, where λ is the porosity and has the value of 0.3~0.4. Therefore, the net sediment transport rate Q over a time duration Δt of wave action is evaluated from the bed elevation change Δh during the same period. Moreover, in this discussion, classifications of "equilibrium transport rate distribution" were determined based on Larson and Krauss [10] theory as follows;

    a. Erosional (Type E); transport directed offshore along with profile.

    b. Accretionary (Type A); transport directed onshore along with profile.

    c. Mixed accretionary and erosional (Type AE); transport directed onshore along the seaward part of the profile and transport directed offshore along shoreward part of the profile.

  A. First series experiment
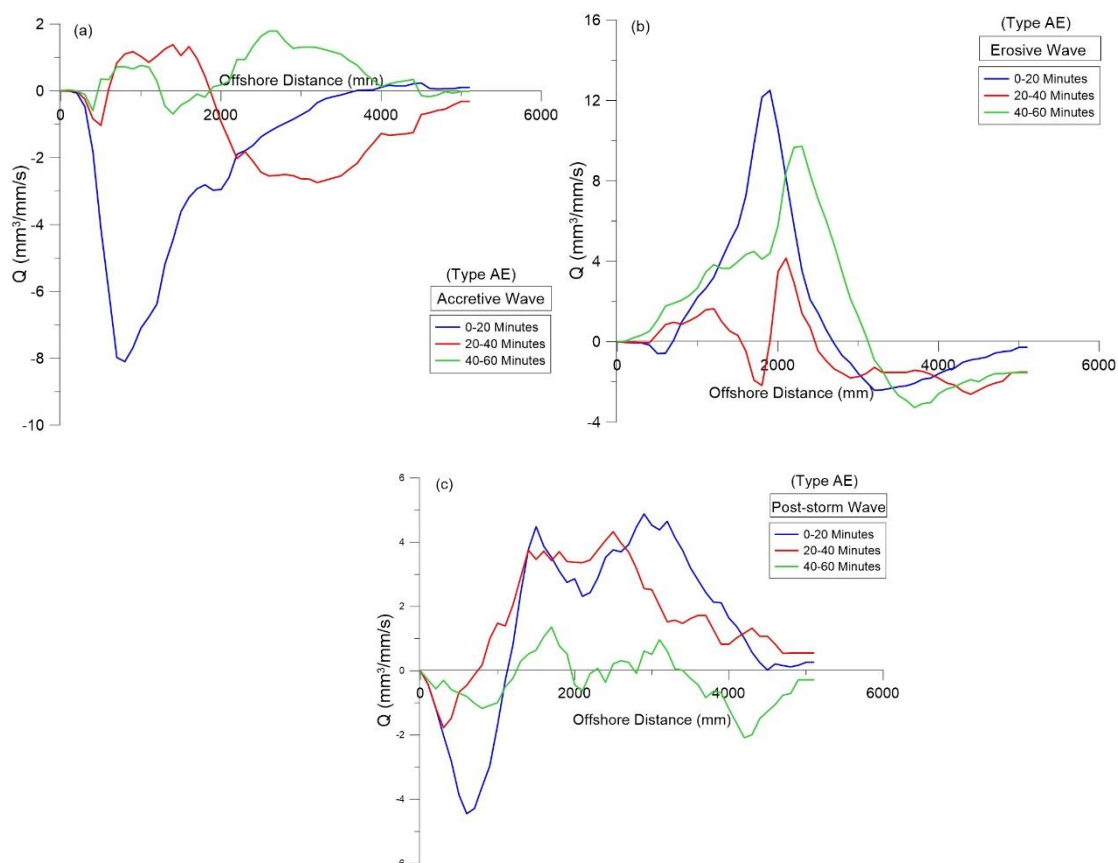
Figure 5.16 Net sediment transport of case-E1

Figure 5.16 shows the spatial distribution of net transport rate Q of case E1. Positive values of Q indicates the net transport toward the offshore direction, while negative Q means the onshore direction. From Fig. 5.16 above reveals that the offshore transport is dominant in the erosive and post-storm wave, while onshore transport takes place in accretive wave condition. Furthermore, the maximum transport rate occurred in the first 20 minutes, and this prevails for all wave condition. The transport rate in every 20 minutes was dissipated. In accretive and post-storm wave condition, the transport rate decreasing by the time, while in the erosive wave the minimum transport rate occurred at 40 minutes wave generation. Moreover, the classification of the equilibrium rate of case-E1 was identified as Type AE.
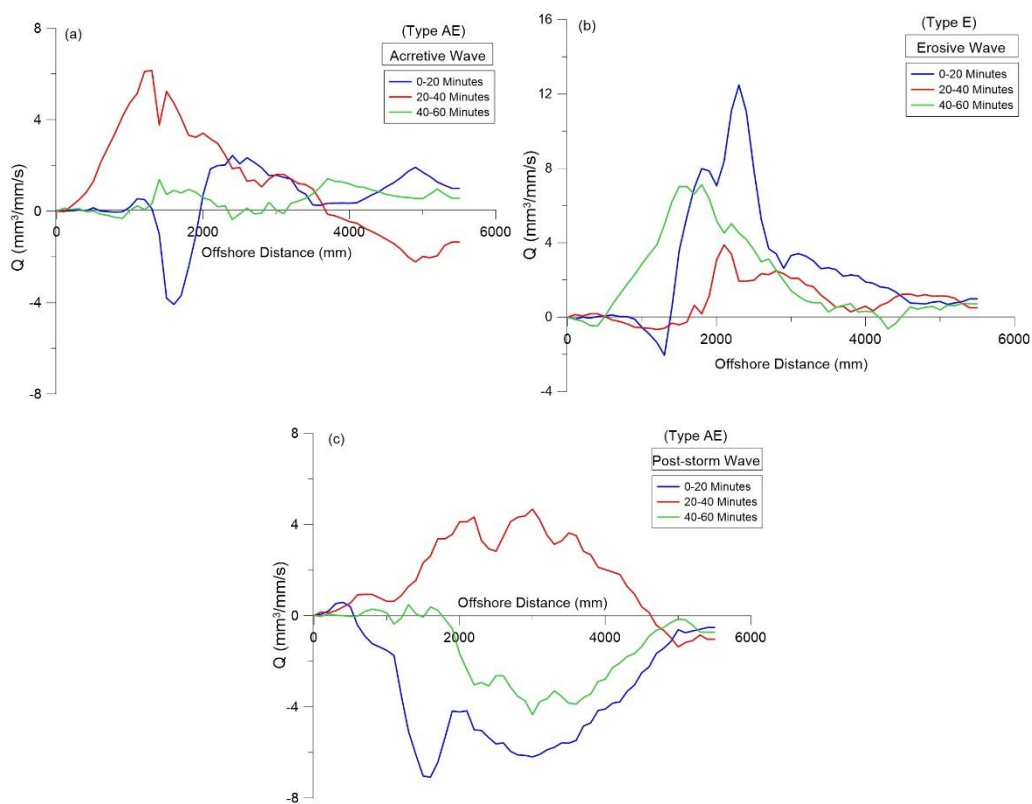
Figure 5.17 Net sediment transport of case-E2

In case-E2, it describes different behavior with case-E1 as shown in Fig. 5.17. The case started with an accretive wave which showed onshore transport predominant nearshore in the first 20 minutes, then in 20 minutes after, nearshore sediment transported offshore and rest of the time the rate became low. It indicates that beach erosion occurs at 40 minutes, despite the accretive wave condition. In erosive wave condition, the rate transport distribution point out the same pattern with case-E1 (Fig. 5.16 b), the peak rate occurred in first 20 minutes, decreasing dramatically in the next 20 minutes and the end of wave run, the rate increased with average was 1.98 mm^2/mm/s or twice higher than average rate in 40 minutes. While in post-

storm condition, inconsistency in transport direction was found. The onshore transport dominated in the first and the last of 20 minutes, while offshore transport occurred in the 40 minutes. Furthermore, the equilibrium transport rate in accretive and post-storm condition was classified in Type AE, while the erosive condition was Type E.
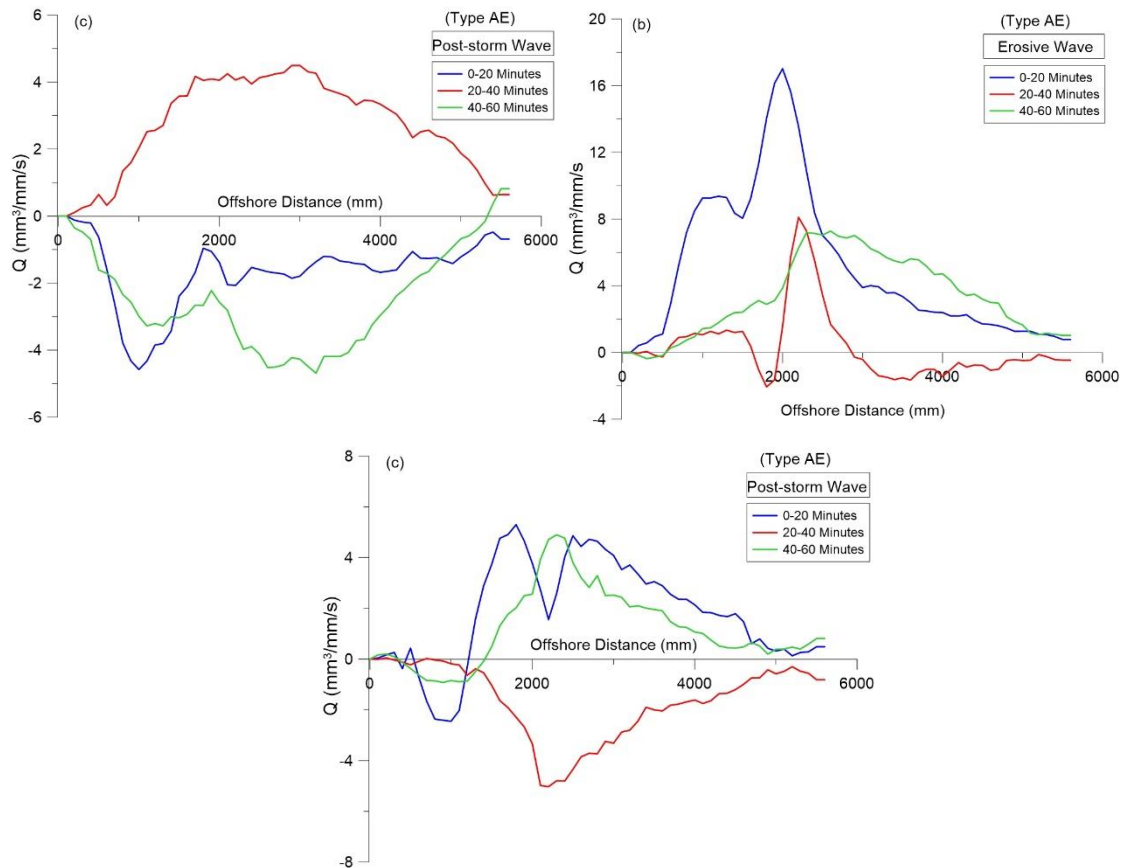
Figure 5.18 Net sediment transport of case-E3

In the last case of the first series experiment, the transport rate of case-E3 showed a balance in transport sediment process as shown in Fig. 5.18. In accretive wave, onshore transport rate dominated in the first 20 minutes, 20 minutes later the direction of transport rate was moved significantly offshore before recovery process occurred in the last 20 minutes which indicates onshore transport took place at this period. In erosive wave, the pattern was the same, but the direction was opposite. In this condition, offshore transport dominated in an almost whole period. Offshore transport initiated in the first 20 minutes. While in the second of 20 minutes, two directions of opposite transport occurred which were nearshore-offshore (minor) and offshore-nearshore (major). Then, the onshore transport direction was controlled fully in the last 20 minutes. On the other hand, in the post-storm wave condition described almost

similar pattern with the erosive wave, it was just onshore transport rate dominated in the second of 20 minutes.
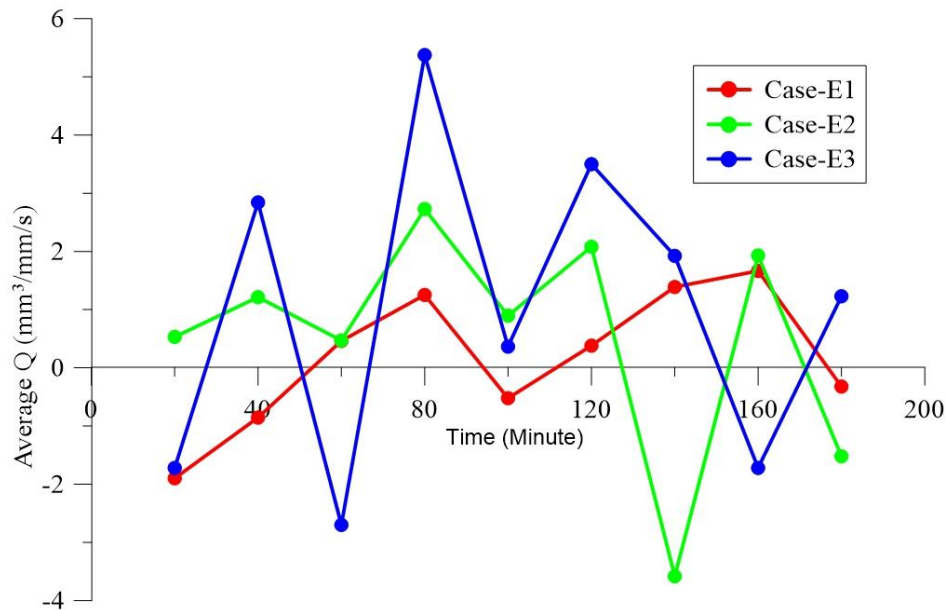
Figure 5.19 Average transport transport overall cases

An average of transport rate of each period of time was estimated to compare all those three cases above which shown in Fig. 5.19. The figure illustrates an average transport rate in succession time from accretive, erosive and post-storm. In this figure, case-E3 had a higher rate on average overall the case, and it mostly dominated offshore transport rate. While case-E2, the fluctuating change in this case was not significant like case-E3, except in 140 to 180 minutes (post-storm condition) which fluctuated dramatically. In case-E1, the distributions of transport rate were scattered evenly between onshore and offshore transport, and however, by looking at the value itself, offshore transport dominated mostly. Furthermore, the average transport rate in this case was identified as the lower than the case of the other.

B. Second series experiment

In this section, the discussion of transport rate is different, which is every single figure represent the case itself as shown in Fig. 5.20. The transport rate estimated is based on the final condition of each wave condition. As the first case, case-T1(without nourishment), the onshore transport rate occurred during the accretive wave, while in the erosive wave, offshore transport dominated nearshore area at 1 to 3 meters, and a minor onshore transport was indicated from the offshore.

In case-T2 where the nourishment built in nearshore, the behavior was interesting. In accretive wave, the offshore transport occurred dominantly along with the profile even it was

small. Immediately after the accretive wave, the nourishment was built. The impact of gravel nourishment showed the response quickly in the erosive wave. The transport rate between onshore and offshore was balanced. The erosion occurred from the beach face to nearshore, just before the area of nourishment (refer to Fig. 5.8). The sand eroded from the beach face-nearshore was transported offshore and formed the bar. While at the same time, the onshore transport took placed in the offshore at 3 – 5 m. The onshore transport was influenced by the existence of gravel nourishment where located at 2.3 to 2.8 m. Furthermore, the gravels nourishment protected dominantly the backside area (offshore) from erosion.
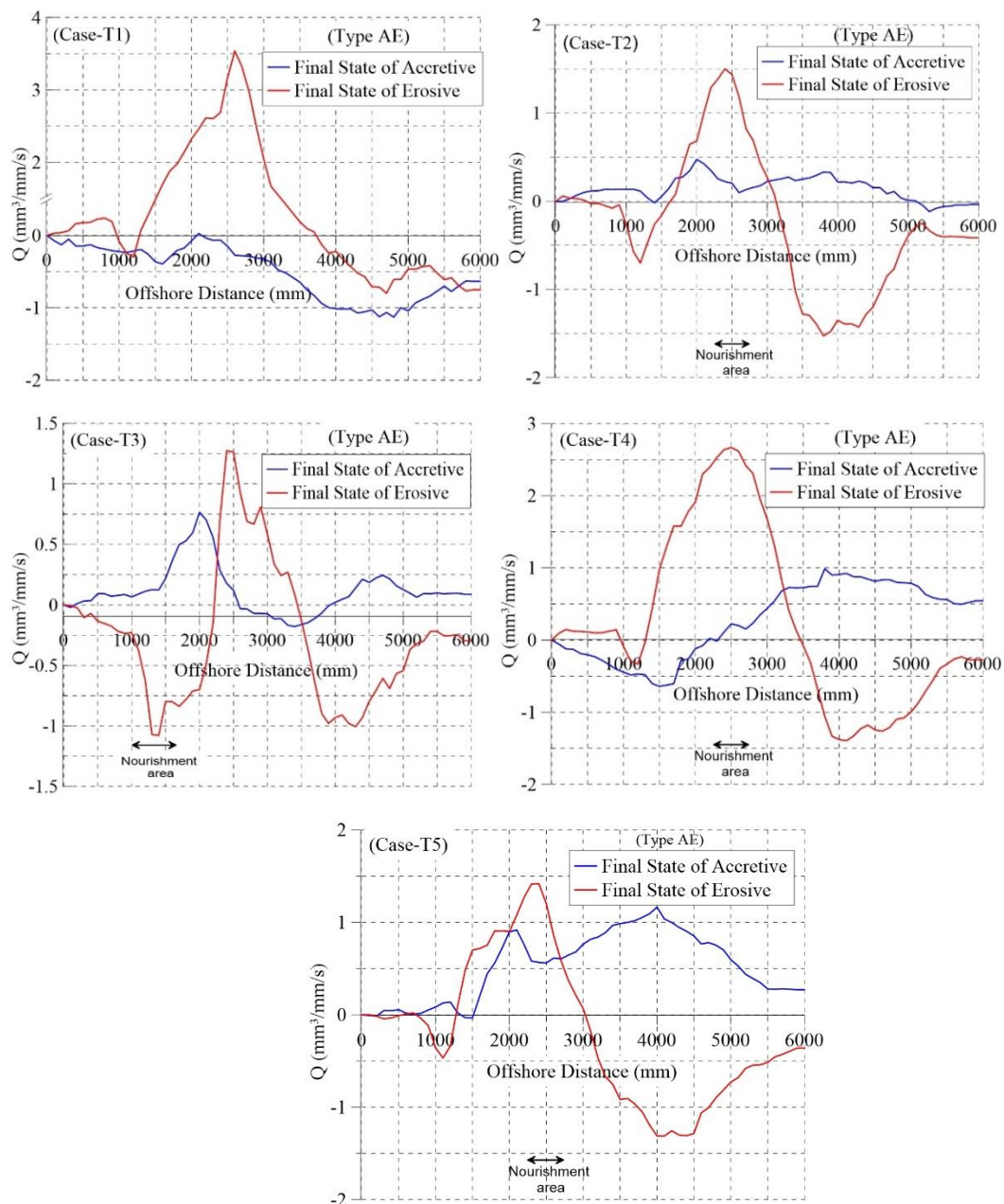
Figure 5.20 Net sediment transport rate of each cases based on different wave condition

In case-T3, the gravel nourishment was placed in the beach face area. In the accretive wave, the offshore transport rate occurred dominantly along the profile body. While in the erosive wave, the transport rate took place in two directions onshore and offshore. The onshore transport occurred in the beach face (foreshore) and offshore zone, whereas erosion in nearshore indicated offshore transport. Since the gravel nourishment was placed in the foreshore, no significant erosion was founded on that area. It means that the gravel nourishment in this state works conditionally in protecting a particular area from erosion.

In case-T4, with 0.035 m^3 volume of gravel, the nourishment was designed in offshore. In the accretive wave, the offshore transport rate was predominant compared to onshore transport. While in the erosive wave, considerable erosion took place from nearshore to offshore (1.3 – 3.5 m) which indicated offshore transport rate. Therefore, the sand eroded along nearshore-offshore were deposited in the backside of the offshore zone. The nourishment which placed at 2.3 – 2.8 m (in middle of the offshore zone) could not detain the erosive wave. Consequently, the gravels nourishment collapsed along with the erosion of the sand layer.

In case-T5, the volume of gravel nourishment was 14 times smaller than case-T2. However, it showed a similar pattern between them. The offshore transport rate predominated at the accretive wave, despite the rate was higher than case-T2, which means the erosion in this state is higher then case-T2 as well. On the otherhand, with the least volume and the location of nourishment, the beach face erosion could not be prevented in erosive wave condition compared to case-T2 and case-T3. However, the area of erosion was similar to case T4, even case-T1 (without nourishment). This could be mean that the volume-factor of gravel nourishment is critical in determining beach protection instead of location-factor because, in the correct estimation of gravel volume, the beach protection could work successfully at any locations, whether offshore or beach face (refer to case T2 and T3).

5.3.4. Armoring and mixture effect on sediment transport

A. First series experiment

In the first series experiment, case E2 was designed with a large volume of gravel nourishment which was placed on the sandy beach as shown in Fig. 5.21. Under erosive wave, the gravel layer (i.e., armor layer) is capable of acting as a shield for the sandy layer (i.e., interface layer) beneath, subsequently it prevents the sandy layer from explosive sand transport (Muhajjir) [11].

Besides, the erosive wave also caused mixing materials between sand and gravels, consequently created the mixture layer. McCarron et. al [12] revealed that the sediment mixture that contained 15 % gravel in the mixture layer could reduce the rate of sediment transport by more than 66% in comparison with the pure sand condition. Therefore, in order to examine the effects of the mixture layer, the sediment sampling was performed in several locations.
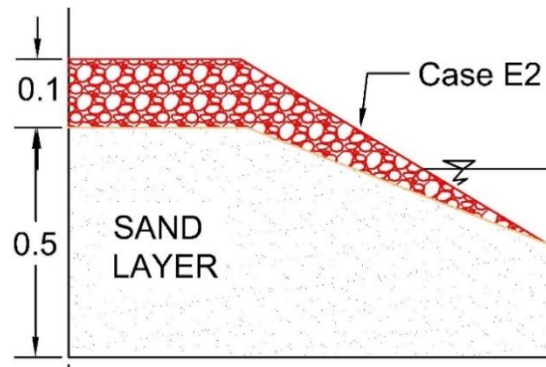
Figure 5.21 Gravel nourishment design for case-E3
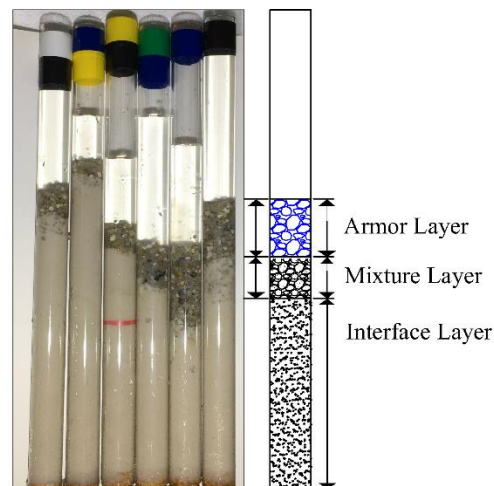
Figure 5.22 Layers of the samples

Figure 5.22 describes the layers of the beach model, which was taken from sediment sampling. There were 14 samples taken in this case. The thickness and ratio of the mixture layer were measured to find a relationship with the transport rate. Both armor-layer and mixture-layer might contribute to reducing sediment transport rate. Figure 5.23 describes two layers (i.e., armor and interface layers) of the profile, which eroded simultaneously between them and formed a trough. From this figure, the armoring-effect is seen obviously. The erosion of the interface layer is following the erosion of the armor layer. The transport of sand layer became suspended (i.e. generally bed load and suspended) due to the existences of armor layer.

Figure 5.23 was captured about 0.5 m from the shoreline, in which the breaking wave took place in this area.
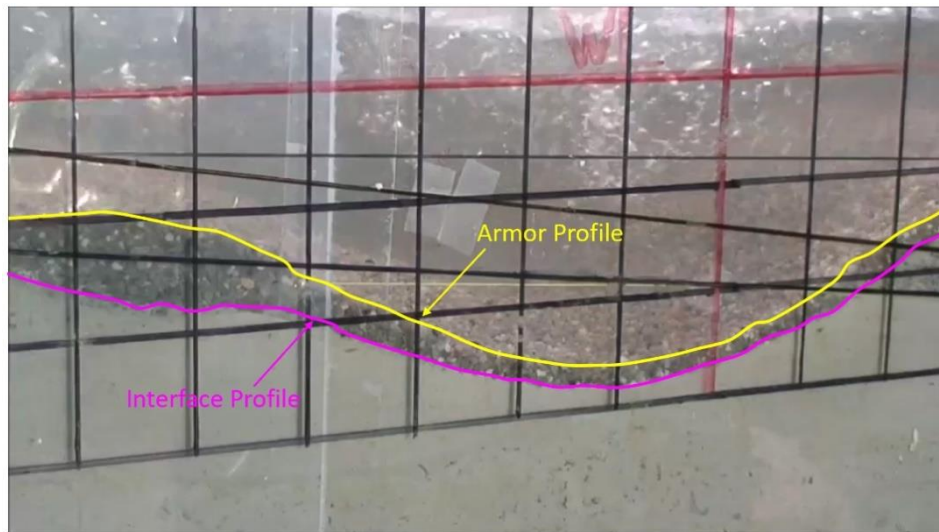
Figure 5.23 Formation of paralell layers as the effect of armoring
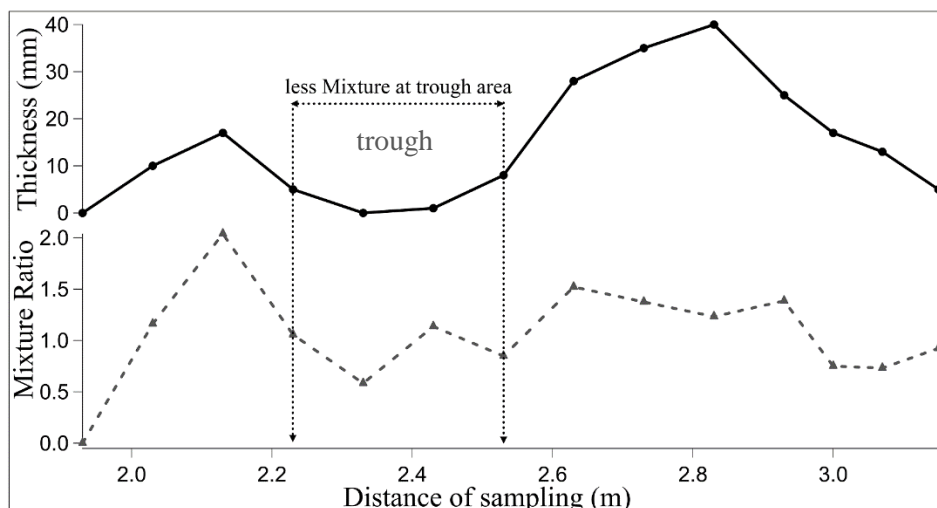
Figure 5.24 Ratio and thickness of the mixture layer

The mixture layers are found to be very thin around a trough as shown in Fig. 5.24. However, at the peaks between the trough, thickness and ratio of the mixture are quite higher. The ratio and thickness of the mixture are also believed contributes to a reduction in the transport rate associated with armoring-effect, which gives reduction impact the most.

Figure 5.25 shows the transport rate overall the cases. Fig. 5.25 could deduce that not all nourishment scheme guarantee work properly, even sometime it could accelerate the erosion in certain area (i.e. case-E3). The transport of case-E3 is even higher than case-E1 (without nourishment). As it is mentioned above section (refer to Fig. 5.6), the gravel nourishment was not sufficient, considering the amount and location of the nourishment design which lead to

severe erosion from beach face to nearshore. Among those three cases, case-E2 gave the lowest rate, which means the armoring and mixture-effect are work evidently.
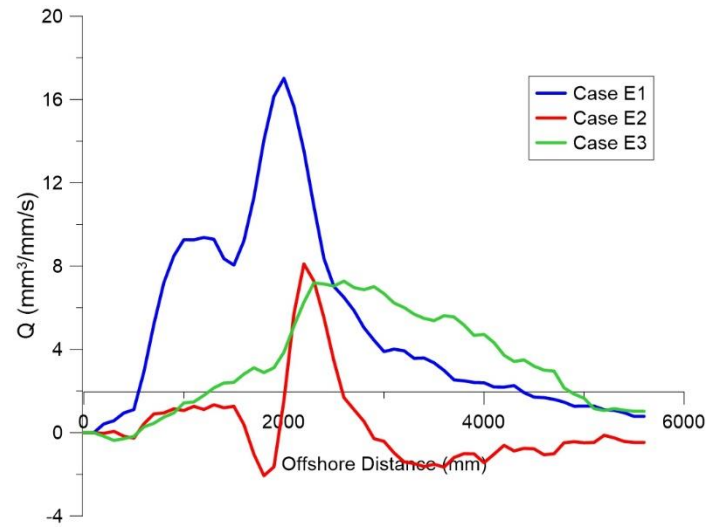
Figure 5.25 Comparison of transport rate overall the cases

B. Second series experiment

In this section, an images analysis is used to discuss the distribution of gravel nourishment together with a ramification of it. Four cases gravel nourishment with different locations and volumes (see Tab.1) was designed to encounter the beach erosion problem. By looking at Fig. 5.26, gravel nourishment in case-T2, T4, and T5 have placed at the same location (offshore). However, with smaller gravel volume than case-T2, the gravel distributed across the beach for case-T4 and T5 were microscopic and thin (i.e., armor and mixture layer); consequently, neither armor nor mixture layer was incapable of detaining the wave hit and led the beach profile collapse by the time.
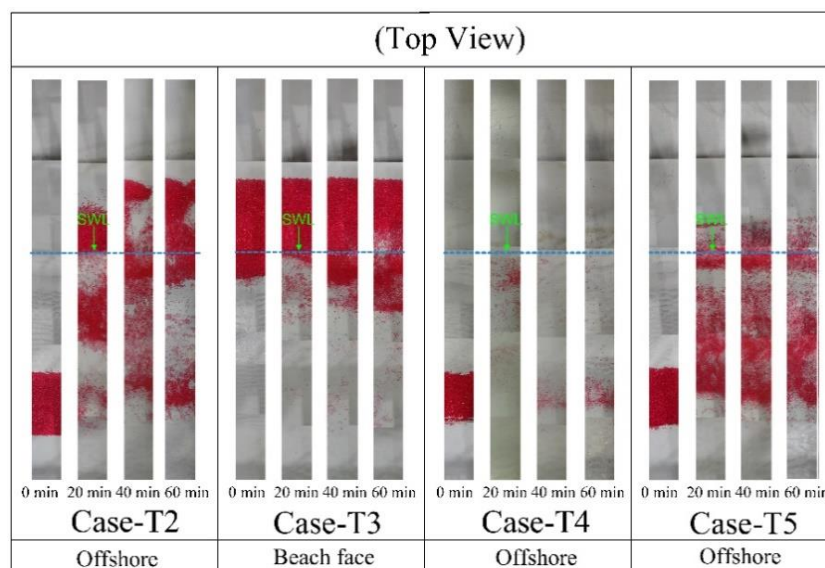
Figure 5.26 Gravel nourishment responses to the wave attack
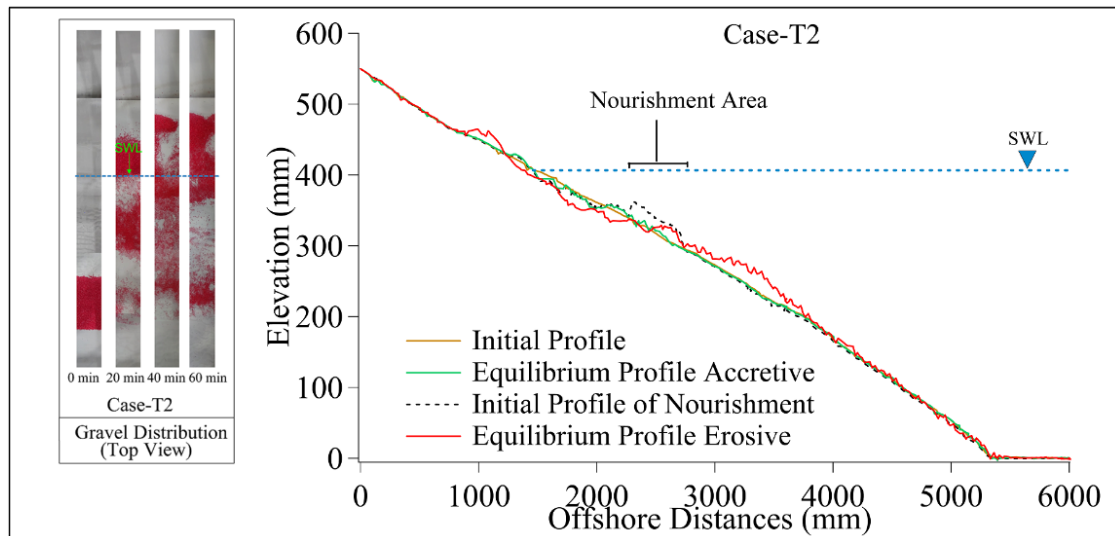
Figure 5.27 Armor layer as the result of gravel distributed which have a role to protect the beach in the case-T2
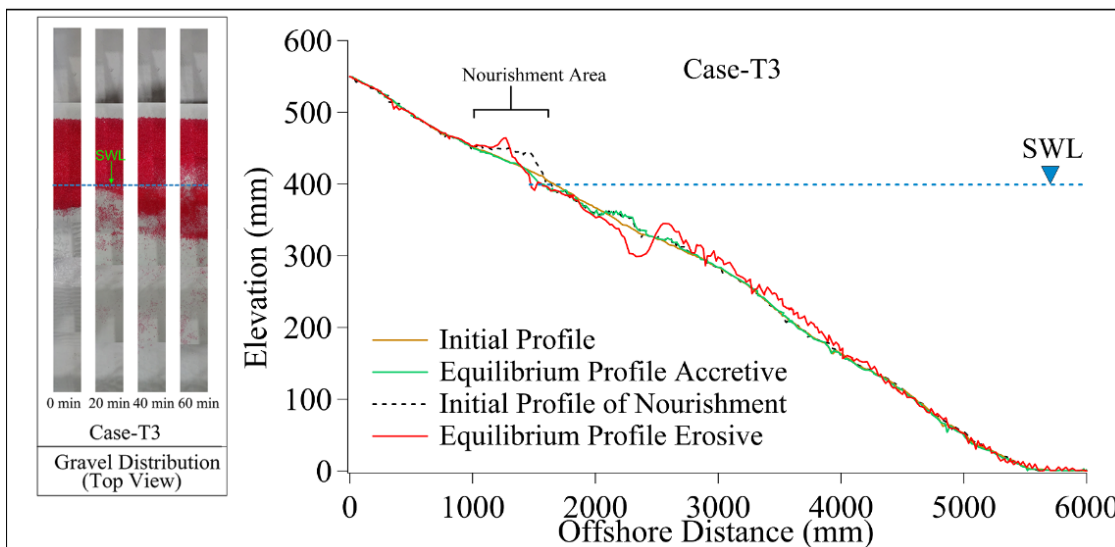
Figure 5.28 Armor layer as the result of gravel distributed which have a role to protect the beach in the case-T3

As it mentioned above section (refer to profile discussion of the second series experiment), there were only two cases which work successfully in mitigating beach erosion for this experiment, which was case-T2 and T3. Both cases had the same volume of gravel nourishment about 0.1 m^3. However, the location of the nourishment distinctly different, in which case-T2 was located in offshore and case-T3 was in beach face zone. As a result, case-T2 could maintained the beach profile from severe erosion both in the beach face and offshore as shown in Fig. 5.27. While case-T3 only preserved the beach face area as shown in Fig. 5.28.

From the above discussion, it could be deduced that the location-factor of gravel nourishment is unreliable compared to volume-factor, in term of determining the critical factor

for mitigation of beach erosion in this experiment. It is substantiated by the results of profile response associated with distributions of gravel (armor layer) across the beach (refer to Fig. 5.27 and 5.28) which justify case-T2 have better performance overall profile body than case-T3 with the same volume, although case-T2 is located offshore. Moreover, the mixture layer could not observe clearly in this analysis, so the effects are not discussed as well.

On the other hand, the armor layer which was distributed as the result of wave impact also promotes the reduction of transport rate in a particular zone (i.e., the zone of gravel distributed). Fig. 5.29 displays the sediment transport rate overall cases. The transport of case-T2 and case-T3 are relatively different. The transport rate in case-T2 prominently was low in the offshore, while small erosion occured nearshore cause transport rate higher than case-T3 in the nearshore. On the contrary, due to well protection in nearshore; consequently, the transport rate in case-T3 becomes low. However, offshore transport was slightly higher than case-T2.
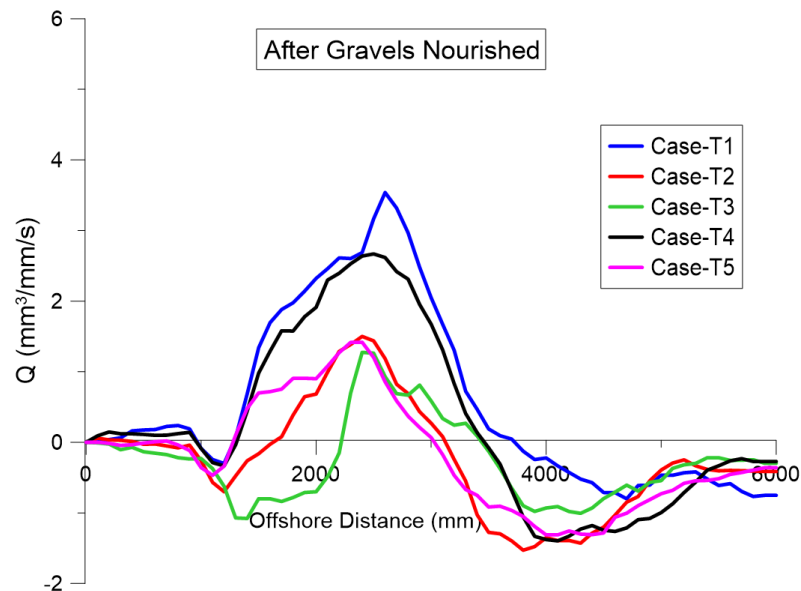
Figure 5.29 Net transport rate of second series experiment

5.4. Conclusions

In this chapter, two scenarios of gravels nourishment were tested to encounter beach erosion problem under experimental condition. The effects of gravel nourishment on the profile are discussed above sections. The significant findings in 2D experiments are addressed separately as follows,

First series experiment:

1. The different volumes of gravel nourishment crucially impact on the response of the beach profile.
2. The nourishment design like case-E3 is easy to collapse by the wave attack. The edge of gravel nourishment is located at sub-aerial (dry-wet zone) which is critical for beach erosion. Hence, the edge should be extended lower under the water to improve the performance of beach protection.
3. The armor and mixture layers revealed to have a significant role in reducing sediment transport rate.

Second series experiment:

1. As well as the first series experiment, determining volume-factor are more critical than location-factor. It is proved by case-T2, with the same volume with case-T3 (0.1 m^3) but the different location (offshore), case-T2 is still able to protect beach face from severe beach erosion.
2. The armoring-effect work successfully for case-T2 and case-T3 in reducing the transport rate in a particular area. The rate between case T2 and T3 are relatively different. The rate in case-T2 is low in offshore, while case-T3 is low in the nearshore. It is due to the volume of gravels nourishment which distributed dominantly offshore and nearshores for case-T2 and case-T3 respectively.

References

1) Stauble, DK., Garcia, AW., Kraus, NC. (1993). *Beach Nourishment Project Response and Design Evaluation: Ocean City, Maryland, Technical Report 1: 1988-1992. Technical Report CERC-93-13*. US Army Engineer Water ways Experiment Station. Coastal Engineering Research Centre, Vicksburg, MS

2) Sorensen R., Beil N. (1988). "Perched Beach Profile Response to Wave Action", *Proceedings 21st Coastal Engineering Conference*, ASCE, 1: 482-492.

3) Risio, MD., Lisi, I., Beltrami, G., Girolamo PD. (2010). "Physical Modeling of the Cross-Shore Short-Term Evolution of Protected and Unprotected Beach Nourishments", *Ocean Engineering*, Vol 37: 777-789.

4) Musumeci, R., Cavallaro, L., Foti, E. (2012). "Performance of Perched Beach Nourishments", Santander, Spain, *Proceedings of 33rd Conference on Coastal Engineering*, Vol 1: 112-125.

5) Farac,i C., Scandura, P., Foti, E. (2014). "Evolution of a Perched Nourished Beach: Comparison Between Field Data And Numerical Results", Seoul, Korea, *Proceedings of 34th Conference on Coastal Engineering*

6) Kumada, T., Uda, T., Ishikawa, T. (2009). "Theory and Field Test of Beach Nourishment Using Coarse Sand and Gravel", *Proc. Coastal Dynamics*, Paper No. 75, pp. 1-11.

7) Kumada, T., Uda, T., Matsu-ura, T., Sumiya, M. (2010). "Field Experiment on Beach Nourishment Using Gravel at Jinkoji Coast", *Proc. 32nd ICCE,* sediment.100, pp.1-13.

8) Yoshioka, A., Uda, T., Aoshima, G., Furuike, K., and Ishikawa, T. (2008). "Field Experiment of Beach Nourishment Considering Change in Grain Size and Prediction of Beach Changes," *Coastal Engineering*, 2694-2706.

9) Dean, RG. (1991). "Equilibrium Beach Profiles: Characteristics and Applications," *Journal of Coastal Research*, Vol. 7(1), 53-84.

10) Larson, M., and Kraus, NC. (1989a). *SBEACH: Numerical Model for Simulating Storm-Induced Beach Change, Report 1: Theory and Model Foundation, Technical Report CERC-89-9*, US Army Engineer Waterways Experiment Station, Coastal Engineering Research Center, Vicksburg, MS.

11) Muhajjir, Suga, H., and Aoki, S. (2018)."Transportation of gravel on the Upper Part of the Sandy Beach," *Proceeding 28th International Offshore and Polar Eng Conf*, Sapporo, ISOPE, 1098-6189.

12) McCarron, C., Howard, N., Van Landaghem, K., Baas, J., and Amoudry, LO. (2016)." Sediment Transport and Bedform Morphodynamics in Sand-Gravel Mixtures," *MARID Conf V*, New South Wales, UK.

Chapter 6
Conclusions

In this section, the results and recommendations of the whole chapters in this research are summarized. This research is triggered by an event of severe beach erosion in Ojigahama Coast, Shingu, Wakayama Prefecture, Japan. This disaster was caused by a storm wave that generated from the typhoon in July 2015. The erosion takes place behind the revetment- under the track of the railway of JR Company. Immediately after the disaster, a temporary (short term) action is done by filling the hole of the erosion with soils, so the operational train could run soon after countermeasure-work is finished. However, a short-term countermeasure is not enough to protect the coast and railway itself from future disaster. In order to prepare a long-term solution, it necessary to study morphodynamics of the beach and wave near the sea. Thus, information and recommendation about nearby coast environment would be given to local government and company, so that they could consider the solution to encounter the issue.

A comprehensive study is conducted in this research through field study and physical experiment. As the first step in this research, the field study is performed to collect information about the characteristics of the beach and waves at Ojigahama Coast. Ojigahama Coast is one of the types of gravel beaches which classified into composite sand-gravel beach. The field study in this research covers the beach topography measurement, wave-current measurement associated with nearby wave data station, and distribution of particles across the beach. The field study had been done from 2016 to 2018, in which in a year, the measurement is conducted 4 – 6 times.

During three years of measurement, some interesting points found in this study, which are the similarity of storm wave condition between 2015, 2017, 2018 and the shoreline retreat as the impact of the storm wave. It is confirmed that a wave height about 10 m and 13 s wave period attack the coast on July 2015. Furthermore, 40 hours wave duration is generated for the wave height over 5 m to 10 m. While there are similar wave heights and periods, occur in 2017 and 2018. Nevertheless, with such erosive wave, there is no severe damage found on the backside of the beach (near revetment) either 2017 or 2018. The waves duration for the wave height over 5 m to 10 m are smaller than the condition in 2015, which are 12 and 32 hours for 2017 and 2018 respectively. However, significant topography change takes place during the storm wave as a result of considerable erosion. Especially in 2018, after continuous-wave

attack (two times of storm wave attack within a month), the shoreline in southern end of the beach (at the erosion area of 2015 or survey lines of 19-22) retreats significantly about 45 m, since then, the shoreline becomes short; it only remains a width of 25 m from the revetment. Moreover, based on topography and wave analyses, it could be deduced that for the wave up to 5 m with wave duration more than 10 hours could cause the shoreline retreat about 15-20 m in one incident. It could be a severe problem if such as wave condition above (up 5 m with wave duration more than 10 hours) happen at least three times in a short time without sufficient beach recovery, the same beach erosion could be repeated in Ojigahama Beach (i.e., the average width is 70-80 m; the shorelines retreat about 15-20 in one time storm wave attack).

The rapid erosion in beach face can not be separated by the characteristic of the beach itself. As it discovers based on field study and experimental condition, the typical composite sand-gravel is very vulnerable to wave, especially in the sub-aerial zone (dry-wet zone). This zone is also the zone in which the shoreline separates the gravel and sand. The sub-aerial zone is critical even for the normal wave (2-4 m), in which under the normal wave conditions the berm (i.e. contained only gravel) is formed on the top the beach. The formation of the berm leads the propagation of the wave and current change when it hit the beach in the next coming wave and produce strong backwash current toward the sea. The strong backwash current pulls a down small amount of gravel to the sea, in which at this circumstance the shape roughness of gravel has a role in accelerating the erosion of the sand layer (i.e. substantial contact/interaction between gravel and sand fractions). Due to this erosion, the profile becomes steeper by the time, and it changes the propagation of wave and current periodically. The steeper profile is formed, the stronger the backwash current is generated. This condition becomes worst under the storm wave, the berm formed is higher, and the erosion becomes more extensive, which followed by steeper profile formation. This cycle keeps repeating until it reaches the equilibrium profile condition.

A couple of experiments 2D and 3D experiment are conducted to complete the step of this research. The purpose of this experiment is to investigate deeply about the morphodynamics of composite sand-gravel beach. Some of the parameters in the experiments are adopted from the condition of disaster in 2015 of Ojigahama Coast. However, the experiment does not intend to model the real condition. The author realizes that not all the parameters on the field could be scaled similarly and perfect with the experiment. There would be a scale-effect issue which might affect the experimental results. Consideration of the scale-effect of each parameter (e.g., sand, gravel, wave height, wave period, wave duration, etc.) and

scale-effect combinations of the parameters are essential, but it needs a comprehensive or specific study to discuss intensely. Moreover, concerning the primary goal of the study which limited to clarify the general characteristics of beach response under experimental condition.

In the 2D experiment, cross-shore morphodynamics of composite sand-gravel beach is studied. Based on the result of the experiment, several findings regarding the characteristics of composite sand-gravel are revealed. Moreover, one of the findings shows a similar characteristic with the real condition of Ojigahama Coast, which is the formation of the berm in storm condition. The formation of the berm under storm condition also often occurs in the pure gravel beach type. The formation of the berm occurs followed by nearshore erosion that forms the steep profile along the nearshore to the offshore, in which this phenomenon could not be seen in the real situation due to none topography measurement is conducted underwater.

Furthermore, the beach recovery is low under a post-storm wave condition. One of the reasons the recovery low is the considerable nearshore erosion. On the other hand, the mixture of thickness and ratio are studied through sediment sampling at 12 locations. In this section, the analysis is done limitedly by assessing only the relationship of mixture ratio and mixture thickness to wave condition. In which, it shows that the ratio and thickness of the mixture are predominant in storm wave condition rather than post-storm wave condition. Furthermore, the correlation between ratio and thickness of the mixture are in good agreement, as the mixture thickness increases, the mixture ration also increases.

In the 3D experiment, longshore sediment transport of composite sand-gravel beach is assessed. This experiment is an advanced study from the 2D experiment. By expanding the scale of the experiment, it is expected that the understanding of the morphodynamics composite sand-gravel beach under longshore condition could be more extensive. The focus of this experiment is the distribution of coloured gravel (blue and red gravel) along or across the beach.

The beach is designed oblique to the wave generator instead generate the oblique wave. By designing this condition, it is expected that the longshore drift could take place at the beach top so that the coloured gravel movement could be seen clearly. The longshore current only develop nearshore, while on the beach top; the strong backwash current occurs and carries down much sediment. Based on the analysis above, it could be conclude that the coloured gravels transport in two steps; first, the gravels moves seaward as the effect of steep profile formation that associated with strong backwash current, secondly, when the gravel reaches nearshore, the gravel would turn to the left side of the beach in following the longshore current

developed. On the other hand, the increase in the water depth led to the different response of topography (profile) change, especially the breaker zone. The breaker zone moves forward toward the beach as the water depth is increased. Consequently, it affects the difference of wave height produced around the breaker zone.

In the last chapter of this research, an additional experiment is carried out to study the countermeasure of beach erosion by using gravel nourishment. By understanding the basic idea of morphodynamics of composite sand-gravel, approximately it could be useful to achieve the objectives of this experiment. There are two objectives in this study, which are to assess the effectiveness of gravel nourishment and to identify the armouring and mixture effect on sediment transport. This study consists of two series experiments, which are done separately. There are three and five cases for the first and second series experiment, respectively. The effectiveness of the gravel nourished is analysed through the profile response to the wave. The purpose of analysis in the sediment sampling is to observe the effect of the mixture and armouring layer. Based on the results of the experiment, the findings are described separately between the first and second series experiment. In the first series experiment, it reveals that the different volumes of gravel nourishment crucially affect the response of the beach profile.

Furthermore, the nourishment design, like case-E3 is easy to collapse by the wave attack. The edge of gravel nourishment is located at sub-aerial (dry-wet zone) which is critical for beach erosion. Hence, the edge should be extended lower under the water to improve the performance of beach protection. On the other hand, the armour and mixture layer reveal to have a significant role in reducing sediment transport rate, which is proved by case E2. While in the second series experiment, two over five cases show a good profile response to storm wave (i.e., the beach protected from severe erosion). Furthermore, there is one crucial finding in this case, in which, determining volume-factor in the design of gravel nourishment are more critical than location-factor. It is proved by case-T2, with the same volume with case-T3 (0.1 m3) but the different location (offshore), case-T2 is still able to protect beach face from severe beach erosion. On the other hand, the armouring-effect work successfully for case-T2 and case-T3 in reducing the transport rate in a particular area (i.e., the reducing effect occurs depends on which zone that the gravel spread dominantly).

Based on the studies, which discuss comprehensively from chapter two to chapter five, a short-term action could be proposed in order to deal with the issue of coastal erosion/shoreline retreat at Ojigahma Beach. One of the countermeasure acts that could be recommended is gravel nourishment. One of the best locations to apply the nourishment is in the sub-aerial zone

(dry-wet zone) as in the case-T3, which discussed details in chapter five. However, this proposal has to be tested under experimental condition before applying in the real condition.

There is still widely space to expand the composite sand-gravel beach study, especially in term of the experimental conditions. Such gravel nourishment with different volume and location as is discussed in chapter five (i.e. limited only on the sandy beach) could be established with different beach type like composite sand-gravel beach. Furthermore, mixing grains (D50) of the gravel could be used in the experiment instead of using the uniform size 2.3 mm like in this study. Moreover, the effect in the different water level or various wave height is also a proper assessment to be developed.